NASA Contractor Report 179469
UTRC-R86-956480-4

1.58

The Effects of Inlet Turbulence and Rotor/Stator Interactions on the Aerodynamics and Heat Transfer of a Large-Scale Rotating Turbine Model

IV—Aerodynamic Data Tabulation

R.P Dring, H.D. Joslyn, and M.F. Blair
United Technologies Research Center
East Hartford, Connecticut

November 1987

Prepared for
Lewis Research Center
Under Contract NAS3-23717

Date for general release May 1988

National Aeronautics and
Space Administration

FOREWORD

This report was prepared for the National Aeronautics and Space Administration, Lewis Research Center by the United Technologies Research Center, East Hartford, Connecticut, under Contract NAS3-23717. The performance period covered by this report was 11 April, 1983 to 11 June, 1986. The project monitor was Dr. Robert J. Simoneau.

R86-956480-4

THE EFFECTS OF INLET TURBULENCE AND ROTOR/STATOR INTERACTIONS ON THE AERODYNAMICS AND HEAT TRANSFER OF A LARGE-SCALE ROTATING TURBINE MODEL

VOLUME IV

AERODYNAMIC DATA TABULATION

TABLE OF CONTENTS

PRECEDING PAGE BLANK NOT FILMED

PAGE ii INTENTIONALLY BLANK

INTRODUCTION

The primary basis currently used by the gas turbine community for heat transfer analysis of turbine airfoils is experimental data obtained in linear cascades. These data have been very valuable in identifying the major heat transfer and fluid flow features of turbine airfoils. The question remains, however, as to how well cascade data translate to the rotating turbine stage. It is known from the work of Lokay and Trushin (ref. 1) that average heat transfer coefficients on the rotor may be as much as 40 percent above the values measured on the same blades without rotation. Recent work by Dunn and Holt (ref. 2) supports the conclusions of reference 1. It is widely recognized that at this time a need exists for a set of heat transfer data from a rotating system which is of sufficient detail to allow careful local comparisons between static cascade and rotor blade distributions. It is important that this data set include sufficient flow field documentation to support the computer analyses being developed today.

Other important questions include the impact of both random and periodic unsteadiness on both the rotor and stator airfoil heat transfer. The random unsteadiness arises from stage inlet turbulence and wake generated turbulence and the periodic unsteadiness arises from blade passing effects. A final question is the influence, if any, of the first stator row and first stator inlet turbulence on the heat transfer of the second stator row after the flow has been passed through the rotor.

OBJECTIVES

The first program objective has been to obtain a detailed set of heat transfer coefficients along the midspan of a stator and a rotor in a rotating turbine stage (fig. 1). The experimental program was designed such that the rotor data could be compared directly with data taken in a static cascade. The data are compared to a standard analysis of blade boundary layer heat transfer which is widely available today. In addition to providing this all-important comparison between rotating and stationary data, this experiment provides important insight to the more elaborate full three-dimensional programs being proposed for future research. A second program objective has been to obtain a detailed set of heat transfer coefficients along the midspan of a stator located in the wake of an upstream turbine stage. The axial location of the second stator relative to the upstream turbine stage is shown in figure 2. Particular focus here was on the relative circumferential location of the first and second stators. Both program objectives were carried out at two levels of inlet turbulence. The low level was on the order of 1 percent while the high level of approximately 10 percent is more typical of combustor exit turbulence intensity. The final program objective is to improve the analytical capability to predict the experimental data.

DESCRIPTION OF EXPERIMENT

1. Turbine Facility

All experimental work for this program was conducted in the United Technologies Research Center Large Scale Rotating Rig (LSRR) shown in figure 2. This test facility was designed for conducting detailed experimental investigations of flow within turbine and compressor blading. Primary considerations were to provide a rig which would: (1) be of sufficient size to permit a high degree of resolution of three-dimensional flows, (2) possess a high degree of flexibility in regard to the configurations which can be tested, and (3) enable measurements to be made directly in the rotating frame of reference.

The facility is of the open circuit type with flow entering through a 12-ft diameter inlet. A 6-in. thick section of honeycomb is mounted at the inlet face to remove any cross flow effects. The inlet smoothly contracts the cross section diameter down to 5-ft. Flow is then passed through a series of three fine mesh screens to reduce the turbulence level. Immediately downstream of the screens is a telescoping section which slides axially and permits access to the test section. The test section consists of an axial series of constant diameter casings enclosing the turbine, compressor or, fan model assemblies. The casings are wholly or partially transparent, which facilitates flow visualization and laser-Doppler-velocimeter studies. The rotor shaft is cantilevered from two downstream bearings thus providing a clean flow path to the most upstream row of test airfoils. Axial length of the test section is 36-in. The rotor is driven or braked by a hydraulic pump and motor system which is capable of maintaining shaft speeds up to 890 rpm. Downstream of the test section flow passes through an annular diffuser into a centrifugal fan and is subsequently exhausted from the rig. A vortex valve is mounted at the fan inlet face for flow rate control.

2. Airfoil Coordinates and Aerodynamics

The surface hub, midspan, and tip coordinates (x,y) of the three airfoil rows (stator 1, rotor and stator 2) are given in Tables 1, 2, and 3 respectively. The aerodynamic documentation of the turbine stage indicated that all parameters were very close to data obtained during prior testing with this turbine model, reference 3. As an example, the first stator and rotor pressure distributions are shown in figures 3a and 3b for the case with the small (15%) axial gap, at the design flow coefficient ($C_x/U_m = 0.78$), and with the inlet turbulence generating grid installed. Agreement with a two-dimensional potential flow calculation (ref. 4) at this midspan location is excellent. The computed surface velocity distributions are used as the input to the suction and pressure surface boundary layer calculations (refs. 5, 6). The resulting calculated suction and pressure surface Stanton number distributions are presented along with the measured results in Volumes I thru III.

3. Inlet Turbulence

As part of the present contract heat transfer distributions through the LSRR turbine blading were examined for both low and high levels of inlet turbulence. Throughout this report the low and high levels are referred to as "grid out" and "grid in" respectively. With the test facility configured in the minimum inlet turbulence arrangement (grid out) the inlet turbulence was approximately 0.5% at an axial location 22% of axial chord ahead of the first stator leading edge. Higher levels of inlet turbulence were produced by installing a biplane grid upstream of the first stator. The turbulence generator consisted of a nearly square array lattice of three concentric rings spaced uniformly in the radial direction with 80 radial bars evenly spaced circumferentially. Both the rings and radial bars were of nearly square 1/2 inch cross-sections. The mesh spacing of the bars was 2.1 inches radially and 4.5 degrees (2.1 in. at mid-annulus) circumferentially. With the grid installed at the inlet turbulence intensity was typically 9.8%. The spanwise distributions at four different circumferential locations (relative to the stator leading edge) are shown in figure 4. The data indicate that the turbulence is spatially uniform, nearly isotropic, and temporally (long time average) steady. This is representative of the level of turbulence measured at the exit of aircraft gas turbine combustors.

4. Heat Transfer Instrumentation

Heat transfer measurements were obtained in this study using low conductivity rigid foam castings of the test airfoils. A uniform heat flux was generated on the surface of the foam test airfoils using electrically heated metal foil strips attached to the model surface. Conduction and radiation effects produced small departures from complete uniformity. Local airfoil surface temperatures were measured using thermocouples welded to the back of the foil while the air temperature was measured using thermocouples in the air stream. The secondary junctions to copper wire were all made on Uniform Temperature Reference blocks (Kaye Instruments, UTR-48N) and the data were recorded using a Hewlett-Packard 300 channel data acquisition unit (3497A/3498A), and an ice point reference (Kaye Instruments, K140-4). A 212 ring slip-ring unit (Wenden Co.) was used to bring heater power onto the rotor and to bring out the thermocouple data. Instrumentation locations for the first stage stator and rotor are given in figures 5a and 5b. Locations for the second stator are given in Volumes I and III.

5. Aerodynamic Instrumentation and Data

The steady aerodynamic measurements consisted of hub and casing flowpath static pressures acquired downstream of each airfoil row, midspan surface static pressure distributions obtained on each airfoil and circumferential distributions of total and static pressures and the flow yaw and pitch angles obtained from a 5 hole pneumatic probe (United Sensors USC-F-152) traverse downstream of each airfoil row. The hub and casing flowpath static pressures and probe traverse data were acquired at stations 2, 3 and 4 (fig. 2). The location of the airfoil surface static pressure measurement sites is given in Tables 7 through 9 in terms of the axial distance (DIST = X/B_x) from the airfoil leading edge tangency plane.

A dedicated online Perkin Elmer (PE 8/16E) minicomputer controls the online calibration of all pressure transducers (Druck model PDCR-22), radial and circumferential positioning and yaw nulling of stationary and rotating frame probes (United Sensors USC-F-152) and the acquisition and online reduction of all steady aerodynamic data. Electrical communication with the rotating frame instrumentation package, transducers and traverse system was through a Fabricast (model 1273) slip-ring assembly mounted on the rotor drive shaft.

High response inter-row velocity and unsteadiness measurements were made by traversing a radially oriented, single element hot film probe (Thermo Systems Inc., TSI model 1211-20) downstream of each airfoil row (stations 2, 3 and 4, fig. 2) at midspan. The probe was calibrated from 40 to 200 feet per second, was powered by a TSI Model 1050 anemometer and was traversed in the stationary frame of reference. Positioning of the hot film probe and data acquisition was controlled by the PE 8/16E minicomputer.

The aerodynamic instrumentation and data are presented in the following Tables and Figures.

Airfoil geometry	Tables 1 through 3
Flowpath static pressures	Tables 4 through 6
Airfoil pressure distributions	Tables 7 through 9, and Figures 3, and 6 through 14
Pitch-averaged unsteadiness	Table 10
Stage-geometry	Figures 1 and 2
Inlet turbulence (Grid In)	Figure 4
Heat transfer instrumentation	Figure 5
5-Hole probe traverse data	Figures 15 through 32
Hot-Film probe traverse data	Figures 33 through 41

A brief overview of the tables and figures containing the aerodynamic data follows:

Flowpath Static Pressures

The hub, mean and outer casing flowpath static pressures at the exit of the first stator, the rotor and the second stator are presented in Tables 4, 5, and 6 respectively. The hub and outer casing flowpath pressures presented are averages based on measured pressures and account for blade-to-blade as well as circumferential (annulus) variations. The mean (i.e. midspan) flowpath static pressure is calculated from a free vortex distribution between the measured hub and outer casing flowpath static pressures (pitch and annulus averages). Results are shown for all three flow coefficients (C_x/U_m = 0.68, 0.78, 0.96), for two first stator/rotor axial spacings (x/B_x = 0.15 and 0.50) and for two inlet turbulence levels (grid out and grid in).

Airfoil Pressure Distributions

Turbine stage (first stator and rotor) airfoil midspan pressure distributions obtained at all three flow coefficients and at axial spacings of 15 and 50 percent axial chord are presented in Tables 7a,b and 8a,b respectively. Tables 7a and 8a contain the data acquired with the grid out; Tables 7b and 8b contain the data acquired with the grid in. The second stator midspan pressure distributions acquired with the grid out and with the grid in for a first stator/rotor axial spacing of 50 percent are presented in Tables 9a and 9b respectively. In all tables (7 through 9), the static pressure coefficient (Cps) is tabulated along with the axial distance (DIST = X/B_x) from the airfoil leading edge tangency plane. The base pressures measured on each airfoil at midspan are also included in the appropriate data set.

The airfoil midspan pressure distribution data are plotted as the symbols in figures 3, and 6 through 14. In figures 6 through 11, all the data sets are presented in terms of a pressure coefficient based on the inlet (station 1) total pressure and the first stator exit (station 2) dynamic pressure, Q2. This permits all of the airfoil data to be compared directly on the same basis. From these results it is clear that the addition of the grid had little impact on the airfoil midspan pressure distributions. Also, it is evident that the first stator midspan pressure distribution was virtually the same at all three flow coefficients. The abbreviations (SS, PS, TE, BP, CG2, CGT1) on the right hand side of the figures represent suction surface, pressure surface, trailing edge, base pressure, airfoil exit static pressure and the rotor inlet relative total pressure respectively. In figures 3 (grid in) and 12 through 14 (grid out), the data is presented along with the results of a potential flow calculation (Ref. 4). Here, the pressure coefficient is based on the inlet total pressure and exit static pressure relative to a particular airfoil row.

Pitch-Averaged Unsteadiness

The average total (U_T), periodic (U_P) and random (U_R) unsteadiness at a single radial/circumferential hot film traverse location in the turbine model are defined in Table 10a. $V_k(t)$ represents the instantaneous film speed measured with a radially oriented single element hot film probe during a specific rotor revolution. It is composed of a periodic component, $\tilde{V}(t)$ and a random component, $v_k'(t)$. Vo is the time average speed at this location. At each radial/circumferential traverse location at stations 2, 3, and 4 (fig. 2), one hundred sets ($N_{rev} = 100$) of instantaneous speed data were acquired and processed (ensemble and time averaged) to obtain the midspan circumferential distributions of average total, periodic and random unsteadiness presented in figures 33 through 41. Measurements were made at all three flow coefficients with the grid out and with the grid in. The midspan circumferential distributions of the average total, periodic and random unsteadiness were pitch averaged and the results are summarized in Tables 10b, 10c, and 10d for the flow coefficients of 0.68, 0.78 and 0.96 respectively.

5-Hole Probe Traverse Data

A single 5 hole pneumatic probe (United Sensor model USC-F-152) was traversed circumferentially at midspan to measure total and static pressures and the flow yaw and pitch angles downstream of each airfoil (stations 2, 3 and 4). The resulting circumferential distributions taken over two first stator pitches are presented in figures 15 through 32. The results obtained with the grid out and with the grid in at three flow coefficients are presented for each airfoil (first stator, rotor and second stator).

The results for each airfoil are presented in the same sequence as that which follows for data in the absolute frame downstream of the first stator (for flow coefficients of 0.68, 0.78 and 0.96).

Figure	Symbol	Quantity	Grid
15a-c	CPTABS CTOT	Total pressure Flow speed	Out
16a-c	CPS CX/UM	Static pressure Axial velocity	Out
17a-c	YAWABS PHI	Flow yaw angle Flow pitch angle	Out
18a-c	CPTABS CTOT	Total pressure Flow speed	In

19a-c	CPS	Static pressure	In
	CX/UM	Axial velocity	
20a-c	YAWABS	Flow yaw angle	In
	PHI	Flow pitch angle	

For the data in the rotating frame downstream of the rotor these quantities are as follows, CPTREL, wTOT, CPS, CX/UM, YAWREL, and PHI.

Hot Film Probe Traverse Data

The midspan circumferential distributions of ensemble-time averaged flow speed (VTAVG) and unsteadiness (total, periodic and random) at the exit of each airfoil are presented in figures 33 through 41. These results were obtained with the grid out and with the grid in by traversing a radially oriented single element hot film probe over two first stator pitches downstream of each airfoil row. Figures 33a to 35b show the results for the first stator, rotor and second stator at a flow coefficient of 0.68 with the grid out and with the grid in. The results obtained at flow coefficients 0.78 and 0.96 are presented in figures 36a and 39a to 41b respectively.

Access to Aerodynamic Data

Copies of the aerodynamic data can be obtained by contacting Robert Dring of UTRC by phone at 203-727-7044.

NOMENCLATURE

B_x	airfoil axial chord
C_p	pressure coefficient (based on turbine inlet total pressure and Q_{U_m})
C_{Tot}	absolute flow speed normalized by U_m
C_x	axial flow speed
P	static pressure
P_T	total pressure
Q_{U_m}	dynamic pressure based on U_m
S	surface arc length from trailing edge
U	streamwise velocity
U_m	rotor midspan wheel speed
U	stage inlet flow velocity
$\overline{U}$	unsteadiness (T: total, R: random, and P: periodic) ($\overline{U}_T = \overline{U}_R + \overline{U}_P$)
W_{Tot}	relative flow speed normalized by U_m
X	axial distance
α	absolute flow angle from axial
β	relative flow angle from axial
ρ	density
ϕ	flow coefficient (C_x/U_m)
$\hat{C}_p$	pressure coefficient (based on turbine inlet total pressure and first stator exit dynamic pressure Q_2)

Superscripts

‾	time average

Subscripts

0	model inlet upstream of turbulence grid
1	first stator inlet
2	first stator exit
3	rotor exit
4	second stator exit
ABS	absolute (stationary) frame
IN	inlet properties relative to airfoil rows
REL	relative frame

REFERENCES

1. Lokay, V. I., and Trushin, V. A.: Heat Transfer from the Gas and Flow-Passage Elements of a Rotating Gas Turbine. Heat Transfer - Soviet Research, Vol. 2, No. 4, July 1970.

2. Dunn, M. G., and Holt, J. L.: The Turbine Stage Heat Flux Measurements. Paper No. 82-1289, AIAA/ASME 18th Joint Propulsion Conference, 21-23, June 1982, Cleveland, Ohio.

3. Dring, R. P., Joslyn, H. D., Hardin, L. W., and Wagner, J. H.: Turbine Rotor-Stator Interaction. ASME J. Eng. for Power, Vol. 104, pp. 729-742, October 1982.

4. Caspar, J. E., Hobbs, D. E. and Davis, R. L.: Calculation of Two-Dimensional Potential Cascade Flow using Finite Area Methods, AIAA Journal, Vol. 18, No. 1, January 1980, pp. 103-109.

5. Carter, J. E., Edwards, D. E. and Werle, M. J.: Coordinate Transformation for Laminar and Turbulent Boundary Layers, AIAA Journal, Vol. 20, No. 2, February 1982, pp. 282-284.

6. Edwards, D. E., Carter, J. E. and Werle, M. J.: Analysis of the Boundary Layer Equations Including a Coordinate Transformation--The ABLE Code, UTRC81-30, 1981.

TABLE 1a
AIRFOIL GEOMETRY

AIRFOIL: FIRST STATOR (HUB)
PITCH (ins.): 6.88865

	LEADING EDGE	TRAILING EDGE
RADIUS (ins.)	0.44485	0.10988
METAL ANGLE (degr.)	90.00395	22.44246
WEDGE ANGLE (degr.)	31.79000	6.85000

	X(ins.)	Y_L(ins.)	Y_U(ins.)
1	0.00000	5.98844	5.98844
2	0.05932	5.76650	6.21038
3	0.11864	5.68598	6.29089
4	0.17796	5.63254	6.34433
5	0.23728	5.59498	6.38189
6	0.29660	5.56902	6.40786
7	0.35592	5.55114	6.42556
8	0.41524	5.53364	6.44182
9	0.47456	5.51555	6.45743
10	0.53388	5.49688	6.47239
11	0.59320	5.47760	6.48668
12	0.74150	5.42681	6.51919
13	0.88980	5.37219	6.54678
14	1.03810	5.31366	6.56894
15	1.18640	5.25111	6.58508
16	1.33470	5.18440	6.59454
17	1.48300	5.11341	6.59667
18	1.63130	5.03800	6.59063
19	1.77960	4.95798	6.57559
20	1.92790	4.87318	6.55065
21	2.07620	4.78339	6.51481
22	2.22450	4.68839	6.46704
23	2.37280	4.58791	6.40627
24	2.52110	4.48160	6.33143
25	2.66940	4.36922	6.24143
26	2.81770	4.25033	6.13530
27	2.96600	4.12450	6.01210
28	3.11430	3.99119	5.87111
29	3.26260	3.84973	5.71175
30	3.41090	3.69938	5.53366
31	3.55920	3.53930	5.33677
32	3.70750	3.36863	5.12118
33	3.85580	3.18656	4.88723
34	4.00410	2.99229	4.63534
35	4.15240	2.78525	4.36603
36	4.30070	2.56517	4.07986
37	4.44900	2.33245	3.77749
38	4.59730	2.08792	3.45958
39	4.74560	1.83271	3.12684
40	4.89390	1.56797	2.78000
41	5.04220	1.29464	2.41981
42	5.19050	1.01365	2.04697
43	5.33880	0.72592	1.66229
44	5.39812	0.60905	1.50524
45	5.45744	0.49120	1.34645
46	5.51676	0.37243	1.18595
47	5.57608	0.25271	1.02380
48	5.63540	0.13213	0.86004
49	5.69472	0.01077	0.69471
50	5.75404	-0.08624	0.52783
51	5.81336	-0.10952	0.35947
52	5.87268	-0.09755	0.18966
53	5.93200	0.00001	0.00001

TABLE 1b
AIRFOIL GEOMETRY

AIRFOIL: FIRST STATOR (MIDSPAN)
PITCH (ins.): 7.71118

	LEADING EDGE	TRAILING EDGE
RADIUS (ins.)	0.44484	0.10987
METAL ANGLE (degr.)	90.00000	21.42000
WEDGE ANGLE (degr.)	31.80000	6.84000

	X(ins.)	Y_L(ins.)	Y_U(ins.)
1	0.00000	6.80766	6.80756
2	0.05932	6.44830	7.15365
3	0.11864	6.43405	7.17319
4	0.17796	6.41912	7.19210
5	0.23728	6.40354	7.21034
6	0.29660	6.38729	7.22791
7	0.35592	6.37035	7.24476
8	0.41524	6.35273	7.26089
9	0.47456	6.33441	7.27624
10	0.53388	6.31540	7.29080
11	0.59320	6.29568	7.30453
12	0.74150	6.24325	7.33502
13	0.88980	6.18623	7.35957
14	1.03810	6.12447	7.37758
15	1.18640	6.05781	7.38835
16	1.33470	5.98603	7.39114
17	1.48300	5.90896	7.38513
18	1.63130	5.82633	7.36940
19	1.77960	5.73787	7.34300
20	1.92790	5.64326	7.30490
21	2.07620	5.54212	7.25403
22	2.22450	5.43404	7.18927
23	2.37280	5.31852	7.10949
24	2.52110	5.19498	7.01363
25	2.66940	5.06273	6.90066
26	2.81770	4.92096	6.76967
27	2.96600	4.76873	6.61989
28	3.11430	4.60490	6.45078
29	3.26260	4.42825	6.26202
30	3.41090	4.23771	6.05354
31	3.55920	4.03254	5.82550
32	3.70750	3.81279	5.57826
33	3.85580	3.57948	5.31230
34	4.00410	3.33397	5.02816
35	4.15240	3.07798	4.72650
36	4.30070	2.81269	4.40803
37	4.44900	2.53937	4.07350
38	4.59730	2.25873	3.72369
39	4.74560	1.97172	3.35942
40	4.89390	1.67884	2.98147
41	5.04220	1.38062	2.59066
42	5.19050	1.07737	2.18773
43	5.33880	0.76951	1.77352
44	5.39812	0.64517	1.60482
45	5.45744	0.52020	1.43448
46	5.51676	0.39451	1.26252
47	5.57608	0.26816	1.08901
48	5.63540	0.14117	0.91397
49	5.69472	0.01364	0.73745
50	5.75404	-0.11456	0.55950
51	5.81336	-0.24329	0.38014
52	5.87268	-0.37263	0.19943
53	5.93200	0.00000	0.00000

ORIGINAL PAGE IS
OF POOR QUALITY

TABLE 1c
AIRFOIL GEOMETRY

AIRFOIL: FIRST STATOR (TIP)
PITCH (ins.): 8.53371

	LEADING EDGE	TRAILING EDGE
RADIUS (ins.)	0.44487	0.10986
METAL ANGLE (degr.)	90.00401	0.25751
WEDGE ANGLE (degr.)	31.79000	6.79000

	X(ins.)	Y_L(ins.)	Y_U(ins.)
1	0.00000	7.57702	7.57702
2	0.05932	7.35507	7.79897
3	0.11864	7.27456	7.87949
4	0.17796	7.22112	7.93293
5	0.23728	7.18355	7.97049
6	0.29660	7.15759	7.99646
7	0.35592	7.13967	8.01409
8	0.41524	7.12193	8.02987
9	0.47456	7.10338	8.04449
10	0.53388	7.08402	8.05803
11	0.59320	7.06383	8.07044
12	0.74150	7.00967	8.09615
13	0.88480	6.95010	8.11406
14	1.03810	6.88487	8.12374
15	1.18640	6.81377	8.12465
16	1.33470	6.73650	8.11627
17	1.48300	6.65274	8.09803
18	1.63130	6.56207	8.06935
19	1.77960	6.46407	8.02955
20	1.92790	6.35817	7.97793
21	2.07620	6.24376	7.91381
22	2.22450	6.12004	7.83635
23	2.37280	5.98609	7.74477
24	2.52110	5.84072	7.63818
25	2.66940	5.68263	7.51566
26	2.81770	5.51023	7.37624
27	2.96600	5.32200	7.21892
28	3.11430	5.11693	7.04264
29	3.26260	4.89526	6.84631
30	3.41090	4.65850	6.62883
31	3.55920	4.40859	6.38910
32	3.70750	4.14741	6.12648
33	3.85580	3.87650	5.84072
34	4.00410	3.59714	5.53208
35	4.15240	3.31031	5.20125
36	4.30070	3.01688	4.84935
37	4.44900	2.71730	4.47775
38	4.59730	2.41223	4.08802
39	4.74560	2.10214	3.68183
40	4.89390	1.78726	3.26080
41	5.04220	1.46798	2.82654
42	5.19050	1.14458	2.38047
43	5.33880	0.81723	1.92403
44	5.39812	0.68529	1.73880
45	5.45744	0.55272	1.55219
46	5.51676	0.41958	1.36422
47	5.57608	0.28587	1.17502
48	5.63540	0.15177	0.98458
49	5.69472	0.01698	0.79299
50	5.75404	-0.08620	0.60033
51	5.81336	-0.10950	0.40661
52	5.87268	-0.09754	0.21192
53	5.93200	0.00001	0.00001

ORIGINAL PAGE IS
OF POOR QUALITY

TABLE 2a
AIRFOIL GEOMETRY

AIRFOIL: FIRST ROTOR (HUB)
PITCH (ins.): 5.41251

	LEADING EDGE	TRAILING EDGE
RADIUS (ins.)	0.34867	0.19000
METAL ANGLE (degr.)	39.56323	25.97078
WEDGE ANGLE (degr.)	31.19000	5.31000

	X(ins.)	Y_L(ins.)	Y_U(ins.)
1	0.00000	2.86604	2.86604
2	0.06341	2.66555	3.08102
3	0.12682	2.59706	3.21151
4	0.19023	2.55545	3.33187
5	0.25364	2.53057	3.44343
6	0.31705	2.51881	3.54722
7	0.38046	2.51882	3.644[illegible]
8	0.44387	2.53062	3.73464
9	0.50728	2.55553	3.81950
10	0.57069	2.59558	3.89912
11	0.63410	2.63747	3.97388
12	0.79262	2.73147	4.14166
13	0.95115	2.81137	4.28528
14	1.10967	2.87832	4.40773
15	1.26820	2.93322	4.51126
16	1.42672	2.97676	4.59755
17	1.58525	3.00948	4.66791
18	1.74377	3.03180	4.72339
19	1.90230	3.04408	4.764[illegible]
20	2.06082	3.04653	4.79267
21	2.21935	3.03939	4.80757
22	2.37787	3.02278	4.80981
23	2.53640	2.99681	4.79963
24	2.69492	2.96157	4.77715
25	2.85345	2.91708	4.74242
26	3.01197	2.86339	4.69537
27	3.17050	2.80050	4.63584
28	3.32902	2.72831	4.56359
29	3.48755	2.64670	4.47823
30	3.64607	2.55547	4.37924
31	3.80460	2.45445	4.26599
32	3.96312	2.34348	4.13761
33	4.12165	2.22234	3.99304
34	4.28017	2.09081	3.83080
35	4.43870	1.94860	3.64903
36	4.59722	1.79535	3.44572
37	4.75575	1.63070	3.21968
38	4.91427	1.45405	2.9[illegible]
39	5.07280	1.26487	2.69996
40	5.23132	1.06245	2.40938
41	5.38985	0.84595	2.10143
42	5.54837	0.61435	1.778[illegible]
43	5.70690	0.36649	1.44378
44	5.77031	0.26245	1.30685
45	5.83372	0.15541	1.16841
46	5.89713	0.04543	1.02861
47	5.96054	-0.06777	0.88753
48	6.02395	-0.16117	0.74527
49	6.08736	-0.19892	0.60194
50	6.15077	-0.20989	0.45759
51	6.21418	-0.19908	0.31233
52	6.27759	-0.16158	0.16622
53	6.34100	-0.01989	-0.01989

TABLE 2b
AIRFOIL GEOMETRY

AIRFOIL: FIRST ROTOR (MIDSPAN)
PITCH (ins.): 6.05879

	LEADING EDGE	TRAILING EDGE
RADIUS (ins.)	0.34872	0.19000
METAL ANGLE (degr.)	42.18646	25.97093
WEDGE ANGLE (degr.)	31.24000	5.31000

	X(ins.)	Y_L(ins.)	Y_U(ins.)
1	0.00000	3.41970	3.41970
2	.06341	3.21919	3.62774
3	0.12682	3.15069	3.74347
4	0.19023	3.10908	3.84906
5	0.25364	3.08419	3.94593
6	0.31705	3.07242	4.03518
7	0.38046	3.07243	4.11769
8	0.44387	3.08422	4.19414
9	0.50728	3.10912	4.26511
10	0.57069	3.14694	4.33106
11	0.63410	3.18401	4.39236
12	0.79262	3.26583	4.52752
13	0.95115	3.33349	4.63984
14	1.10967	3.38822	4.73220
15	1.26820	3.43094	4.80674
16	1.42672	3.46228	4.86506
17	1.58525	3.48271	4.90837
18	1.74377	3.49248	4.93760
19	1.90230	3.49176	4.95347
20	2.06082	3.48053	4.95652
21	2.21935	3.45868	4.94712
22	2.37787	3.42596	4.92555
23	2.53640	3.38201	4.89193
24	2.69492	3.32633	4.84632
25	2.85345	3.25830	4.78863
26	3.01197	3.17735	4.71868
27	3.17050	3.08283	4.63616
28	3.32902	2.97433	4.54063
29	3.48755	2.85162	4.43151
30	3.64607	2.71488	4.30799
31	3.80460	2.56463	4.16905
32	3.96312	2.40136	4.01334
33	4.12165	2.22577	3.83912
34	4.28017	2.03852	3.64406
35	4.43870	1.84022	3.42595
36	4.59722	1.63139	3.18387
37	4.75575	1.41252	2.91861
38	4.91427	1.18402	2.63221
39	5.07280	0.94623	2.32774
40	5.23132	0.69955	2.00932
41	5.38985	0.44403	1.67680
42	5.54837	0.18008	1.33571
43	5.70690	-0.09214	0.98699
44	5.77031	-0.20337	0.84573
45	5.83372	-0.31578	0.70359
46	5.89713	-0.42949	0.56065
47	5.96054	-0.54448	0.41698
48	6.02395	-0.63800	0.27261
49	6.08736	-0.67575	0.12765
50	6.15077	-0.68673	-0.01791
51	6.21418	-0.67591	-0.16397
52	6.27759	-0.63841	-0.31052
53	6.34100	-0.49672	-0.49672

TABLE 2c
AIRFOIL GEOMETRY

AIRFOIL: FIRST ROTOR (TIP)
PITCH (ins.): 6.70506

	LEADING EDGE	TRAILING EDGE
RADIUS (ins.)	0.34881	0.19000
METAL ANGLE (degr.)	46.66805	25.96767
WEDGE ANGLE (degr.)	31.26000	5.31000

	X(ins.)	Y_L(ins.)	Y_U(ins.)
1	0.00000	3.97348	3.97348
2	0.06341	3.77294	4.17548
3	0.12682	3.70443	4.27381
4	0.19023	3.66280	4.36353
5	0.25364	3.63790	4.44573
6	0.31705	3.62612	4.52127
7	0.38046	3.62611	4.59084
8	0.44387	3.63787	4.65499
9	0.50728	3.66275	4.71419
10	0.57069	3.69488	4.76883
11	0.63410	3.72462	4.81924
12	0.79262	3.78887	4.92848
13	0.95115	3.83974	5.01637
14	1.10967	3.87814	5.08539
15	1.26820	3.90472	5.13737
16	1.42672	3.91989	5.17369
17	1.58525	3.92388	5.19537
18	1.74377	3.91674	5.20321
19	1.90230	3.89838	5.19778
20	2.06082	3.86851	5.17950
21	2.21935	3.82665	5.14862
22	2.37787	3.77210	5.10529
23	2.53640	3.70385	5.04954
24	2.69492	3.62049	4.98122
25	2.85345	3.52015	4.90012
26	3.01197	3.40033	4.80585
27	3.17050	3.25903	4.69788
28	3.32902	3.09581	4.57543
29	3.48755	2.91352	4.43757
30	3.64607	2.71577	4.28296
31	3.80460	2.50562	4.10990
32	3.96312	2.28505	3.91608
33	4.12165	2.05587	3.69853
34	4.28017	1.81890	3.45544
35	4.43870	1.57520	3.18730
36	4.59722	1.32521	2.89675
37	4.75575	1.06966	2.58780
38	4.91427	0.80884	2.26420
39	5.07280	0.54319	1.92951
40	5.23132	0.27306	1.58629
41	5.38985	-0.00136	1.23664
42	5.54837	-0.27975	0.88207
43	5.70690	-0.56201	0.52368
44	5.77031	-0.67597	0.37945
45	5.83372	-0.79046	0.23478
46	5.89713	-0.90562	0.08974
47	5.96054	-1.02119	-0.05569
48	6.02395	-1.11481	-0.20147
49	6.08736	-1.15257	-0.34753
50	6.15077	-1.16355	-0.49387
51	6.21418	-1.15274	-0.64045
52	6.27759	-1.11524	-0.78726
53	6.34100	-0.97355	-0.97355

ORIGINAL PAGE IS
OF POOR QUALITY

TABLE 3a

AIRFOIL GEOMETRY

AIRFOIL: SECOND STATOR (HUB)
PITCH (ins.): 5.41251

	LEADING EDGE	TRAILING EDGE
RADIUS (ins.)	0.34999	0.19000
METAL ANGLE (degr.)	41.01068	4.98619
WEDGE ANGLE (degr.)	29.91000	8.91000

	X(ins.)	Y_L(ins.)	Y_U(ins.)
1	0.00000	3.68263	3.68263
2	0.06452	3.48015	3.89472
3	0.12904	3.41120	4.01869
4	0.19356	3.36955	4.13494
5	0.25808	3.34493	4.24410
6	0.32260	3.33372	4.34672
7	0.38712	3.33462	4.44321
8	0.45164	3.34773	4.53406
9	0.51616	3.37461	4.61958
10	0.58068	3.41583	4.70006
11	0.64520	3.45739	4.77576
12	0.80650	3.55269	4.94580
13	0.96780	3.63560	5.09069
14	1.12910	3.70599	5.21287
15	1.29040	3.76376	5.31424
16	1.45170	3.80880	5.39634
17	1.61300	3.84106	5.46037
18	1.77430	3.86048	5.50735
19	1.93560	3.86704	5.53806
20	2.09690	3.86072	5.55317
21	2.25820	3.84153	5.55319
22	2.41950	3.80950	5.53852
23	2.58080	3.76468	5.50948
24	2.74210	3.70714	5.46629
25	2.90340	3.63698	5.40908
26	3.06470	3.55430	5.33790
27	3.22600	3.45921	5.25273
28	3.38730	3.35188	5.15348
29	3.54860	3.23245	5.03995
30	3.70990	3.10111	4.91189
31	3.87120	2.95802	4.76892
32	4.03250	2.80339	4.61058
33	4.19380	2.63745	4.43628
34	4.35510	2.46037	4.24527
35	4.51640	2.27244	4.03662
36	4.67770	2.07384	3.80928
37	4.83900	1.86483	3.56222
38	5.00030	1.64569	3.29479
39	5.16160	1.41663	3.00662
40	5.32290	1.17789	2.69784
41	5.48420	0.92975	2.36890
42	5.64550	0.67246	2.02068
43	5.80680	0.40629	1.65431
44	5.87132	0.29738	1.50296
45	5.93584	0.18710	1.34900
46	6.00036	0.07548	1.19252
47	6.06488	-0.03748	1.03361
48	6.12940	-0.13608	0.87238
49	6.19392	-0.17738	0.70890
50	6.25844	-0.18997	0.54327
51	6.32296	-0.17996	0.37560
52	6.38748	-0.14267	0.20595
53	6.15200	0.00000	0.00000

TABLE 3b
AIRFOIL GEOMETRY

AIRFOIL: SECOND STATOR (MIDSPAN)
PITCH (ins.): 6.05879

	LEADING EDGE	TRAILING EDGE
RADIUS (ins.)	0.34999	0.19000
METAL ANGLE (degr.)	45.66800	25.00000
WEDGE ANGLE (degr.)	27.50000	6.50000

	X(ins.)	Y_L(ins.)	Y_U(ins.)
1	0.00000	4.10291	4.10291
2	0.06452	3.47786	4.30650
3	0.12904	3.52885	4.40610
4	0.19356	3.57793	4.50013
5	0.25808	3.62510	4.58895
6	0.32260	3.67035	4.67285
7	0.38712	3.71368	4.75210
8	0.45164	3.75508	4.82695
9	0.51616	3.79454	4.89760
10	0.58068	3.83206	4.96425
11	0.64520	3.86762	5.02707
12	0.80650	3.94796	5.16834
13	0.96780	4.01599	5.28865
14	1.12910	4.07162	5.38963
15	1.29040	4.11482	5.47259
16	1.45170	4.14552	5.53859
17	1.61300	4.16371	5.58849
18	1.77430	4.16934	5.62296
19	1.93560	4.16244	5.64258
20	2.09690	4.14298	5.64778
21	2.25820	4.11101	5.63888
22	2.41950	4.06655	5.61615
23	2.58080	4.00965	5.57973
24	2.74210	3.94037	5.52972
25	2.90340	3.85879	5.46611
26	3.06470	3.76498	5.38882
27	3.22600	3.65906	5.29771
28	3.38730	3.54111	5.19255
29	3.54860	3.41127	5.07300
30	3.70990	3.26967	4.93863
31	3.87120	3.11644	4.78891
32	4.03250	2.95172	4.62316
33	4.19380	2.77568	4.44053
34	4.35510	2.58849	4.24001
35	4.51640	2.39030	4.02052
36	4.67770	2.18130	3.78134
37	4.83900	1.96166	3.52218
38	5.00030	1.73160	3.24330
39	5.16160	1.49128	2.94535
40	5.32290	1.24090	2.62941
41	5.48420	0.98064	2.29682
42	5.64550	0.71074	1.94914
43	5.80680	0.43141	1.58790
44	5.87132	0.31707	1.43996
45	5.93584	0.20126	1.29018
46	6.00036	0.08400	1.13867
47	6.06488	-0.03471	0.98552
48	6.12940	-0.15484	0.83080
49	6.19392	-0.27639	0.67459
50	6.25844	-0.39934	0.51699
51	6.32296	-0.52368	0.35805
52	6.38748	-0.64939	0.19786
53	6.45200	0.00000	0.00000

TABLE 3c

AIRFOIL GEOMETRY

AIRFOIL: SECOND STATOR (TIP)
PITCH (ins.): 6.70506

	LEADING EDGE	TRAILING EDGE
RADIUS (ins.)	0.35006	0.19000
METAL ANGLE (degr.)	50.49115	24.98778
WEDGE ANGLE (degr.)	25.12000	4.09000

	X(ins.)	Y_L(ins.)	Y_U(ins.)
1	0.00000	4.53429	4.53429
2	0.06452	4.33178	4.73679
3	0.12904	4.26282	4.81836
4	0.19356	4.22116	4.89463
5	0.25808	4.19652.	4.96641
6	0.32260	4.18530	5.03396
7	0.38712	4.18619	5.09751
8	0.45164	4.19929	5.15728
9	0.51616	4.22602	5.21343
10	0.58068	4.25762	5.26613
11	0.64520	4.28729	5.31552
12	0.80650	4.35297	5.42538
13	0.96780	4.40647	5.51708
14	1.12910	4.44777	5.59199
15	1.29040	4.47683	5.65117
16	1.45170	4.49364	5.69551
17	1.61300	4.49819	5.72567
18	1.77430	4.49045	5.74219
19	1.93560	4.47047	5.74550
20	2.09690	4.43822	5.73590
21	2.25820	4.39375	5.71360
22	2.41950	4.33706	5.67874
23	2.58080	4.26823	5.63135
24	2.74210	4.18728	5.57140
25	2.90340	4.09426	5.49876
26	3.06470	3.98924	5.41323
27	3.22600	3.87229	5.31449
28	3.38730	3.74348	5.20215
29	3.54860	3.60289	5.07566
30	3.70990	3.45062	4.93435
31	3.87120	3.28675	4.77738
32	4.03250	3.11139	4.60366
33	4.19380	2.92465	4.41196
34	4.35510	2.72666	4.20118
35	4.51640	2.51749	3.97077
36	4.67770	2.29731	3.72077
37	4.83900	2.06620	3.45177
38	5.00030	1.82436	3.16495
39	5.16160	1.57187	2.86176
40	5.32290	1.30889	2.54389
41	5.48420	1.03553	2.21304
42	5.64550	0.75199	1.87091
43	5.80680	0.45841	1.51902
44	5.87132	0.33818	1.37585
45	5.93584	0.21639	1.23140
46	6.00036	0.09302	1.08577
47	6.06488	-0.03190	0.93902
48	6.12940	-0.13607	0.79122
49	6.19392	-0.17738	0.64244
50	6.25844	-0.18996	0.49272
51	6.32296	-0.17995	0.34214
52	6.38748	-0.14267	0.19073
53	6.45200	0.00000	0.00000

TABLE 4

FLOWPATH STATIC PRESSURES AT 1ST STATOR EXIT (STA. 2)

$C_{Ps} = (P_{To} - P) / Q_{Um}$

RUN/PT	ϕ	GRID IN/OUT	X/Bx	HUB	MEAN*	OUTER CASING
13/1	0.68	OUT	0.15	4.306	3.588	3.074
31/2		IN	0.15	4.927	4.225	3.722
79/1		OUT	0.50	4.106	3.395	2.887
83/3		IN	0.50	5.040	4.270	3.720
12/1	0.78	OUT	0.15	5.616	4.680	4.010
30/3		IN	0.15	6.518	5.599	4.942
80/4		OUT	0.50	5.414	4.477	3.806
82/2		IN	0.50	6.589	5.592	4.879
14/1	0.96	OUT	0.15	8.695	7.261	6.235
32/2		IN	0.15	9.826	8.468	7.497
81/2		OUT	0.50	8.129	6.736	5.739
81/7		IN	0.50	9.892	8.422	7.370

* Calculated from a free vortex distribution between the measured hub and outer casing flowpath static pressures (pitch and annulus averages).

TABLE 5

FLOWPATH STATIC PRESSURES AT ROTOR EXIT (STA. 3)

RUN/PT	ϕ	GRID IN/OUT	X/Bx	$C_{Ps} = (P_{To} - P) / Q_{Um}$ HUB	MEAN*	OUTER CASING
13/1	0.68	OUT	0.15	5.271	5.308	5.334
31/2		IN	0.15	6.024	5.984	5.956
79/1		OUT	0.50	5.042	5.061	5.075
83/3		IN	0.50	5.951	5.971	5.982
12/1	0.78	OUT	0.15	6.729	6.709	6.694
30/3		IN	0.15	7.832	7.709	7.621
80/4		OUT	0.50	6.535	6.509	6.490
82/2		IN	0.50	7.690	7.685	7.682
14/1	0.96	OUT	0.15	9.751	9.791	9.819
32/2		IN	0.15	11.491	11.245	11.069
81/2		OUT	0.50	9.514	9.352	9.236
81/7		IN	0.50	11.286	11.108	10.930

* Calculated from a free vortex distribution between the measured hub and outer casing flowpath static pressures (pitch and annulus averages).

TABLE 6

FLOWPATH STATIC PRESSURES AT 2ND STATOR EXIT (STA. 4)

RUN/PT	ϕ	GRID IN/OUT	X/Bx	$C_{Ps} = (P_{To} - P) / Q_{Um}$ HUB	MEAN*	OUTER CASING
13/1	0.68	OUT	0.15	5.405	5.377	5.357
31/2		IN	0.15	6.041	5.991	5.955
86/4		OUT	0.50	7.606	7.009	6.582
90/2		IN	0.50	8.717	8.079	7.623
12/1	0.78	OUT	0.15	6.871	6.777	6.710
30/3		IN	0.15	7.807	7.724	7.664
87/1		OUT	0.50	9.690	8.924	8.377
89/2		IN	0.50	11.133	10.311	9.722
14/1	0.96	OUT	0.15	10.256	10.017	9.846
32/2		IN	0.15	11.458	11.227	11.061
88/1		OUT	0.50	14.157	12.942	12.074
88/3		IN	0.50	16.207	14.914	14.028

* Calculated from a free vortex distribution between the measured hub and outer casing flowpath static pressures (pitch and annulus averages).

ORIGINAL PAGE IS
OF POOR QUALITY

TABLE 7a

TURBINE STAGE MIDSPAN PRESSURE DISTRIBUTIONS

AXIAL GAP 15%
GRID OUT
$CP = (PTO - P)/1/2\,\rho U_m^2$

$\phi = 0.68$		$\phi = 0.78$		$\phi = 0.96$	
STATOR-1		**STATOR-1**		**STATOR-1**	
CFT1	0.000	CPT1	0.000	CPT1	0.000
CFS2	3.588	CPS2	4.680	CPS2	7.261
SUCTION SURFACE		SUCTION SURFACE		SUCTION SURFACE	
DIST	CPS	DIST	CPS	DIST	CPS
0.012	1.665	0.012	2.165	0.012	3.368
0.070	2.215	0.070	2.895	0.070	4.465
0.251	3.731	0.251	4.857	0.251	7.507
0.426	5.275	0.426	6.841	0.426	10.588
0.554	5.015	0.554	6.519	0.554	10.067
0.651	4.659	0.651	6.061	0.651	9.322
0.734	4.336	0.734	5.589	0.734	8.680
0.809	4.089	0.809	5.303	0.809	8.164
0.879	3.961	0.879	5.116	0.879	7.869
0.945	3.349	0.945	4.318	0.945	6.666
1.000	3.578	1.000	4.863	1.000	7.429
PRESSURE SURFACE		PRESSURE SURFACE		PRESSURE SURFACE	
DIST	CPS	DIST	CPS	DIST	CPS
0.005	0.059	0.005	0.103	0.005	0.129
0.027	0.108	0.027	0.136	0.027	0.207
0.066	0.219	0.066	0.285	0.066	0.437
0.251	0.233	0.251	0.292	0.251	0.477
0.423	0.294	0.423	0.369	0.423	0.598
0.564	0.436	0.564	0.568	0.564	0.875
0.667	0.792	0.667	1.046	0.667	1.563
0.789	1.382	0.789	1.795	0.789	2.771
0.886	2.228	0.886	2.917	0.886	4.456
0.967	3.643	0.967	4.738	0.967	7.284
BASE PRESSURE		BASE PRESSURE		BASE PRESSURE	
DIST	CPS	DIST	CPS	DIST	CPS
0.990	3.755	0.990	4.652	.990	7.217
ROTOR-1		**ROTOR-1**		**ROTOR-1**	
CFTR2	2.567	CFTR2	3.143	CFTR2	4.192
CFS3	5.307	CPS3	6.709	CPS3	9.791
SUCTION SURFACE		SUCTION SURFACE		SUCTION SURFACE	
DIST	CPS	DIST	CPS	DIST	CPS
0.005	4.532	0.005	7.164	0.005	14.024
0.011	4.893	0.011	7.229	0.011	13.014
0.117	5.770	0.117	7.727	0.117	12.832
0.269	6.311	0.269	8.294	0.269	12.823
0.437	6.370	0.437	8.116	0.437	12.165
0.578	6.450	0.578	8.277	0.578	12.170
0.695	6.365	0.695	8.022	0.695	11.911
0.785	5.912	0.785	7.450	0.785	11.137
0.863	5.732	0.863	7.322	0.863	10.917
0.937	5.630	0.937	7.212	0.937	10.631
1.003	5.523	1.003	7.069	1.003	10.474
PRESSURE SURFACE		PRESSURE SURFACE		PRESSURE SURFACE	
DIST	CPS	DIST	CPS	DIST	CPS
0.012	2.658	0.012	3.482	0.012	5.946
0.049	2.791	0.049	3.243	0.049	4.215
0.089	2.975	0.089	3.441	0.089	4.593
0.248	2.757	0.246	3.326	0.248	4.496
0.426	2.723	0.426	3.331	0.426	4.465
0.570	2.863	0.570	3.476	0.570	4.747
0.678	3.138	0.678	3.856	0.678	5.317
0.775	3.568	0.775	4.426	0.775	6.167
0.868	4.241	0.868	5.250	0.868	7.559
0.952	5.515	0.952	6.881	0.952	10.234
BASE PRESSURE		BASE PRESSURE		BASE PRESSURE	
DIST	CPS	DIST	CPS	DIST	CPS
0.985	5.570	0.985	7.128	0.985	10.502

TABLE 7b

TURBINE STAGE MIDSPAN PRESSURE DISTRIBUTIONS

AXIAL GAP: 15%
GRID IN
$CP = (PTO - P)/1/2\, \rho\, U_m^2$

	$\phi = 0.68$		$\phi = 0.78$		$\phi = 0.96$	
STATOR-1						
	CPT1	0.708	CPT1	0.934	CPT1	1.403
	CPS2	4.225	CPS2	5.599	CPS2	8.468
SUCTION SURFACE	DIST	CPS	DIST	CPS	DIST	CPS
	0.012	2.386	0.012	3.190	0.012	4.749
	0.070	2.891	0.070	3.823	0.070	5.791
	0.251	4.337	0.251	5.723	0.251	6.661
	0.426	5.778	0.426	7.678	0.426	11.607
	0.554	5.574	0.554	7.426	0.554	11.148
	0.651	5.257	0.651	6.937	0.651	10.423
	0.734	4.980	0.734	6.596	0.734	9.854
	0.809	4.711	0.809	6.237	0.809	9.415
	0.879	4.595	0.879	6.056	0.879	9.123
	0.945	3.997	0.945	5.276	0.945	7.930
	1.000	4.407	1.000	5.882	1.000	8.744
PRESSURE SURFACE	DIST	CPS	DIST	CPS	DIST	CPS
	0.005	0.792	0.005	1.035	0.005	1.575
	0.027	0.801	0.027	1.066	0.027	1.629
	0.066	0.933	0.066	1.224	0.066	1.862
	0.251	0.946	0.251	1.251	0.251	1.875
	0.423	1.005	0.423	1.334	0.423	2.000
	0.564	1.143	0.564	1.509	0.564	2.274
	0.687	1.479	0.687	1.972	0.687	2.969
	0.789	2.069	0.789	2.724	0.789	4.113
	0.886	2.892	0.886	3.826	0.886	5.817
	0.967	[illegible].352	0.967	5.735	0.967	8.712
BASE PRESSURE	DIST	CPS	DIST	CPS	DIST	CPS
	0.990	4.228	0.990	5.638	0.990	8.489
ROTOR-1						
	CPTR2	3.447	CPTR2	4.279	CPTR2	5.778
	CPS3	5.984	CPS3	7.709	CPS3	11.245
SUCTION SURFACE	DIST	CPS	DIST	CPS	DIST	CPS
	0.005	5.342	0.005	7.839	0.005	14.921
	0.011	5.529	0.011	7.986	0.011	13.463
	0.117	6.436	0.117	8.795	0.117	14.008
	0.269	7.122	0.269	9.362	0.269	14.009
	0.437	7.152	0.437	9.123	0.437	13.388
	0.578	7.206	0.578	9.289	0.578	13.437
	0.695	7.145	0.695	9.099	0.695	13.128
	0.785	6.678	0.785	8.528	0.785	17.460
	0.863	6.500	0.863	8.469	0.863	12.241
	0.937	6.459	0.937	8.188	0.937	12.063
	1.003	6.376	1.003	8.159	1.003	11.836
PRESSURE SURFACE	DIST	CPS	DIST	CPS	DIST	CPS
	0.012	3.495	0.012	4.651	0.012	7.499
	0.049	3.722	0.049	4.402	0.049	5.779
	0.089	3.859	0.089	4.663	0.089	6.123
	0.248	3.645	0.248	4.463	0.248	6.031
	0.426	3.593	0.426	4.461	0.426	6.056
	0.570	3.786	0.570	4.641	0.570	6.327
	0.678	4.039	0.678	5.069	0.678	6.875
	0.775	4.441	0.775	5.579	0.775	7.709
	0.868	5.068	0.868	6.452	0.868	9.074
	0.952	6.335	0.952	8.145	0.952	11.683
BASE PRESSURE	DIST	CPS	DIST	CPS	DIST	CPS
	0.985	6.398	0.985	8.217	0.985	12.005

TABLE 8a

TURBINE STAGE MIDSPAN PRESSURE DISTRIBUTIONS

AXIAL GAP: 50%
GRID OUT
$CP = (PTO - P)/1/2\ \rho U_m^2$

STATOR-1

	$\phi = 0.68$	$\phi = 0.78$	$\phi = 0.96$
CPT1	0.000	0.000	0.000
CPS2	3.395	4.477	6.736

SUCTION SURFACE

DIST	CPS ($\phi = 0.68$)	CPS ($\phi = 0.78$)	CPS ($\phi = 0.96$)
0.012	1.617	2.117	3.215
0.070	2.156	2.859	4.328
0.251	3.557	4.705	7.115
0.426	5.043	6.731	10.112
0.554	4.848	6.423	9.726
0.651	4.507	5.953	8.960
0.734	4.170	5.532	8.276
0.809	3.943	5.216	7.856
0.879	3.816	5.031	7.604
0.945	3.639	4.808	7.232
1.000	3.624	4.705	7.173

PRESSURE SURFACE

DIST	CPS ($\phi = 0.68$)	CPS ($\phi = 0.78$)	CPS ($\phi = 0.96$)
0.005	0.086	0.111	0.180
0.027	0.084	0.108	0.159
0.066	0.192	0.254	0.381
0.251	0.222	0.292	0.435
0.423	0.290	0.374	0.565
0.564	0.429	0.563	0.843
0.687	0.777	1.019	1.536
0.789	1.347	1.779	2.678
0.886	2.166	2.864	4.298
0.967	3.492	4.650	6.971

BASE PRESSURE

DIST	CPS ($\phi = 0.68$)	CPS ($\phi = 0.78$)	CPS ($\phi = 0.96$)
0.990	3.456	4.535	6.852

ROTOR-1

	$\phi = 0.68$	$\phi = 0.78$	$\phi = 0.96$
CPTR2	2.585	3.184	4.100
CPS3	5.061	6.509	9.352

SUCTION SURFACE

DIST	CPS ($\phi = 0.68$)	CPS ($\phi = 0.78$)	CPS ($\phi = 0.96$)
0.005	4.052	6.477	12.857
0.011	4.267	6.507	11.828
0.117	5.252	7.211	11.744
0.269	5.906	7.903	11.829
0.437	5.946	7.722	11.252
0.578	6.031	7.754	11.146
0.695	5.902	7.591	10.880
0.785	5.497	7.017	10.278
0.863	5.319	6.925	10.001
0.937	5.321	6.889	9.882
1.003	5.214	6.746	9.722

PRESSURE SURFACE

DIST	CPS ($\phi = 0.68$)	CPS ($\phi = 0.78$)	CPS ($\phi = 0.96$)
0.012	2.648	3.579	5.922
0.049	2.768	3.236	4.141
0.089	2.890	3.411	4.342
0.248	2.707	3.267	4.280
0.426	2.724	3.360	4.463
0.570	2.841	3.501	4.662
0.678	3.003	3.681	5.062
0.775	3.358	4.216	5.927
0.868	3.724	4.830	6.900
0.952	5.063	6.569	9.436

BASE PRESSURE

DIST	CPS ($\phi = 0.68$)	CPS ($\phi = 0.78$)	CPS ($\phi = 0.96$)
0.985	5.079	6.636	9.591

ORIGINAL PAGE IS
OF POOR QUALITY

TABLE 8b

TURBINE STAGE MIDSPAN PRESSURE DISTRIBUTIONS

AXIAL GAP: 50%
GRID IN
$CP = (PTO - P)/1/2\, \rho\, U_m^2$

$\phi = 0.68$

STATOR-1

CPT1	0.717
CPS2	4.270

SUCTION SURFACE

DIST	CPS
0.012	2.346
0.070	2.940
0.251	4.379
0.426	5.977
0.554	5.745
0.651	5.345
0.734	5.119
0.809	4.878
0.879	4.713
0.945	4.549
1.000	4.554

PRESSURE SURFACE

DIST	CPS
0.005	0.797
0.027	0.799
0.066	0.911
0.251	0.946
0.423	1.005
0.564	1.160
0.687	1.520
0.789	2.105
0.886	2.990
0.967	4.438

BASE PRESSURE

DIST	CPS
0.990	4.338

ROTOR-1

CPTR2	3.386
CPS3	5.964

SUCTION SURFACE

DIST	CPS
0.005	5.203
0.011	5.272
0.117	6.240
0.269	6.825
0.437	6.837
0.578	6.981
0.695	6.835
0.785	6.356
0.863	6.225
0.937	6.174
1.003	6.178

PRESSURE SURFACE

DIST	CPS
0.012	3.401
0.049	3.487
0.089	3.645
0.248	3.474
0.426	3.531
0.678	3.793
0.775	4.158
0.868	4.662
0.952	6.071

BASE PRESSURE

DIST	CPS
0.985	6.017

$\phi = 0.78$

STATOR-1

CPT1	0.934
CPS2	5.592

SUCTION SURFACE

DIST	CPS
0.012	3.105
0.070	3.890
0.251	5.819
0.426	7.921
0.554	7.569
0.651	7.054
0.734	6.711
0.809	6.408
0.879	6.230
0.945	6.002
1.000	6.013

PRESSURE SURFACE

DIST	CPS
0.005	1.069
0.027	1.060
0.066	1.214
0.251	1.240
0.423	1.329
0.564	1.532
0.687	2.011
0.789	2.801
0.886	3.893
0.967	5.875

BASE PRESSURE

DIST	CPS
0.990	5.721

ROTOR-1

CPTR2	4.128
CPS3	7.685

SUCTION SURFACE

DIST	CPS
0.005	7.971
0.011	7.684
0.117	8.700
0.269	9.157
0.437	8.988
0.578	9.009
0.695	8.715
0.785	8.311
0.863	7.918
0.937	8.098
1.003	7.831

PRESSURE SURFACE

DIST	CPS
0.012	4.654
0.049	4.194
0.089	4.392
0.248	4.311
0.426	4.315
0.570	4.516
0.678	4.718
0.775	5.282
0.868	5.987
0.952	7.922

BASE PRESSURE

DIST	CPS
0.985	7.894

$\phi = 0.96$

STATOR-1

CPT1	1.418
CPS2	8.422

SUCTION SURFACE

DIST	CPS
0.012	4.755
0.070	5.892
0.251	8.695
0.426	11.852
0.554	11.314
0.651	10.678
0.734	10.134
0.809	9.679
0.879	9.353
0.945	9.080
1.000	9.051

PRESSURE SURFACE

DIST	CPS
0.005	1.587
0.027	1.593
0.066	1.813
0.251	1.886
0.423	1.991
0.564	2.310
0.687	2.997
0.789	4.203
0.886	5.938
0.967	8.873

BASE PRESSURE

DIST	CPS
0.990	8.591

ROTOR-1

CPTR2	5.710
CPS3	11.194

SUCTION SURFACE

DIST	CPS
0.005	15.107
0.011	13.042
0.117	13.722
0.269	13.926
0.437	13.121
0.578	12.949
0.695	12.685
0.785	12.066
0.863	11.836
0.937	11.670
1.003	11.603

PRESSURE SURFACE

DIST	CPS
0.012	7.767
0.049	5.712
0.089	5.946
0.248	5.858
0.426	6.002
0.570	6.265
0.678	6.620
0.775	7.532
0.868	8.635
0.952	11.388

BASE PRESSURE

DIST	CPS
0.985	11.517

TABLE 9a

STATOR-2 MIDSPAN PRESSURE DISTRIBUTIONS

AXIAL GAP: 50%
GRID OUT
$CP = (PTO - P)/1/2\, \rho U_m^2$

$\phi = 0.68$		$\phi = 0.78$		$\phi = 0.96$	
STATOR-2		STATOR-2		STATOR-2	
CPT3	4.551	CPT3	5.570	CPT3	7.700
CPS4	7.009	CPS4	8.924	CPS4	12.942
SUCTION	SURFACE	SUCTION	SURFACE	SUCTION	SURFACE
DIST	CPS	DIST	CPS	DIST	CPS
0.000	5.392	0.000	7.479	0.000	12.329
0.022	5.096	0.022	6.796	0.022	11.687
0.135	6.106	0.135	8.110	0.135	12.670
0.291	7.428	0.291	9.658	0.291	14.485
0.459	8.004	0.459	10.176	0.459	14.932
0.598	8.160	0.598	10.385	0.598	15.217
0.704	8.144	0.704	10.428	0.704	15.258
0.791	7.894	0.791	10.115	0.791	14.705
0.868	7.670	0.868	9.807	0.868	14.303
0.933	7.629	0.933	9.706	0.933	14.091
0.995	7.587	0.995	9.681	0.995	14.065
PRESSURE	SURFACE	PRESSURE	SURFACE	PRESSURE	SURFACE
DIST	CPS	DIST	CPS	DIST	CPS
0.023	4.602	0.023	6.019	0.023	9.708
0.107	4.958	0.107	6.146	0.107	8.424
0.265	4.747	0.265	5.870	0.265	8.117
0.425	4.758	0.425	5.832	0.425	8.078
0.564	4.861	0.564	5.983	0.564	8.423
0.679	5.117	0.679	6.341	0.679	9.028
0.777	5.551	0.777	6.901	0.777	9.989
0.865	6.132	0.865	7.706	0.865	11.253
0.946	7.192	0.946	9.128	0.946	13.418
BASE	PRESSURE	BASE	PRESSURE	BASE	PRESSURE
DIST	CPS	DIST	CPS	DIST	CPS
0.986	7.271	0.986	9.292	0.986	13.535

ORIGINAL PAGE IS
OF POOR QUALITY

TABLE 9b

STATOR-2 MIDSPAN PRESSURE DISTRIBUTIONS

AXIAL GAP: 50%
GRID IN
$CP = (PTO - P)/1/2\ \rho U_m^2$

$\phi = 0.68$		$\phi = 0.78$		$\phi = 0.96$	
STATOR-2		STATOR-2		STATOR-2	
CPT3	5.483	CPT3	6.801	CPT3	9.560
CPS4	8.079	CPS4	10.311	CPS4	14.914
SUCTION SURFACE		SUCTION SURFACE		SUCTION SURFACE	
DIST	CPS	DIST	CPS	DIST	CPS
0.000	6.380	0.000	8.669	0.000	14.162
0.022	6.099	0.022	8.237	0.022	13.408
0.135	7.167	0.135	9.477	0.135	14.706
0.291	8.512	0.291	11.113	0.291	16.578
0.459	9.107	0.459	11.689	0.459	17.206
0.598	9.273	0.598	11.944	0.598	17.370
0.704	9.297	0.704	11.920	0.704	17.341
0.791	9.012	0.791	11.578	0.791	16.716
0.868	8.785	0.868	11.265	0.868	16.286
0.933	8.695	0.933	11.170	0.933	15.980
0.995	8.691	0.995	11.061	0.995	16.003
PRESSURE SURFACE		PRESSURE SURFACE		PRESSURE SURFACE	
DIST	CPS	DIST	CPS	DIST	CPS
0.023	5.601	0.023	7.288	0.023	11.839
0.107	5.901	0.107	7.344	0.107	10.193
0.265	5.672	0.265	7.069	0.265	9.899
0.425	5.700	0.425	7.074	0.425	9.945
0.564	5.810	0.564	7.280	0.564	10.258
0.679	6.078	0.679	7.633	0.679	10.888
0.777	6.500	0.777	8.219	0.777	11.839
0.865	7.170	0.865	9.076	0.865	13.267
0.946	8.301	0.946	10.551	0.946	15.433
BASE PRESSURE		BASE PRESSURE		BASE PRESSURE	
DIST	CPS	DIST	CPS	DIST	CPS
0.986	8.328	0.986	10.679	0.986	15.400

TABLE 10a

DEFINITION OF AVERAGE TOTAL, PERIODIC, AND RANDOM UNSTEADINESS

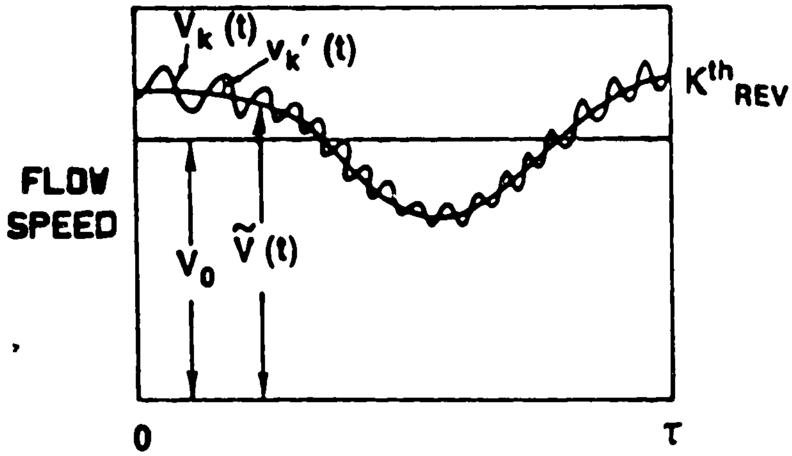

$$\bar{U}_T = \frac{1}{N_{REV}} \sum_{K=1}^{N_{REV}} \frac{1}{\tau} \int_0^{\tau} (V_k(t) - V_0)^2 \, dt \Big/ V_{REF}^2$$

$$\bar{U}_T = \frac{1}{\tau} \int_0^{\tau} (\tilde{V}(t) - V_0)^2 \, dt \Big/ V_{REF}^2 + \frac{1}{N_{REV}} \sum_{K=1}^{N_{REV}} \frac{1}{\tau} \int_0^{\tau} v_k'^2 \, dt \Big/ V_{REF}^2$$

$$\bar{U}_T = \bar{U}_P + \bar{U}_R$$

TABLE 10b

PITCH AVERAGED UNSTEADINESS RESULTS AT Cx/Um = 0.68

	TOTAL $\sqrt{\overline{U}_T}$	RANDOM $\sqrt{\overline{U}_R}$	PERIODIC $\sqrt{\overline{U}_P}$
1st STATOR EXIT			
• GRID OUT	0.024	0.018	0.014
• GRID IN	0.034	0.030	0.014
ROTOR EXIT			
• GRID OUT	0.155	0.115	0.101
• GRID IN	0.154	0.132	0.078
2nd STATOR EXIT			
• GRID OUT	0.057	0.054	0.017
• GRID IN	0.058	0.056	0.016

TABLE 10c

PITCH AVERAGED UNSTEADINESS RESULTS AT Cx/Um = 0.78

	TOTAL $\sqrt{\overline{U}_T}$	RANDOM $\sqrt{\overline{U}_R}$	PERIODIC $\sqrt{\overline{U}_P}$
1st STATOR EXIT			
• GRID OUT	0.030	0.022	0.019
• GRID IN	0.036	0.031	0.017
ROTOR EXIT			
• GRID OUT	0.155	0.120	0.096
• GRID IN	0.155	0.137	0.069
2nd STATOR EXIT			
• GRID OUT	0.061	0.058	0.020
• GRID IN	0.061	0.058	0.017

TABLE 10d

PITCH AVERAGED UNSTEADINESS RESULTS AT Cx/Um = 0.96

	TOTAL $\sqrt{\overline{U}_T}$	RANDOM $\sqrt{\overline{U}_R}$	PERIODIC $\sqrt{\overline{U}_P}$
1st STATOR EXIT			
• GRID OUT	0.028	0.018	0.020
• GRID IN	0.037	0.030	0.020
ROTOR EXIT			
• GRID OUT	0.159	0.123	0.098
• GRID IN	0.169	0.146	0.084
2nd STATOR EXIT			
• GRID OUT	0.071	0.066	0.026
• GRID IN	0.073	0.068	0.025

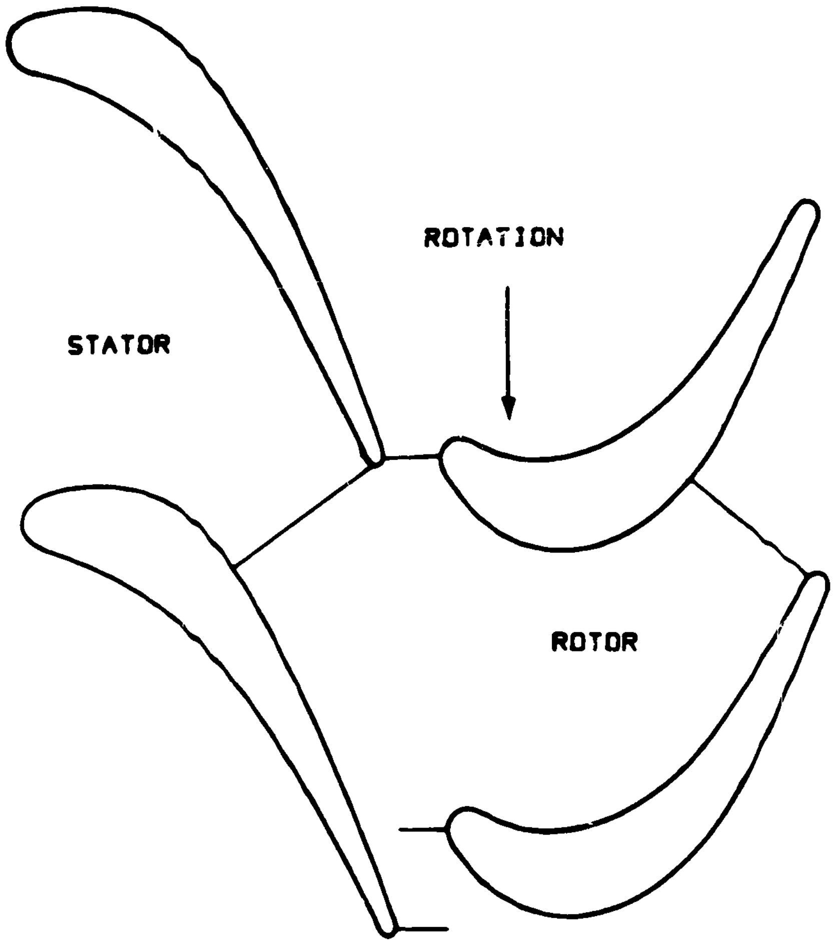

FIG. 1 TURBINE STAGE AT 15% AXIAL GAP

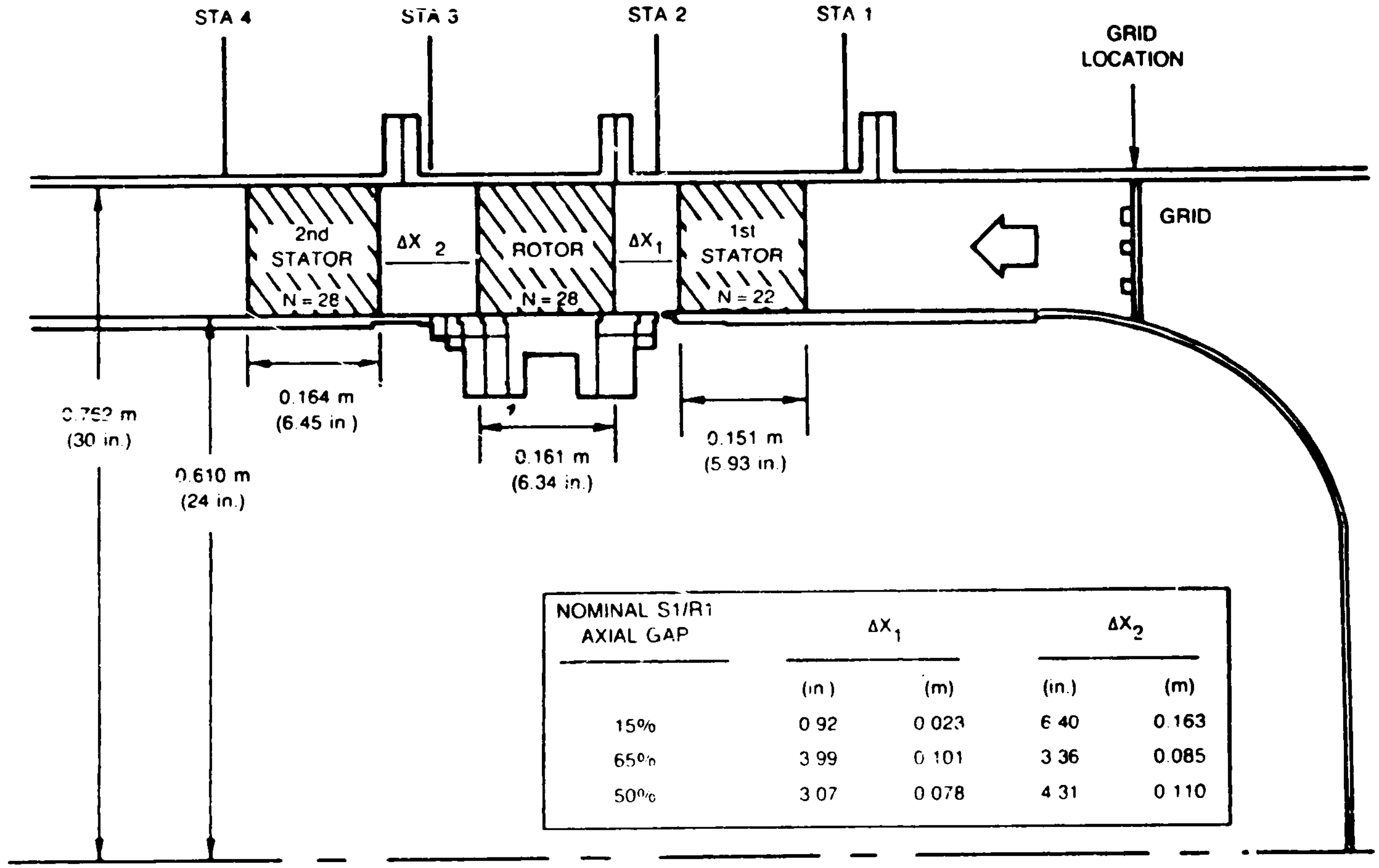

NOMINAL S1/R1 AXIAL GAP	ΔX_1		ΔX_2	
	(in.)	(m)	(in.)	(m)
15%	0.92	0.023	6.40	0.163
65%	3.99	0.101	3.36	0.085
50%	3.07	0.078	4.31	0.110

FIG. 2 UNITED TECHNOLOGIES RESEARCH CENTER LARGE SCALE ROTATING RIG

FIRST STATOR PRESSURE DISTRIBUTION

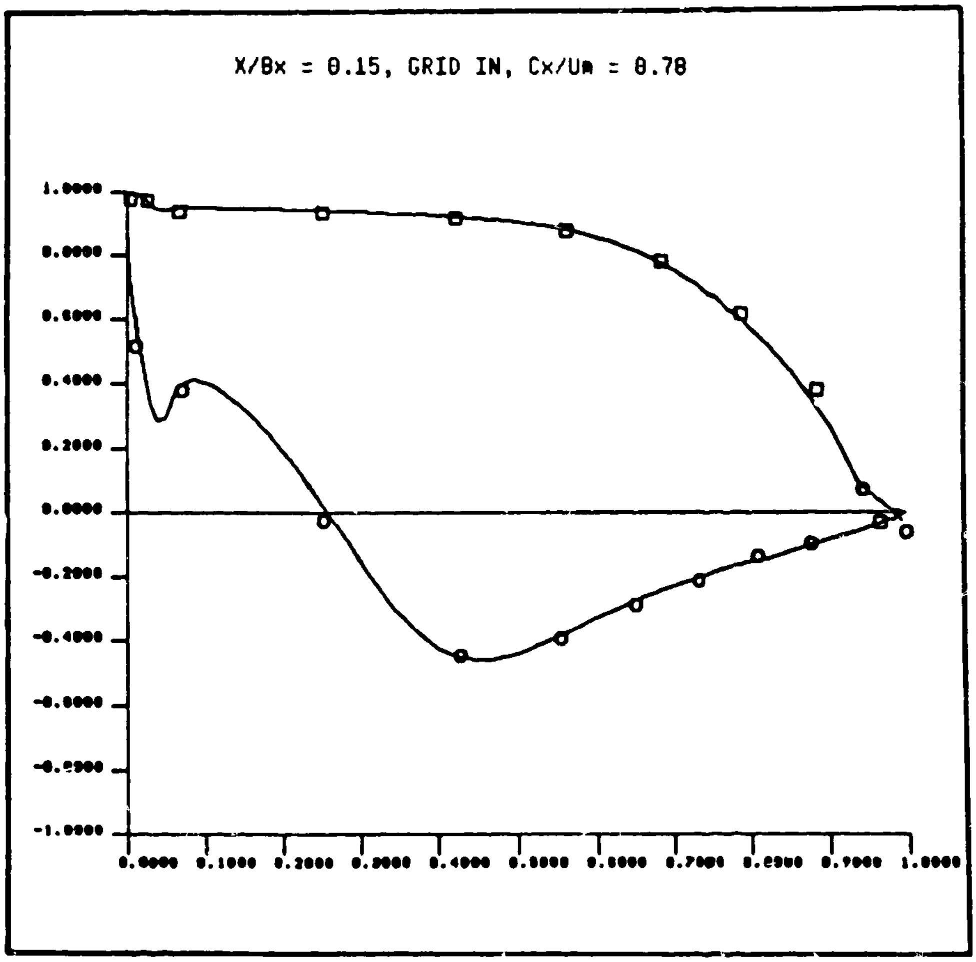

FIG. 3a

ROTOR PRESSURE DISTRIBUTION

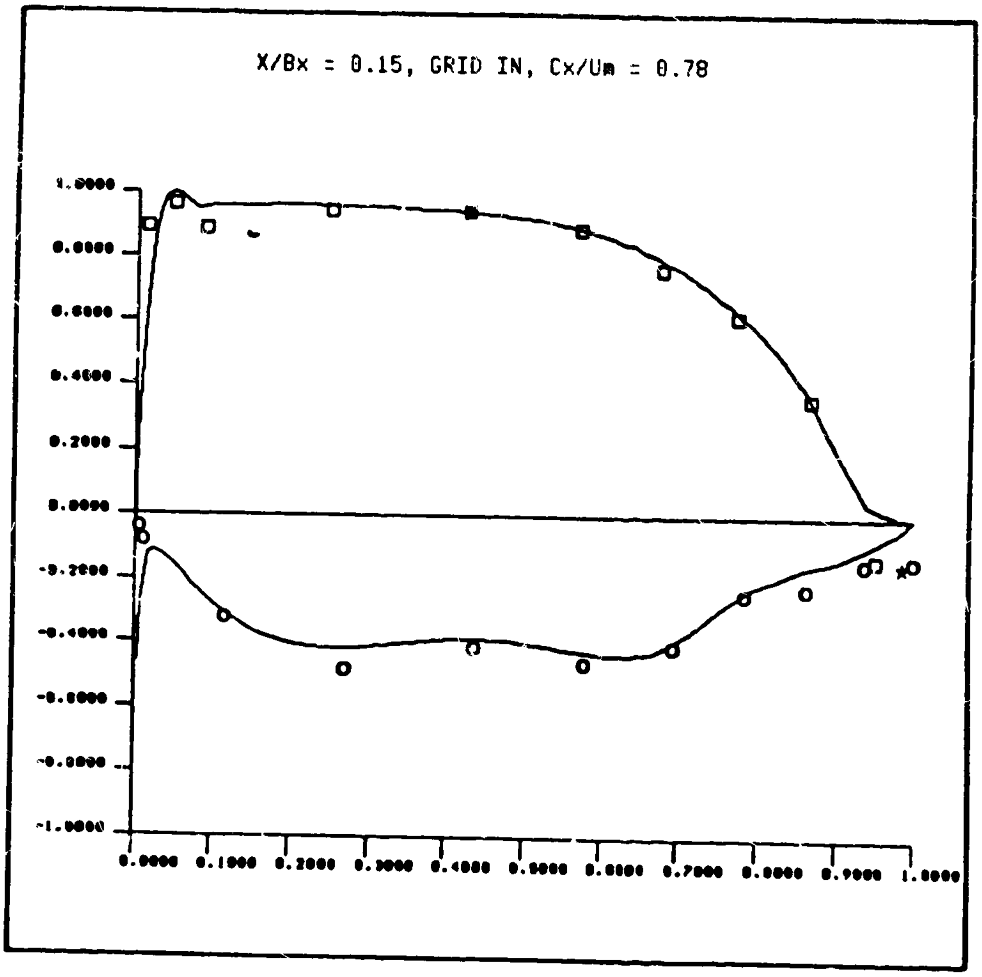

FIG. 3b

STREAMWISE TURBULENCE (RMS)

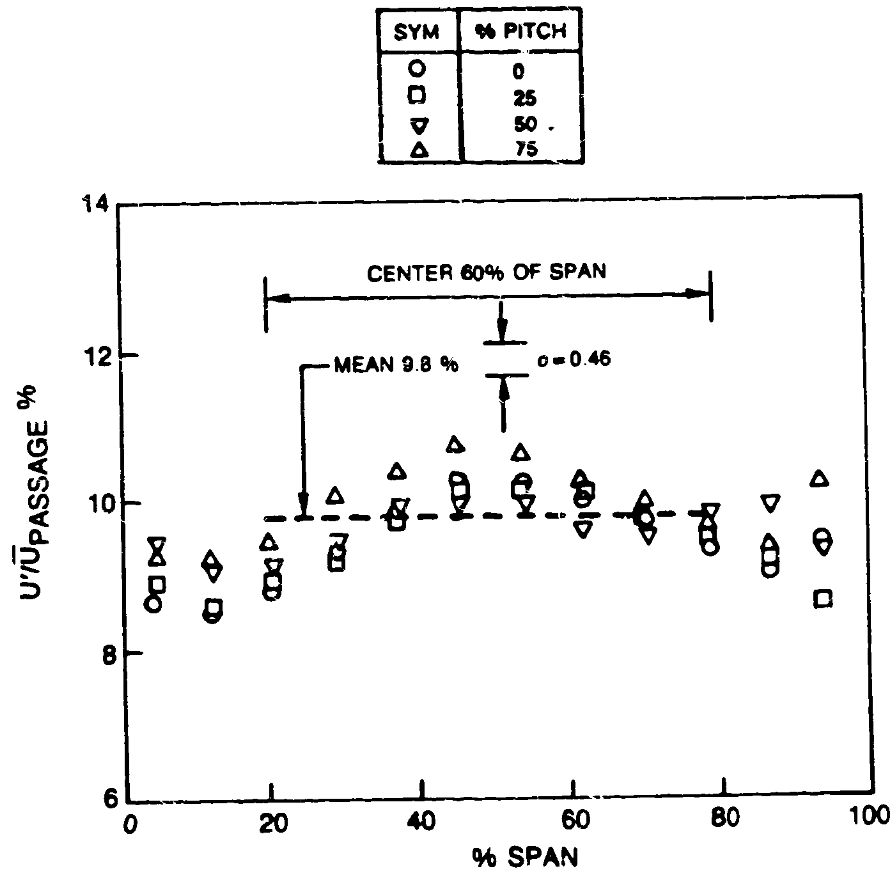

FIG. 4

B_x = 5.932 in.   TOTAL ARC LENGTH = 20.334 in.

S=0 at S'=11.11 in.

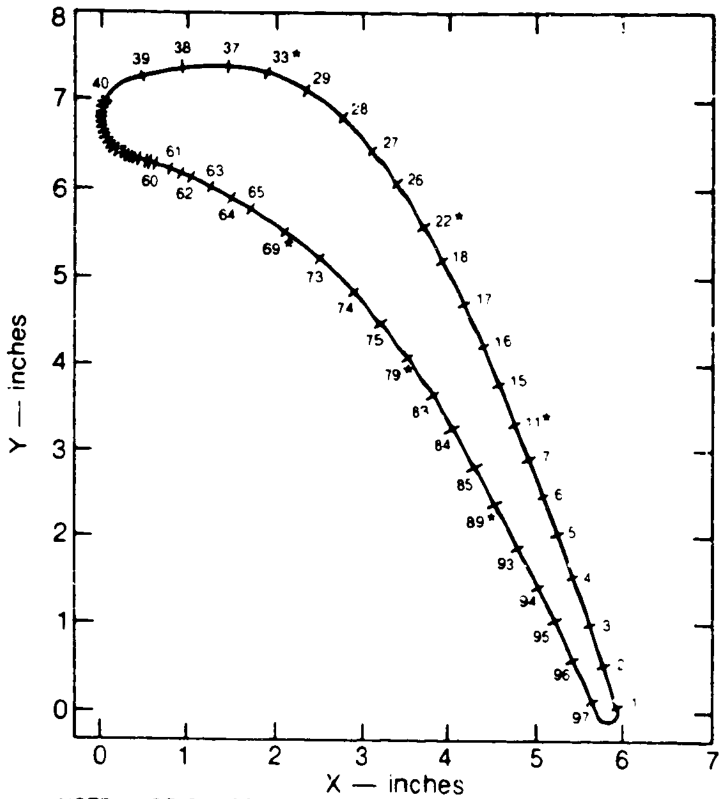

NOTE — ORIGIN OF ARC LENGTH (S) IS THE AXIAL TRAILING EDGE (MAXIMUM X). S INCREASES MOVING COUNTERCLOCKWISE

SUCTION SURFACE AIRFOIL TC's 1-60
PRESSURE SURFACE AIRFOIL TC's 40-97

T C #	X/B_x	S'/B_x
1	0.995	0.012
2	0.968	0.096
3	0.941	0.181
4	0.915	0.265
5	0.887	0.349
6	0.858	0.434
7	0.829	0.518
11*	0.799	0.602
15	0.767	0.686
16	0.735	0.771
17	0.700	0.855
18	0.663	0.939
22*	0.620	1.024
26	0.575	1.108
27	0.524	1.192
28	0.464	1.277
29	0.396	1.361
33*	0.324	1.445
37	0.169	1.529
38	0.155	1.614

T C #	X/B_x	S'/B_x
39	0.073	1.698
40	0.007	1.782
41	0.004	1.791
42	0.001	1.799
43	0.000	1.808
44	0.000	1.816
45	0.001	1.824
46	0.002	1.833
47	0.005	1.841
48	0.008	1.850
49	0.013	1.858
50	0.018	1.867
51	0.023	1.875
52	0.030	1.883
53	0.037	1.892
54	0.044	1.900
55	0.052	1.909
56	0.060	1.917
57	0.068	1.926
58	0.076	1.934

T C #	X/B_x	S'/B_x
59	0.084	1.942
60	0.092	1.951
61	0.130	1.993
62	0.172	2.035
63	0.209	2.077
64	0.246	2.119
65	0.285	2.162
69*	0.356	2.246
73	0.421	2.330
74	0.484	2.414
75	0.538	2.499
79*	0.590	2.583
83	0.637	2.667
84	0.679	2.752
85	0.723	2.836
89*	0.764	2.9[illegible]
93	0.802	3.004
94	0.840	3.089
95	0.878	3.173
96	0.914	3.257
97	0.949	3.342

* AT THESE AXIAL STATIONS T.C.s LOCATED AT 50% SPAN AND ±8.3, 16.6 AND 25% AWAY FROM MIDSPAN

FIG. 5a INSTRUMENTATION DIAGRAM FOR THE FIRST STAGE STATOR

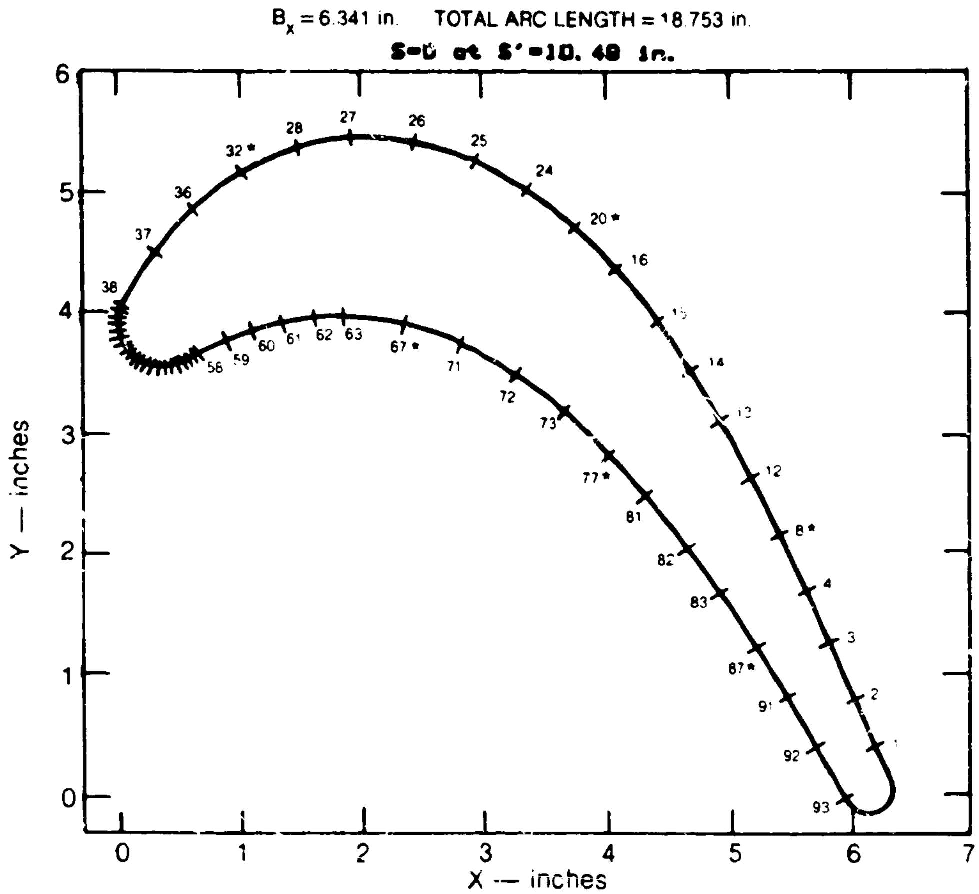

NOTE — ORIGIN OF ARC LENGTH (S) IS THE AXIAL TRAILING EDGE (MAXIMUM X). S INCREASES MOVING COUNTERCLOCKWISE

SUCTION SURFACE AIRFOIL TC s 1-58
PRESSURE SURFACE AIRFOIL TC s 38-93

T C #	X/B_x	S'/B_x
1	0.975	0.069
2	0.945	0.148
3	0.912	0.227
4	0.878	0.306
8*	0.845	0.385
12	0.811	0.463
13	0.773	0.542
14	0.735	0.621
15	0.692	0.700
16	0.643	0.779
20*	0.588	0.858
24	0.525	0.936
25	0.456	1.015
26	0.382	1.094
27	0.303	1.173
28	0.226	1.252
32*	0.155	1.331
36	0.095	1.410
37	0.044	1.488
38	0.003	1.567

T C #	X/B_x	S'/B_x
39	0.001	1.575
40	0.000	1.583
41	0.000	1.591
42	0.002	1.599
43	0.004	1.607
44	0.007	1.615
45	0.012	1.622
46	0.017	1.630
47	0.023	1.638
48	0.030	1.646
49	0.037	1.654
50	0.044	1.662
51	0.052	1.670
52	0.061	1.678
53	0.068	1.686
54	0.076	1.693
55	0.083	1.701
56	0.090	1.709
57	0.096	1.717
58	0.103	1.725

T C #	X/B_x	S'/B_x
59	0.139	1.764
60	0.172	1.804
61	0.211	1.843
62	0.251	1.883
63	0.290	1.922
67*	0.371	2.000
71	0.445	2.080
72	0.513	2.159
73	0.574	2.237
77*	0.629	2.316
81	0.680	2.395
82	0.730	2.474
83	0.774	2.553
87*	0.820	2.632
91	0.856	2.711
92	0.899	2.789
93	0.940	2.868

* AT THESE AXIAL STATIONS T C s LOCATED AT 50% SPAN AND ± 8.3, 16.6 AND 25% AWAY FROM MIDSPAN

FIG. 5b INSTRUMENTATION DIAGRAM FOR THE FIRST STAGE ROTOR

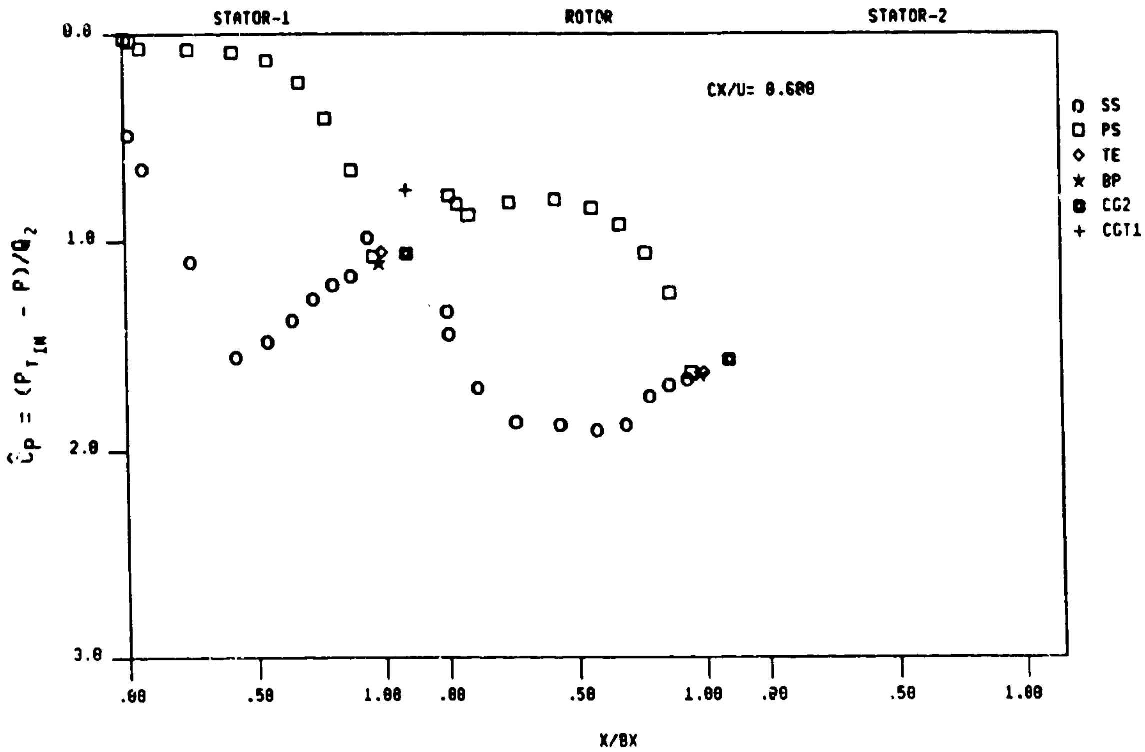

FIG. 6a AIRFOIL MIDSPAN PRESSURE DISTRIBUTIONS,
X/Bx = 0.15, GRID OUT, Cx/Um = 0.68

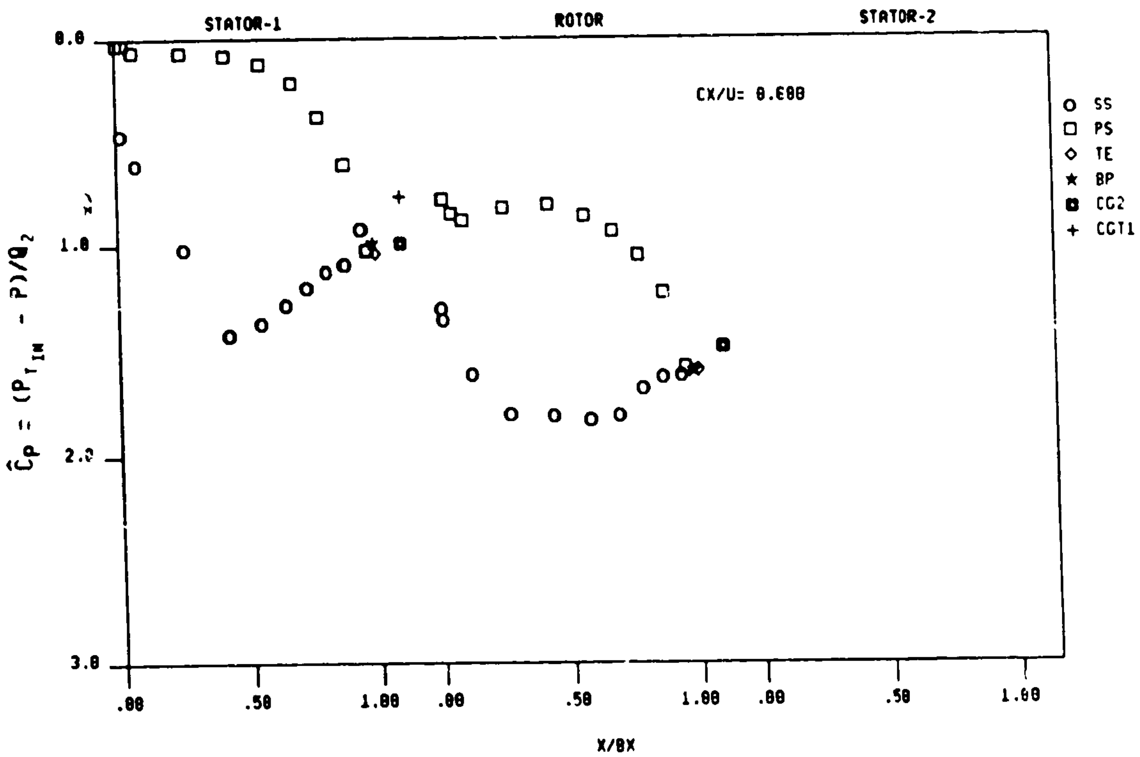

FIG. 6b AIRFOIL MIDSPAN PRESSURE DISTRIBUTIONS,
X/Bx = 0.15, GRID IN, Cx/Um = 0.68

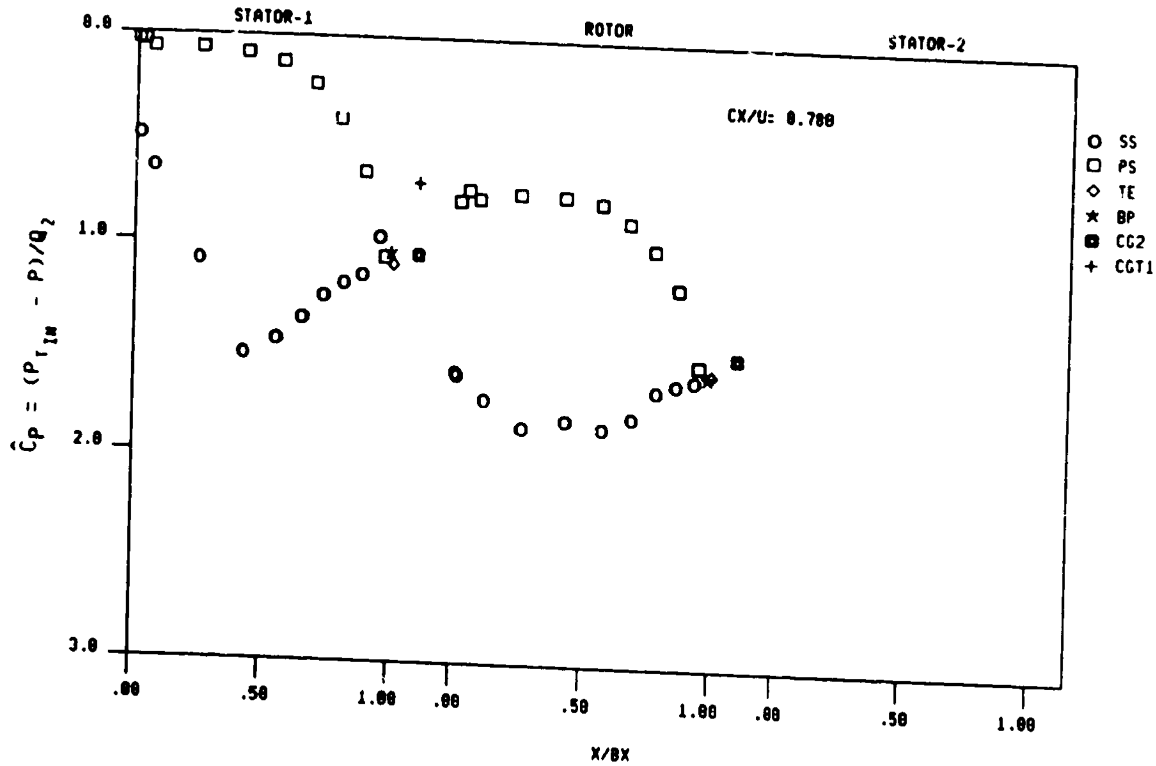

FIG. 7a AIRFOIL MIDSPAN PRESSURE DISTRIBUTIONS, X/Bx = 0.15, GRID OUT, Cx/Um = 0.78

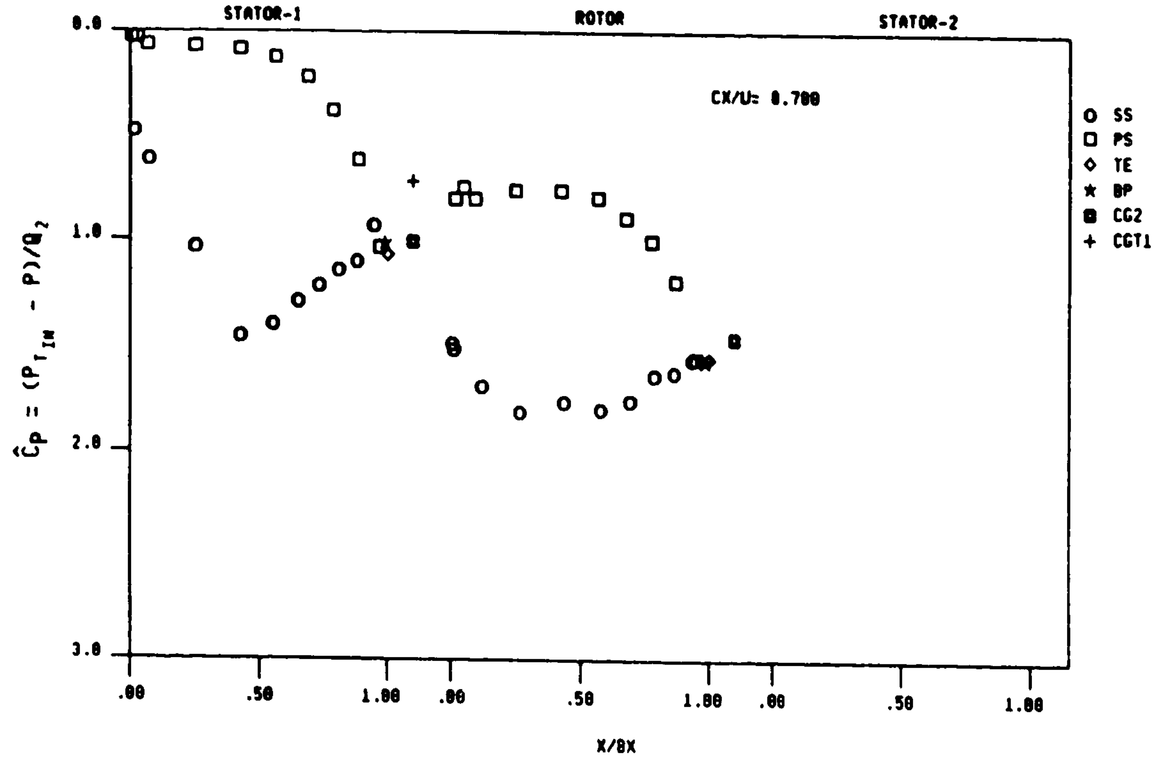

FIG. 7b AIRFOIL MIDSPAN PRESSURE DISTRIBUTIONS,
X/Bx = 0.15, GRID IN, Cx/Um = 0.78

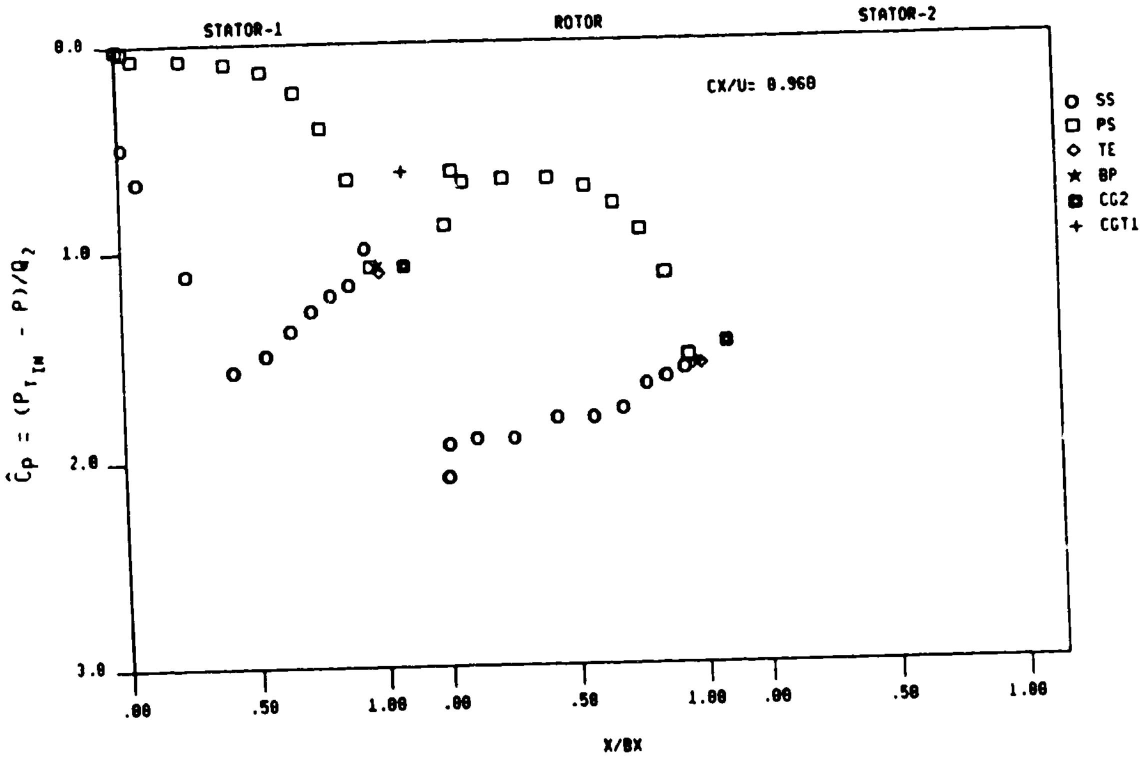

FIG. 8a AIRFOIL MIDSPAN PRESSURE DISTRIBUTIONS, X/Bx = 0.15, GRID OUT, Cx/Um = 0.96

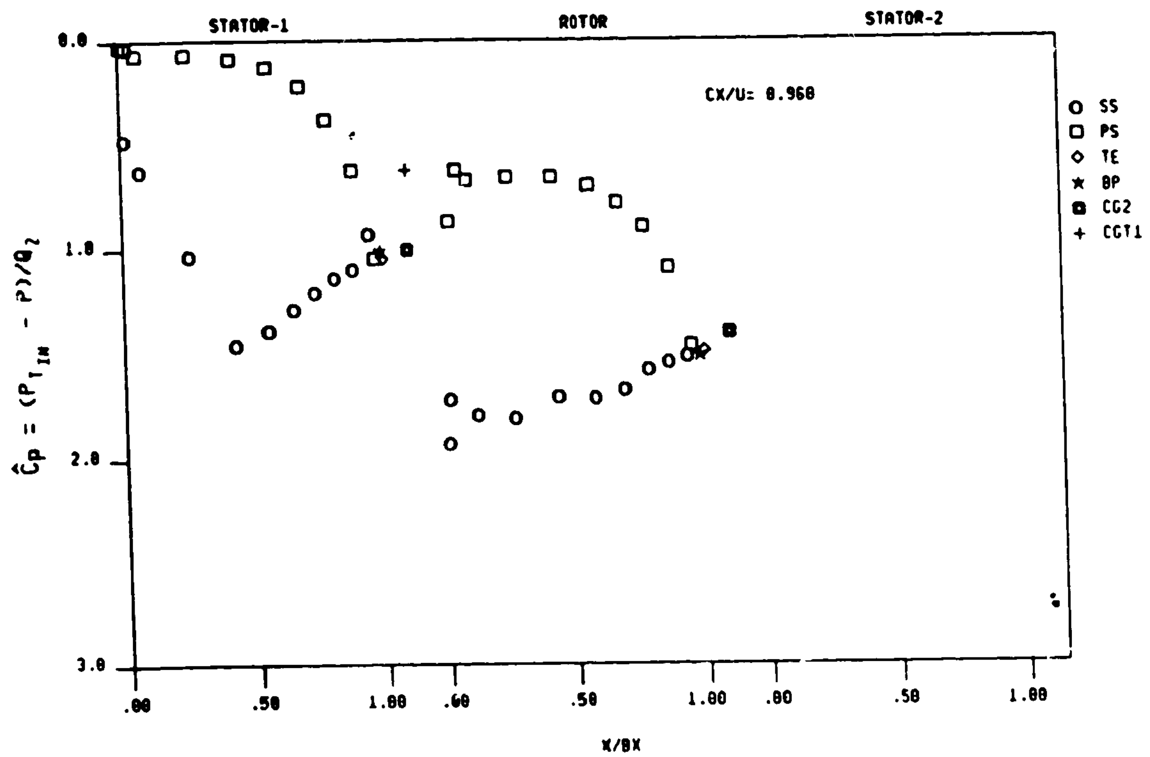

FIG. 8b AIRFOIL MIDSPAN PRESSURE DISTRIBUTIONS,
X/Bx = 0.15, GRID IN, Cx/Um = 0.96

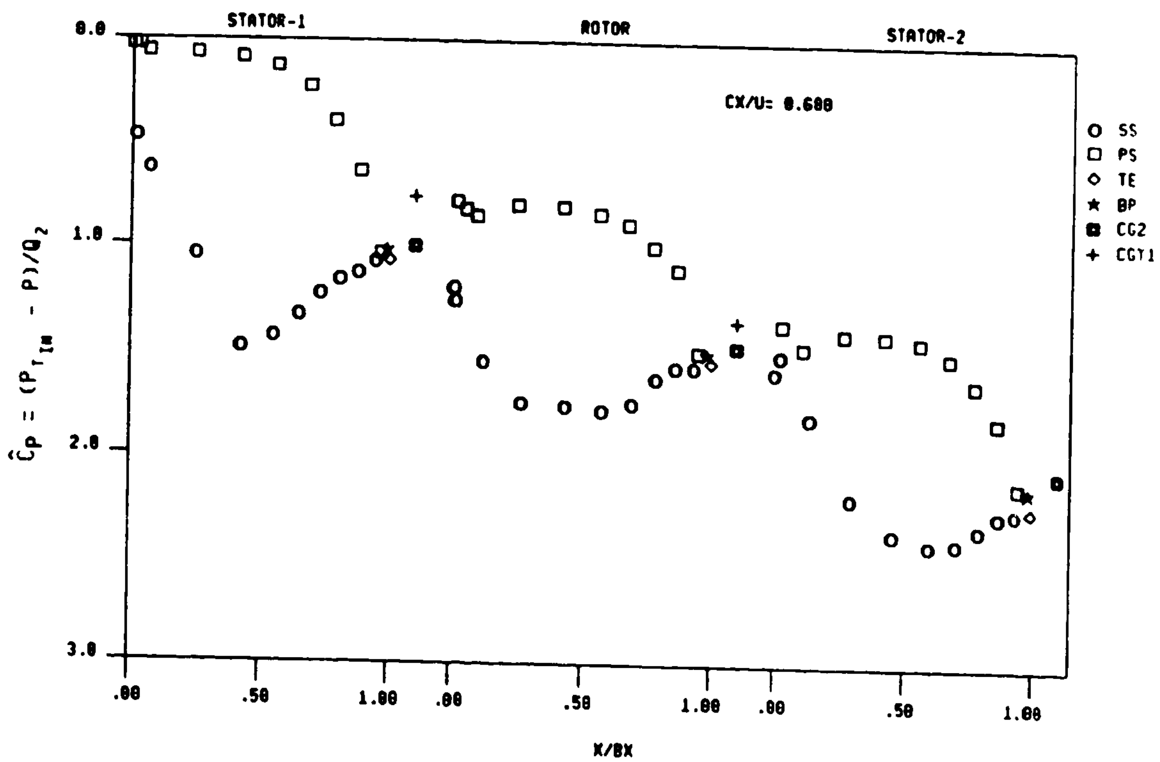

FIG. 9a AIRFOIL MIDSPAN PRESSURE DISTRIBUTIONS, X/Bx = 0.50, GRID OUT, Cx/Um = 0.68

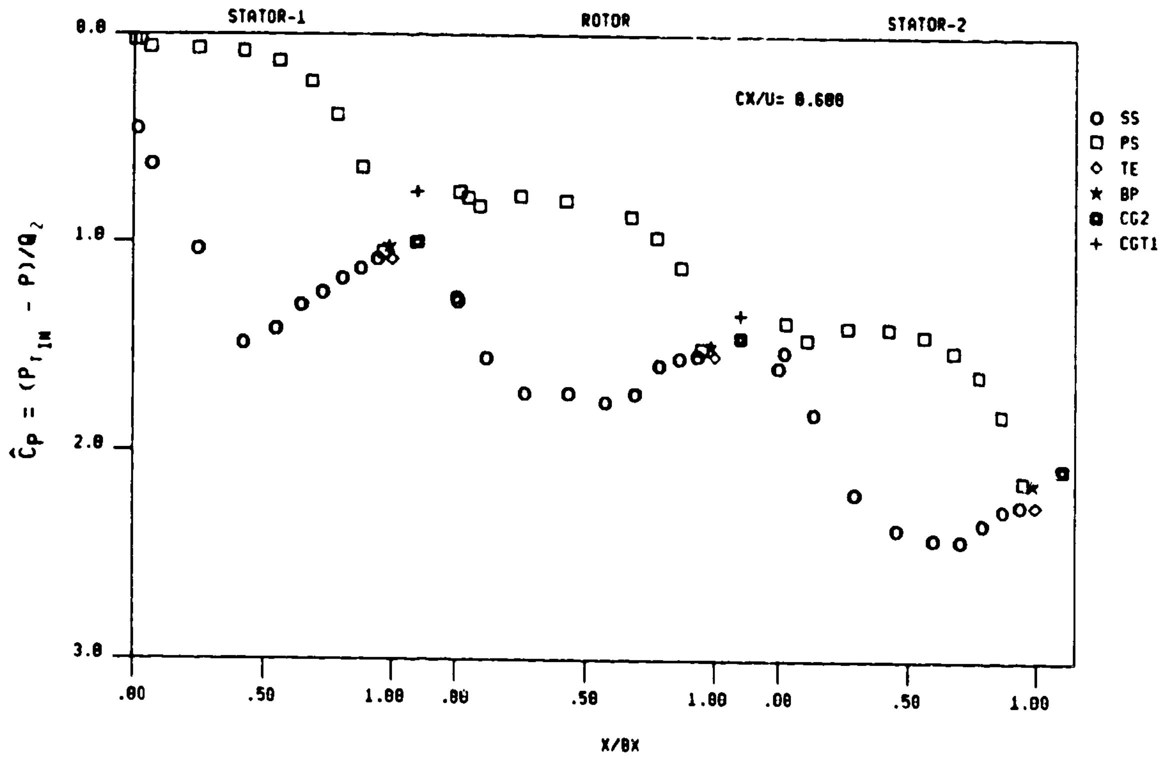

FIG. 9b AIRFOIL MIDSPAN PRESSURE DISTRIBUTIONS,
X/Bx = 0.50, GRID IN, Cx/Um = 0.68

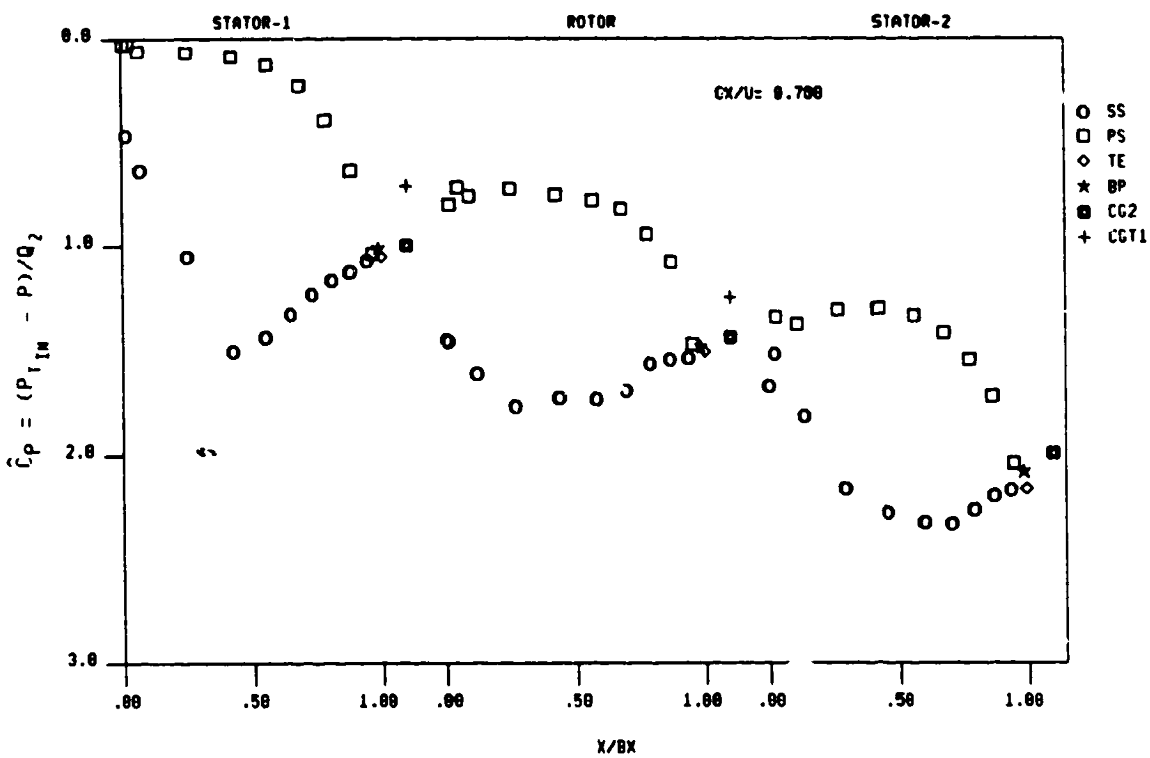

FIG. 10a AIRFOIL MIDSPAN PRESSURE DISTRIBUTIONS,
X/Bx = 0.50, GRID OUT, Cx/Um = 0.78

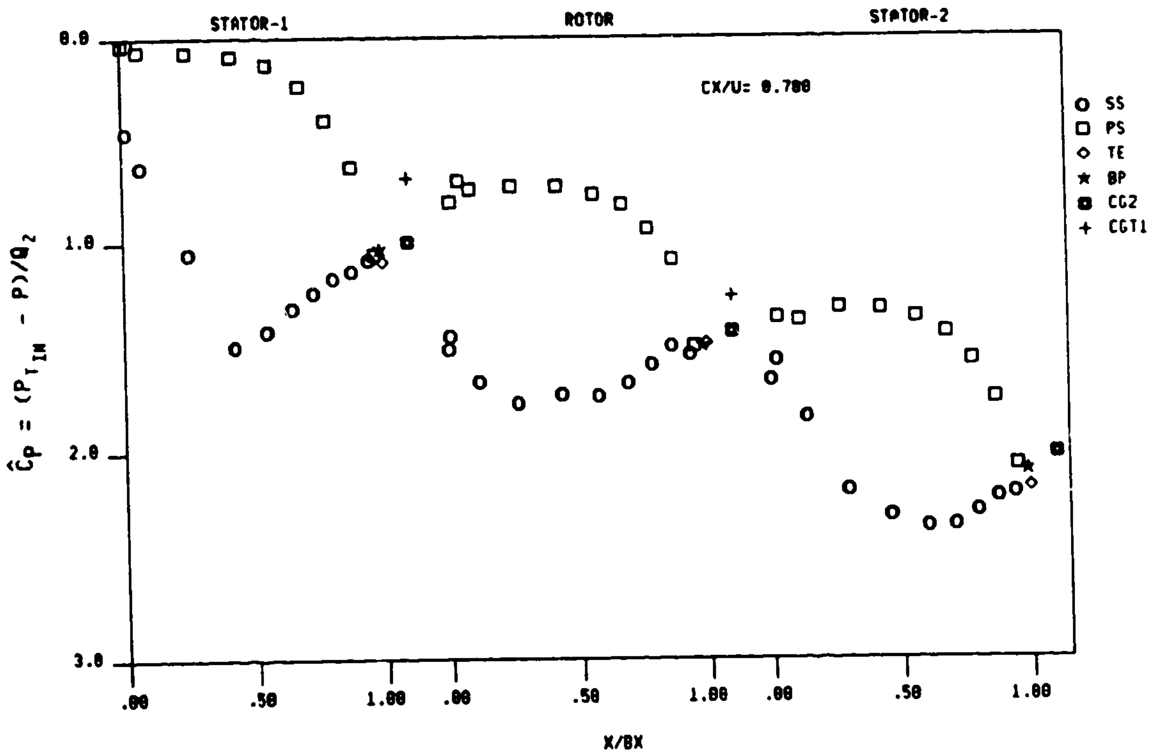

FIG. 10b AIRFOIL MIDSPAN PRESSURE DISTRIBUTIONS,
X/Bx = 0.50, GRID IN, Cx/Um = 0.78

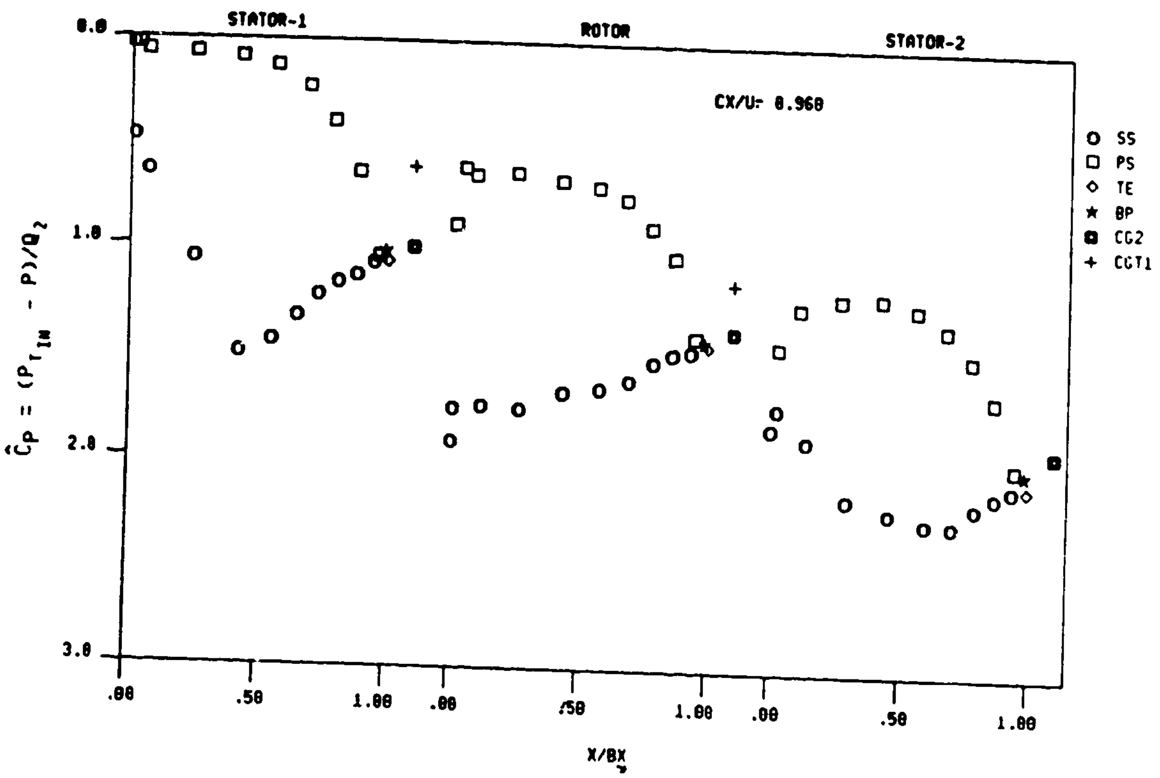

FIG. 11a AIRFOIL MIDSPAN PRESSURE DISTRIBUTIONS, X/Bx = 0.50, GRID OUT, Cx/Um = 0.96

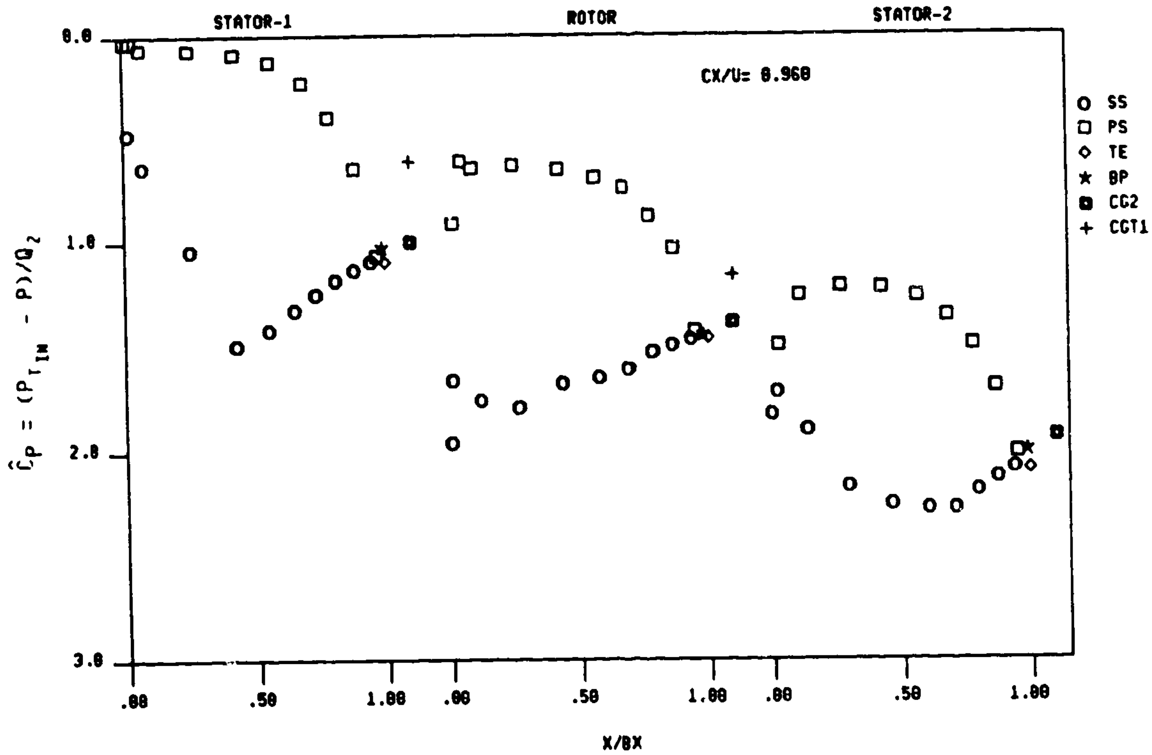

FIG. 11b AIRFOIL MIDSPAN PRESSURE DISTRIBUTIONS, X/Bx = 0.50, GRID IN, Cx/Um = 0.96

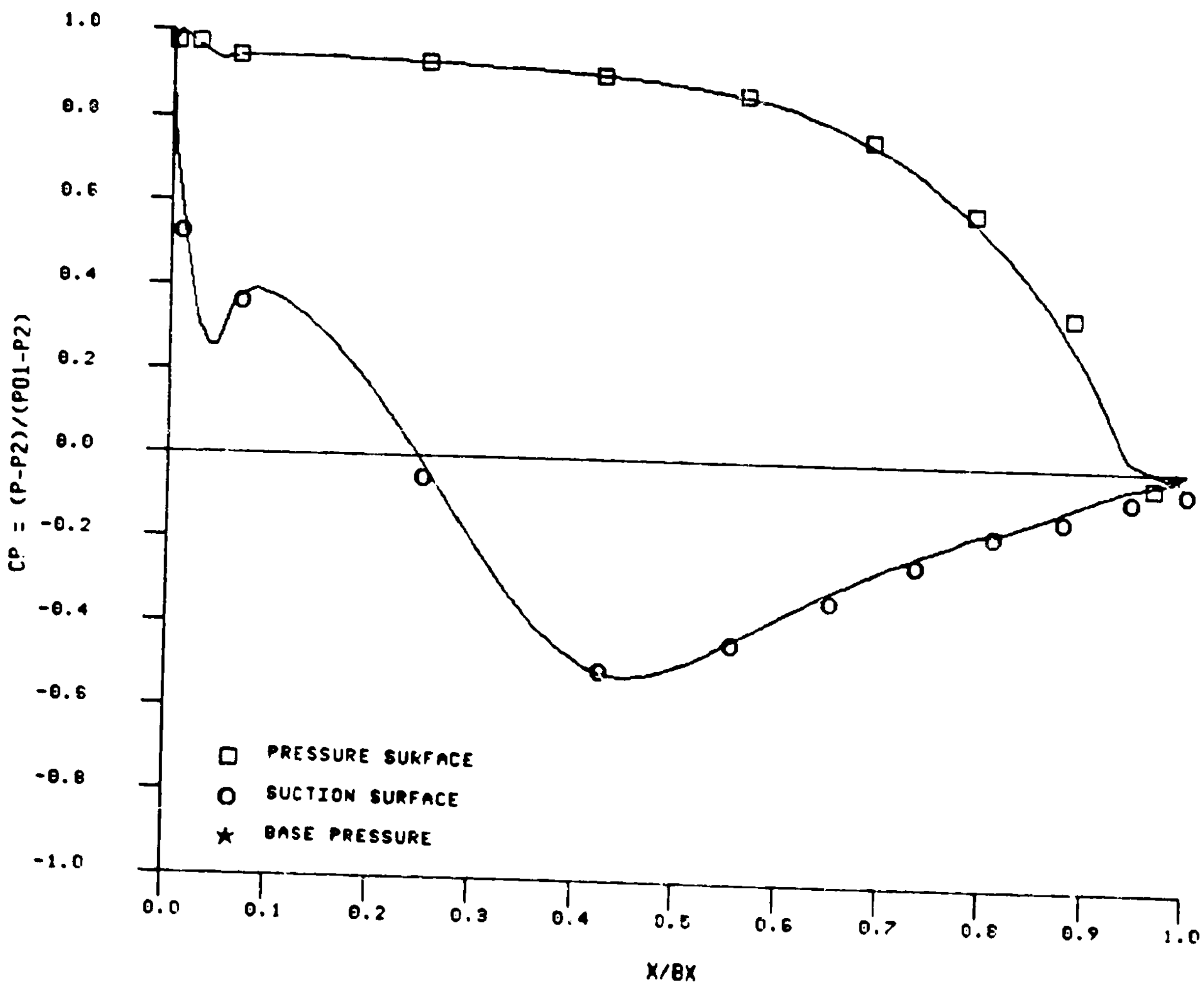

FIG. 12 FIRST STATOR PRESSURE DISTRIBUTION, ϕ = 0.78

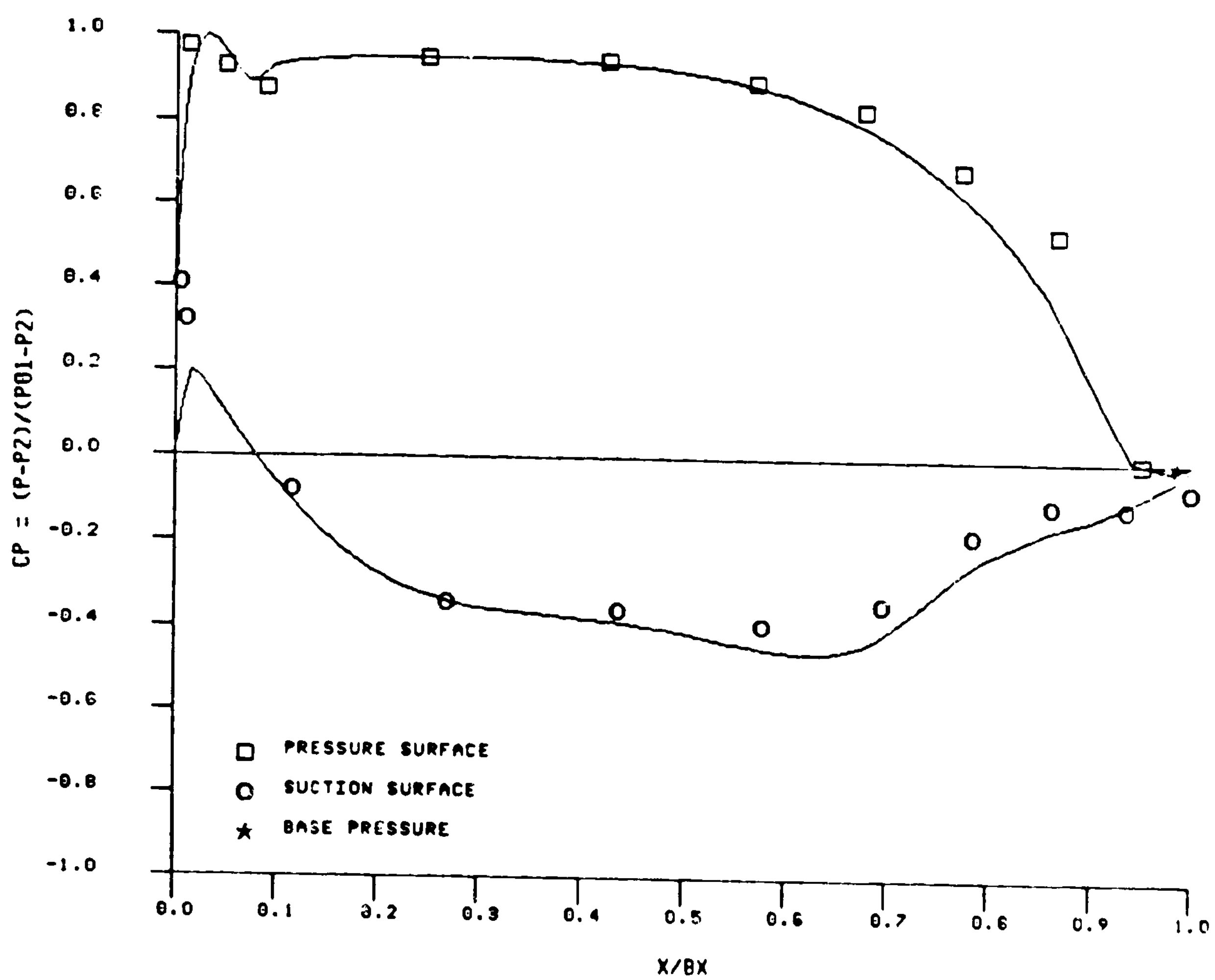

FIG. 13a ROTOR PRESSURE DISTRIBUTION. ϕ = 0.68

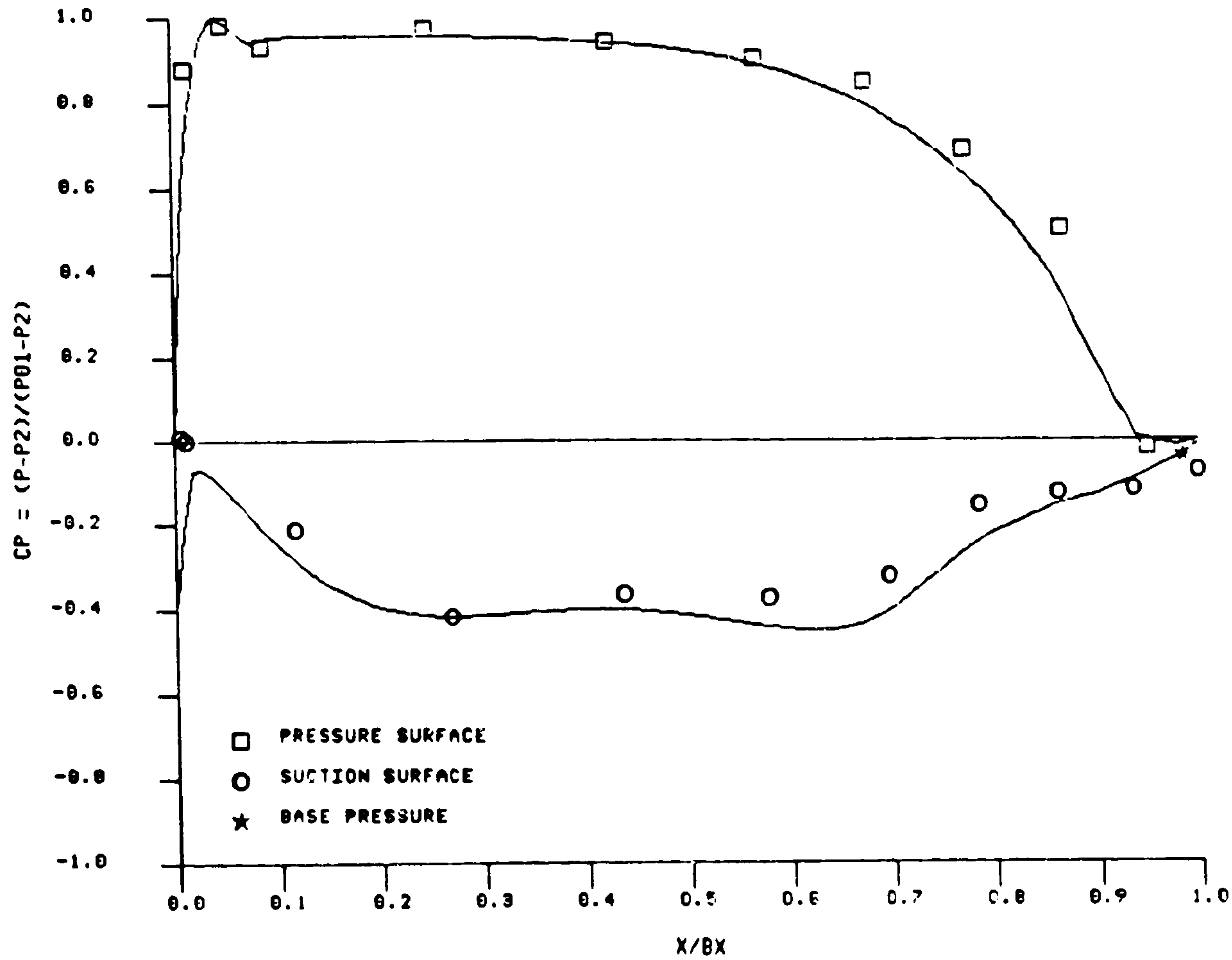

FIG. 13b ROT(R PRESSURE DISTRIBUTION, ϕ = 0.78

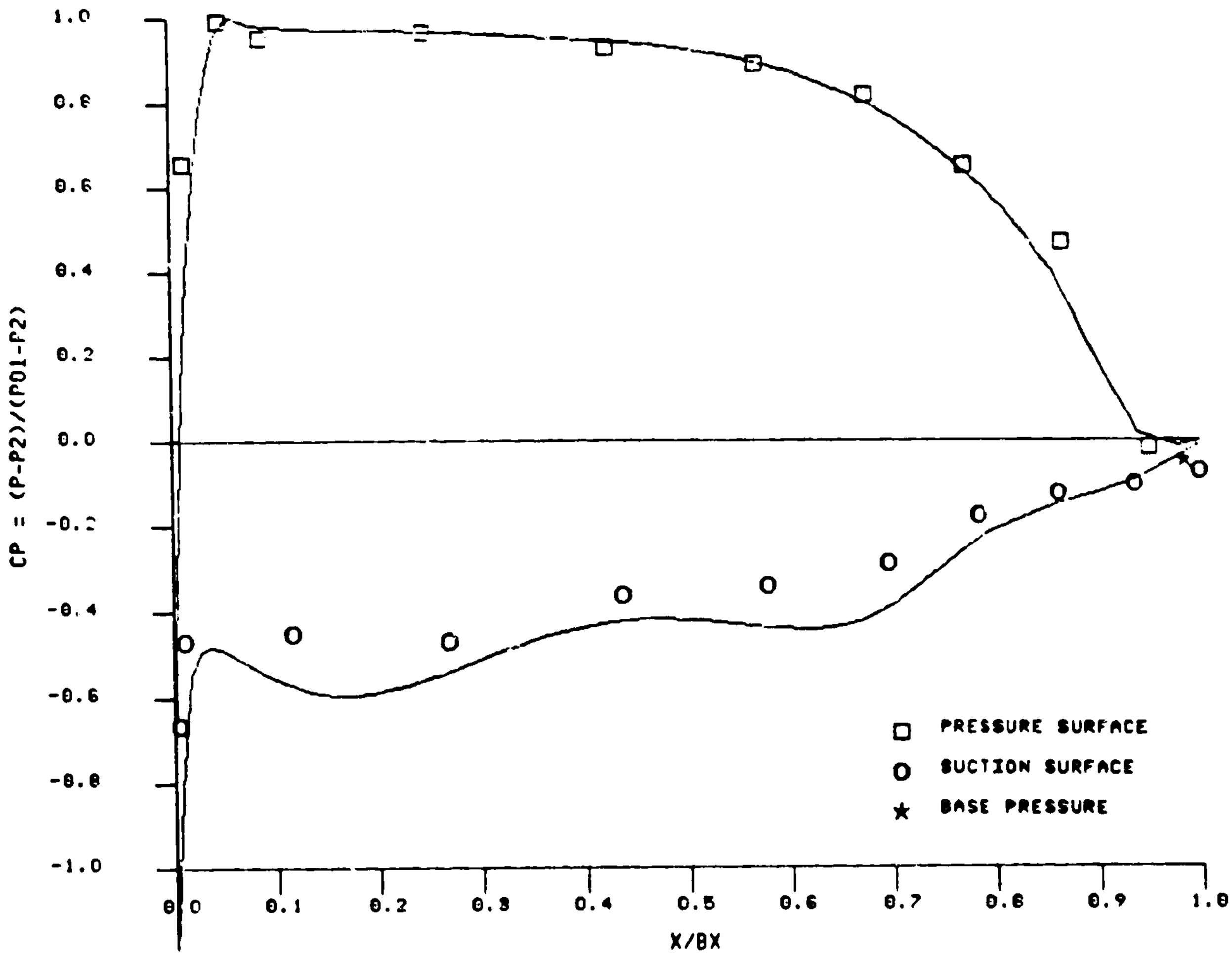

FIG. 13c ROTOR PRESSURE DISTRIBUTION, ϕ = 0.96

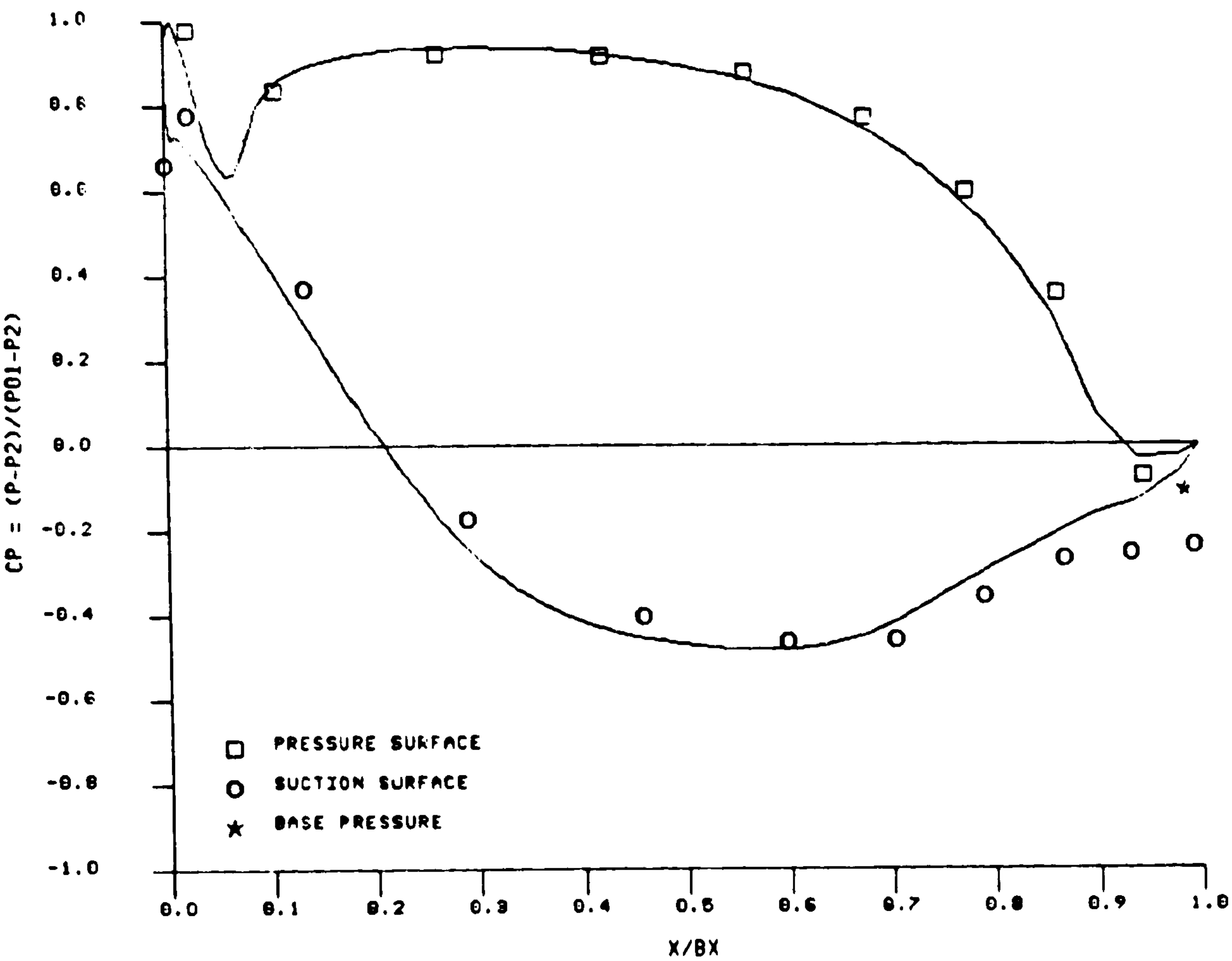

FIG. 14a SECOND STATOR PRESSURE DISTRIBUTION, $\phi = 0.68$

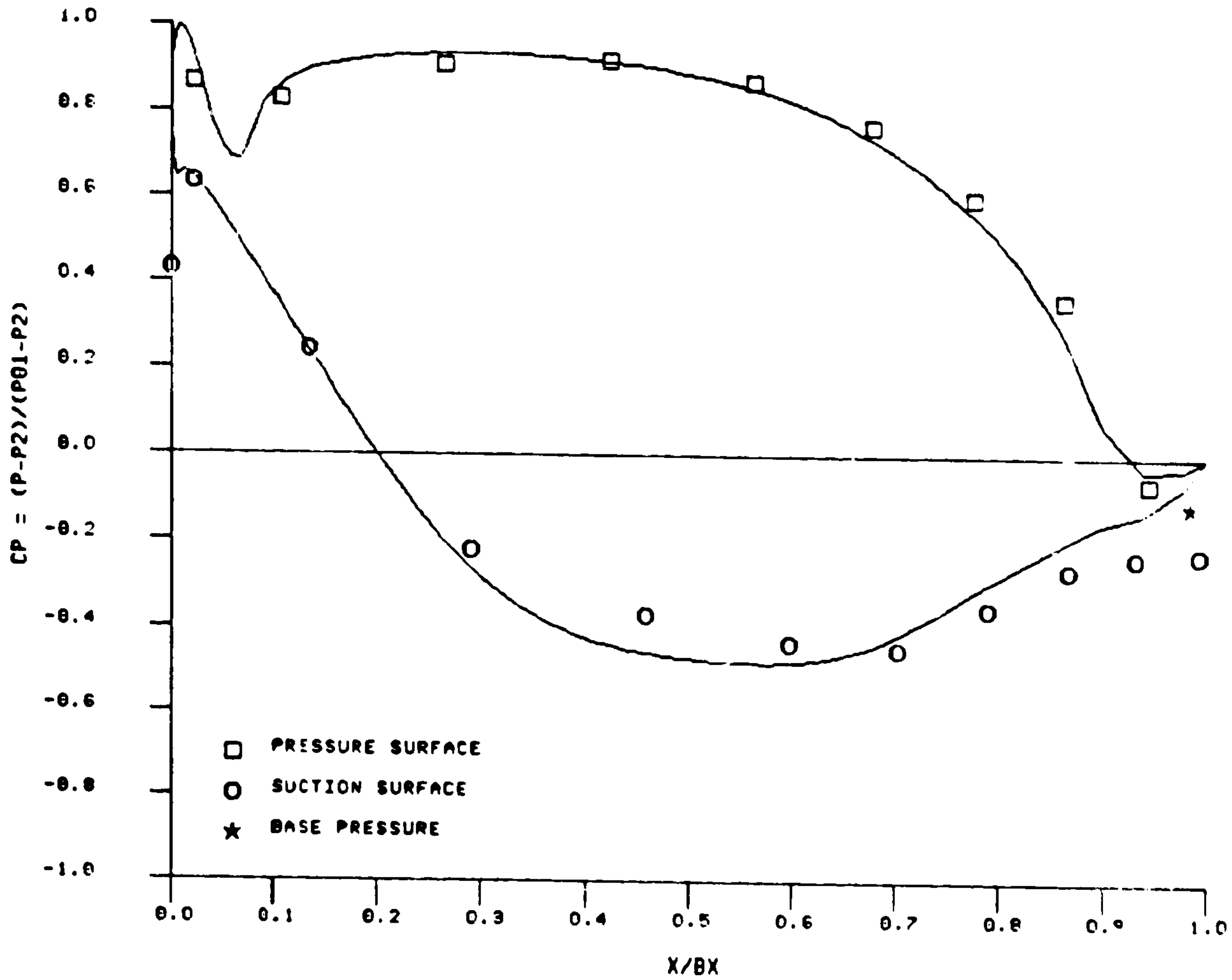

FIG. 14b SECOND STATOR PRESSURE DISTRIBUTION, ϕ = 0.78

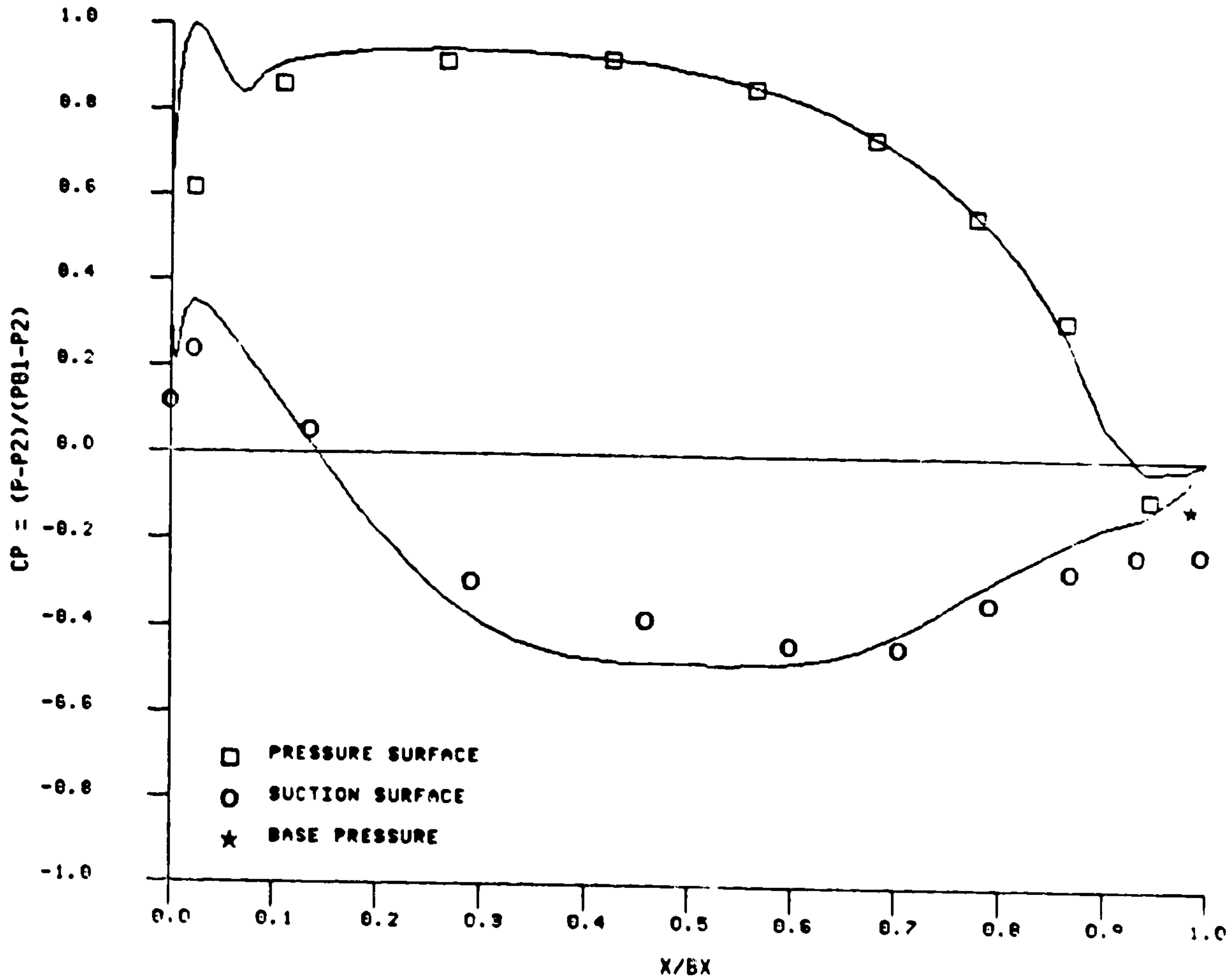

FIG. 14c SECOND STATOR PRESSURE DISTRIBUTION, ϕ = 0.96

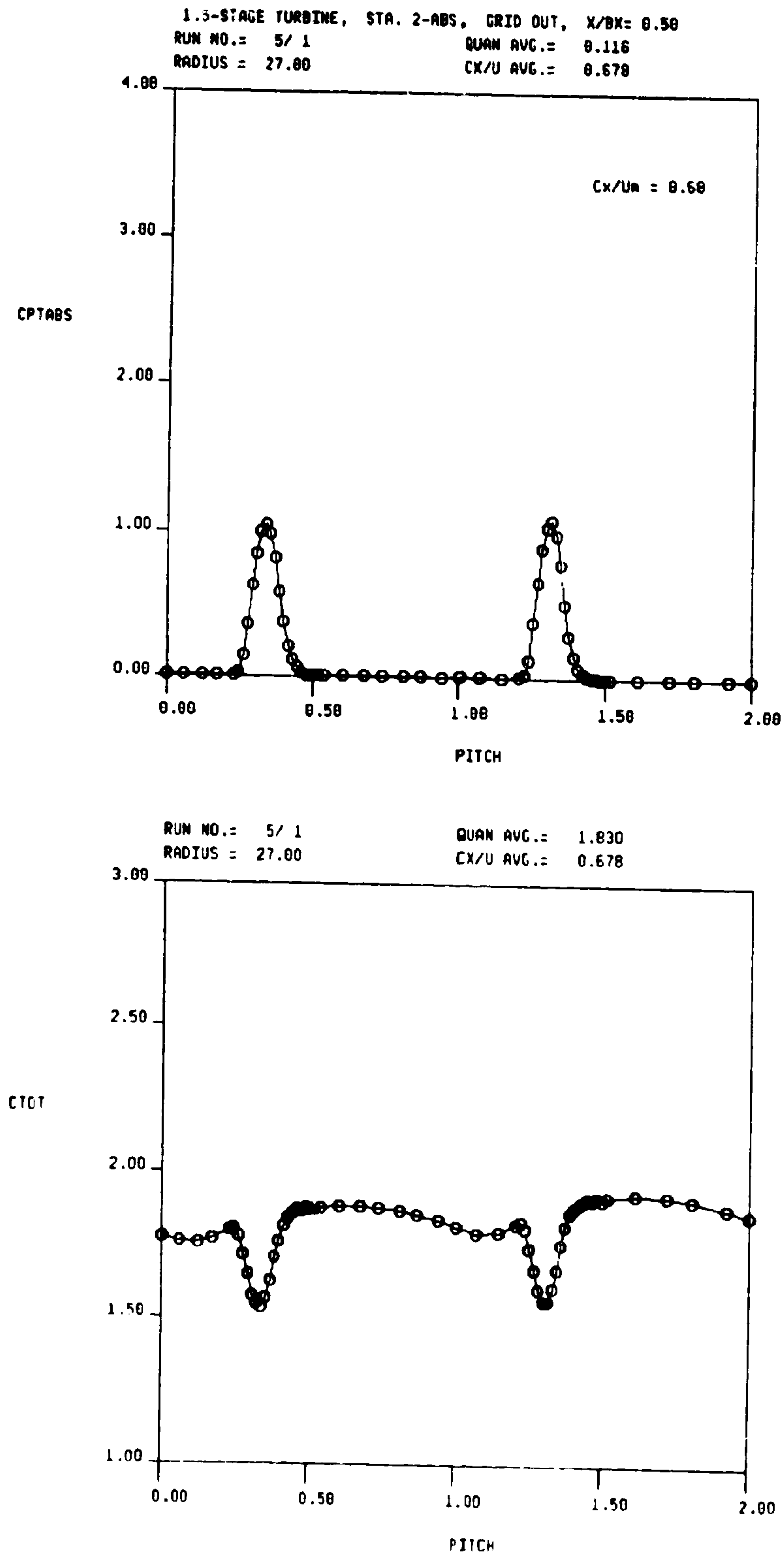

FIG. 15a ABSOLUTE TOTAL PRESSURE AND VELOCITY FROM 5-HOLE PROBE TRAVERSE AT 1ST STATOR EXIT (X/Bx = 0.17), GRID OUT

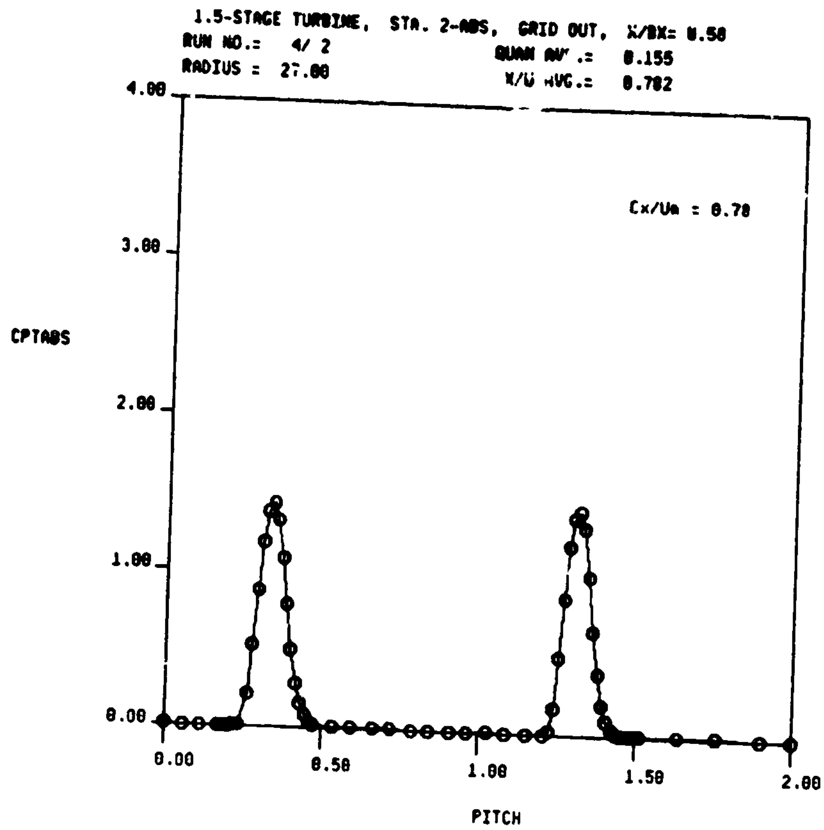

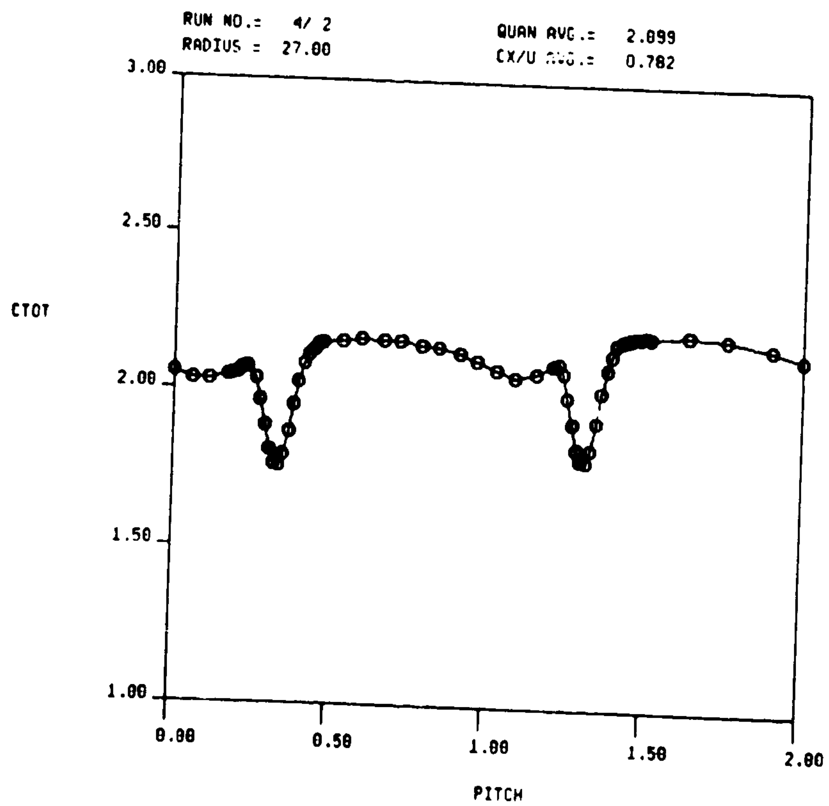

FIG. 15b ABSOLUTE TOTAL PRESSURE AND VELOCITY FROM 5-HOLE PROBE TRAVERSE AT 1ST STATOR EXIT (X/Bx = 0.17), GRID OUT

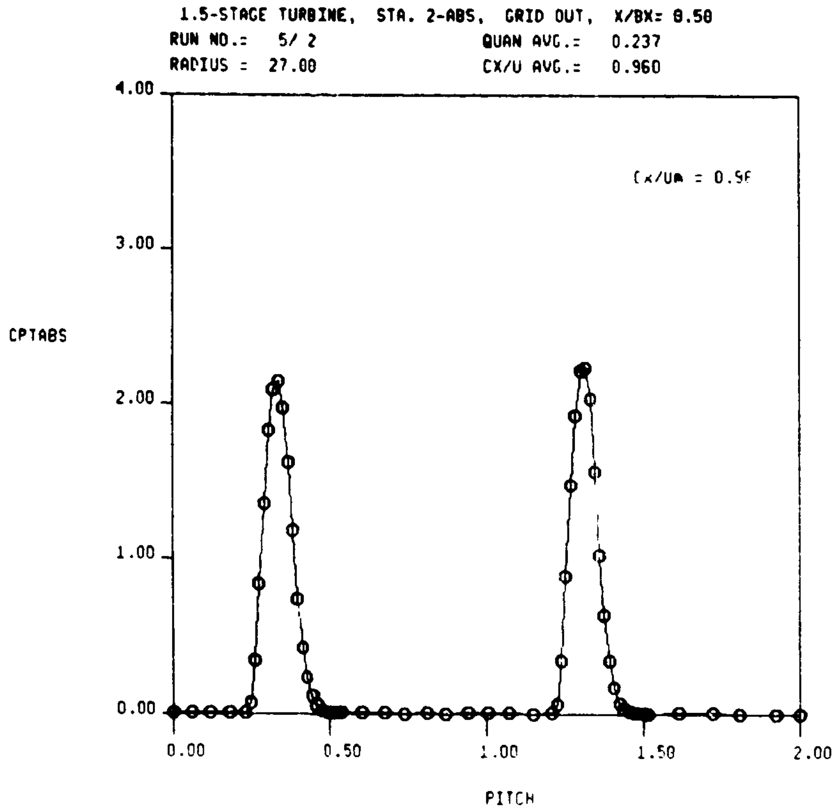

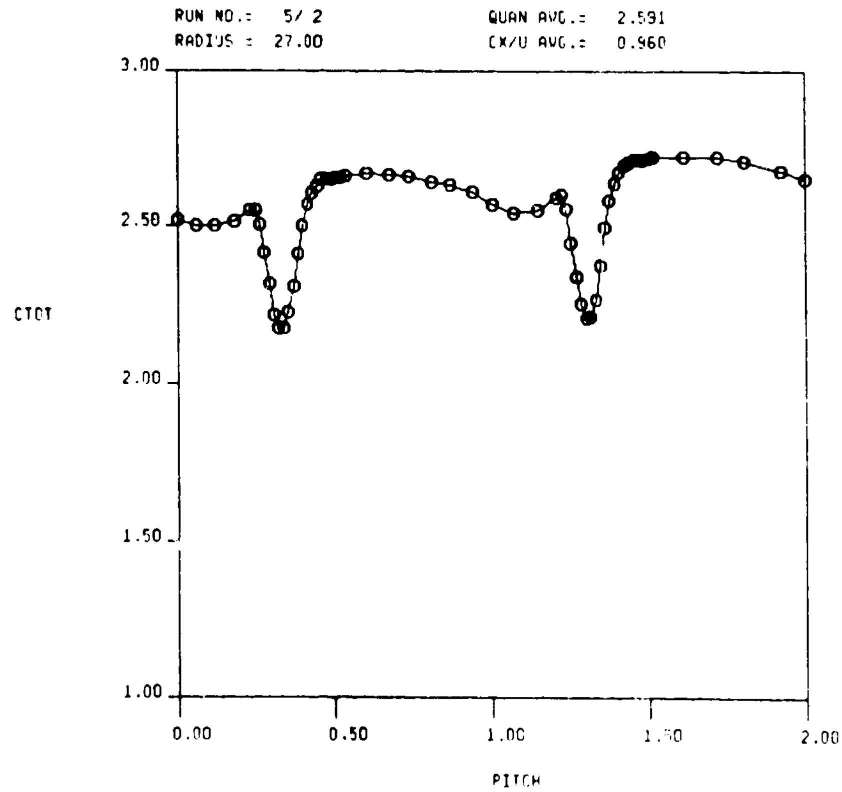

FIG. 15c ABSOLUTE TOTAL PRESSURE AND VELOCITY FROM 5-HOLE PROBE TRAVERSE AT 1ST STATOR EXIT (X/Bx = 0.17), GRID OUT

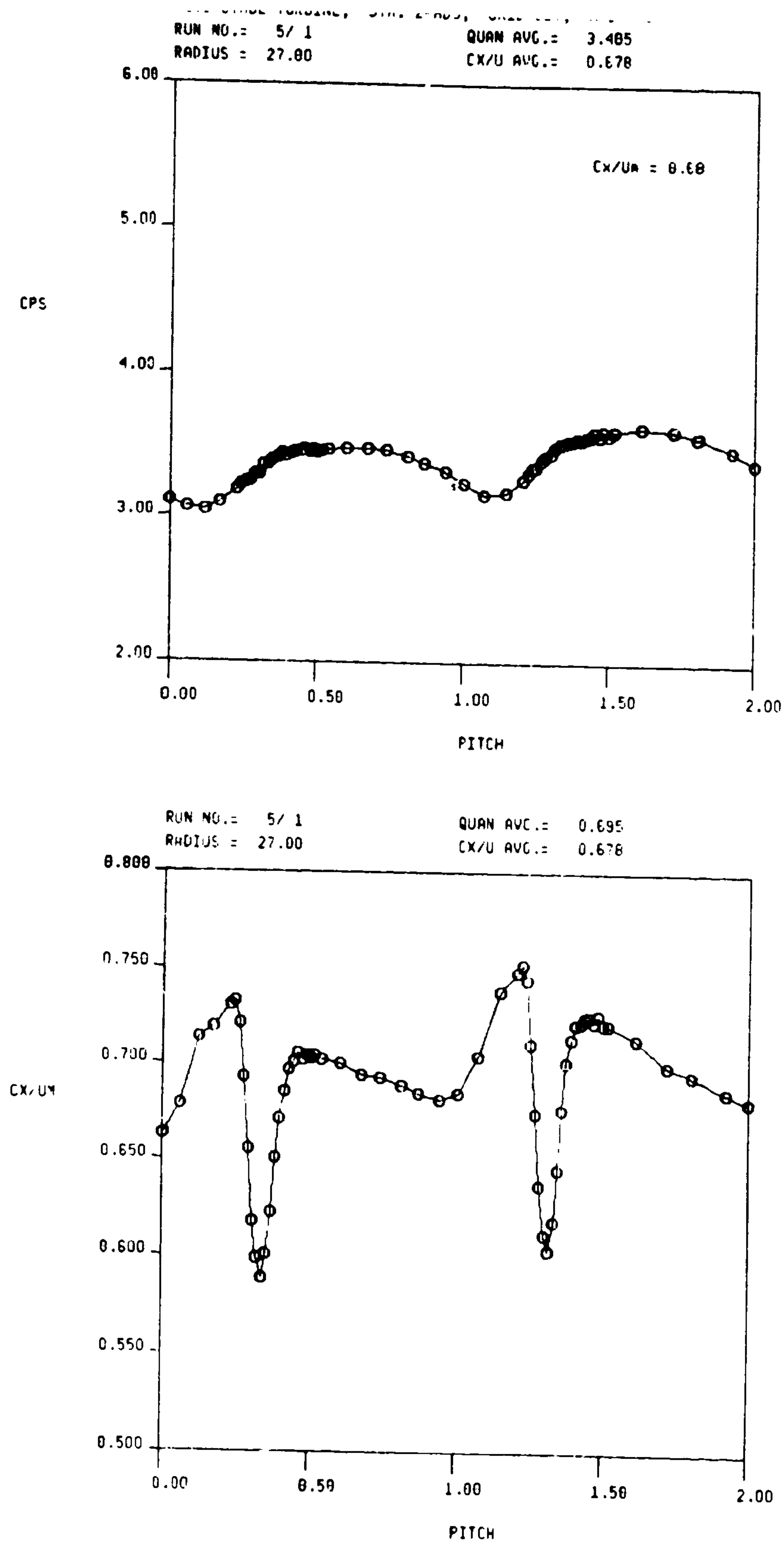

FIG. 16a STATIC PRESSURE AND AXIAL VELOCITY FROM 5-HOLE PROBE TRAVERSE AT 1ST STATOR EXIT (X/Bx = 0.17), GRID OUT

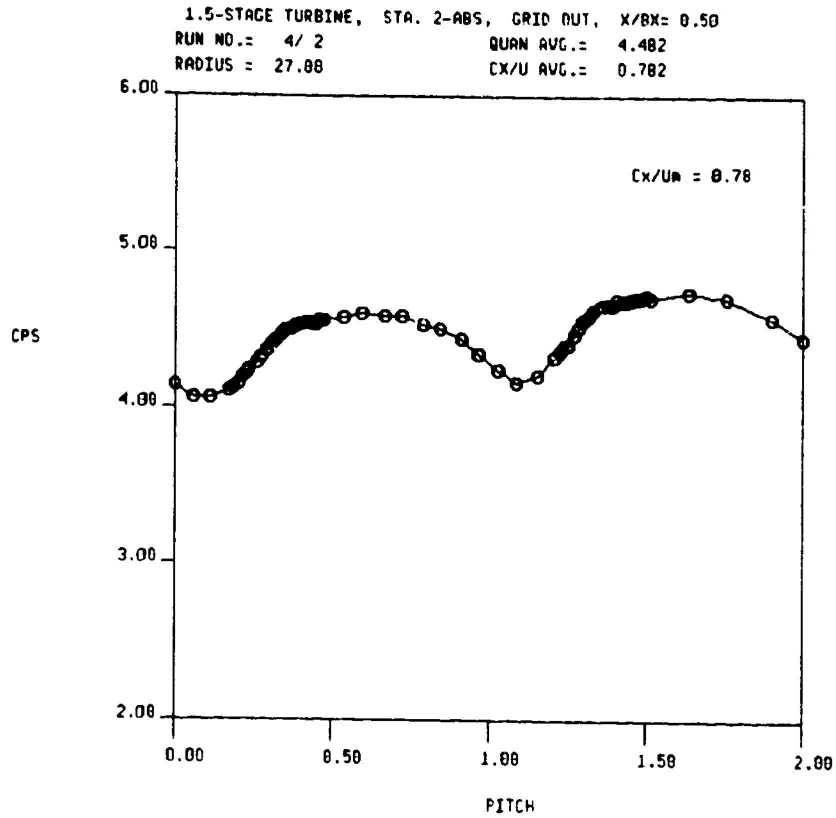

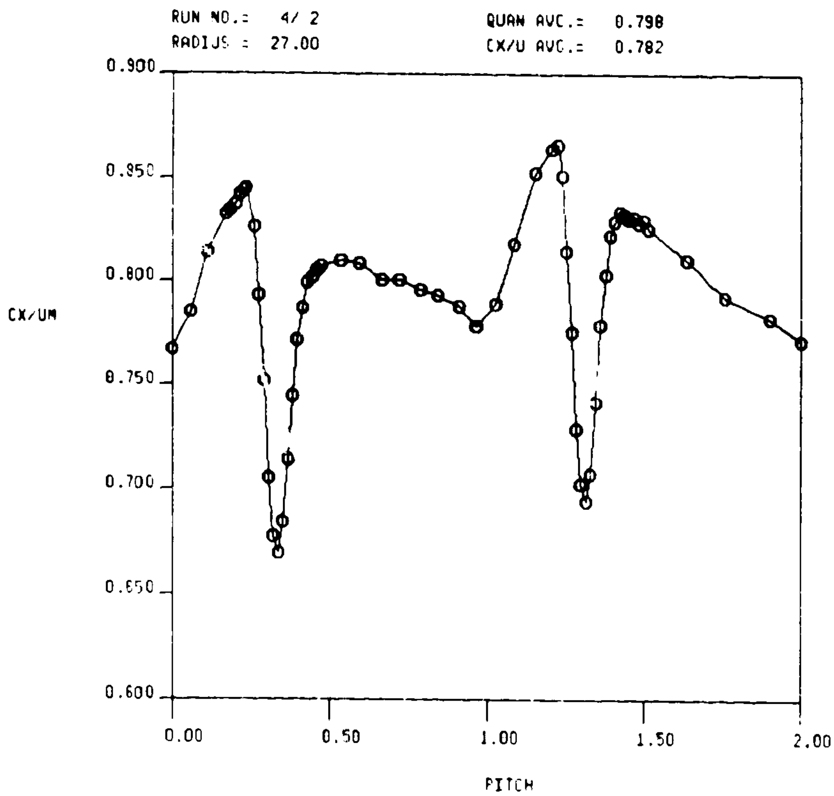

ORIGINAL PAGE IS
OF POOR QUALITY

FIG. 16b STATIC PRESSURE AND AXIAL VELOCITY FROM 5-HOLE PROBE TRAVERSE AT 1ST STATOR EXIT (X/Bx = 0.17), GRID OUT

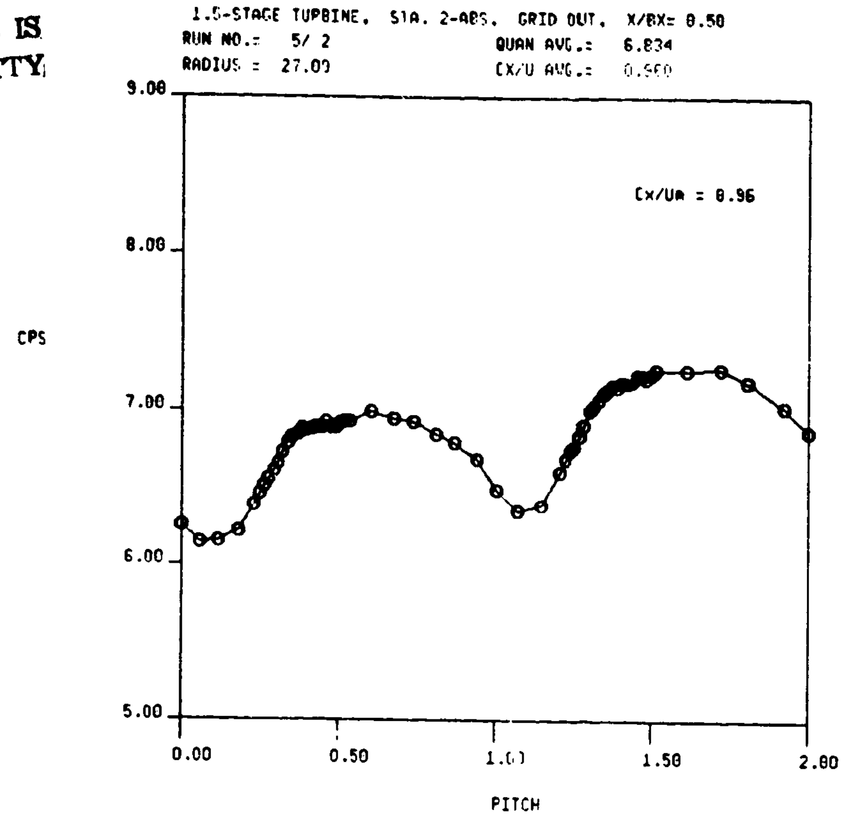

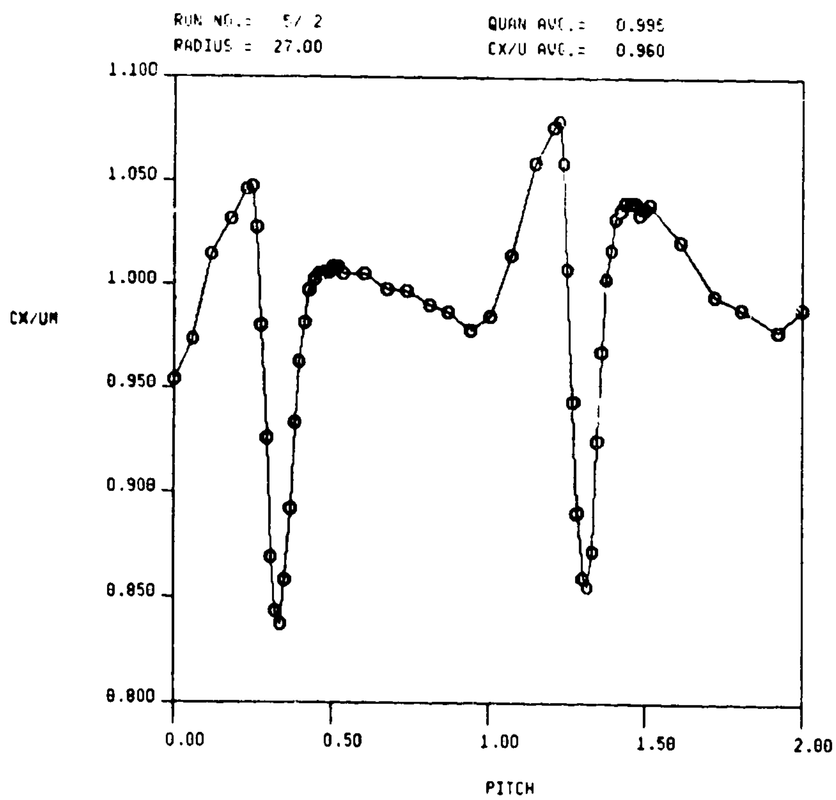

FIG. 16c STATIC PRESSURE AND AXIAL VELOCITY FROM 5-HOLE PROBE TRAVERSE AT 1ST STATOR EXIT (X/Bx = 0.17), GRID OUT

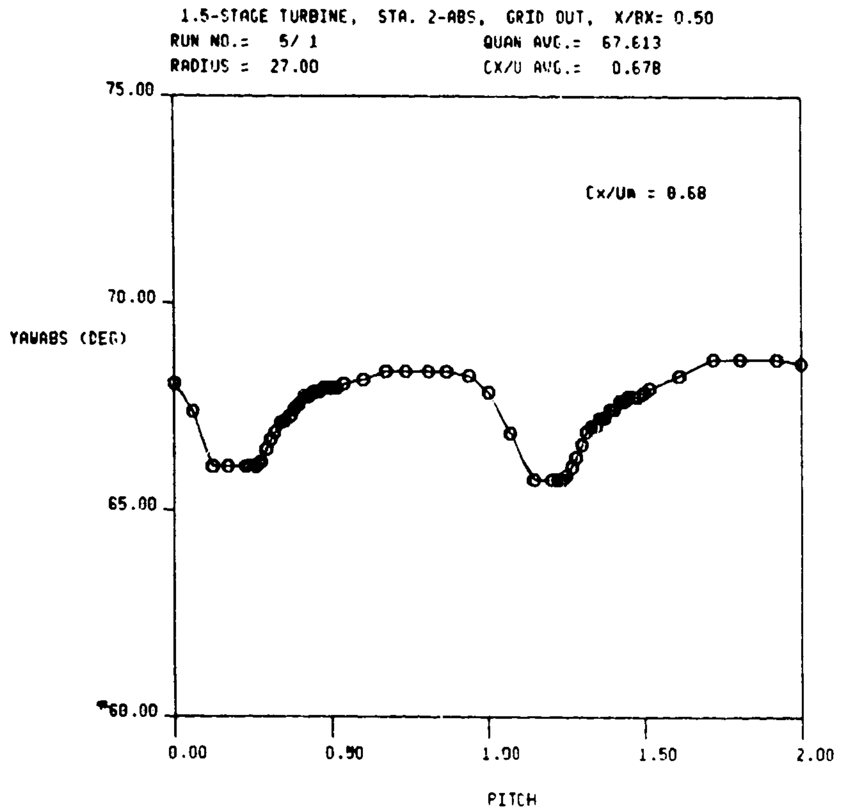

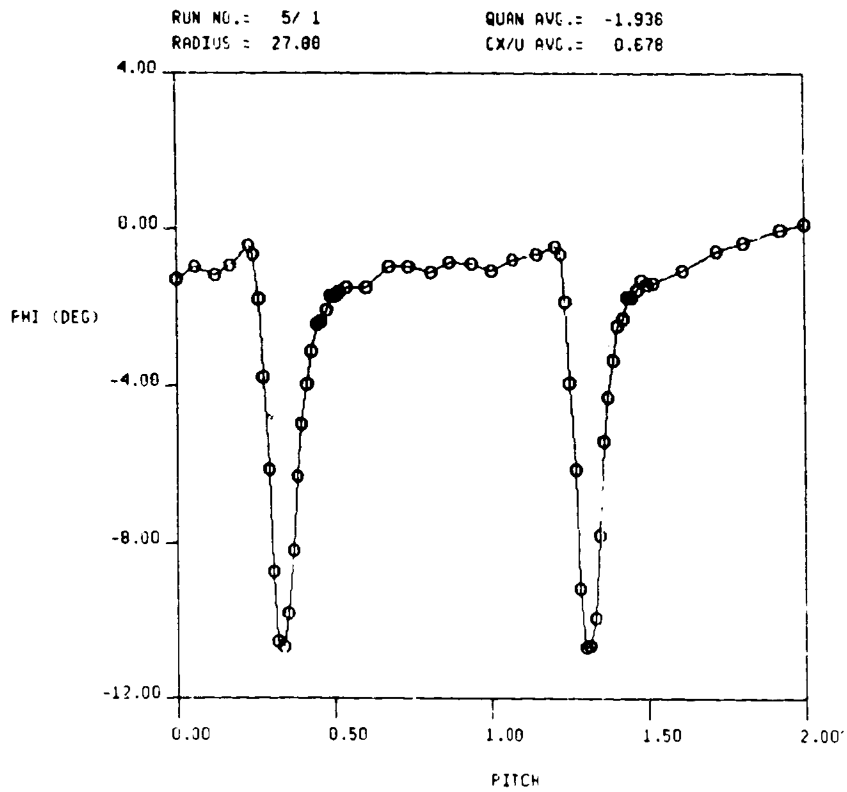

ORIGINAL PAGE IS OF POOR QUALITY

FIG. 17a ABSOLUTE YAW AND PITCH ANGLES FROM 5-HOLE PROBE TRAVERSE AT 1ST STATOR EXIT (X/Bx = 0.17), GRID OUT

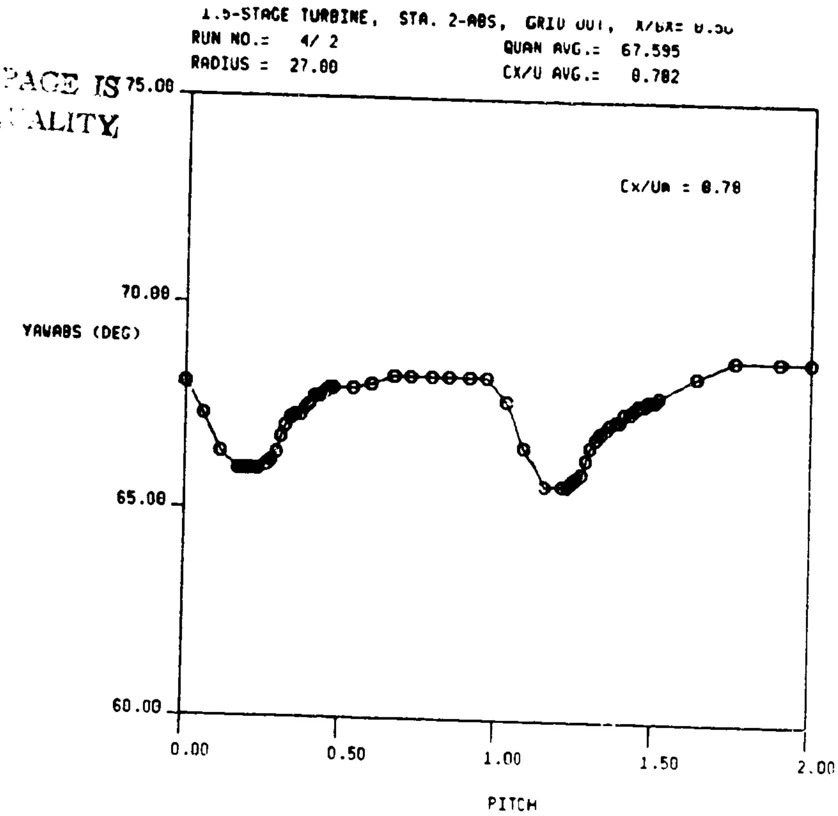

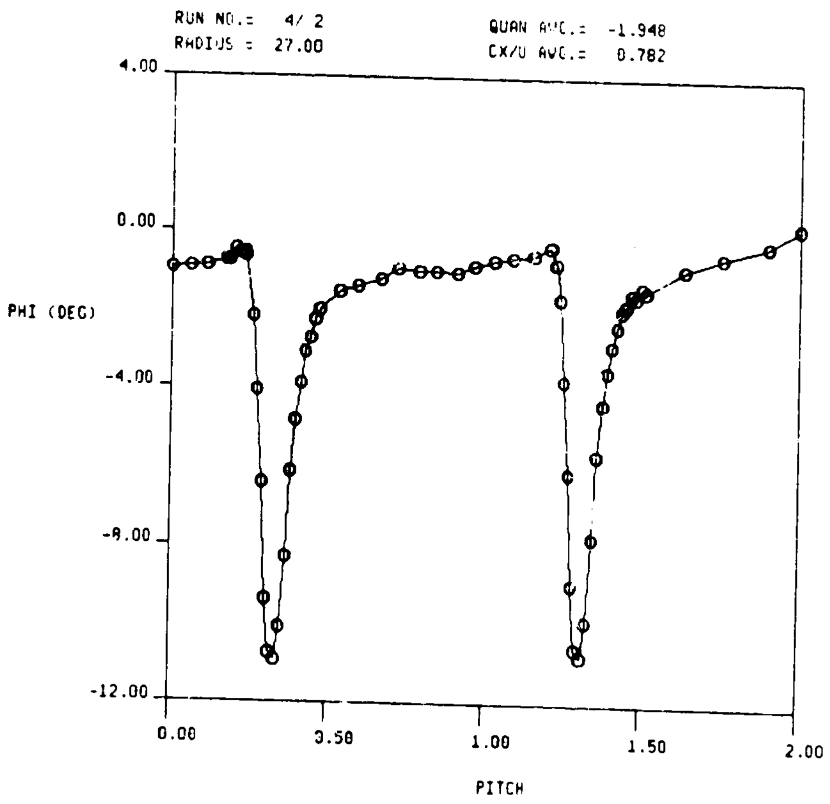

FIG. 17b ABSOLUTE YAW AND PITCH ANGLES FROM 5-HOLE PROBE TRAVERSE AT 1ST STATOR EXIT (X/Bx = 0.17), GRID OUT

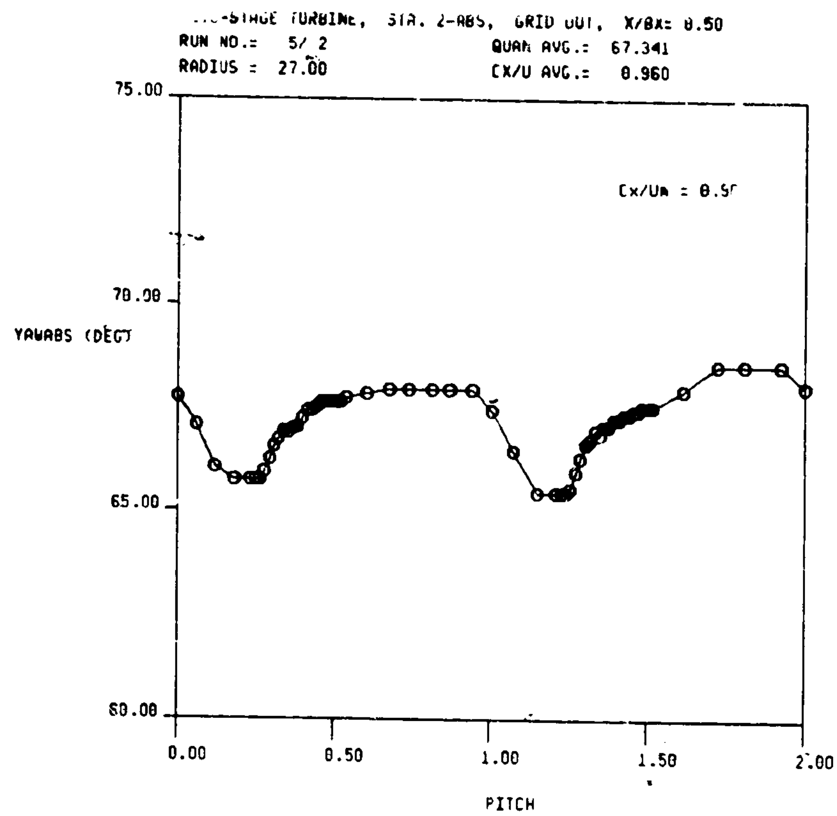

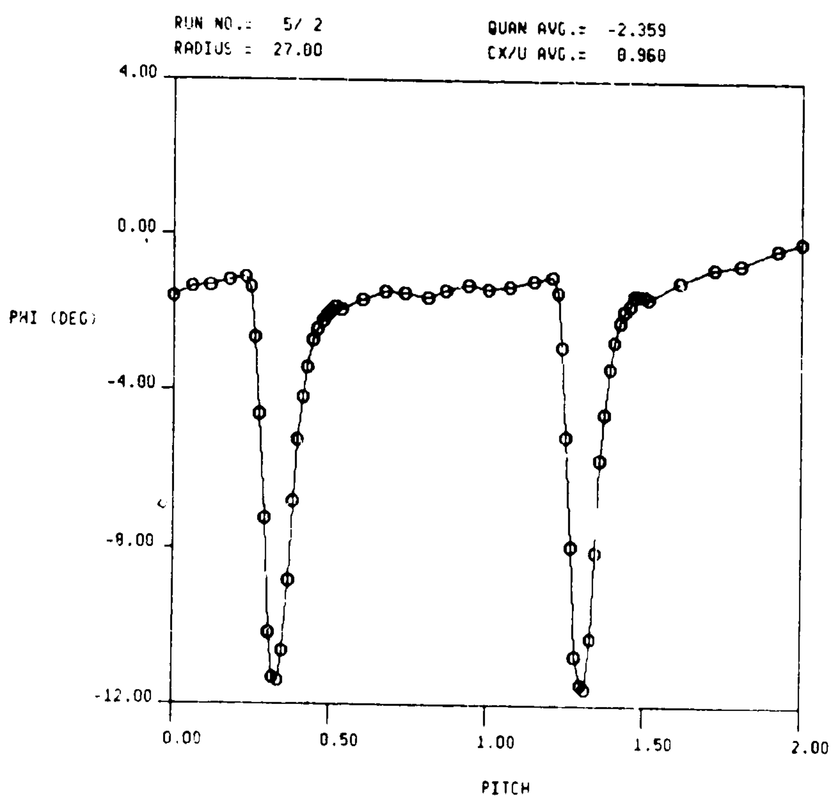

ORIGINAL PAGE IS
OF POOR QUALITY

FIG. 17c ABSOLUTE YAW AND PITCH ANGLES FROM 5-HOLE PROBE TRAVERSE AT 1ST STATOR EXIT (X/Bx = 0.17), GRID OUT

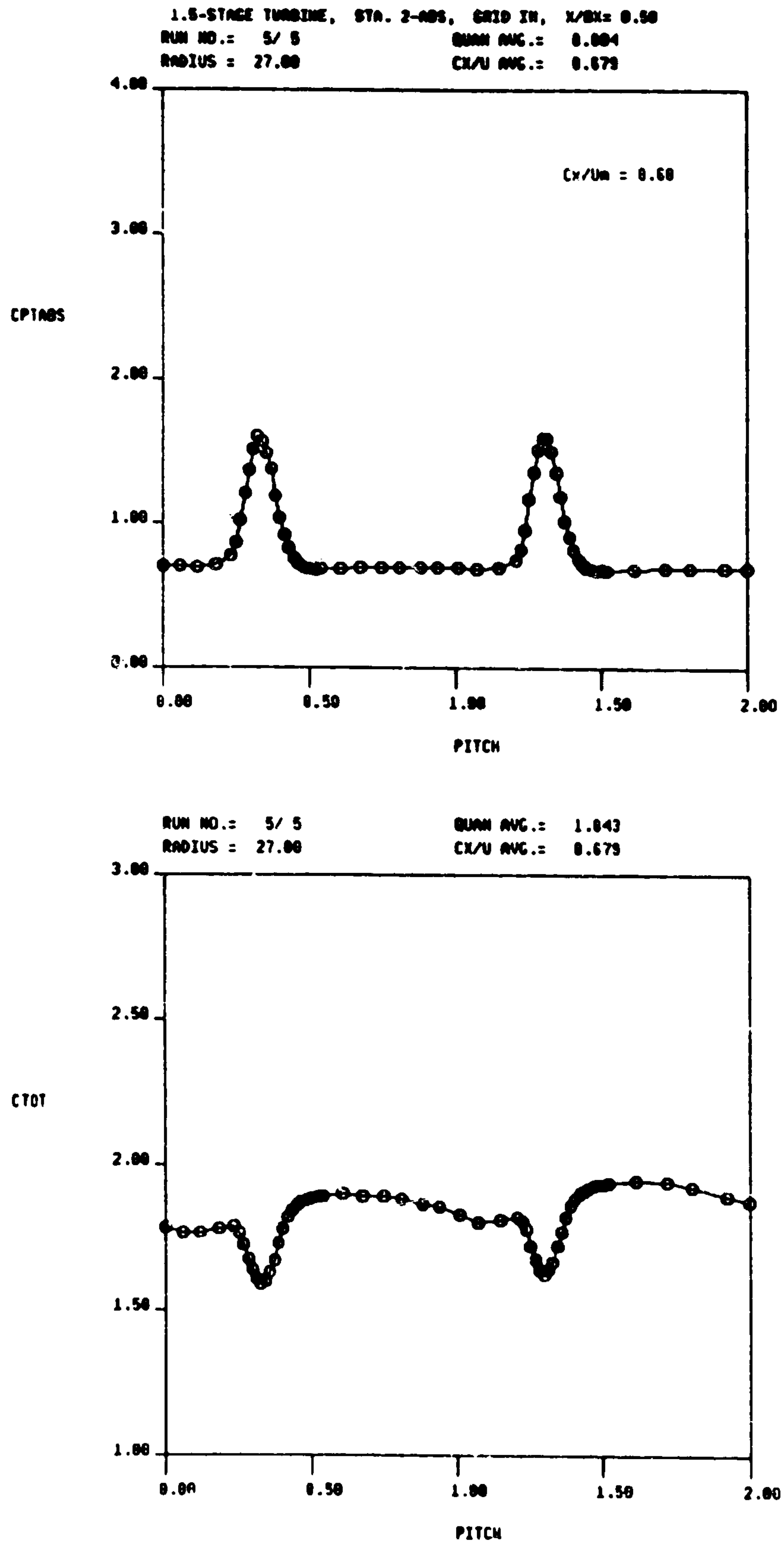

FIG. 18a ABSOLUTE TOTAL PRESSURE AND VELOCITY FROM 5-HOLE PROBE TRAVERSE AT 1ST STATOR EXIT (X/Bx = 0.17), GRID IN

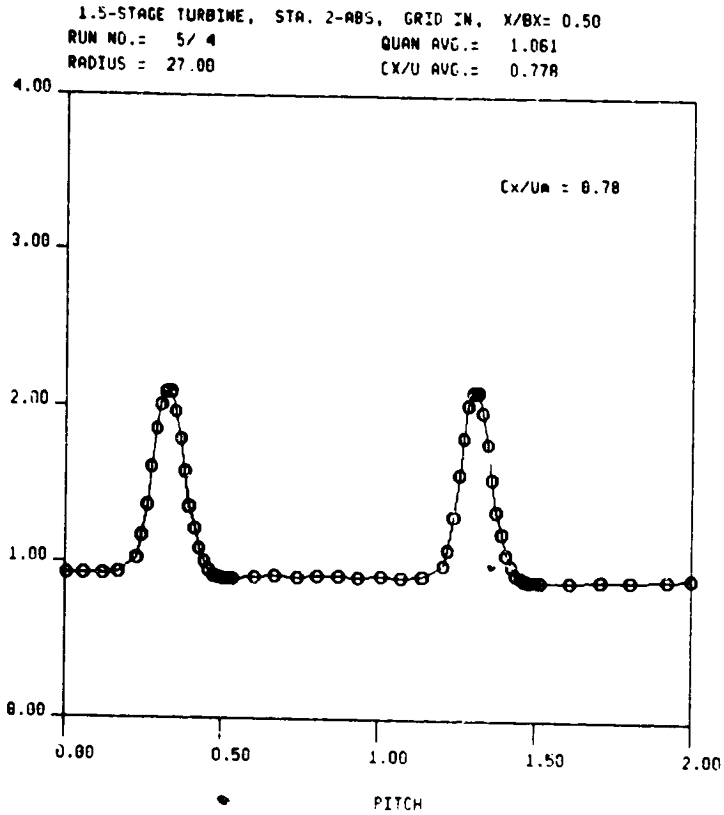

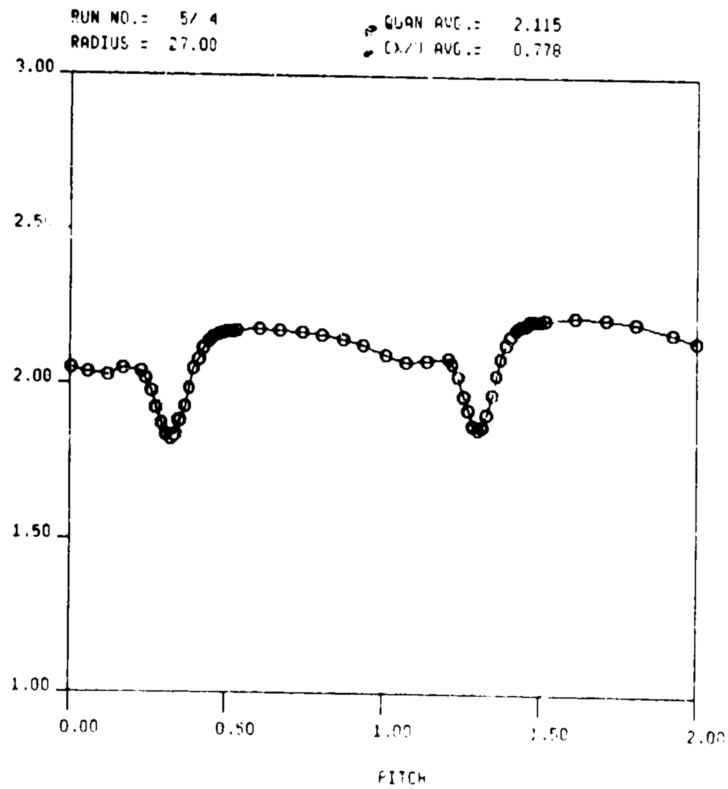

ORIGINAL PAGE IS
OF POOR QUALITY

FIG. 18b ABSOLUTE TOTAL PRESSURE AND VELOCITY FROM 5-HOLE PROBE TRAVERSE AT 1ST STATOR EXIT (X/Bx = 0.17), GRID IN

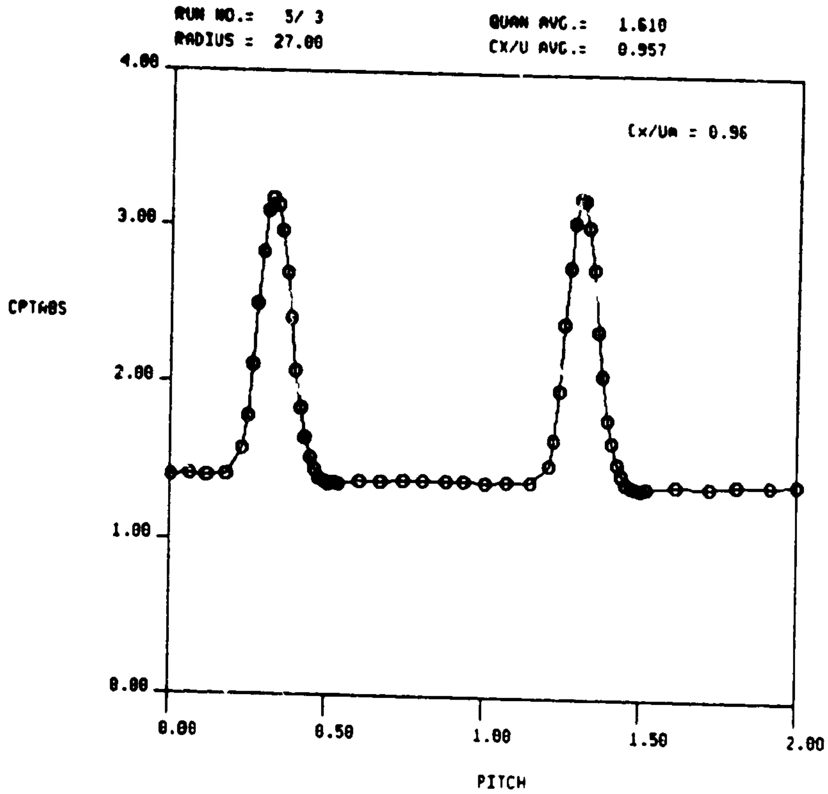

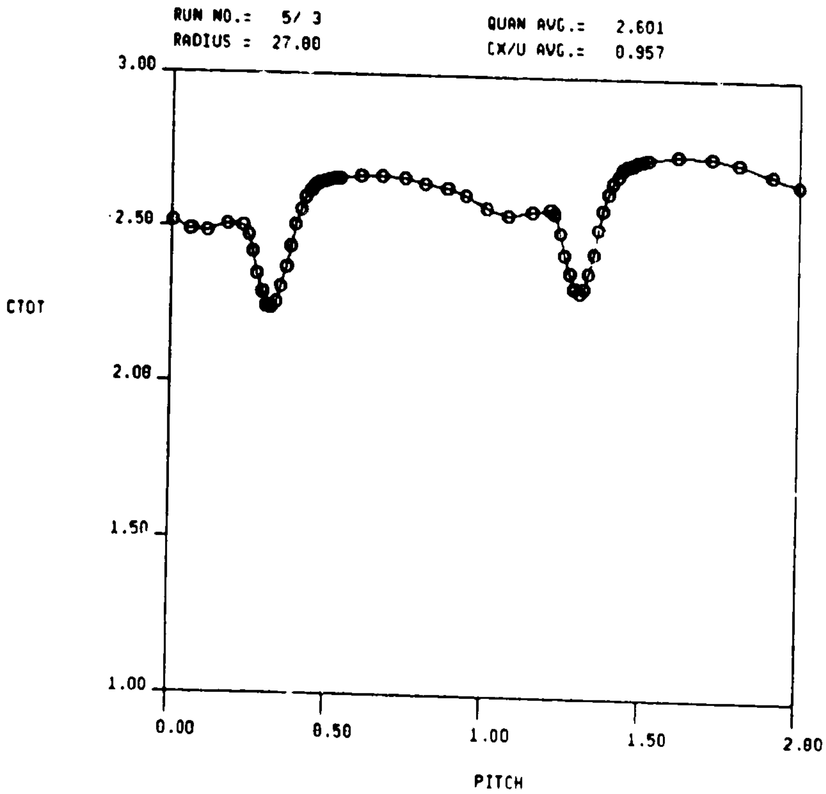

FIG. 18c ABSOLUTE TOTAL PRESSURE AND VELOCITY FROM 5-HOLE PROBE TRAVERSE AT 1ST STATOR EXIT (X/Bx = 0.17), GRID IN

ORIGINAL PAGE IS
OF POOR QUALITY

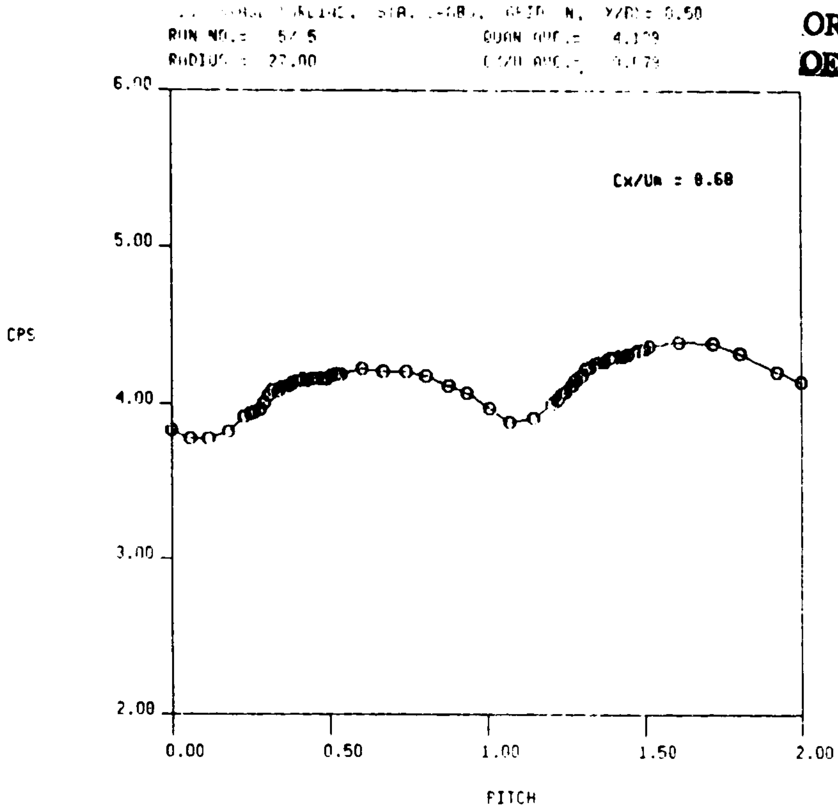

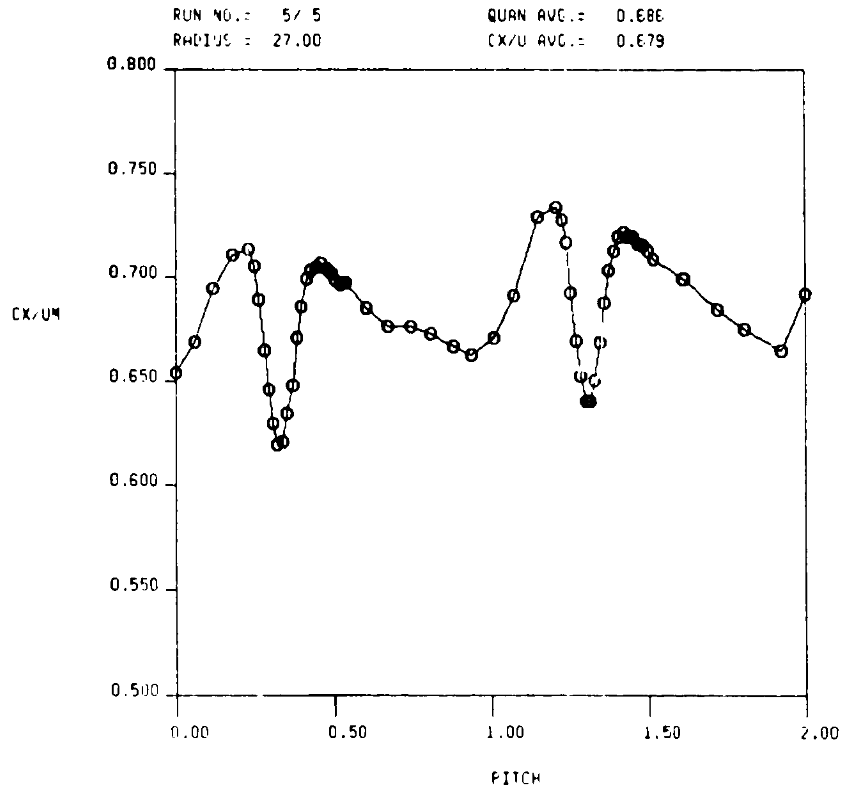

FIG. 19a STATIC PRESSURE AND AXIAL VELOCITY FROM 5-HOLE PROBE TRAVERSE AT 1ST STATOR EXIT (X/Bx = 0.17), GRID IN

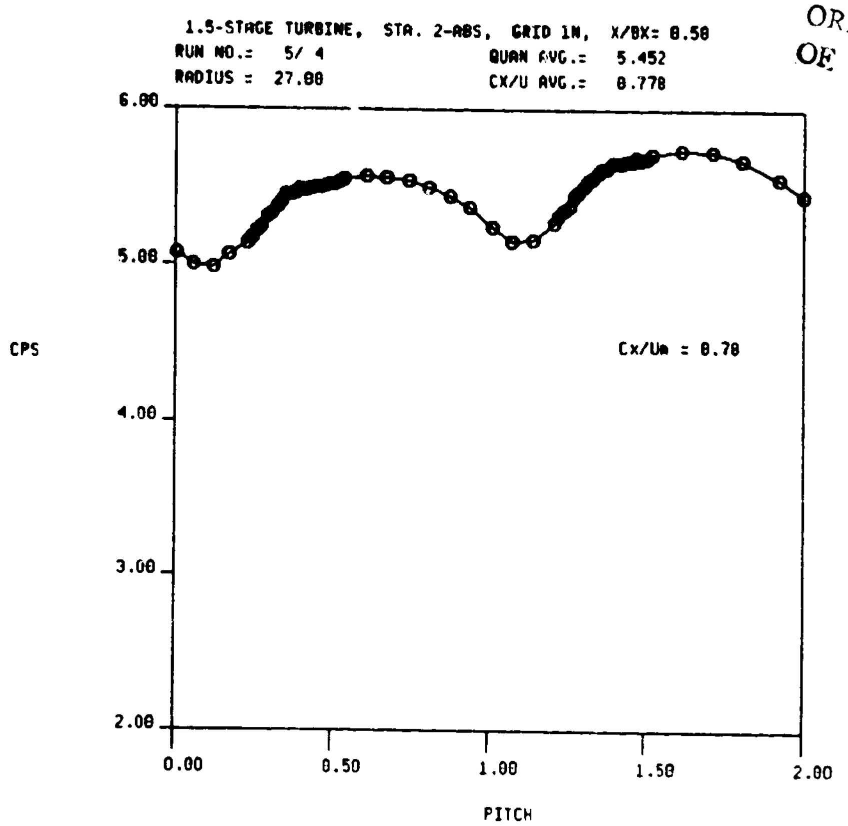

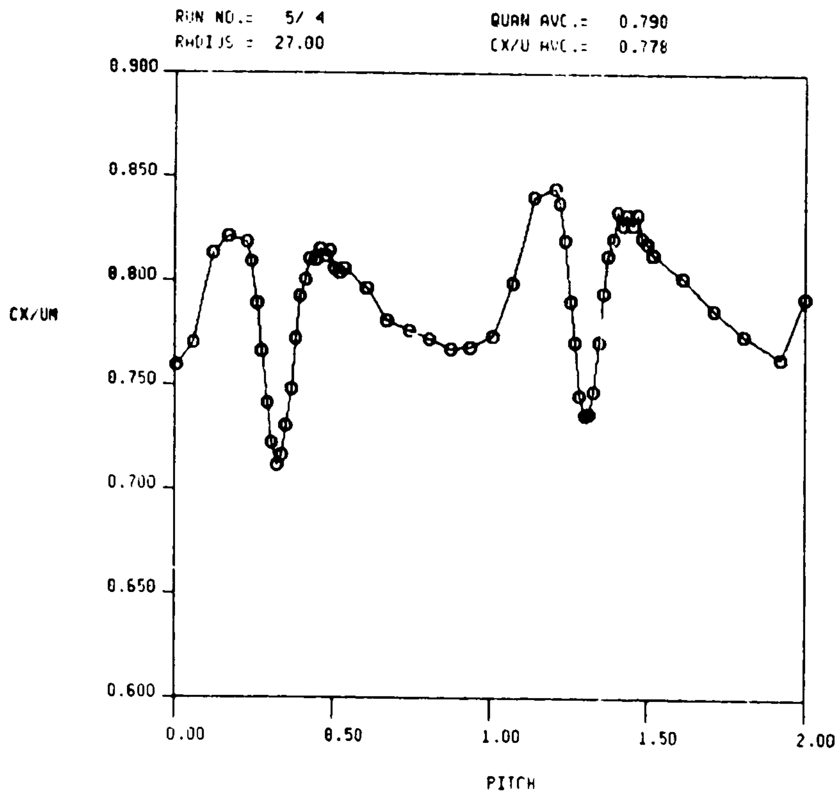

FIG. 19b STATIC PRESSURE AND AXIAL VELOCITY FROM 5-HOLE PROBE TRAVERSE AT 1ST STATOR EXIT (X/Bx = 0.17), GRID IN

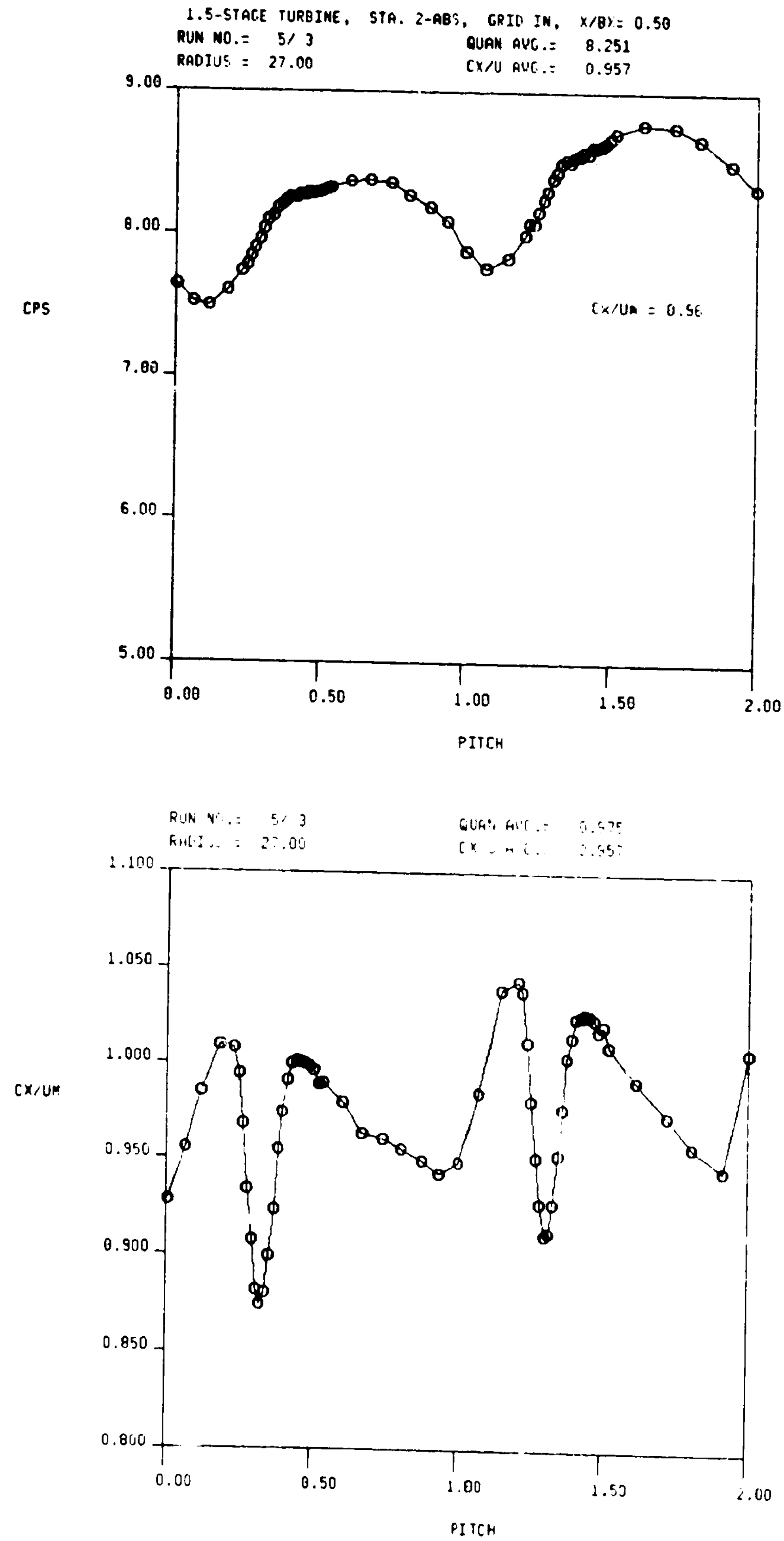

FIG. 19c STATIC PRESSURE AND AXIAL VELOCITY FROM 5-HOLE PROBE TRAVERSE AT 1ST STATOR EXIT (X/Bx = 0.17), GRID IN

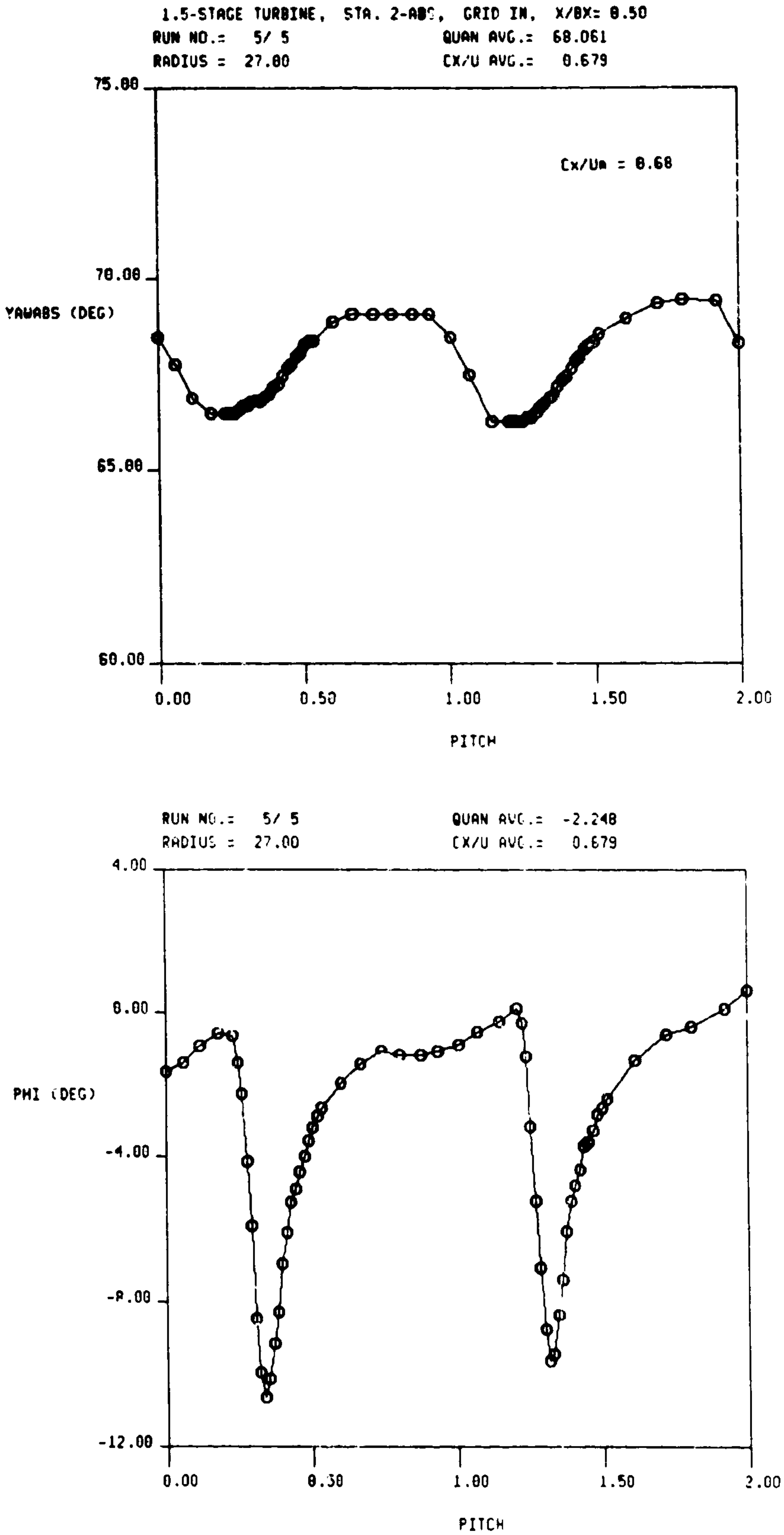

FIG. 20a ABSOLUTE YAW AND PITCH ANGLES FROM 5-HOLE PROBE TRAVERSE AT 1ST STATOR EXIT (X/Bx = 0.17), GRID IN

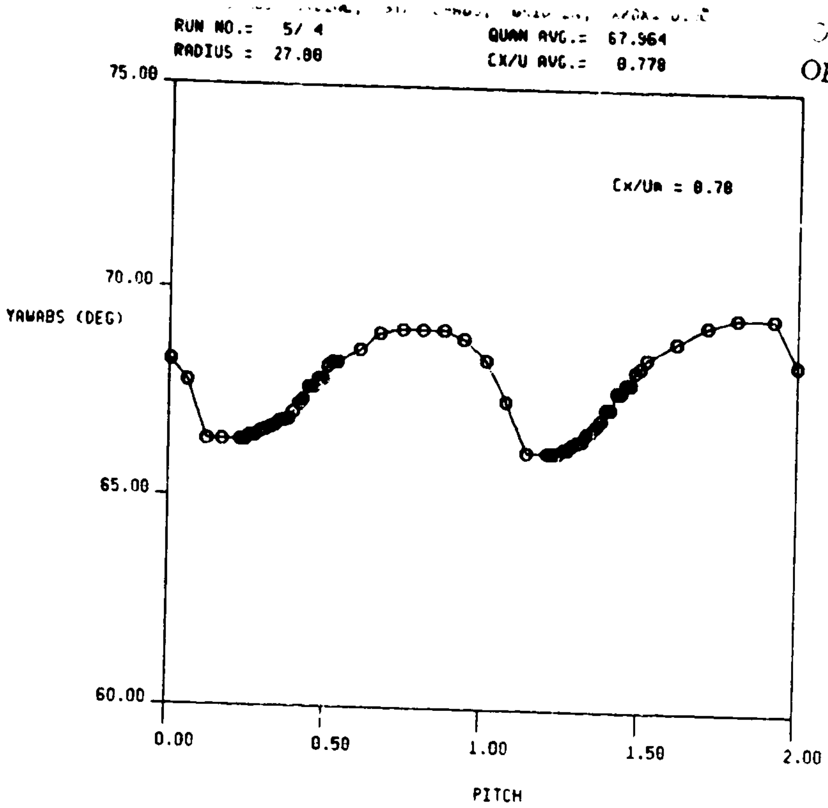

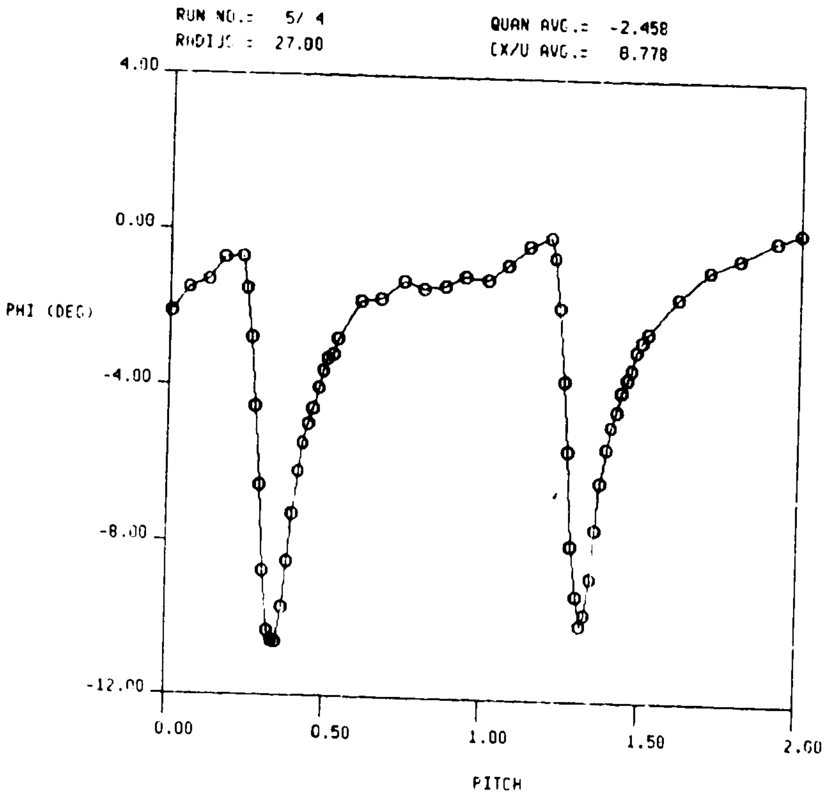

FIG. 20b ABSOLUTE YAW AND PITCH ANGLES FROM 5-HOLE PROBE TRAVERSE AT 1ST STATOR EXIT (X/Bx = 0.17), GRID IN

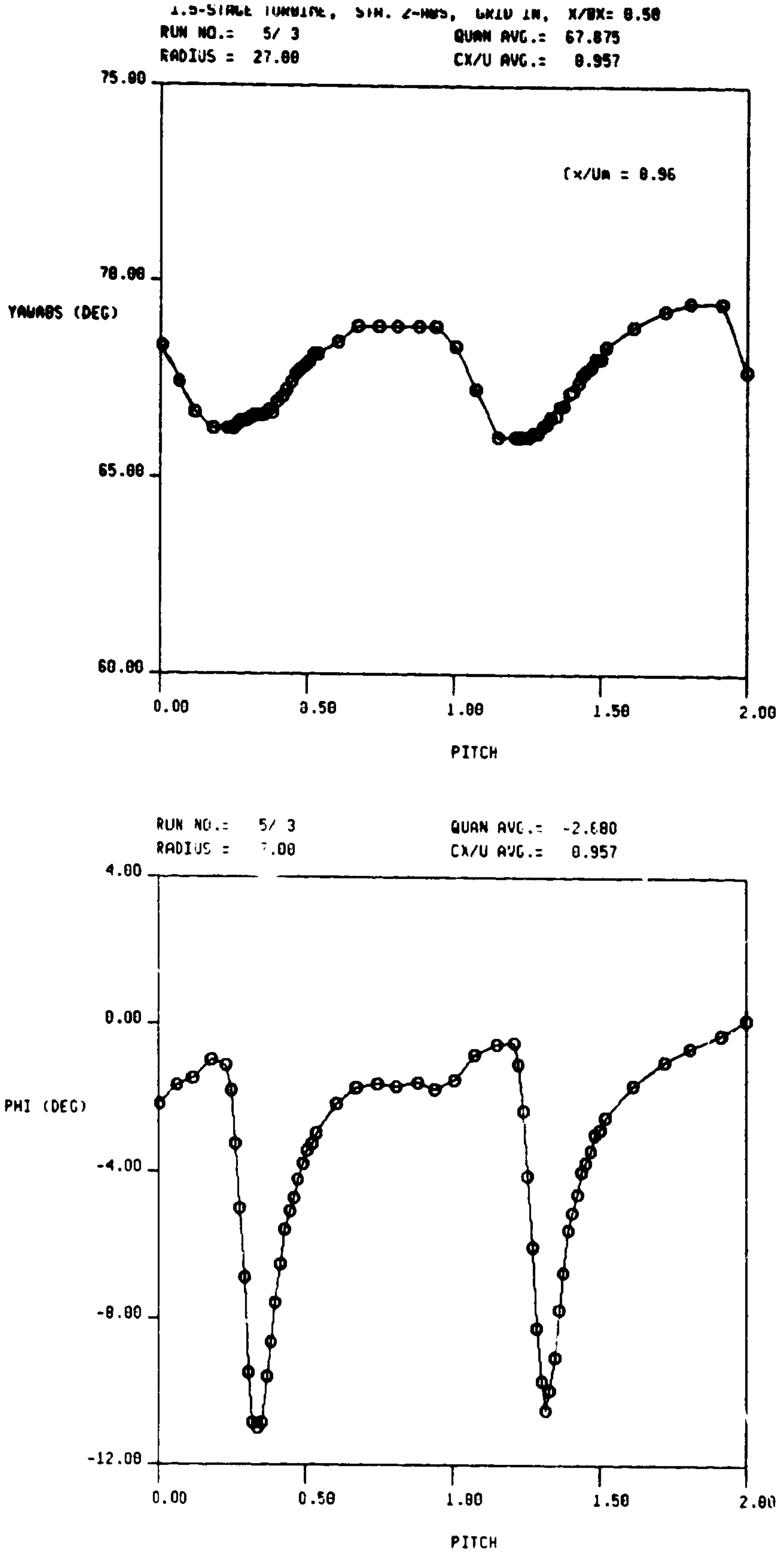

FIG. 20c ABSOLUTE YAW AND PITCH ANGLES FROM 5-HOLE PROBE TRAVERSE AT 1ST STATOR EXIT (X/Bx = 0.17), GRID IN

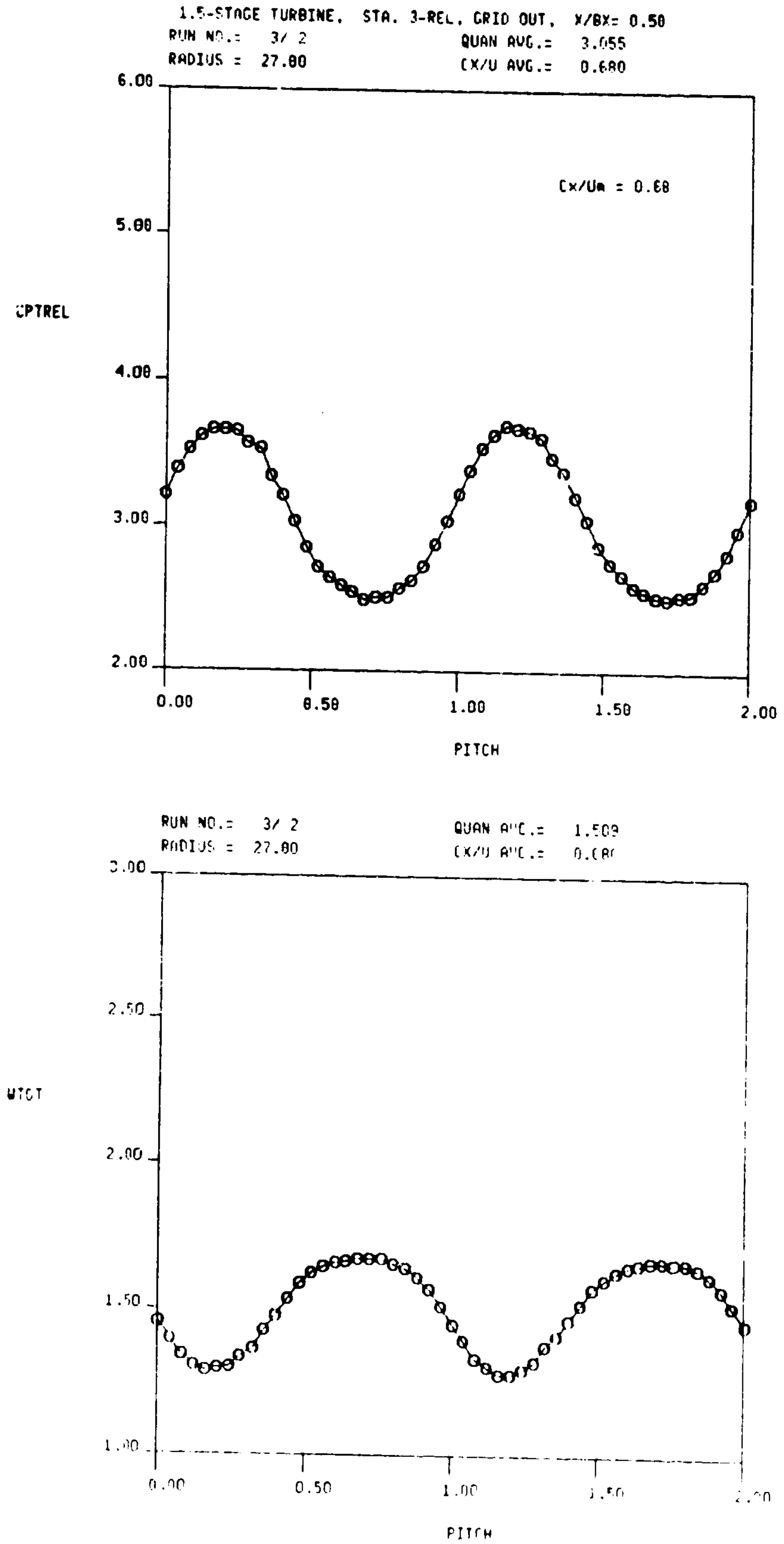

FIG. 21a RELATIVE TOTAL PRESSURE AND VELOCITY FROM 5-HOLE PROBE TRAVERSE AT ROTOR EXIT (X/Bx = 0.36), GRID OUT

OPIGINAL PAGE IS
OF POOR QUALITY

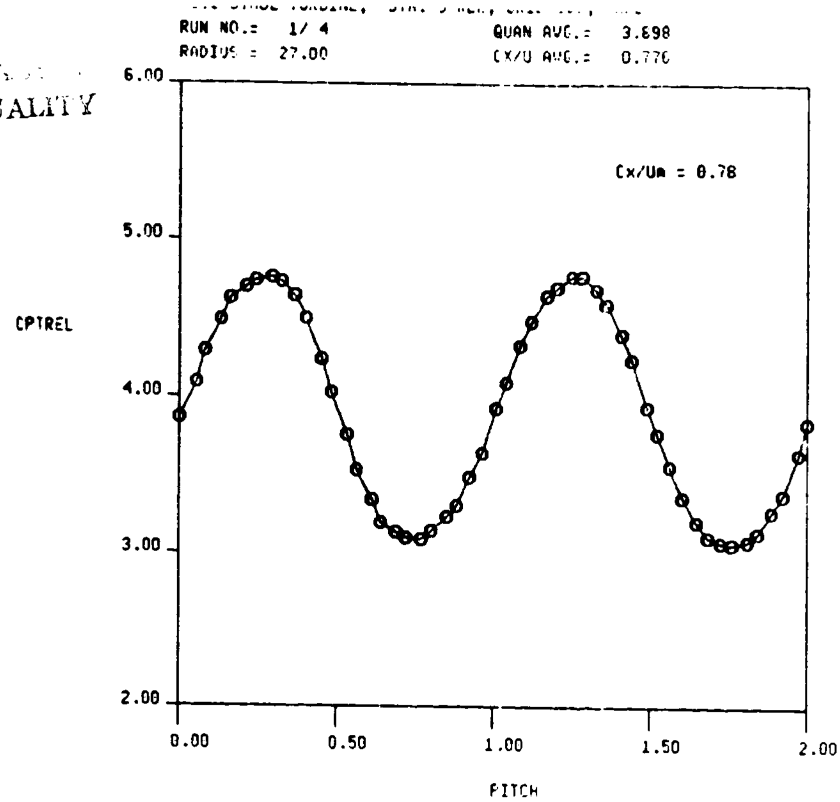

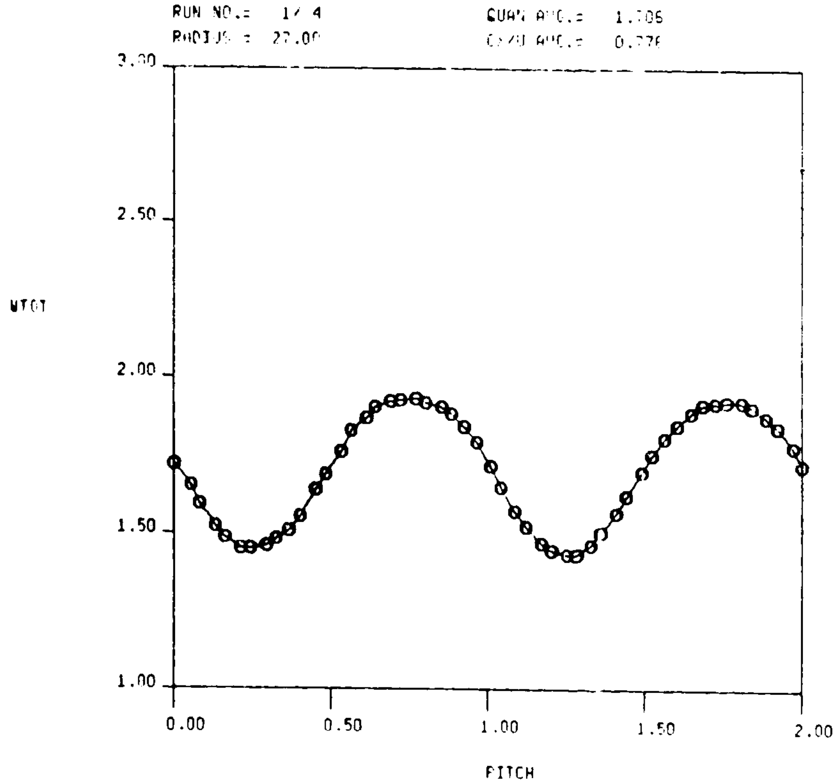

FIG. 21b RELATIVE TOTAL PRESSURE AND VELOCITY FROM 5-HOLE PROBE TRAVERSE AT ROTOR EXIT (X/Bx = 0.36), GRID OUT

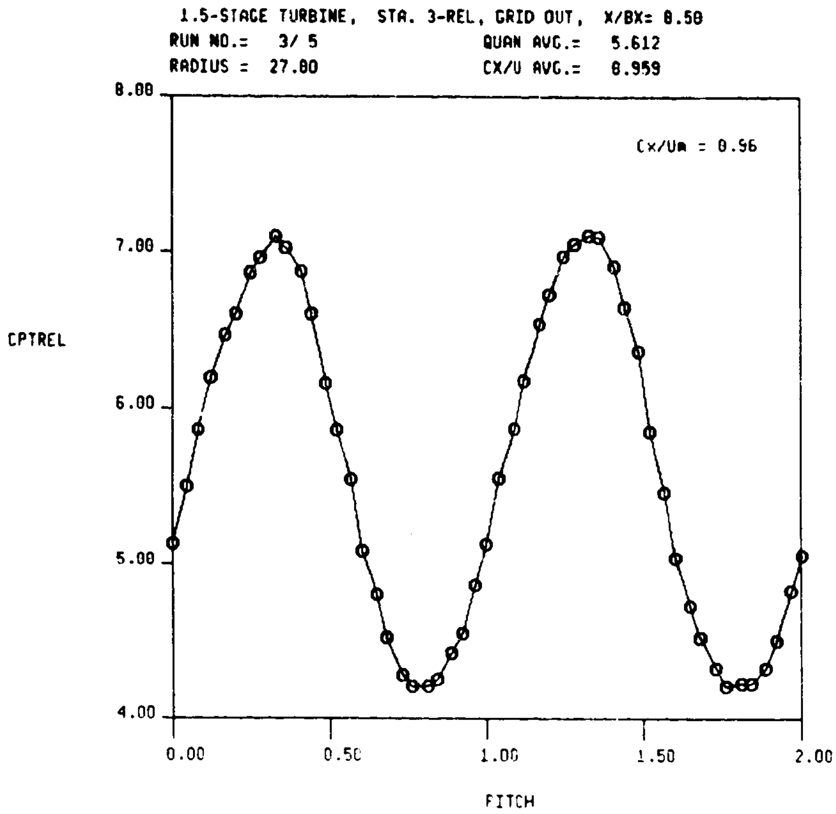

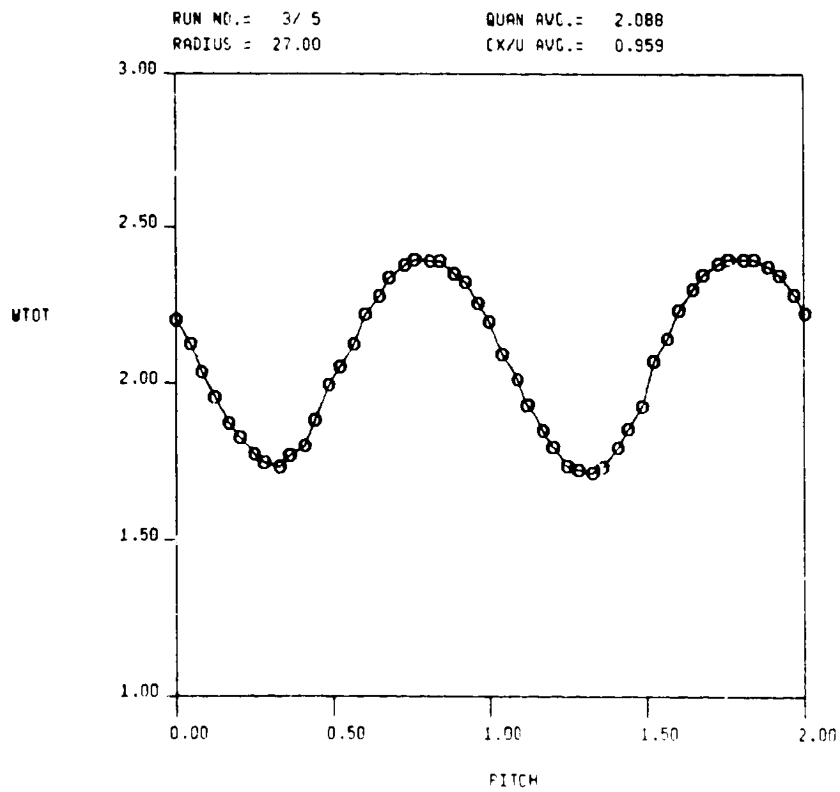

FIG. 21c RELATIVE TOTAL PRESSURE AND VELOCITY FROM 5-HOLE PROBE TRAVERSE AT ROTOR EXIT (X/Bx = 0.36), GRID OUT

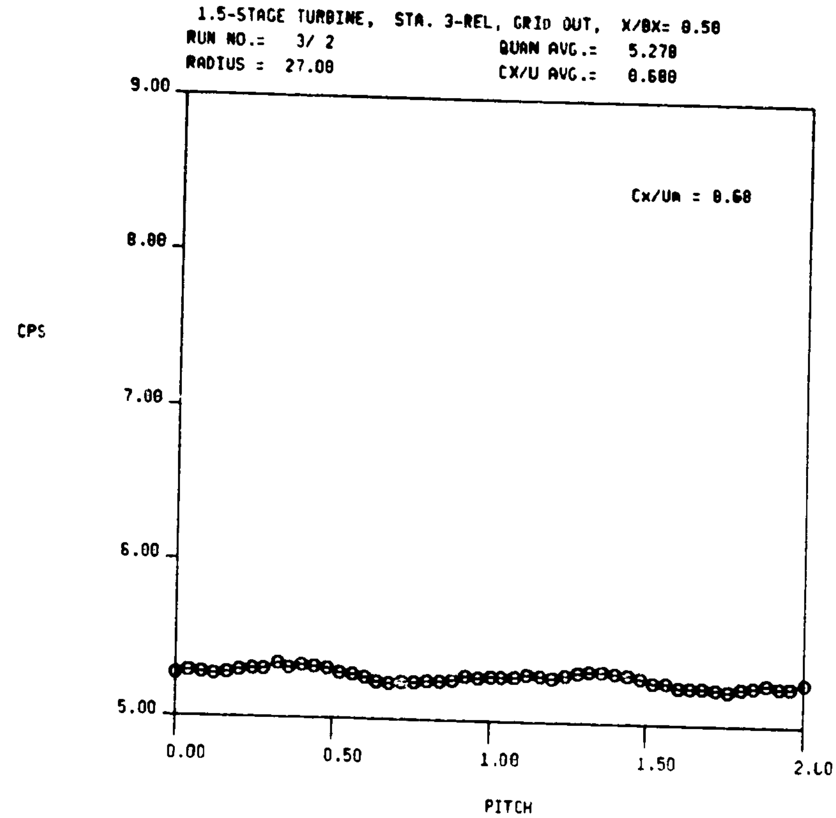

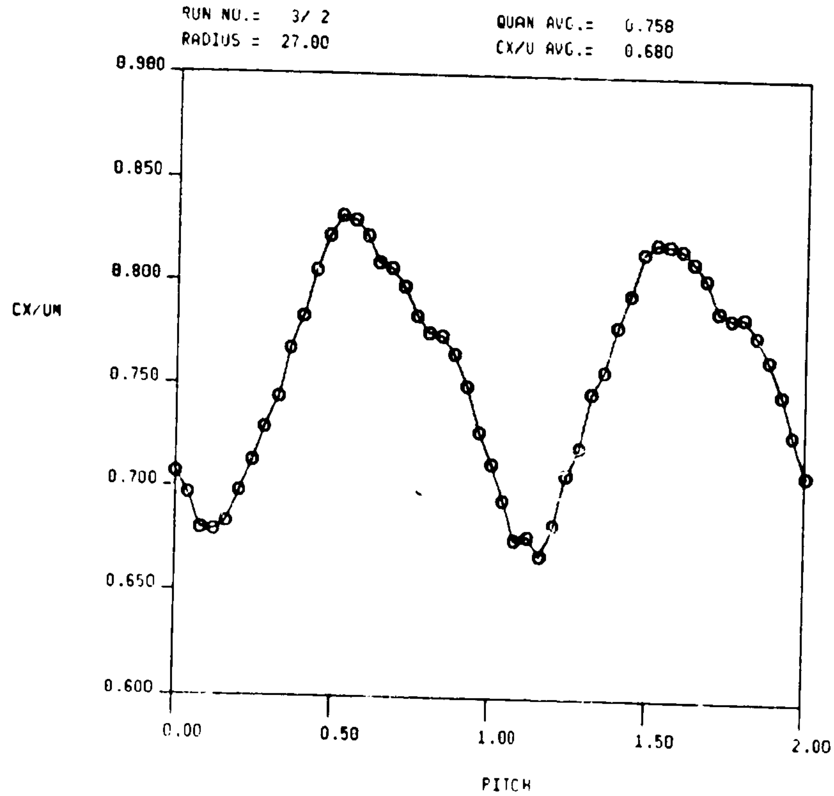

FIG. 22a STATIC PRESSURE AND AXIAL VELOCITY FROM 5-HOLE PROBE TRAVERSE AT ROTOR EXIT (X/Bx = 0.36), GRID OUT

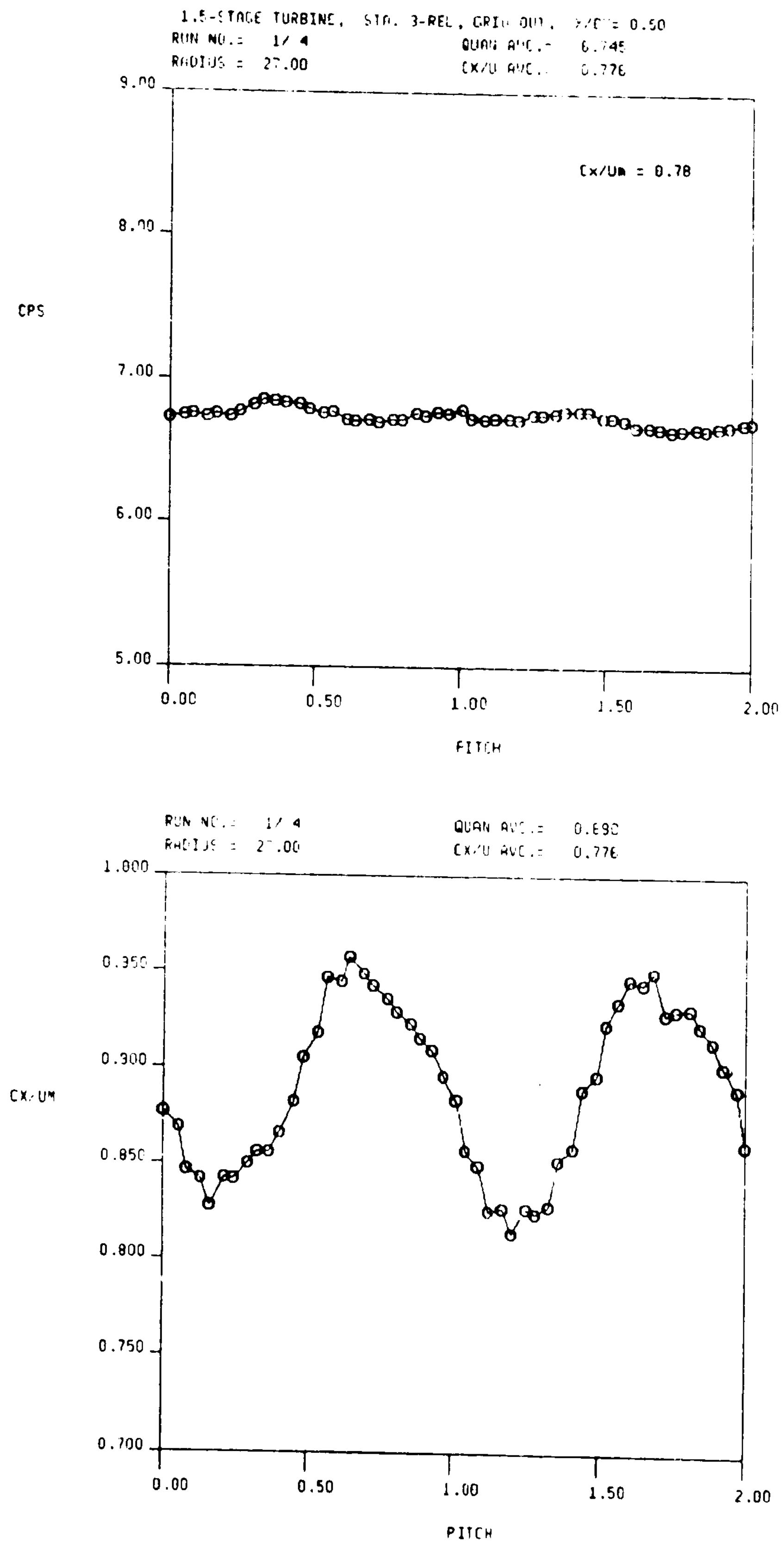

FIG. 22b STATIC PRESSURE AND AXIAL VELOCITY FROM 5-HOLE PROBE TRAVERSE AT ROTOR EXIT (X/Bx = 0.36), GRID OUT

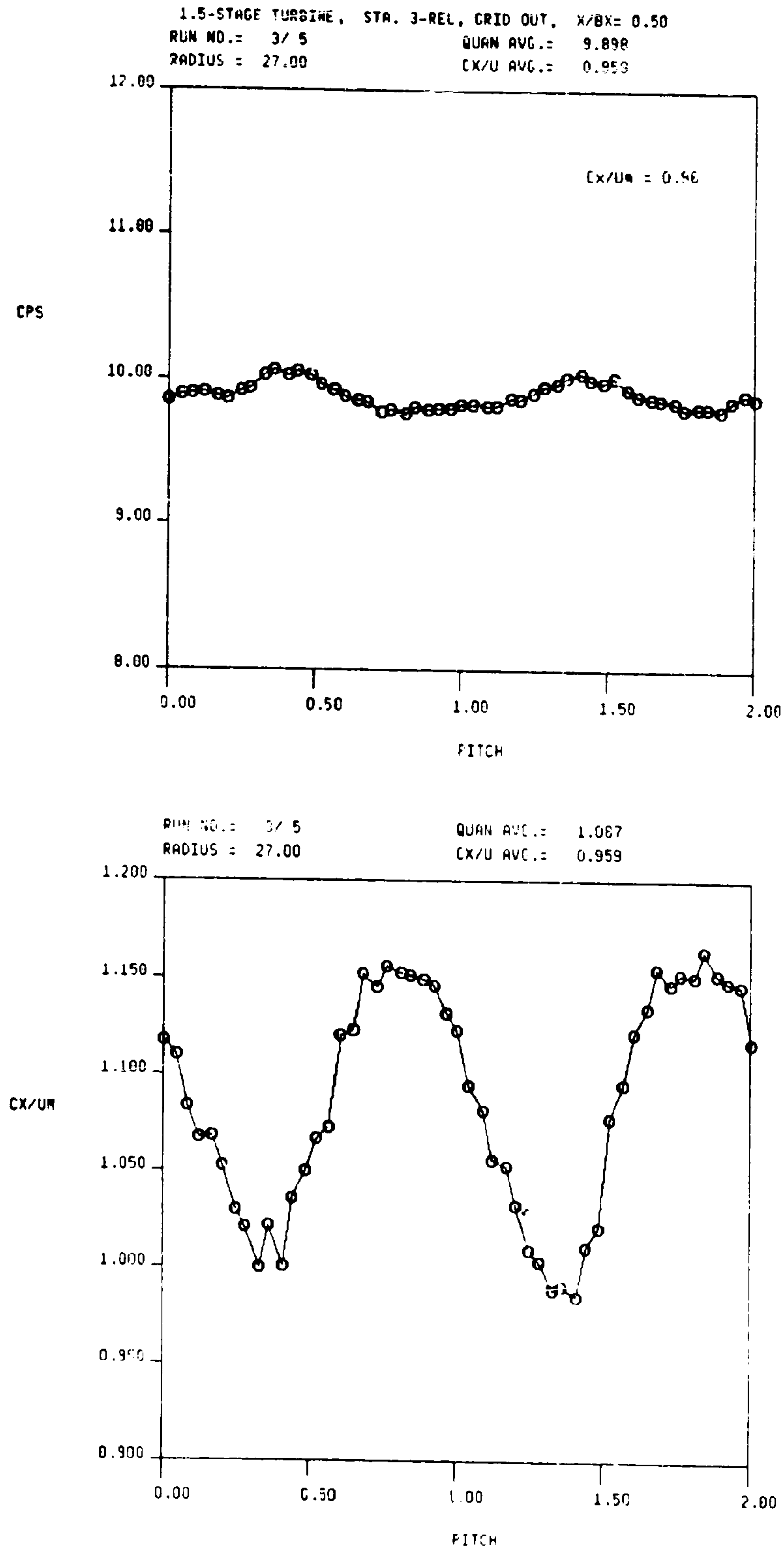

FIG. 22c STATIC PRESSURE AND AXIAL VELOCITY FROM 5-HOLE PROBE TRAVERSE AT ROTOR EXIT (X/Bx = 0.36), GRID OUT

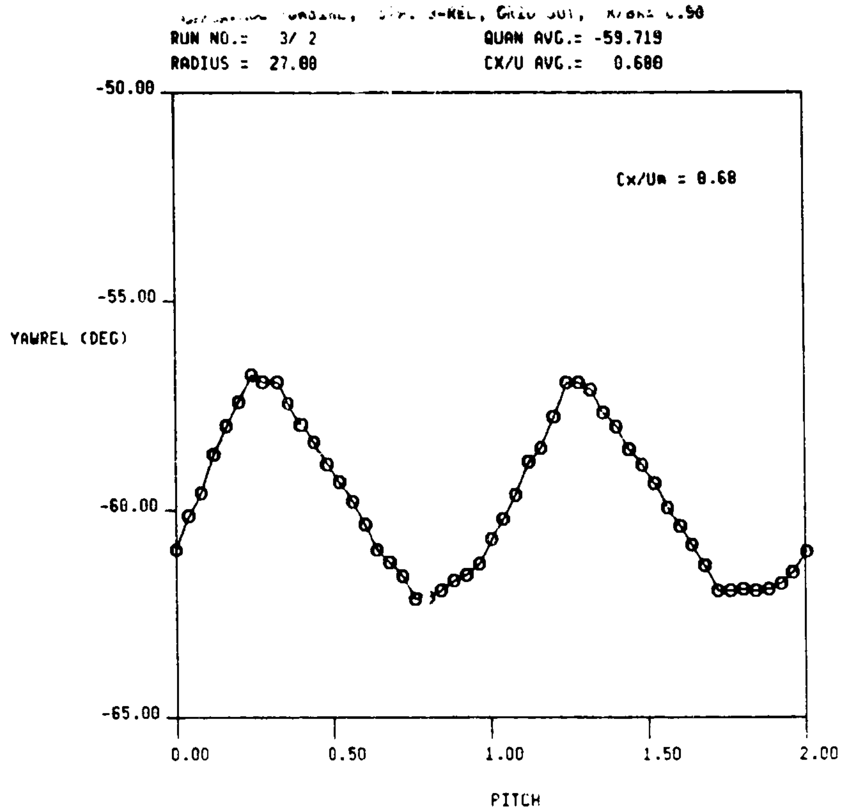

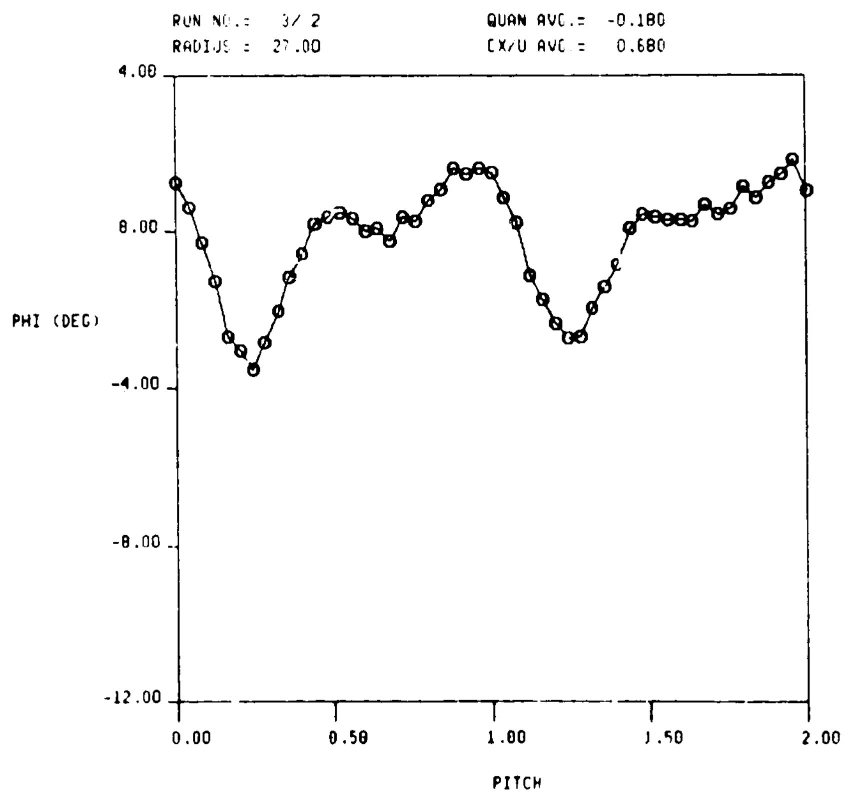

FIG. 23a RELATIVE YAW AND PITCH ANGLES FROM 5-HOLE PROBE TRAVERSE AT ROTOR EXIT (X/Bx = 0.36), GRID OUT

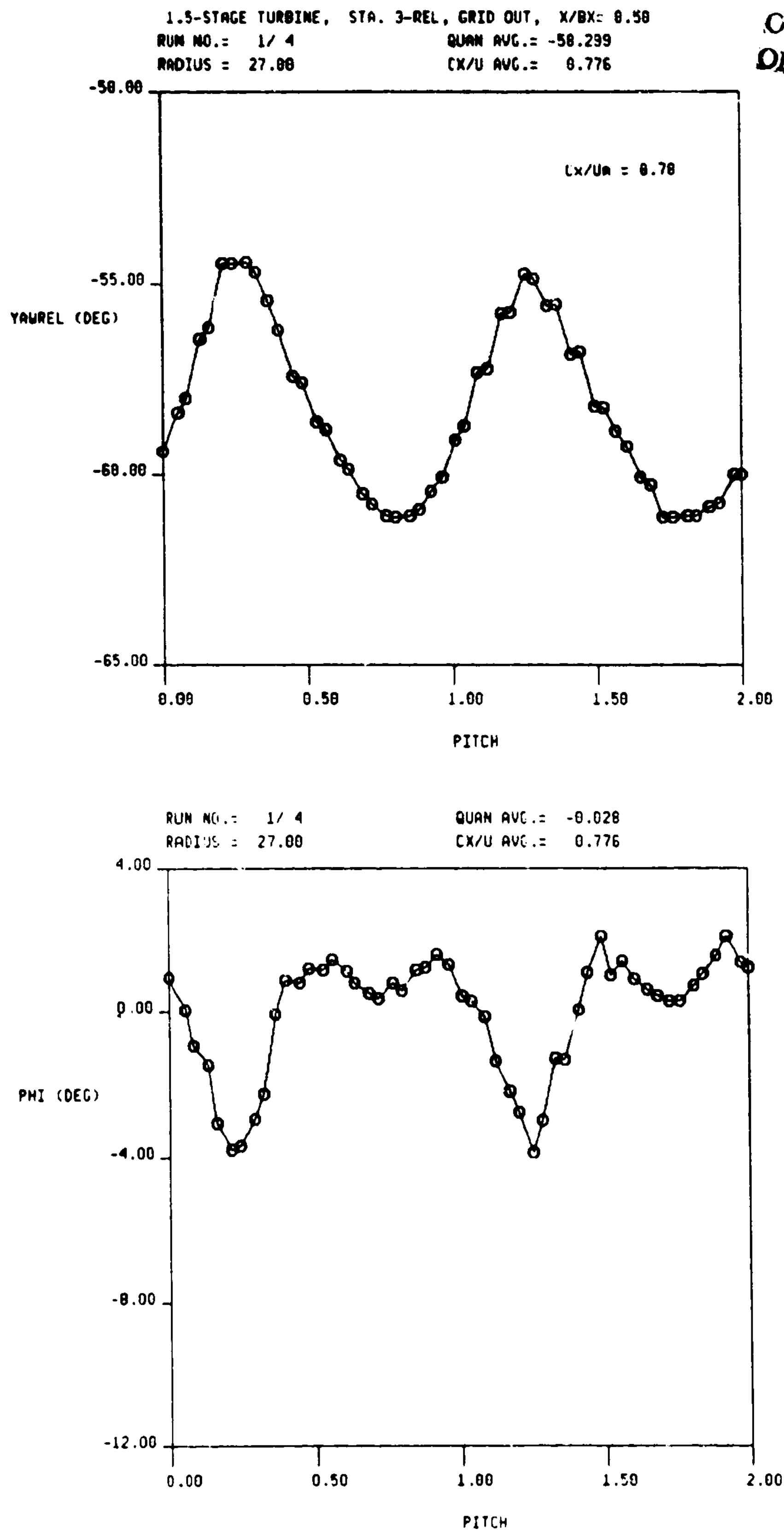

FIG. 23b RELATIVE YAW AND PITCH ANGLES FROM 5-HOLE PROBE TRAVERSE AT ROTOR EXIT (X/Bx = 0.36), GRID OUT

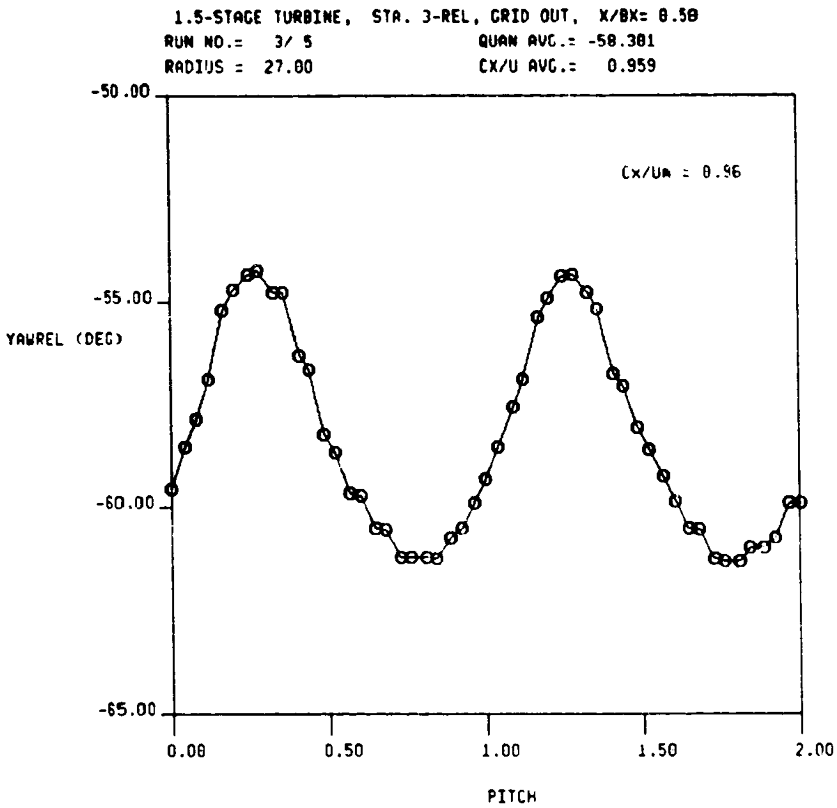

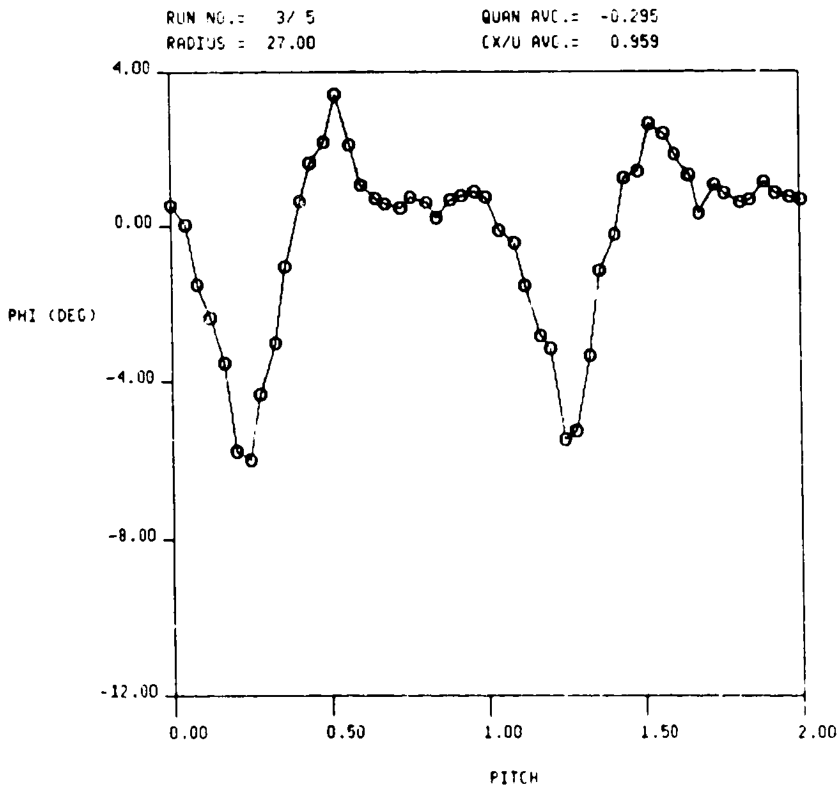

FIG. 23c RELATIVE YAW AND PITCH ANGLES FROM 5-HOLE PROBE TRAVERSE AT ROTOR EXIT (X/Bx = 0.36), GRID OUT

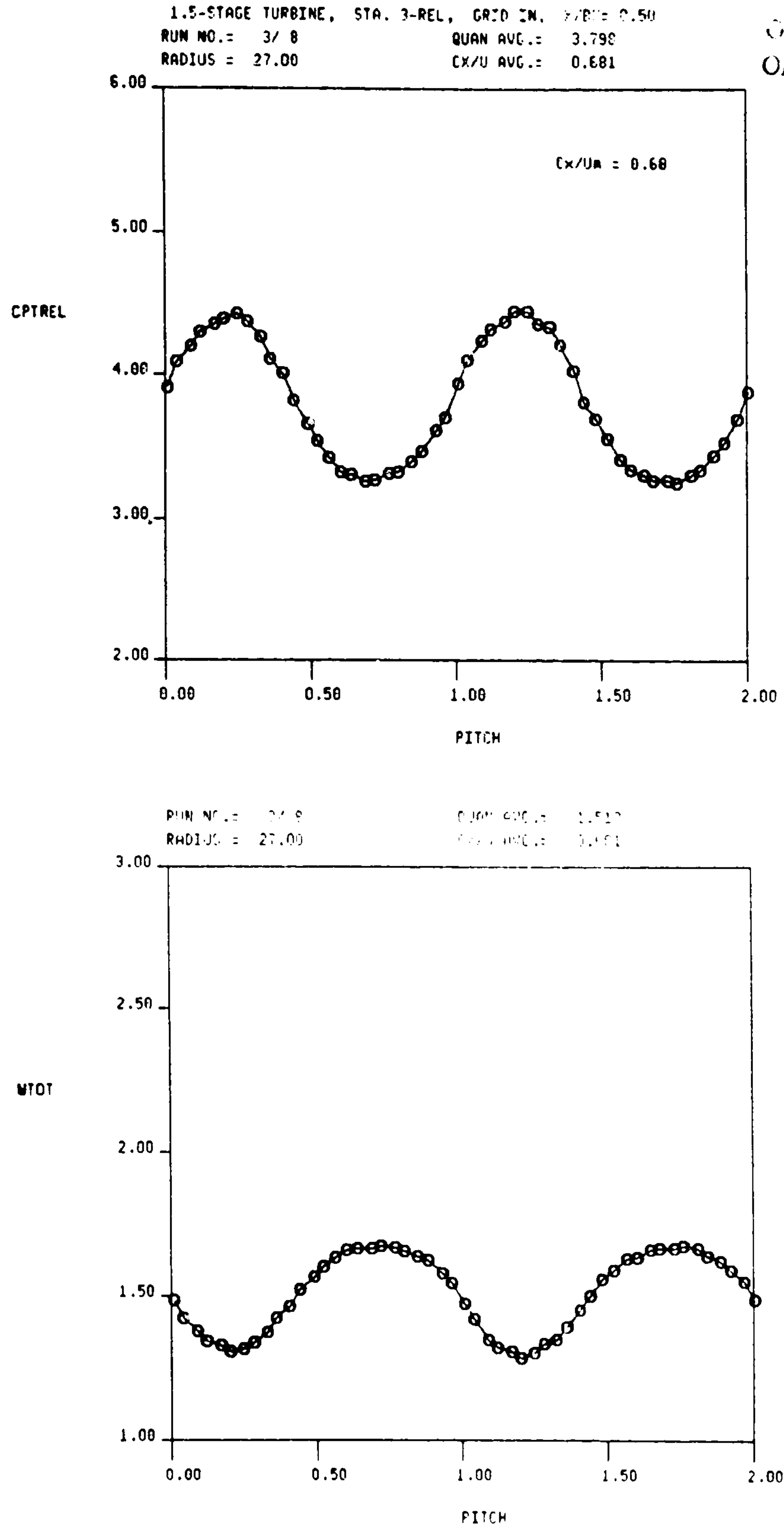

FIG. 24a RELATIVE TOTAL PRESSURE AND VELOCITY FROM 5-HOLE PROBE TRAVERSE AT ROTOR EXIT (X/Bx = 0.36), GRID IN

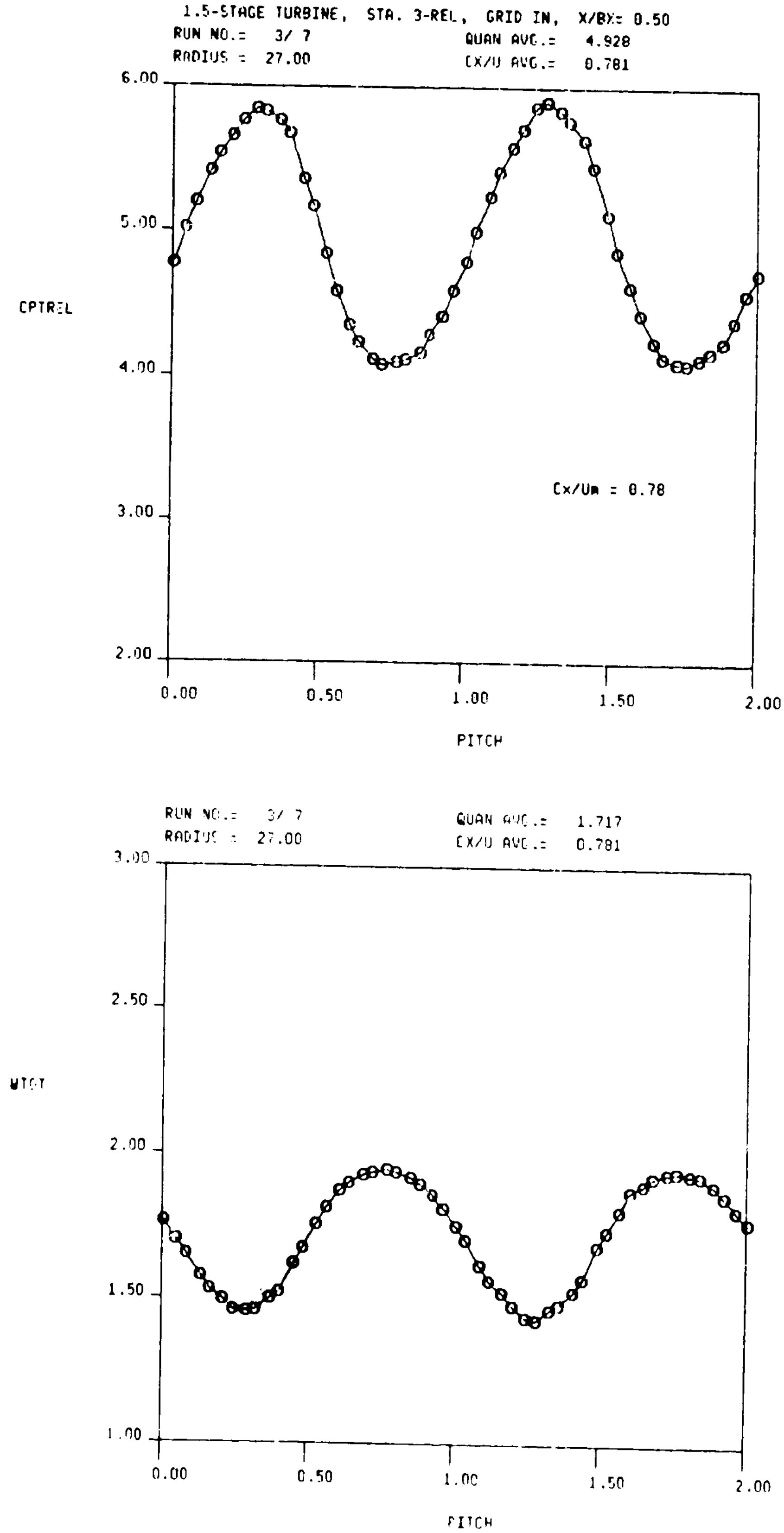

FIG. 24b RELATIVE TOTAL PRESSURE AND VELOCITY FROM 5-HOLE PROBE TRAVERSE AT ROTOR EXIT (X/Bx = 0.36), GRID IN

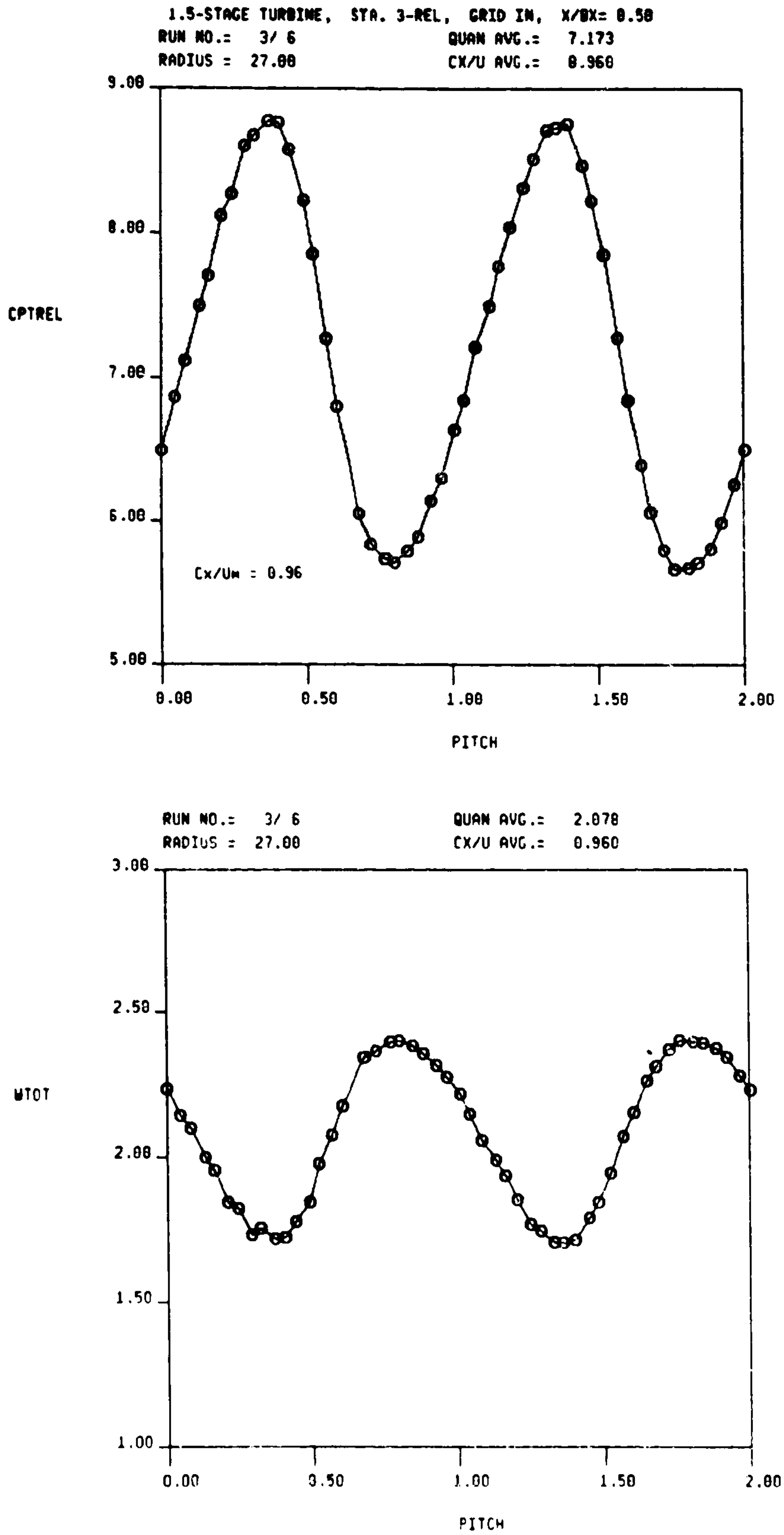

FIG. 24c RELATIVE TOTAL PRESSURE AND VELOCITY FROM 5-HOLE PROBE TRAVERSE AT ROTOR EXIT (X/Bx = 0.36), GRID IN

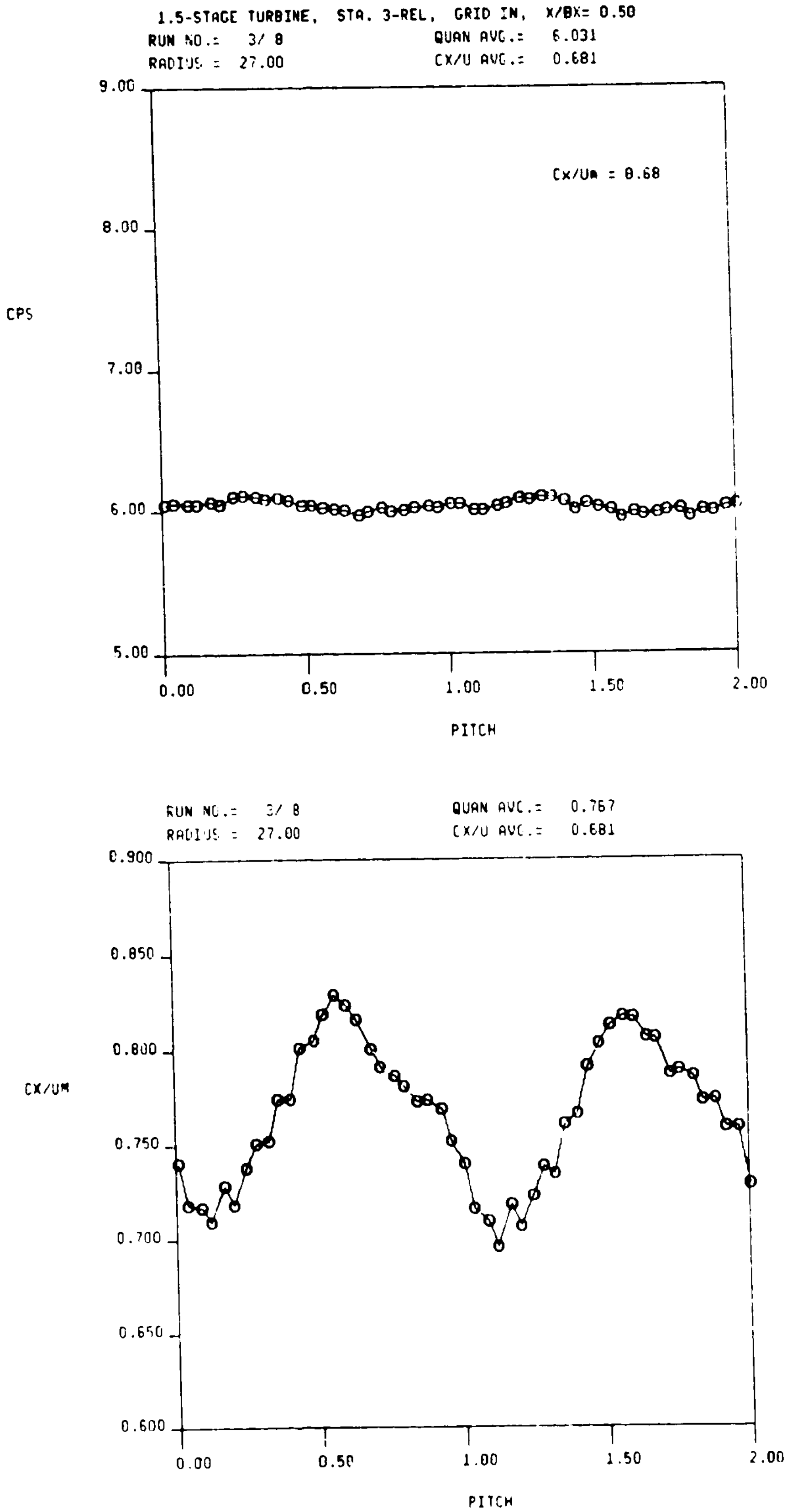

FIG. 25a STATIC PRESSURE AND AXIAL VELOCITY FROM 5-HOLE PROBE TRAVERSE AT ROTOR EXIT (X/Bx = 0.36), GRID IN

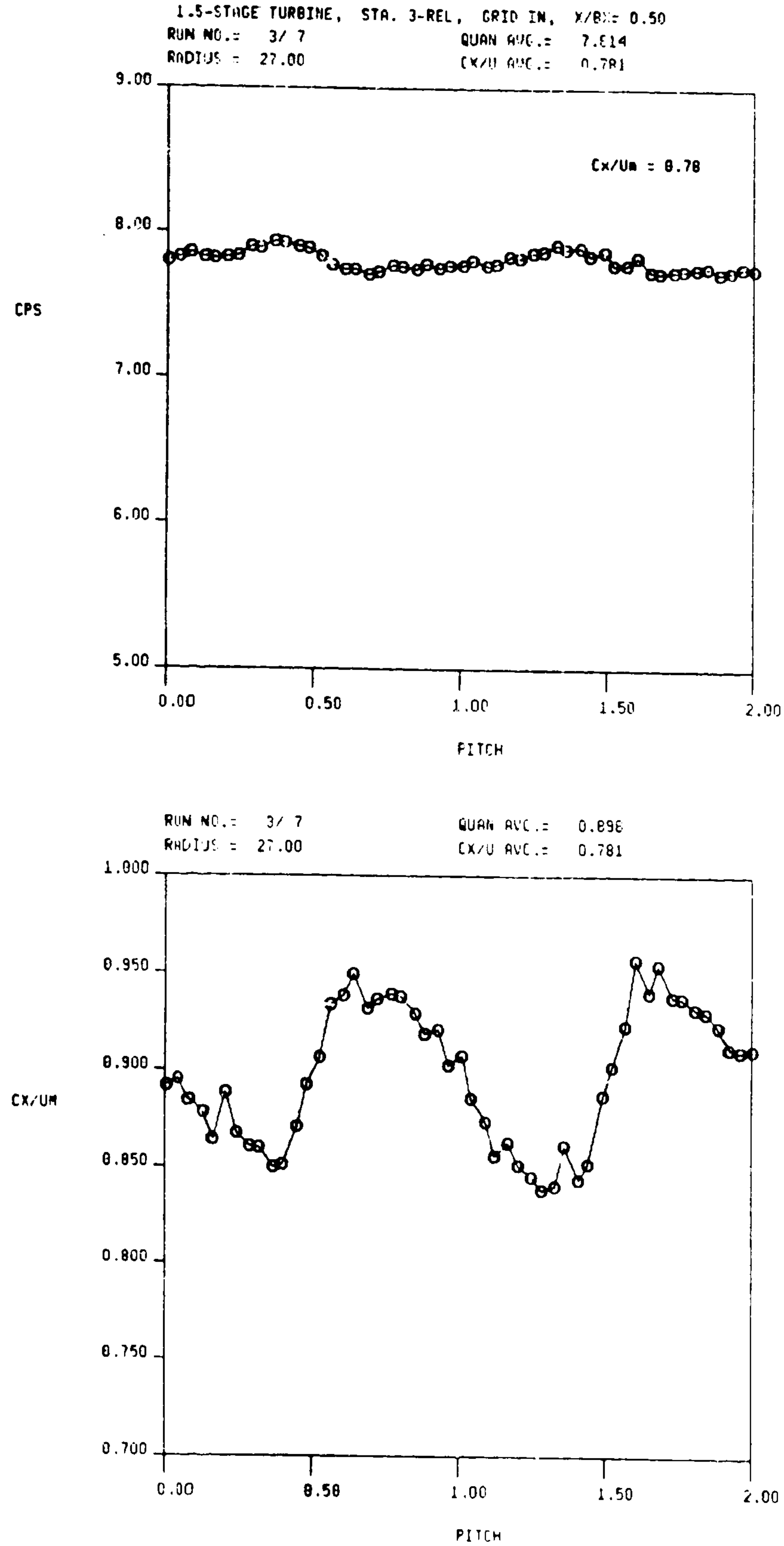

FIG. 25b STATIC PRESSURE AND AXIAL VELOCITY FROM 5-HOLE PROBE TRAVERSE AT ROTOR EXIT (X/Bx = 0.36), GRID IN

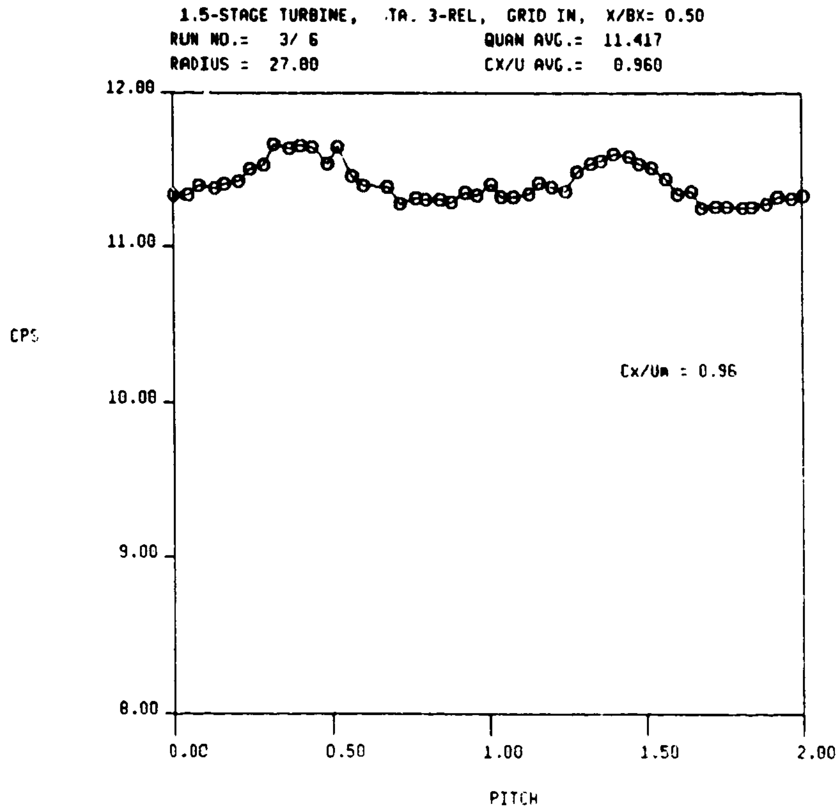

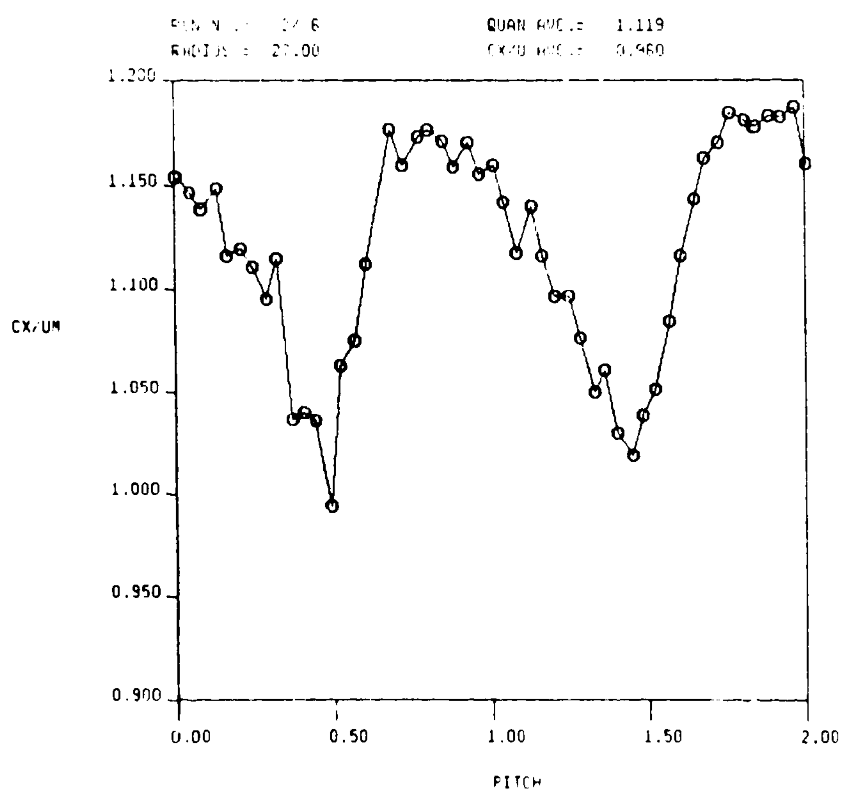

FIG. 25c STATIC PRESSURE AND AXIAL VELOCITY FROM 5-HOLE PROBE TRAVERSE AT ROTOR EXIT (X/Bx = 0.36), GRID IN

ORIGINAL PAGE IS OF POOR QUALITY

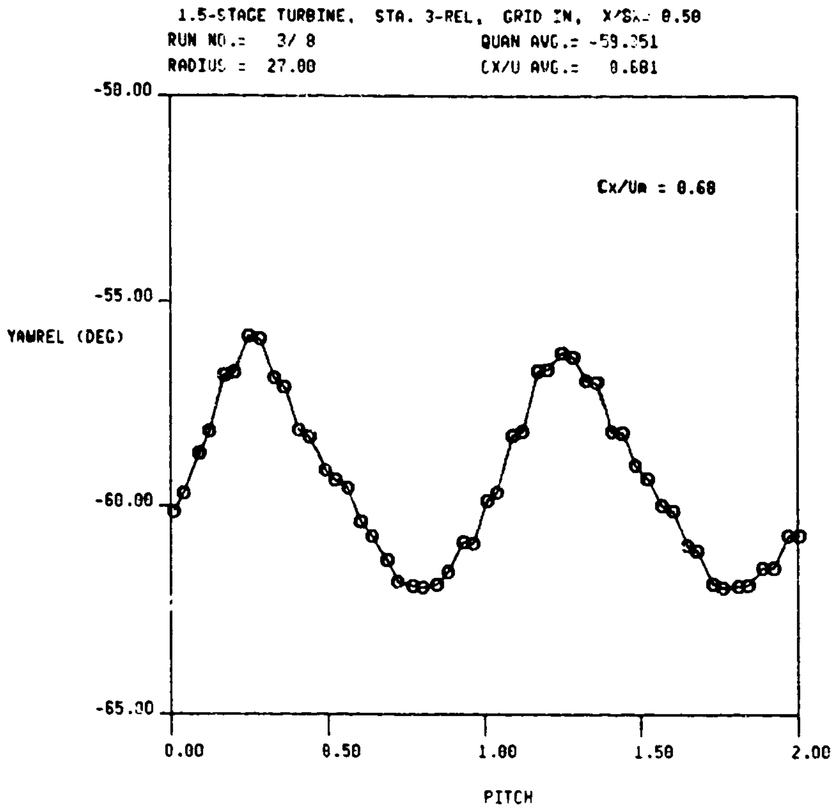

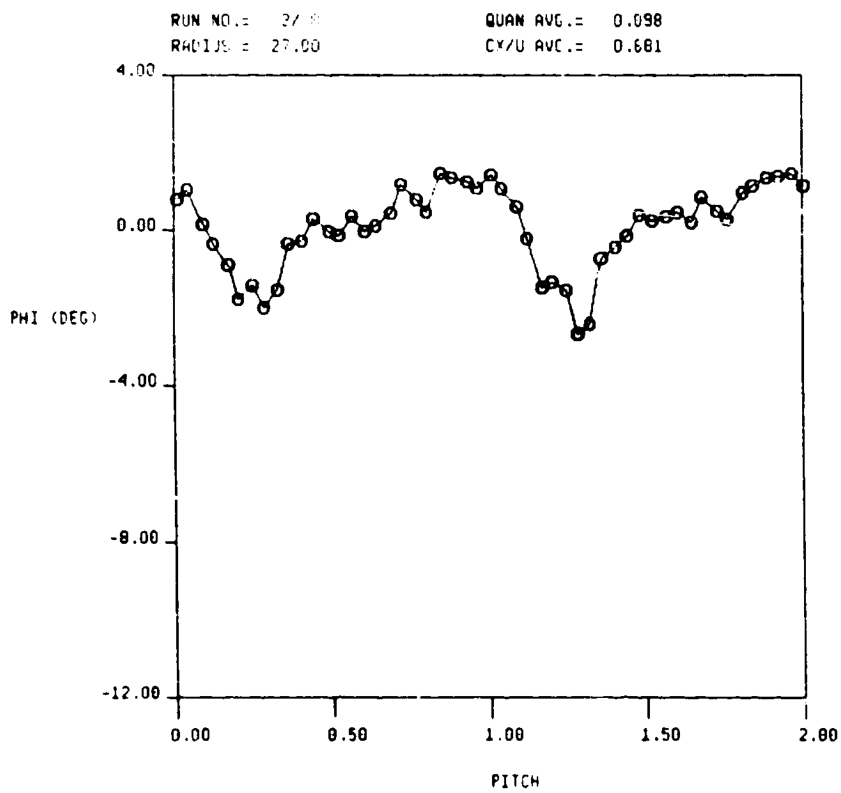

FIG. 26a RELATIVE YAW AND PITCH ANGLES FROM 5-HOLE PROBE TRAVERSE AT ROTOR EXIT (X/Bx = 0.36), GRID IN

C-2

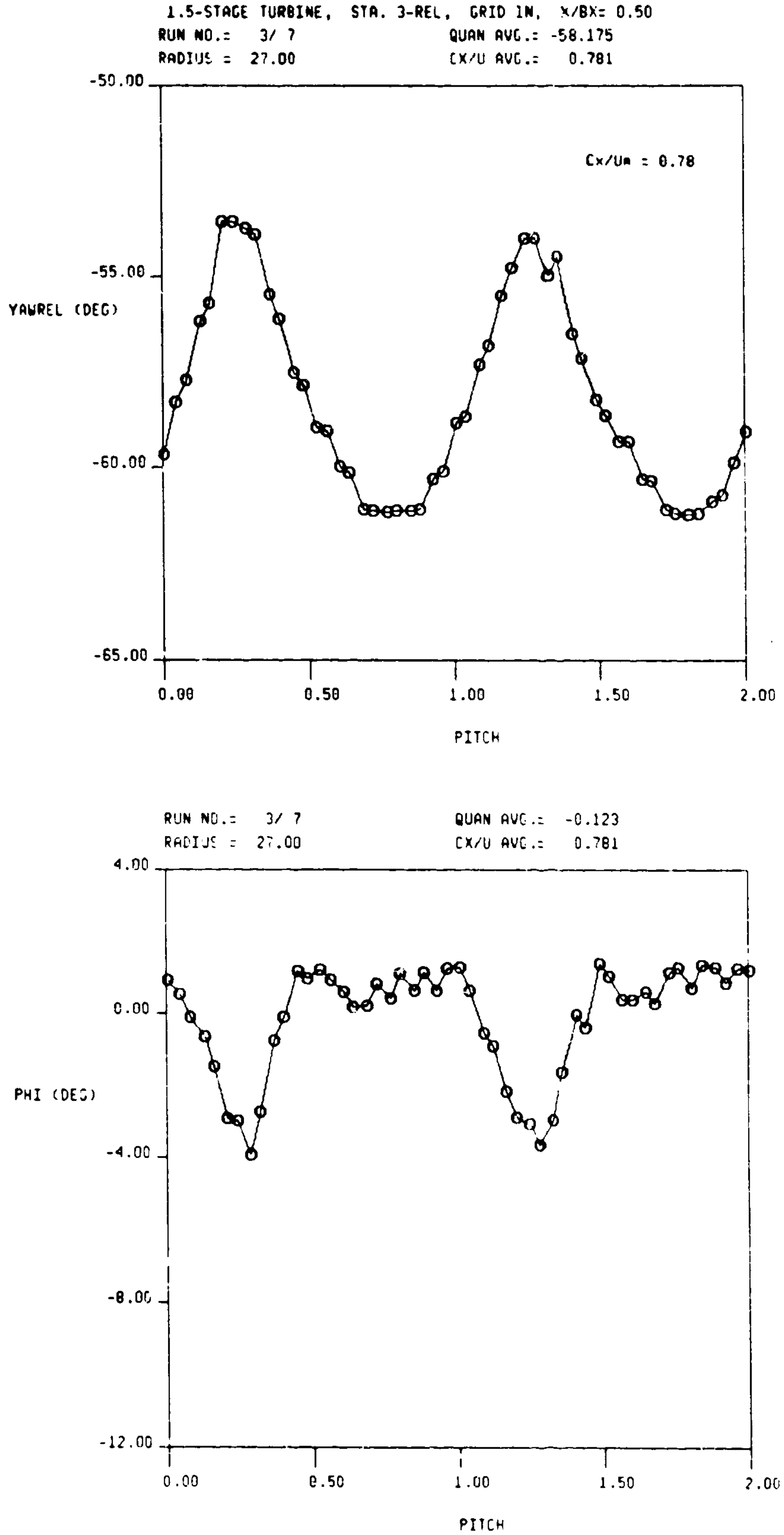

FIG. 26b RELATIVE YAW AND PITCH ANGLES FROM 5-HOLE PROBE TRAVERSE AT ROTOR EXIT (X/Bx = 0.36), GRID IN

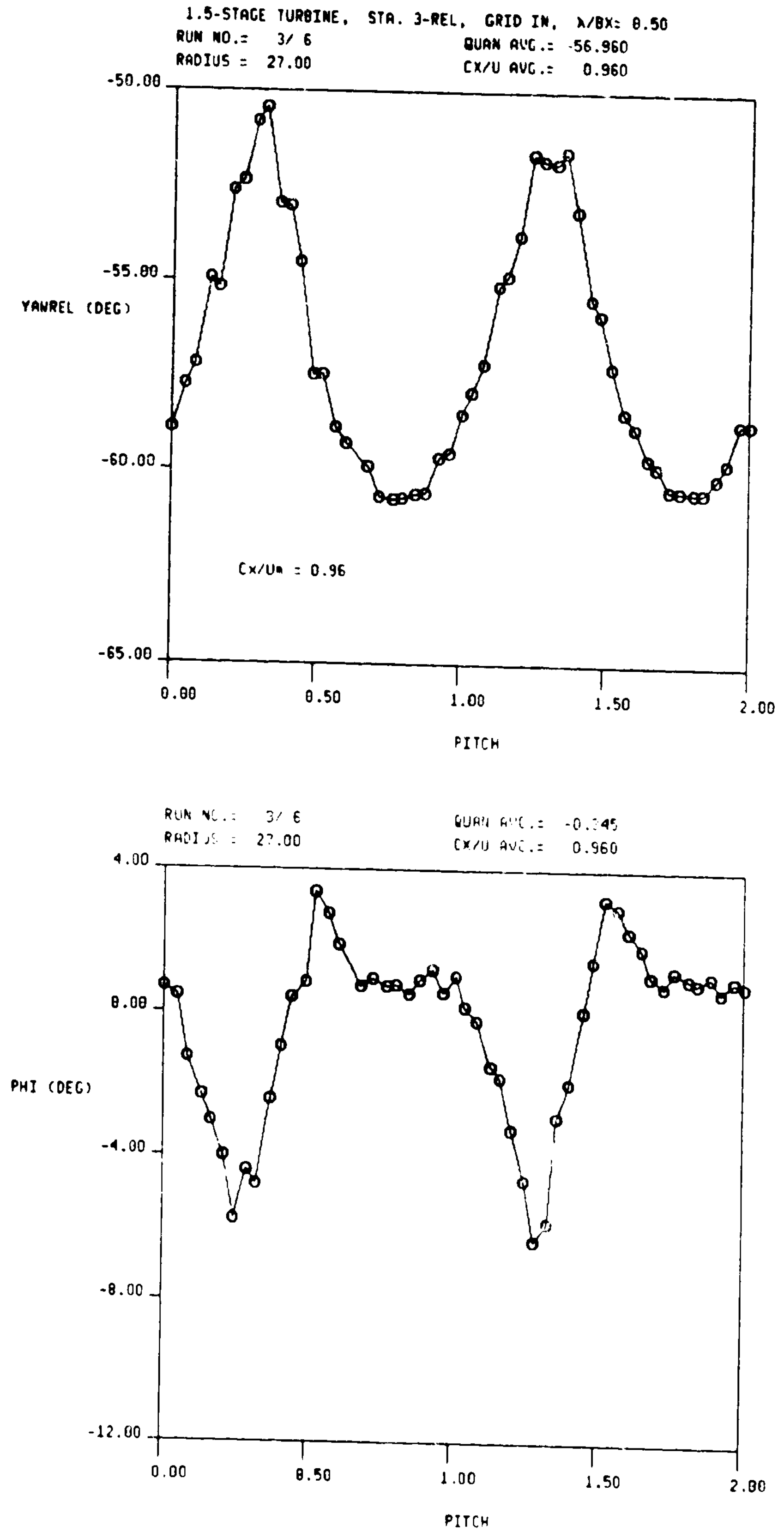

FIG. 26c RELATIVE YAW AND PITCH ANGLES FROM 5-HOLE PROBE TRAVERSE AT ROTOR EXIT (X/Bx = 0.36), GRID IN

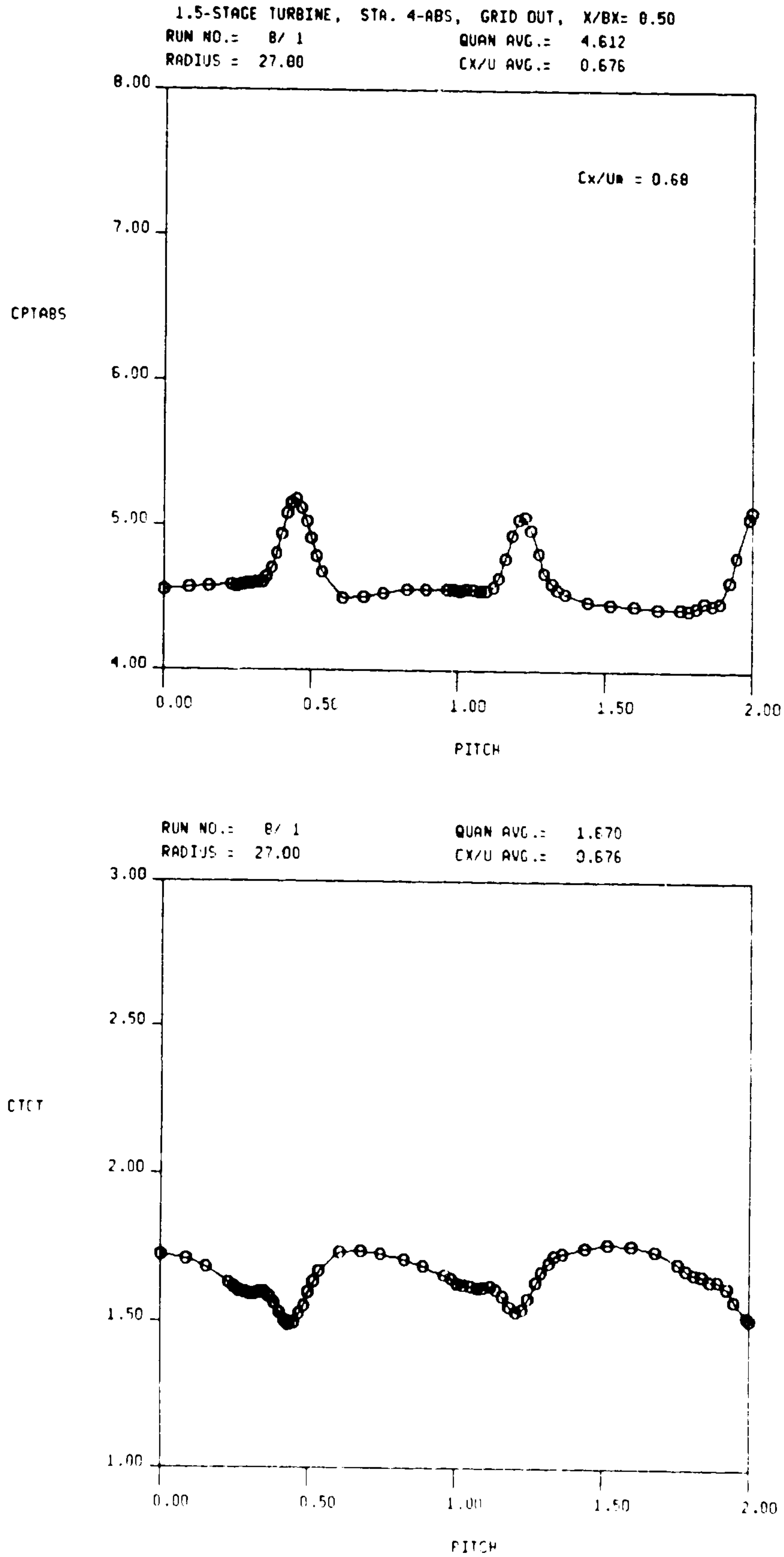

FIG. 27a ABSOLUTE TOTAL PRESSURE AND VELOCITY FROM 5-HOLE PROBE TRAVERSE AT 2ND STATOR EXIT (X/Bx = 0.14), GRID OUT

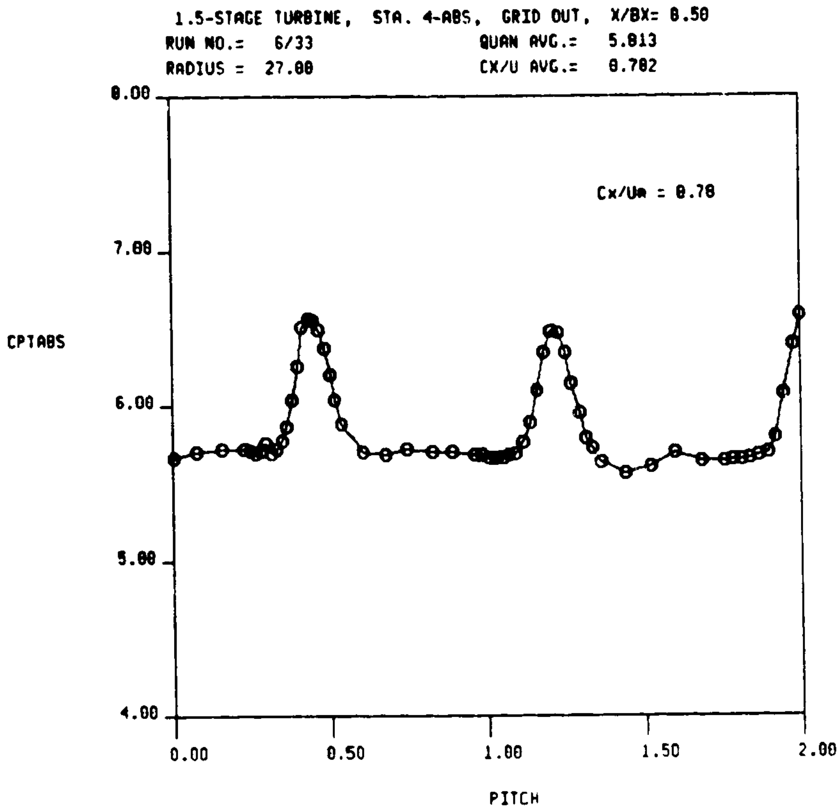

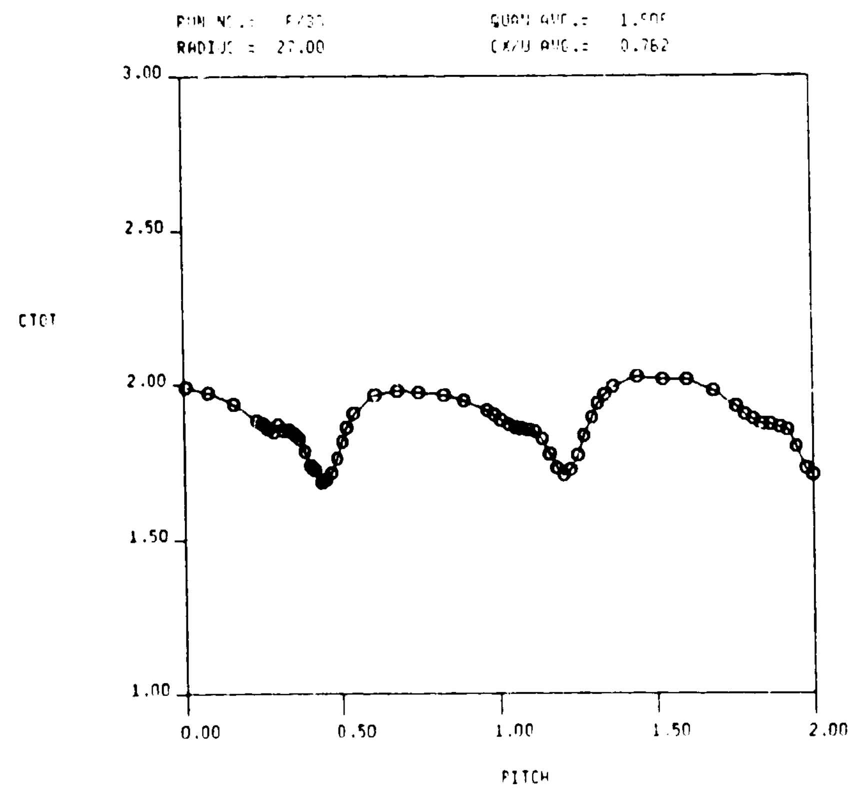

FIG. 27b ABSOLUTE TOTAL PRESSURE AND VELOCITY FROM 5-HOLE PROBE TRAVERSE AT 2ND STATOR EXIT (X/Bx = 0.14), GRID OUT

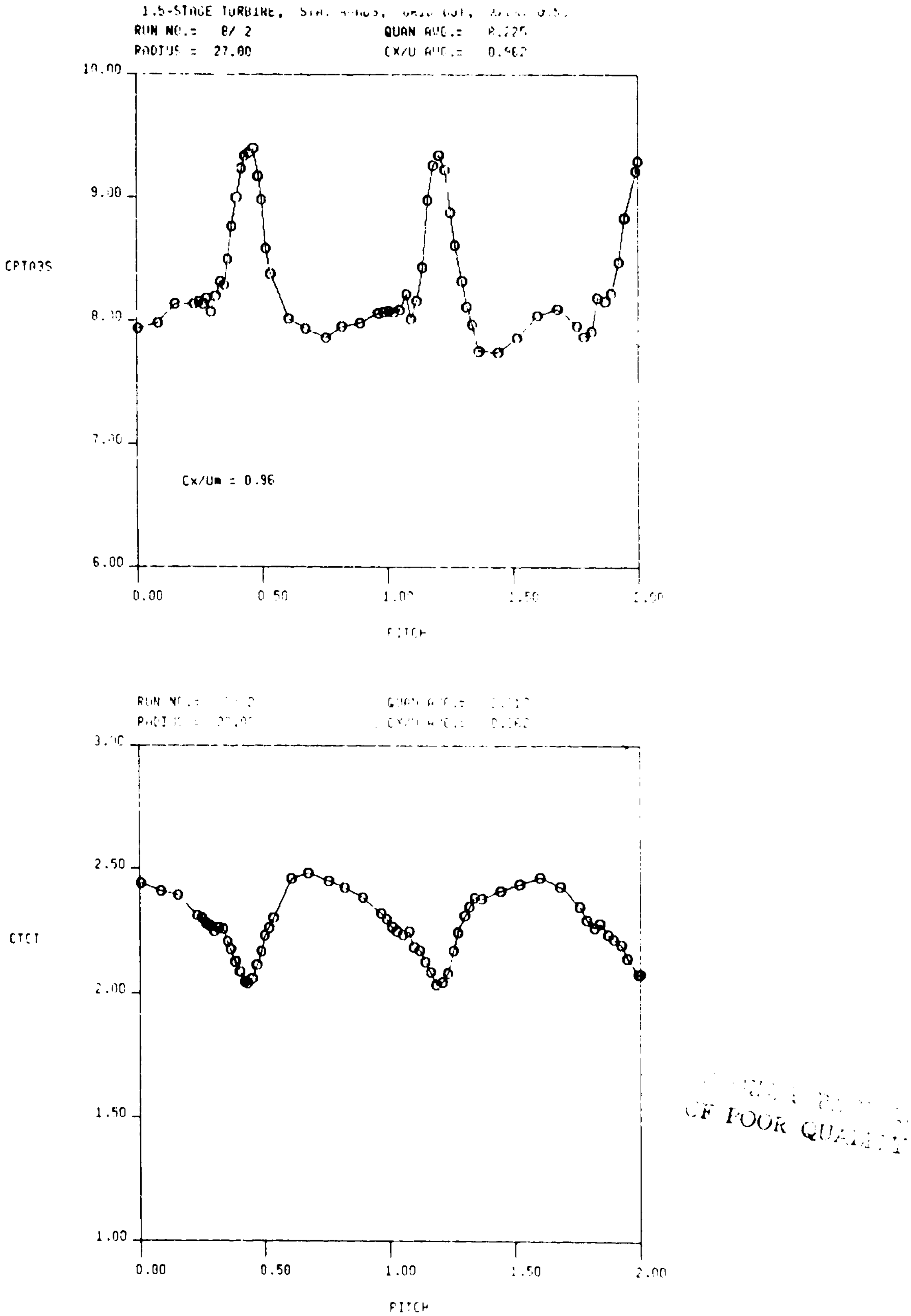

FIG. 27c ABSOLUTE TOTAL PRESSURE AND VELOCITY FROM 5-HOLE PROBE TRAVERSE AT 2ND STATOR EXIT (X/Bx = 0.14), GRID OUT

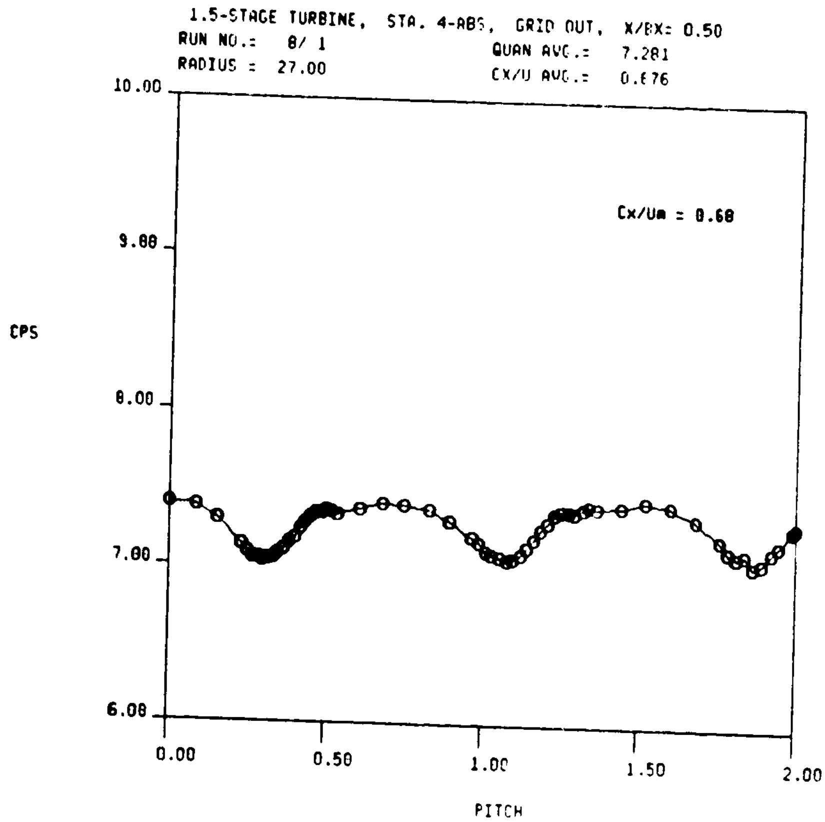

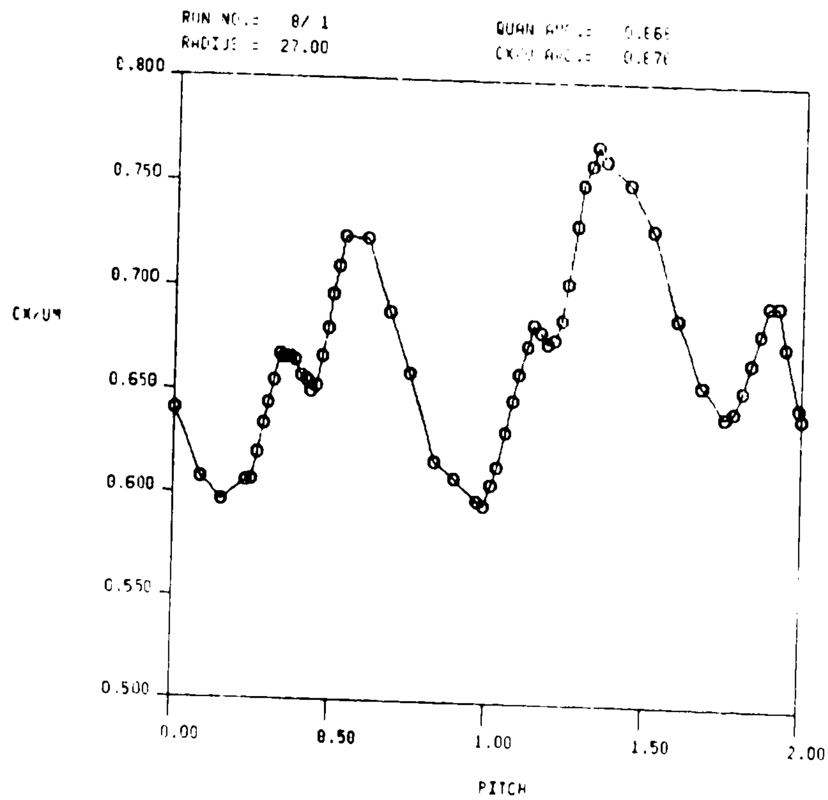

FIG. 28a STATIC PRESSURE AND AXIAL VELOCITY FROM 5-HOLE PROBE TRAVERSE AT 2ND STATOR EXIT (X/Bx = 0.14), GRID OUT

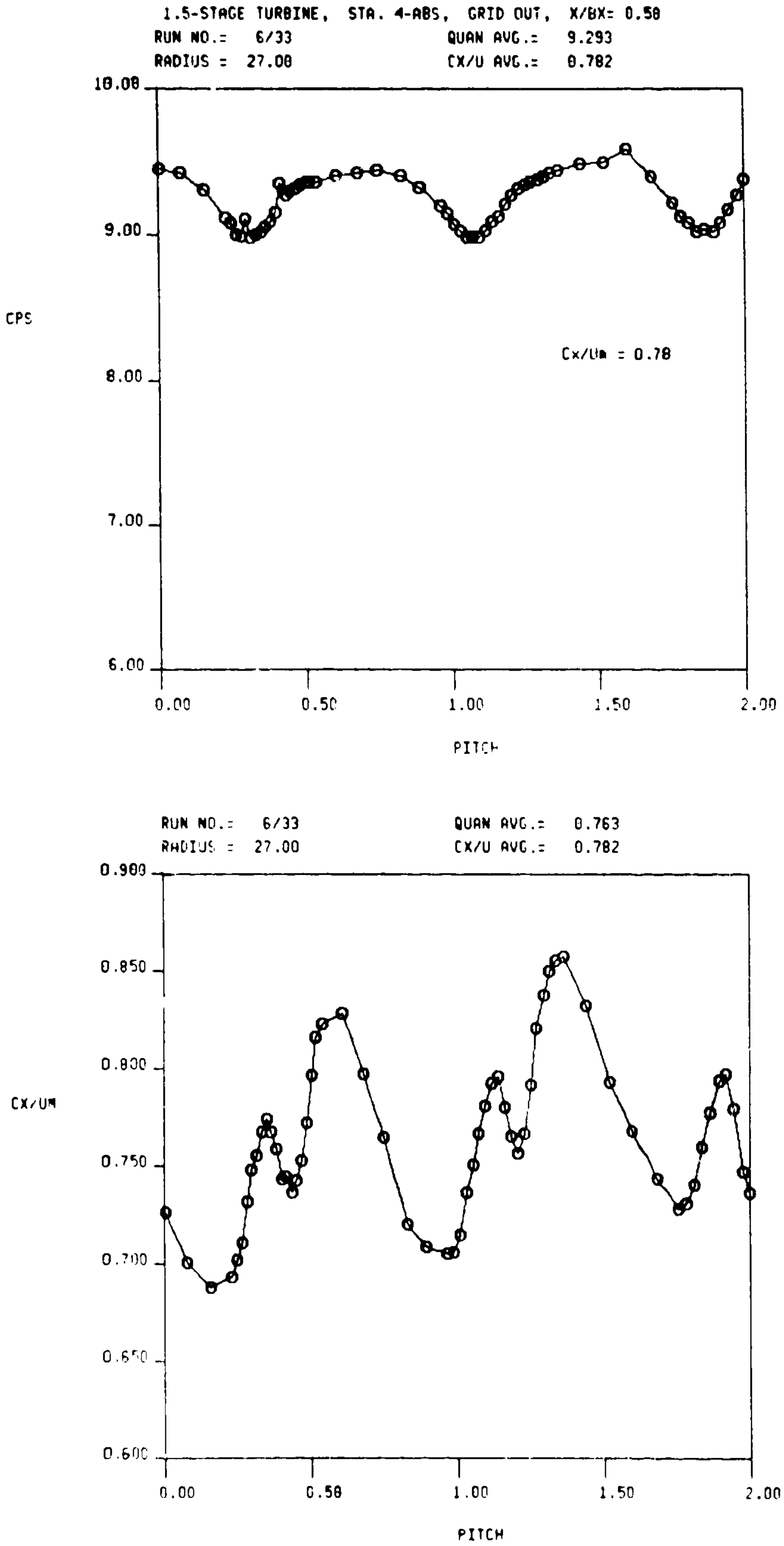

FIG. 28b STATIC PRESSURE AND AXIAL VELOCITY FROM 5-HOLE PROBE TRAVERSE AT 2ND STATOR EXIT (X/Bx = 0.14), GRID OUT

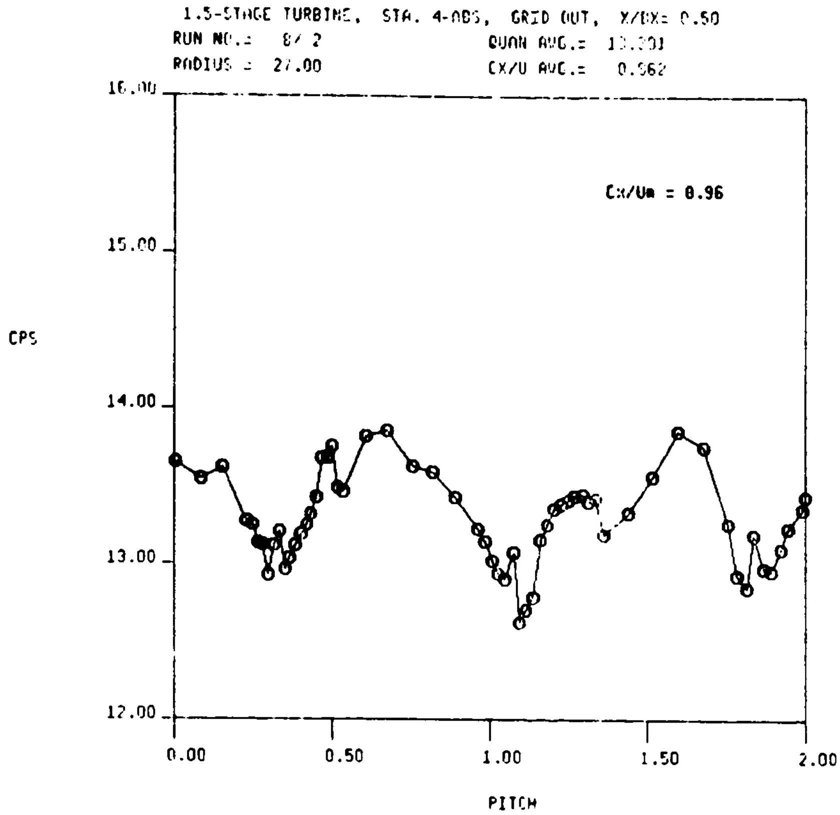

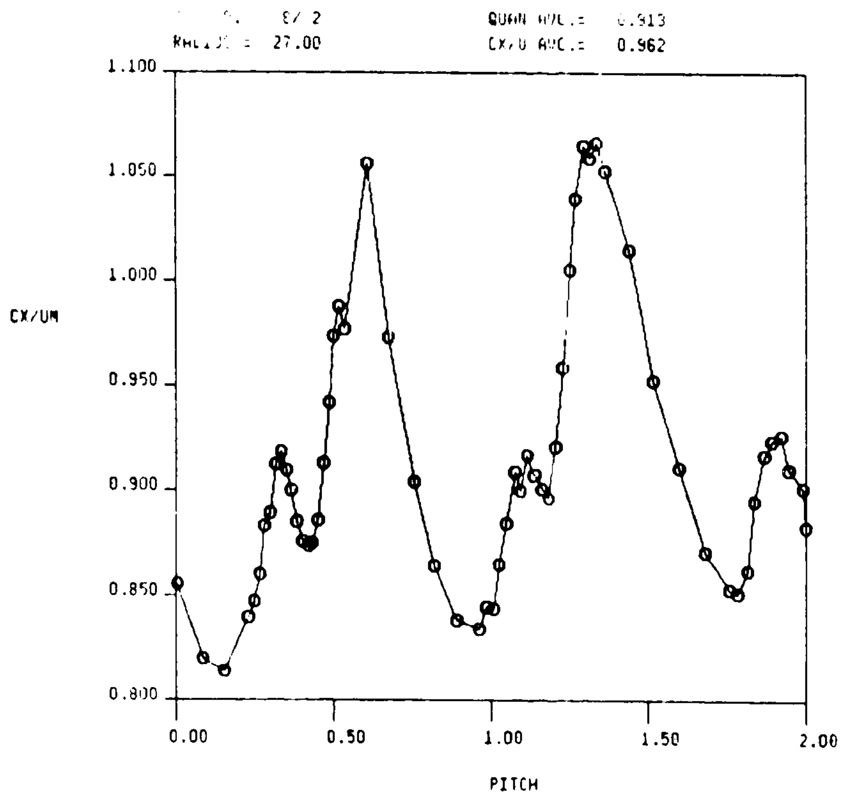

FIG. 28c STATIC PRESSURE AND AXIAL VELOCITY FROM 5-HOLE PROBE TRAVERSE AT 2ND STATOR EXIT (X/Bx = 0.14), GRID OUT

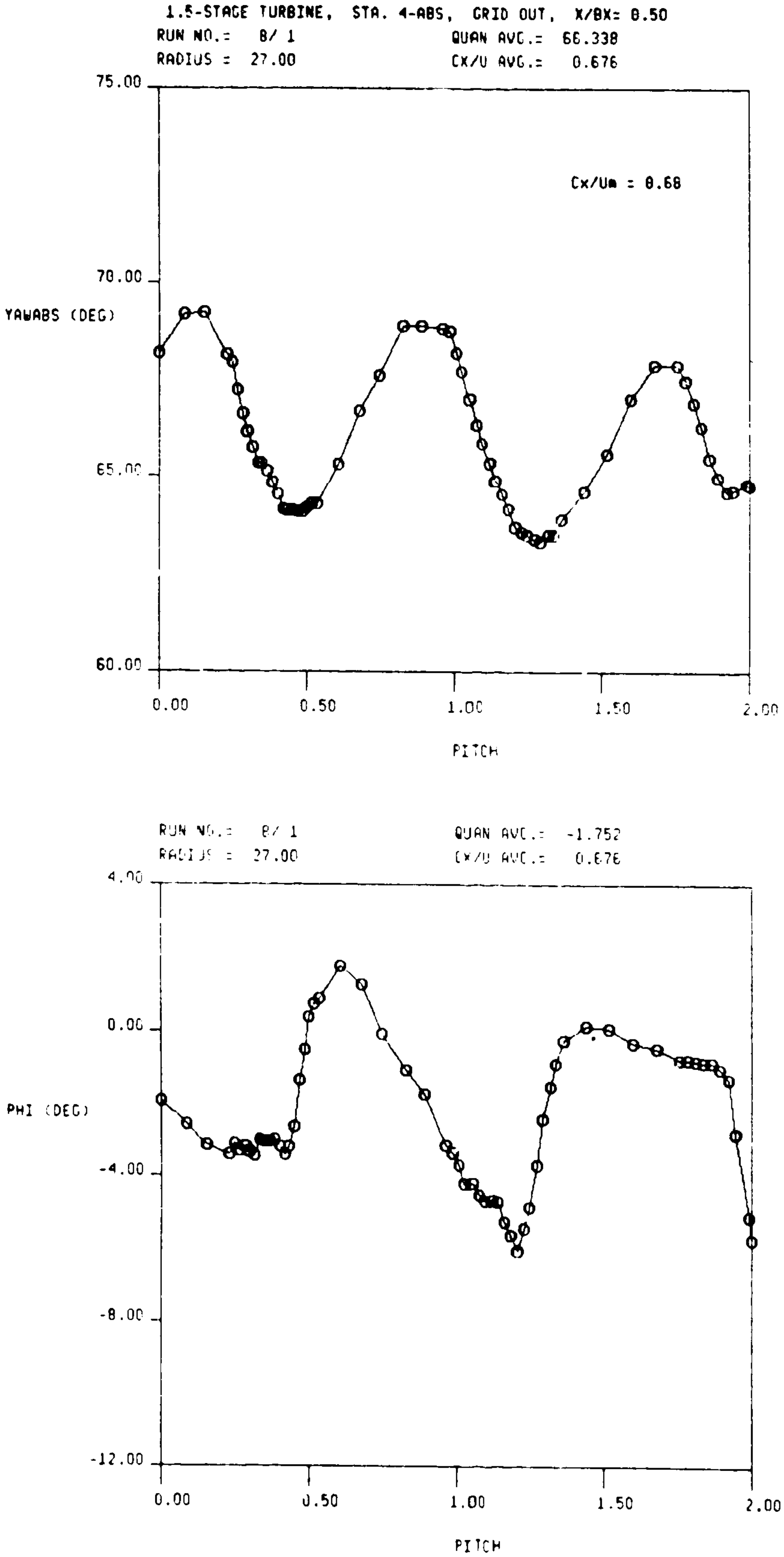

FIG. 29a ABSOLUTE YAW AND PITCH ANGLES FROM 5-HOLE PROBE TRAVERSE AT 2ND STATOR EXIT (X/Bx = 0.14), GRID OUT

ORIGINAL PAGE IS OF POOR QUALITY

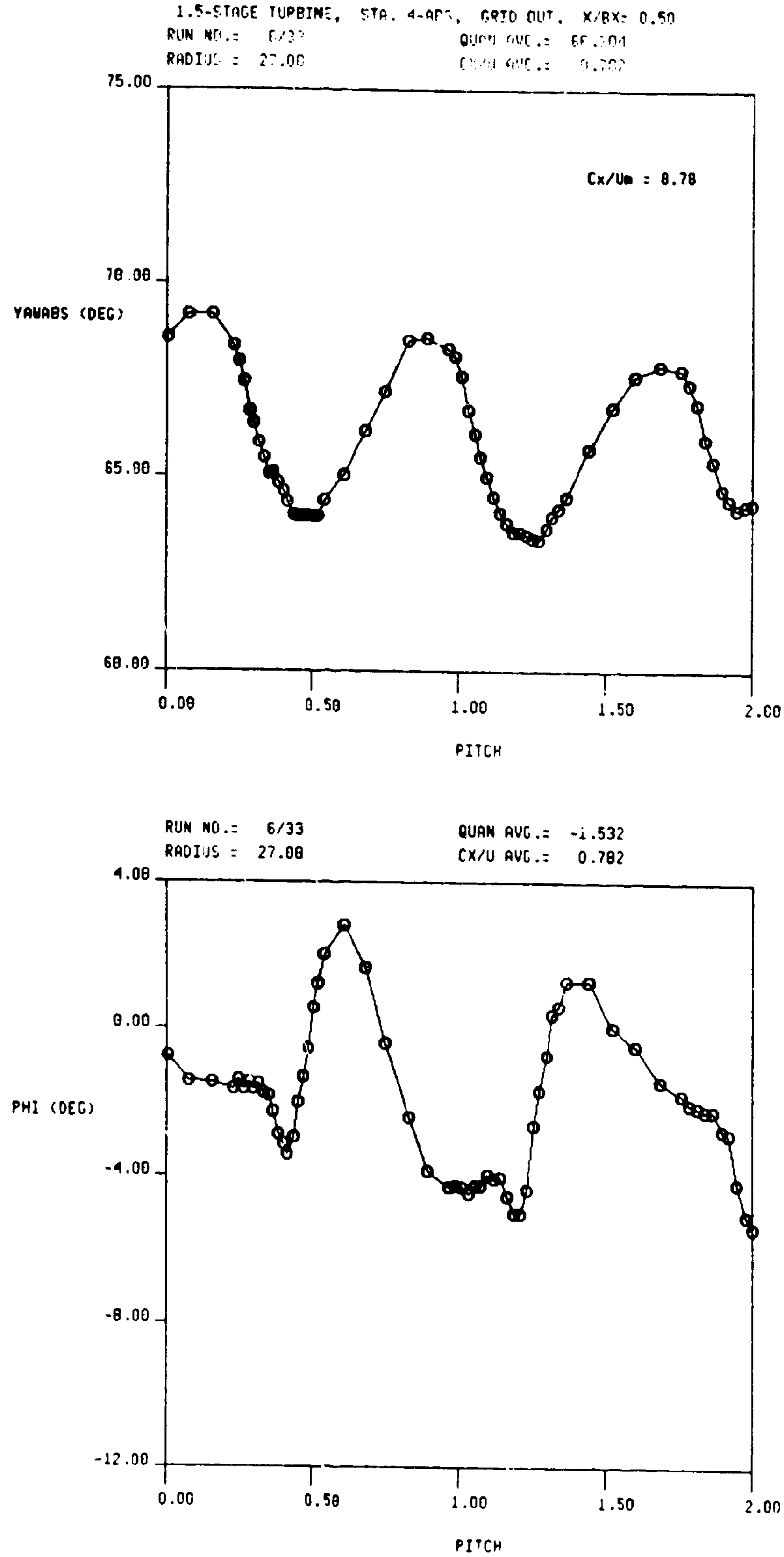

FIG. 29b ABSOLUTE YAW AND PITCH ANGLES FROM 5-HOLE PROBE TRAVERSE AT 2ND STATOR EXIT (X/Bx = 0.14), GRID OUT

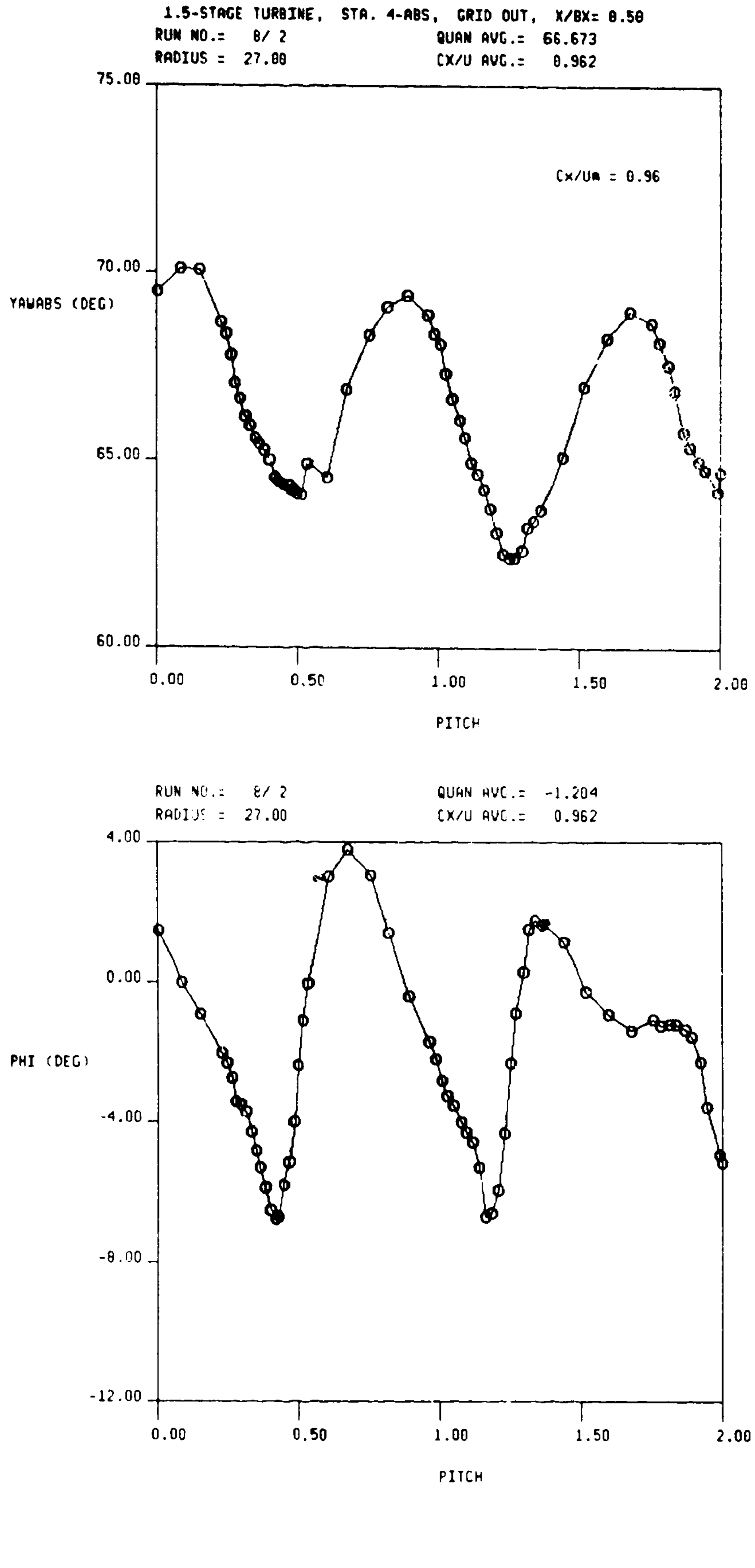

FIG. 29c ABSOLUTE YAW AND PITCH ANGLES FROM 5-HOLE PROBE TRAVERSE AT 2ND STATOR EXIT (X/Bx = 0.14), GRID OUT

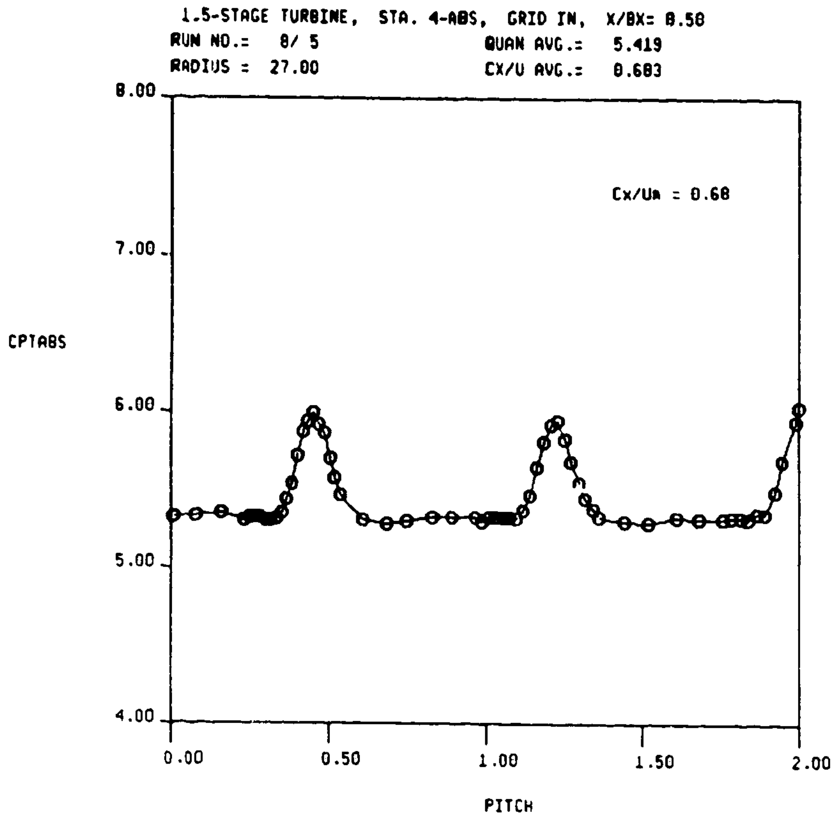

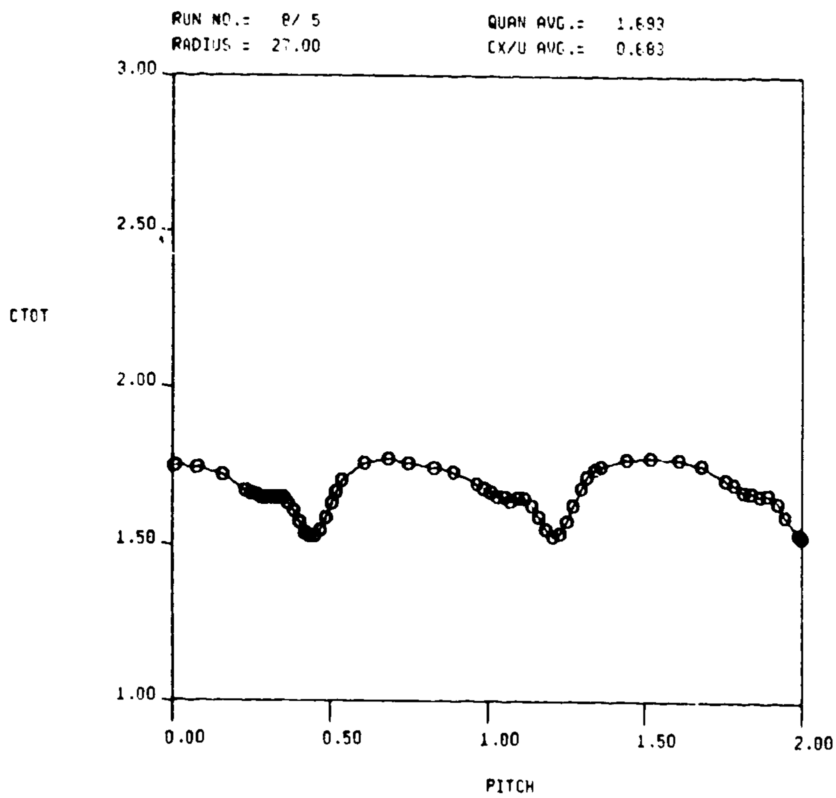

FIG. 30a ABSOLUTE TOTAL PRESSURE AND VELOCITY FROM 5-HOLE PROBE TRAVERSE AT 2ND STATOR EXIT (X/Bx = 0.14), GRID IN

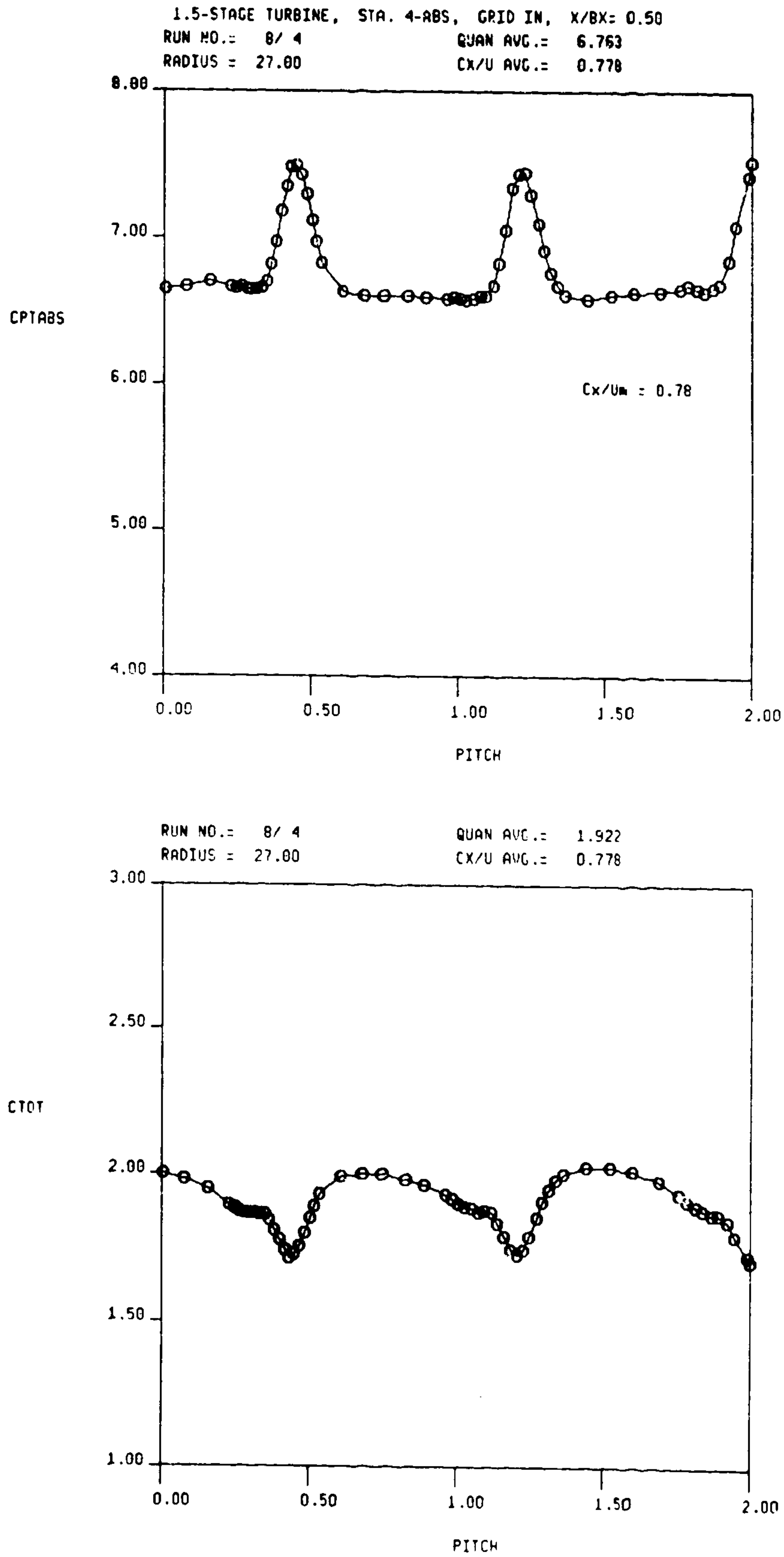

FIG. 30b ABSOLUTE TOTAL PRESSURE AND VELOCITY FROM 5-HOLE PROBE TRAVERSE AT 2ND STATOR EXIT (X/Bx = 0.14), GRID IN

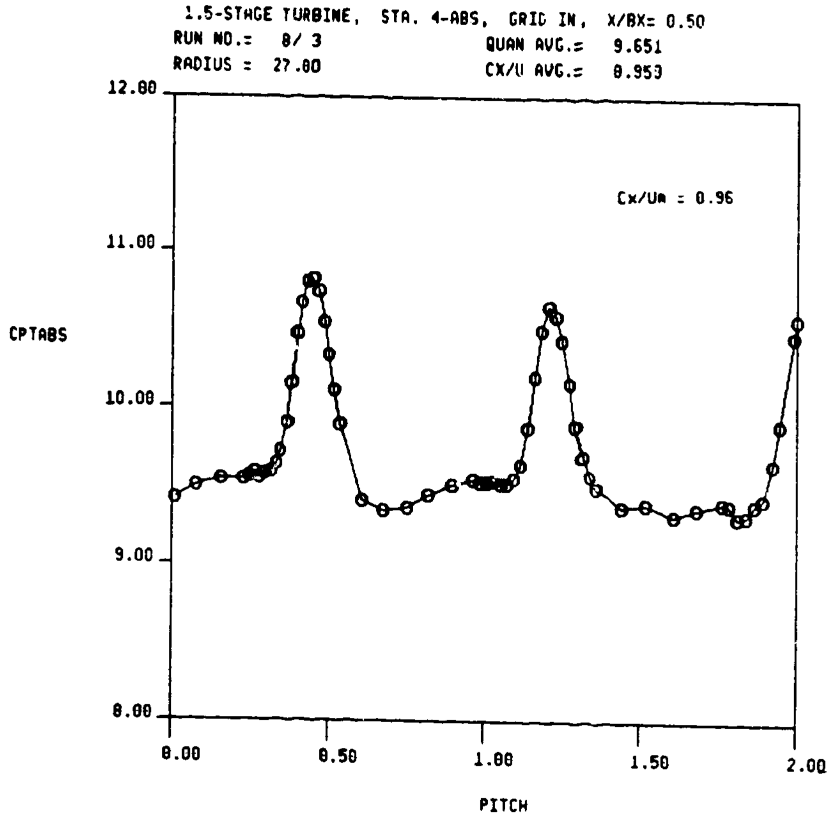

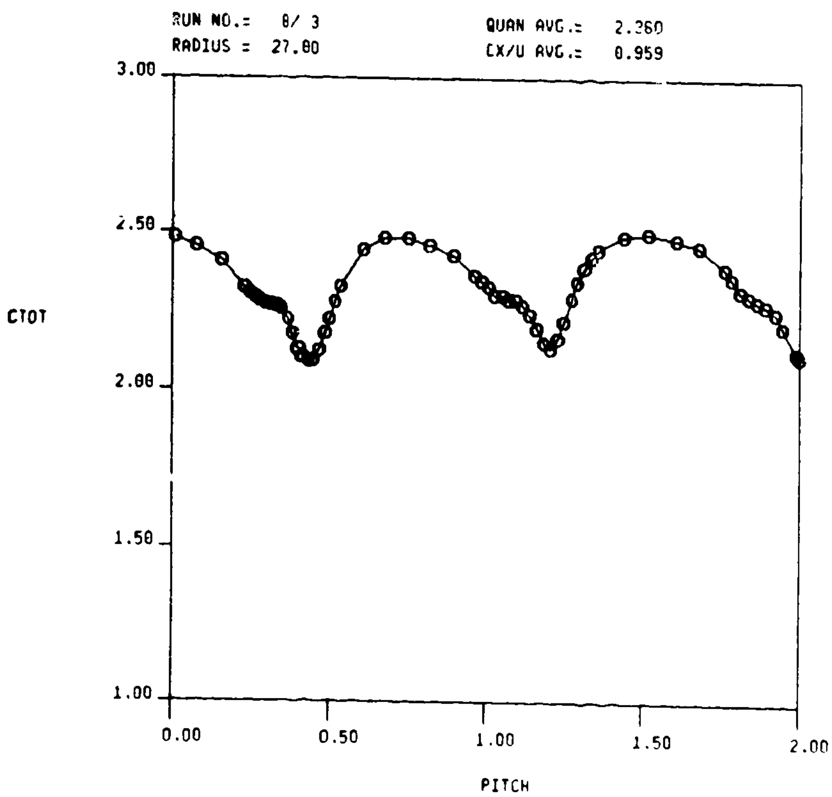

FIG. 30c ABSOLUTE TOTAL PRESSURE AND VELOCITY FROM 5-HOLE PROBE TRAVERSE AT 2ND STATOR EXIT (X/Bx = 0.14), GRID IN

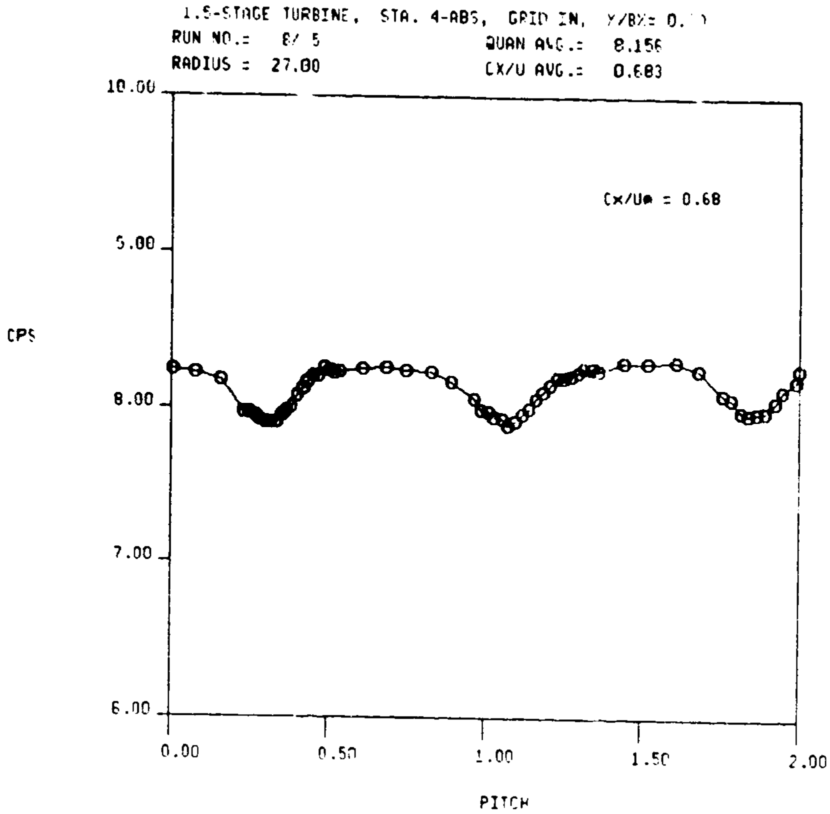

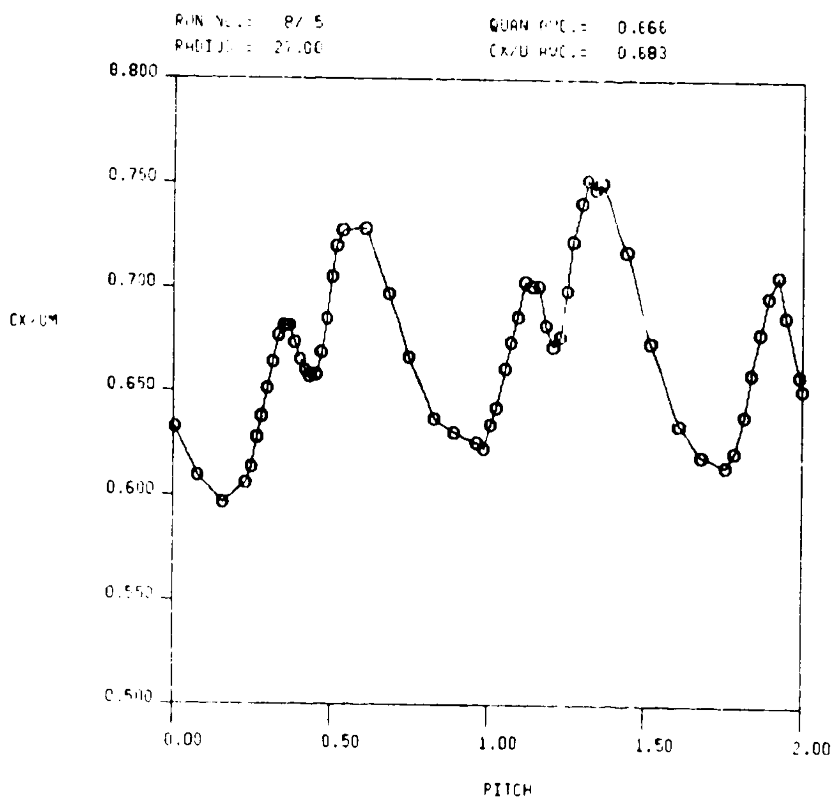

FIG. 31a STATIC PRESSURE AND AXIAL VELOCITY FROM 5-HOLE PROBE TRAVERSE AT 2ND STATOR EXIT (X/Bx = 0.14), GRID IN

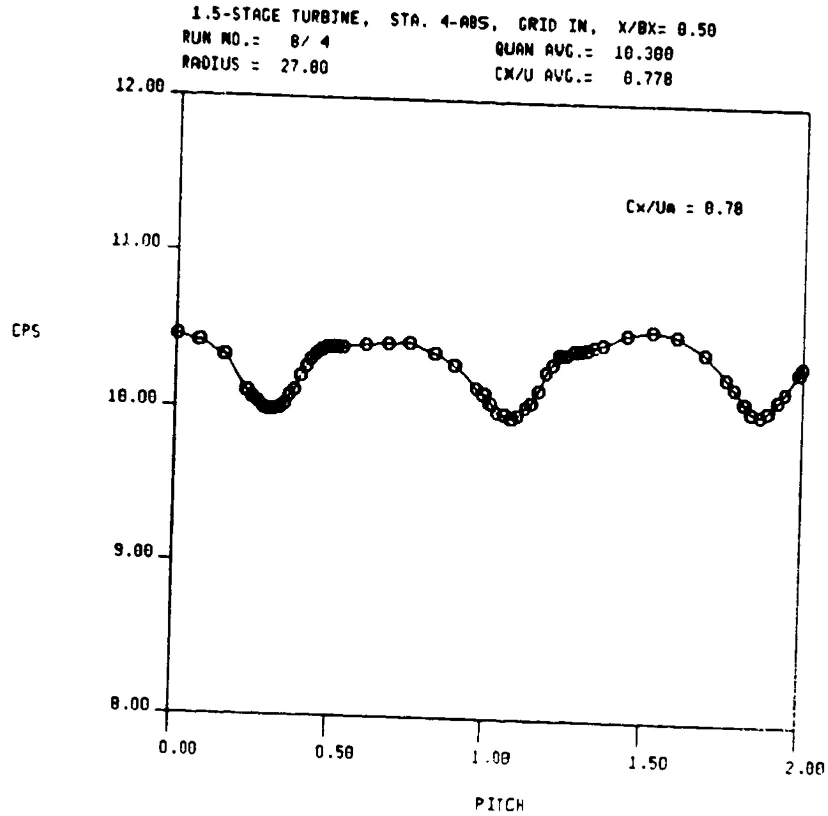

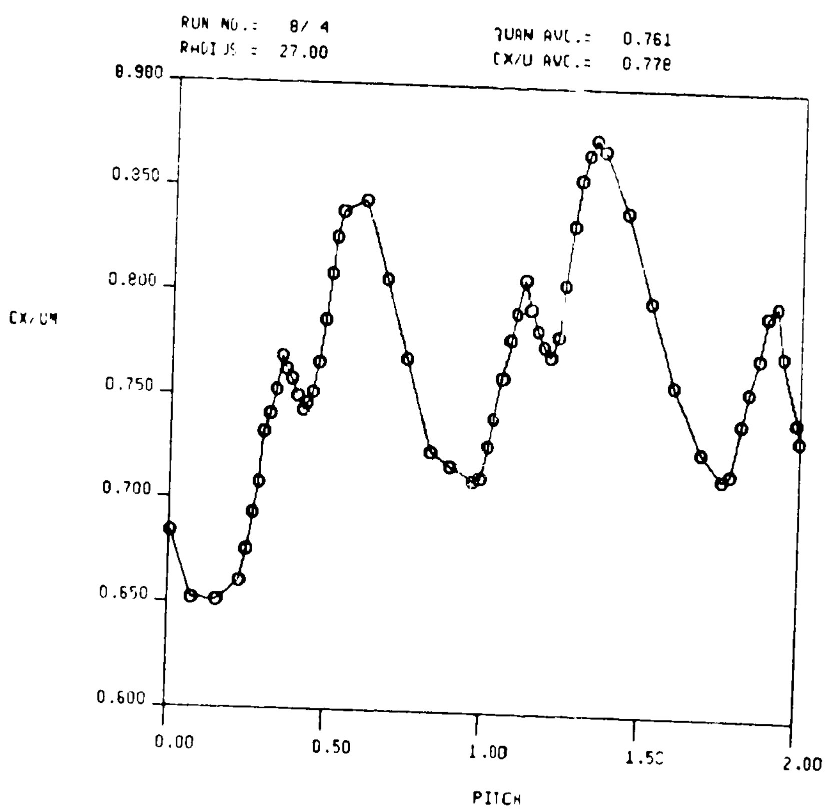

FIG. 31b STATIC PRESSURE AND AXIAL VELOCITY FROM 5-HOLE PROBE TRAVERSE AT 2ND STATOR EXIT (X/Bx = 0.14), GRID IN

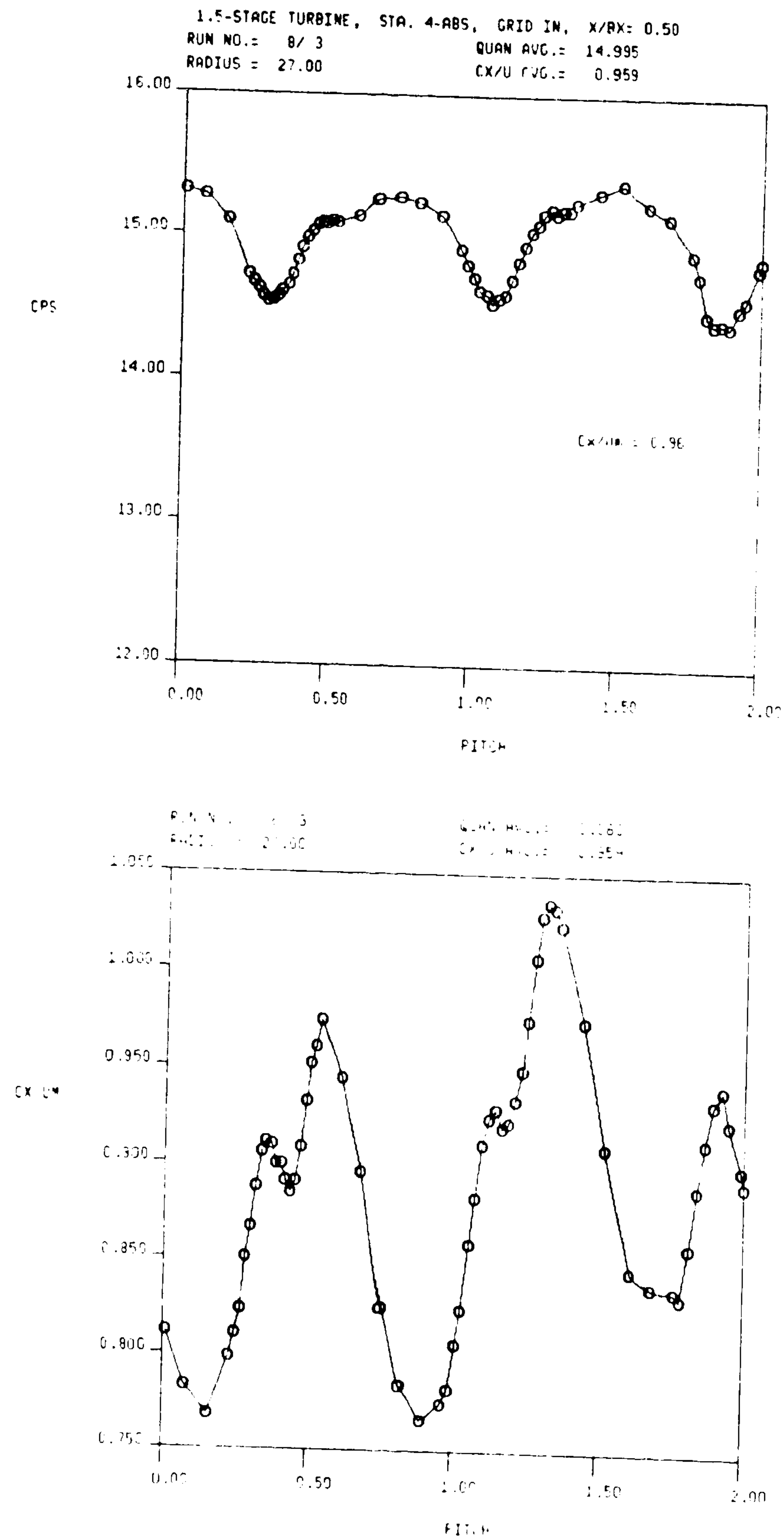

ORIGINAL PAGE IS OF POOR QUALITY

FIG. 31c STATIC PRESSURE AND AXIAL VELOCITY FROM 5-HOLE PROBE TRAVERSE AT 2ND STATOR EXIT (X/Bx = 0.14), GRID IN

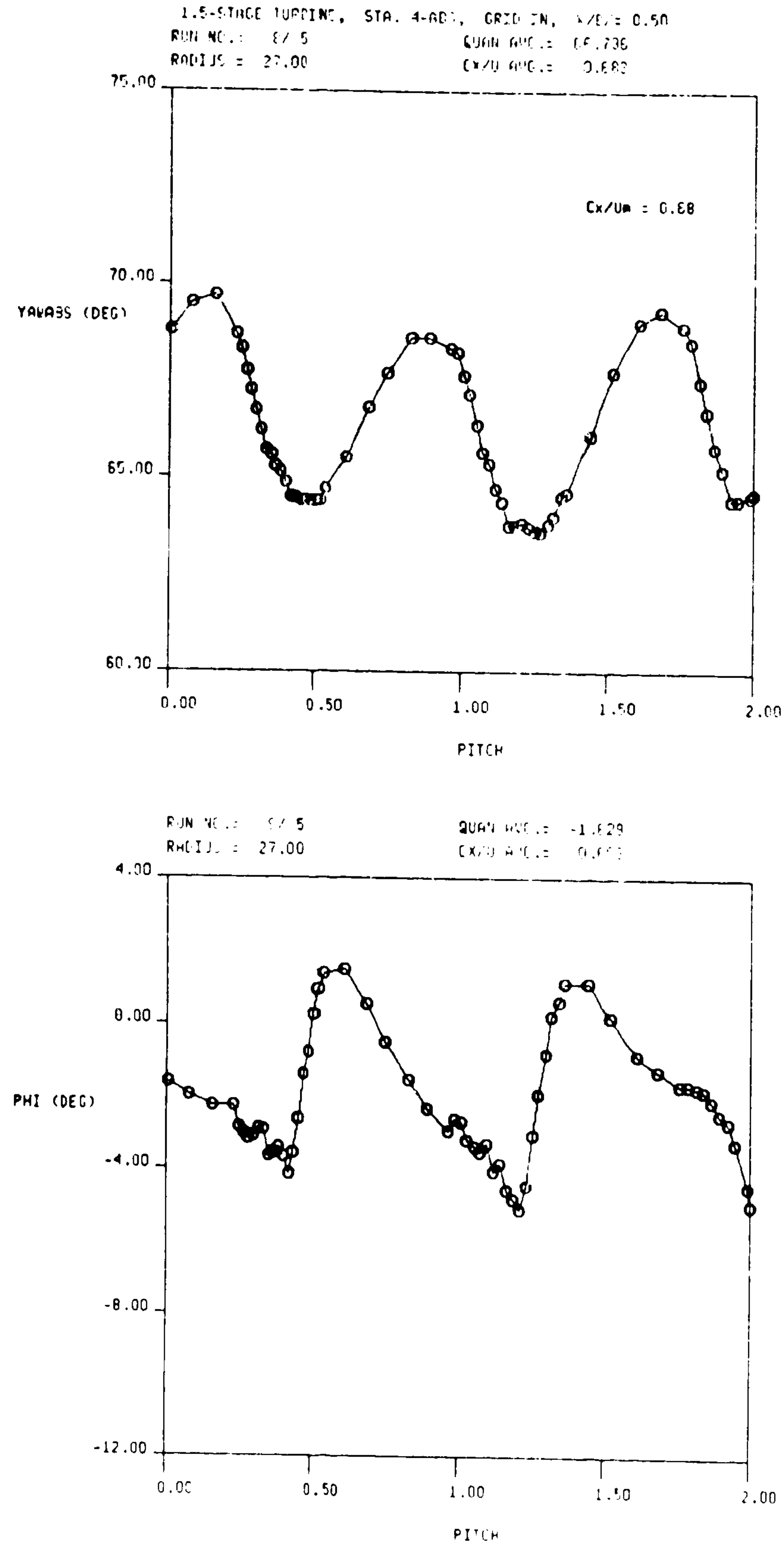

FIG. 32a ABSOLUTE YAW AND PITCH ANGLES FROM 5-HOLE PROBE TRAVERSE AT 2ND STATOR EXIT (X/Bx = 0.14), GRID IN

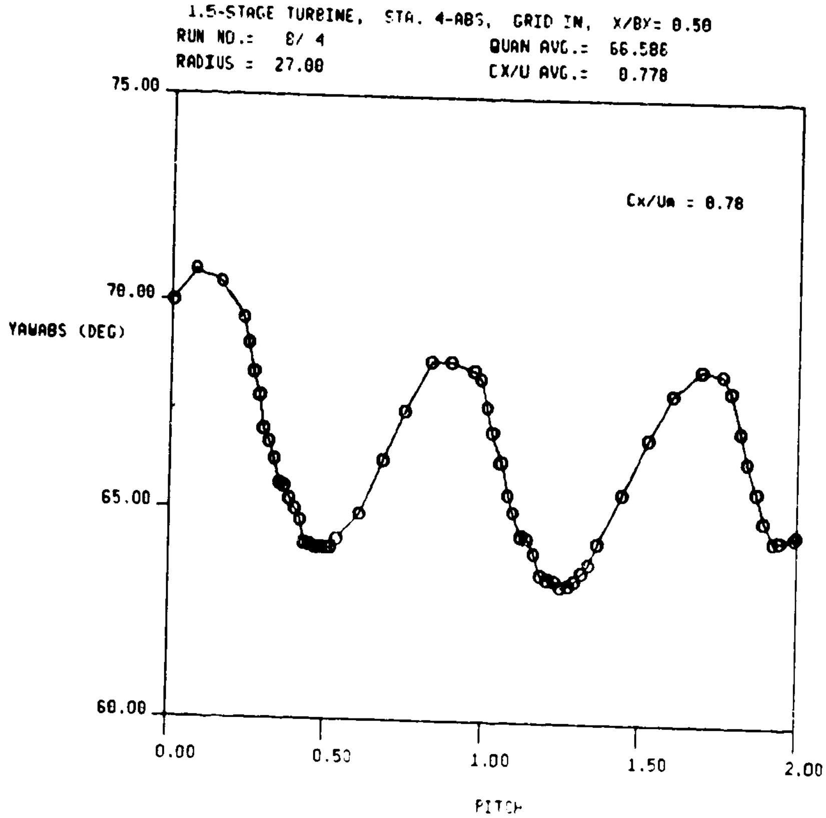

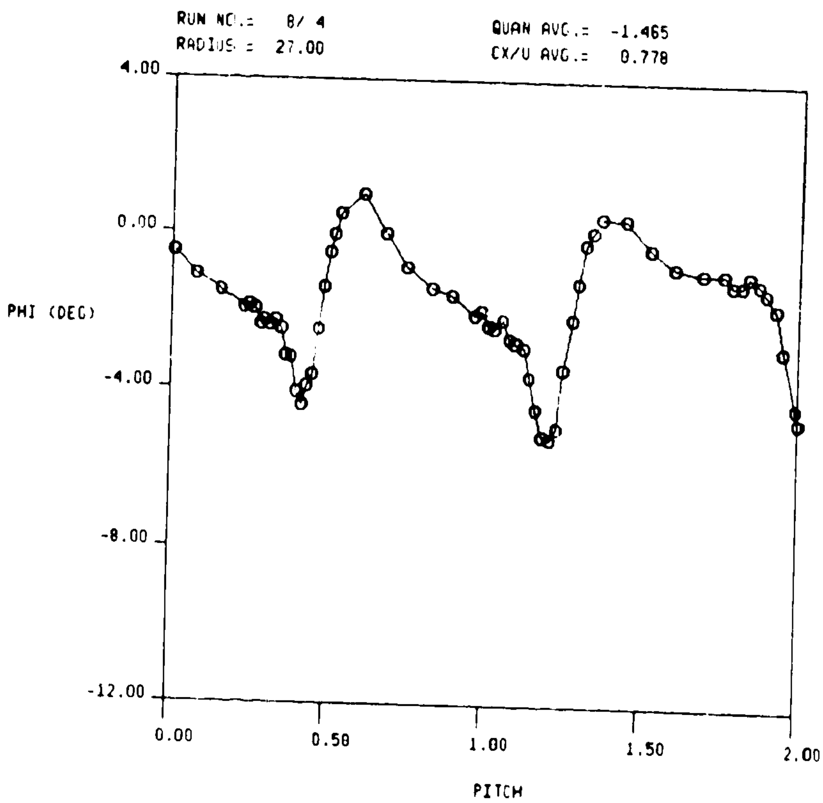

ORIGINAL PAGE IS OF POOR QUALITY

FIG. 32b ABSOLUTE YAW AND PITCH ANGLES FROM 5-HOLE PROBE TRAVERSE AT 2ND STATOR EXIT (X/Bx = 0.14), GRID IN

ORIGINAL PAGE IS
OF POOR QUALITY

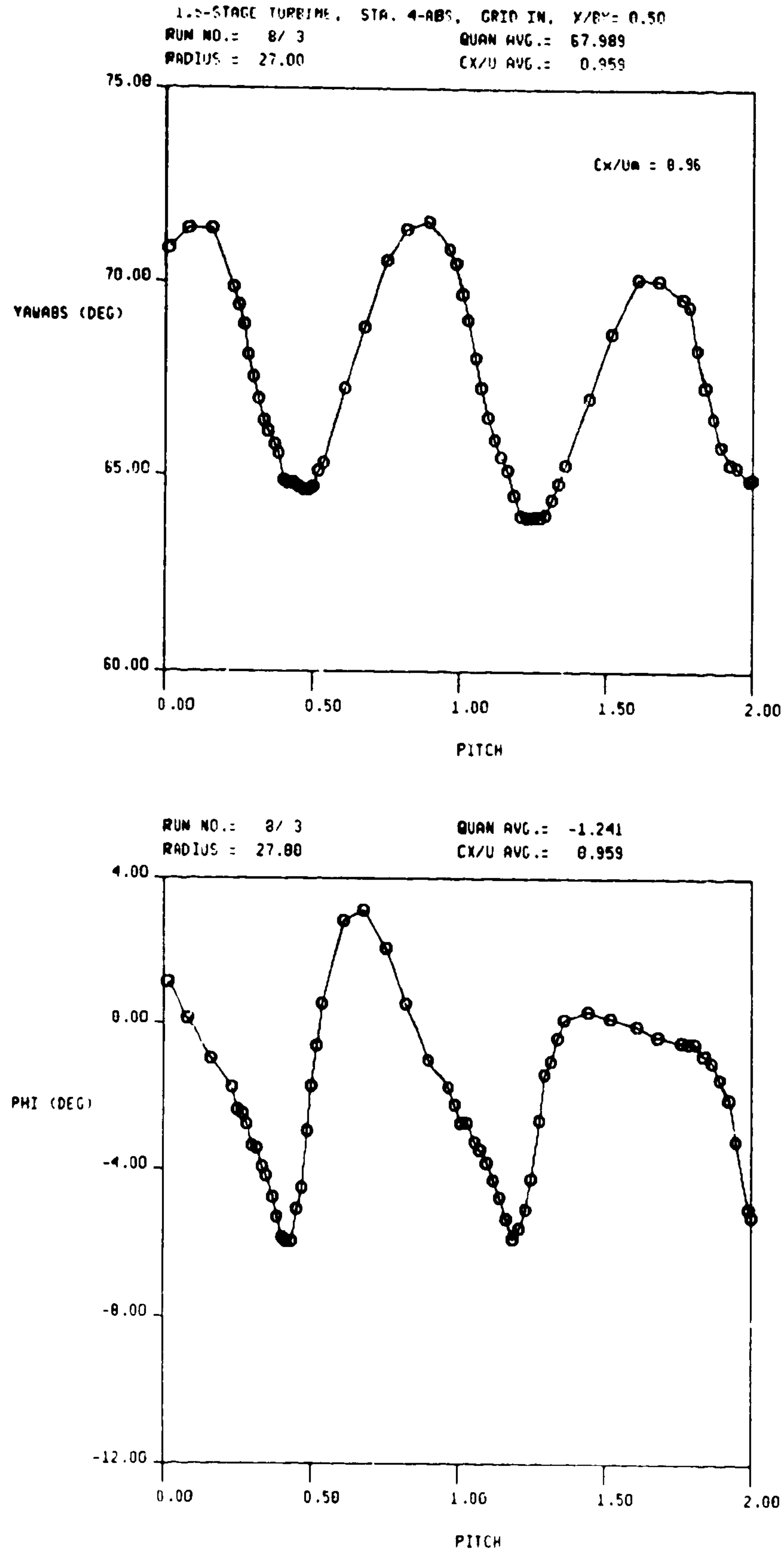

FIG. 32c ABSOLUTE YAW AND PITCH ANGLES FROM 5-HOLE PROBE TRAVERSE AT 2ND STATOR EXIT (X/Bx = 0.14), GRID IN

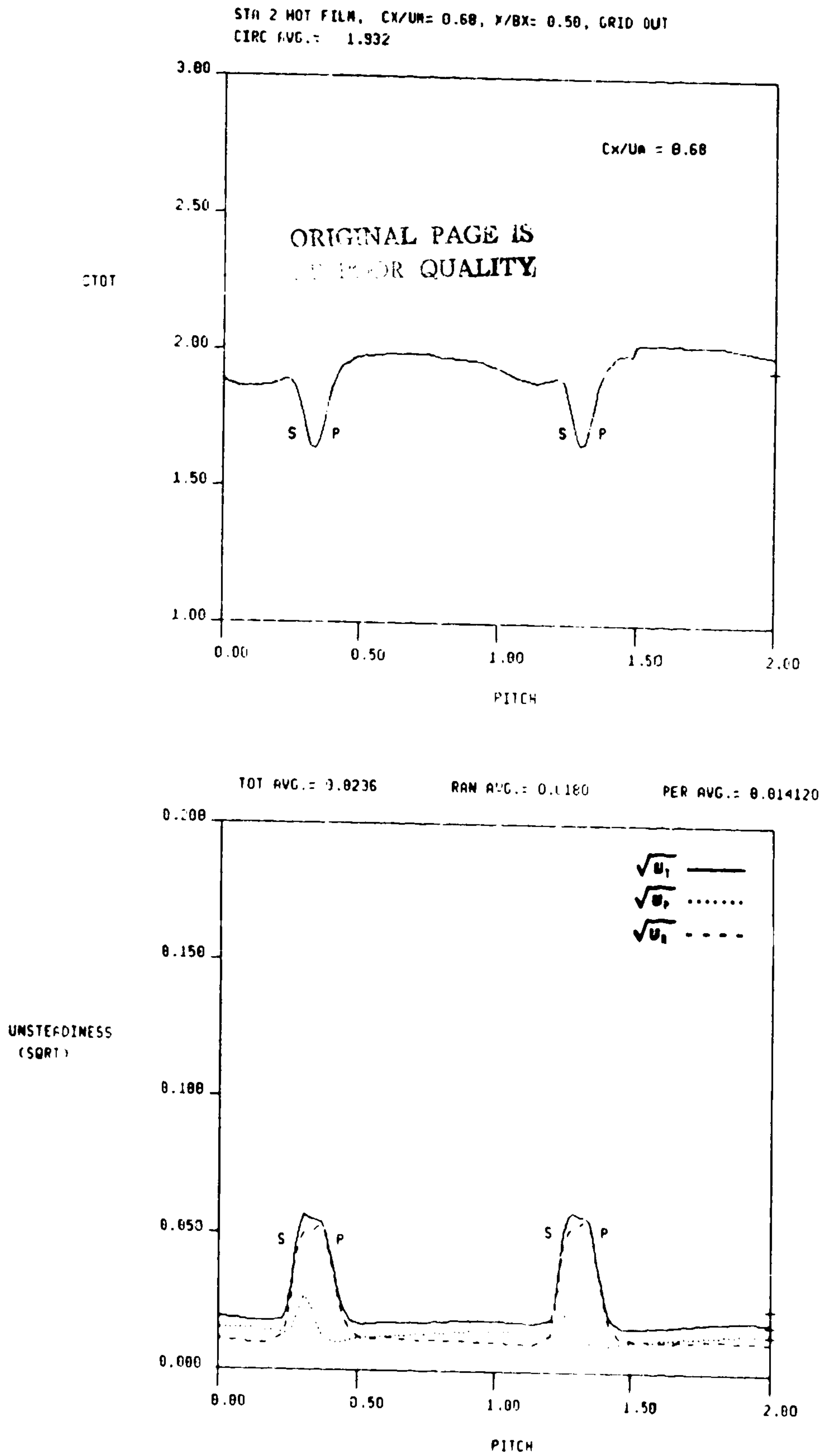

ORIGINAL PAGE IS
OF POOR QUALITY

FIG. 33a CIRCUMFERENTIAL DISTRIBUTION OF TIME AVERAGED SPEED AND UNSTEADINESS AT 1ST STATOR EXIT, GRID OUT

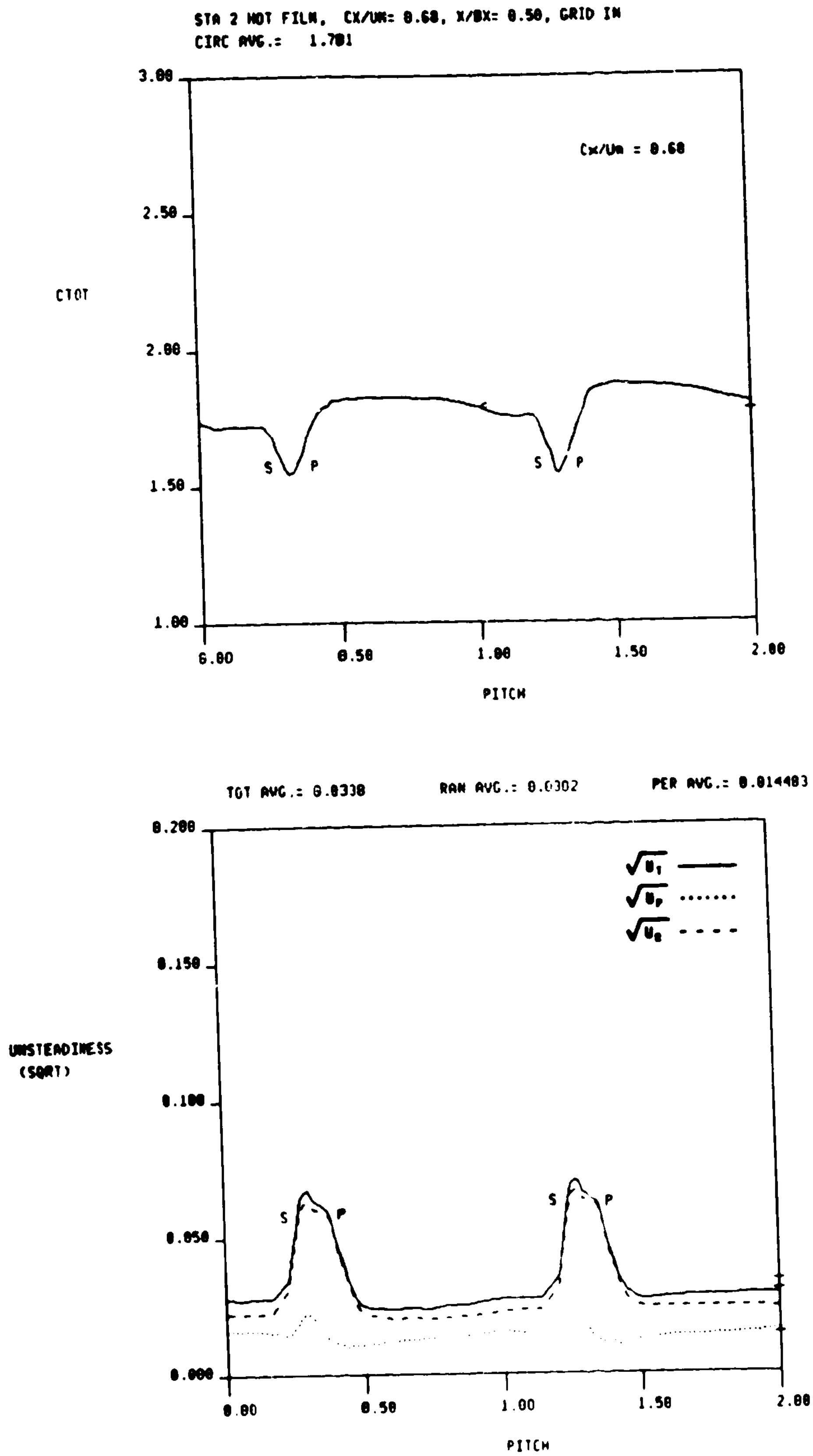

FIG. 33b CIRCUMFERENTIAL DISTRIBUTION OF TIME AVERAGED SPEED AND UNSTEADINESS AT 1ST STATOR EXIT, GRID IN

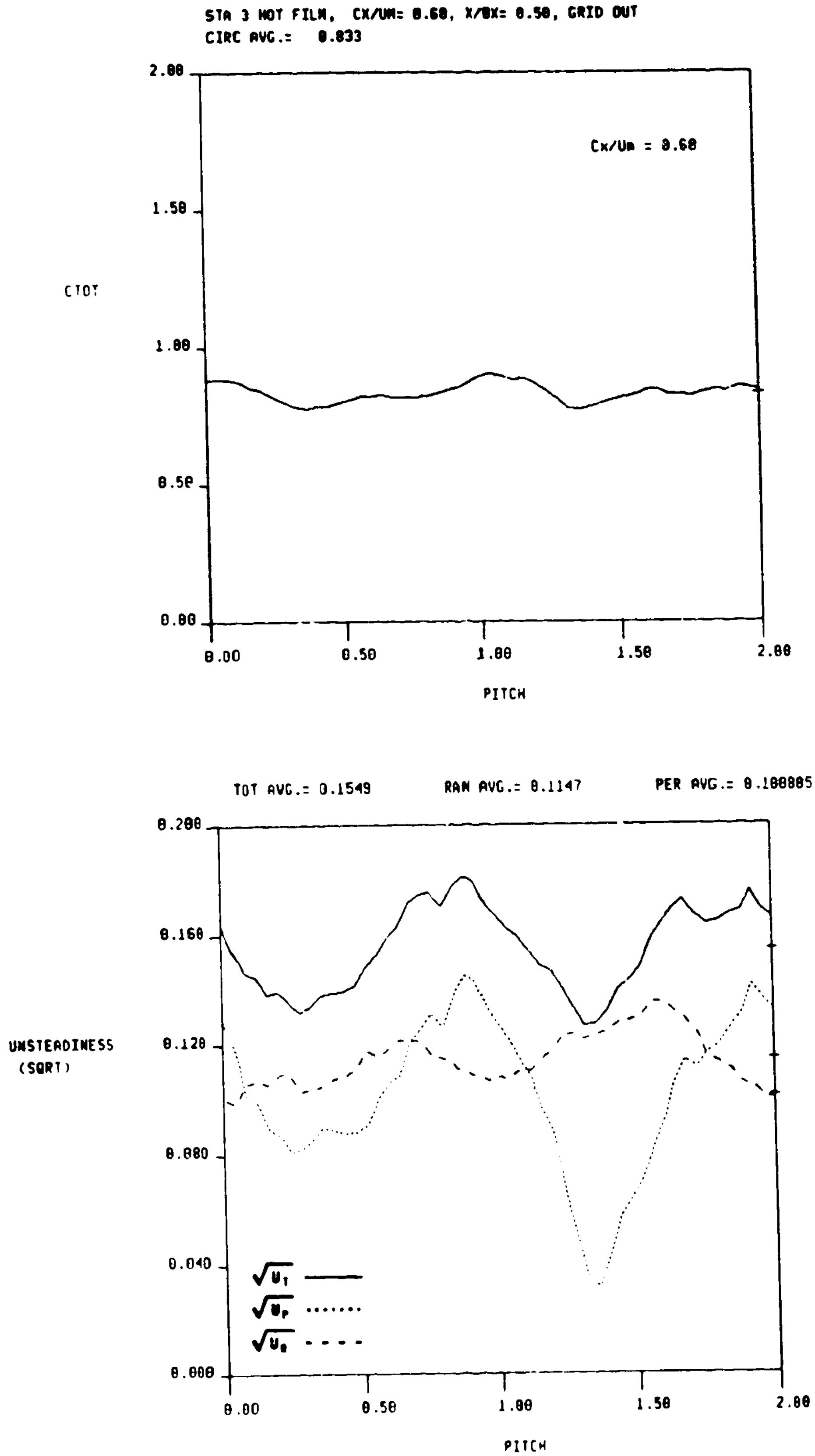

FIG. 34a CIRCUMFERENTIAL DISTRIBUTION OF TIME AVERAGED SPEED AND UNSTEADINESS AT ROTOR EXIT, GRID OUT

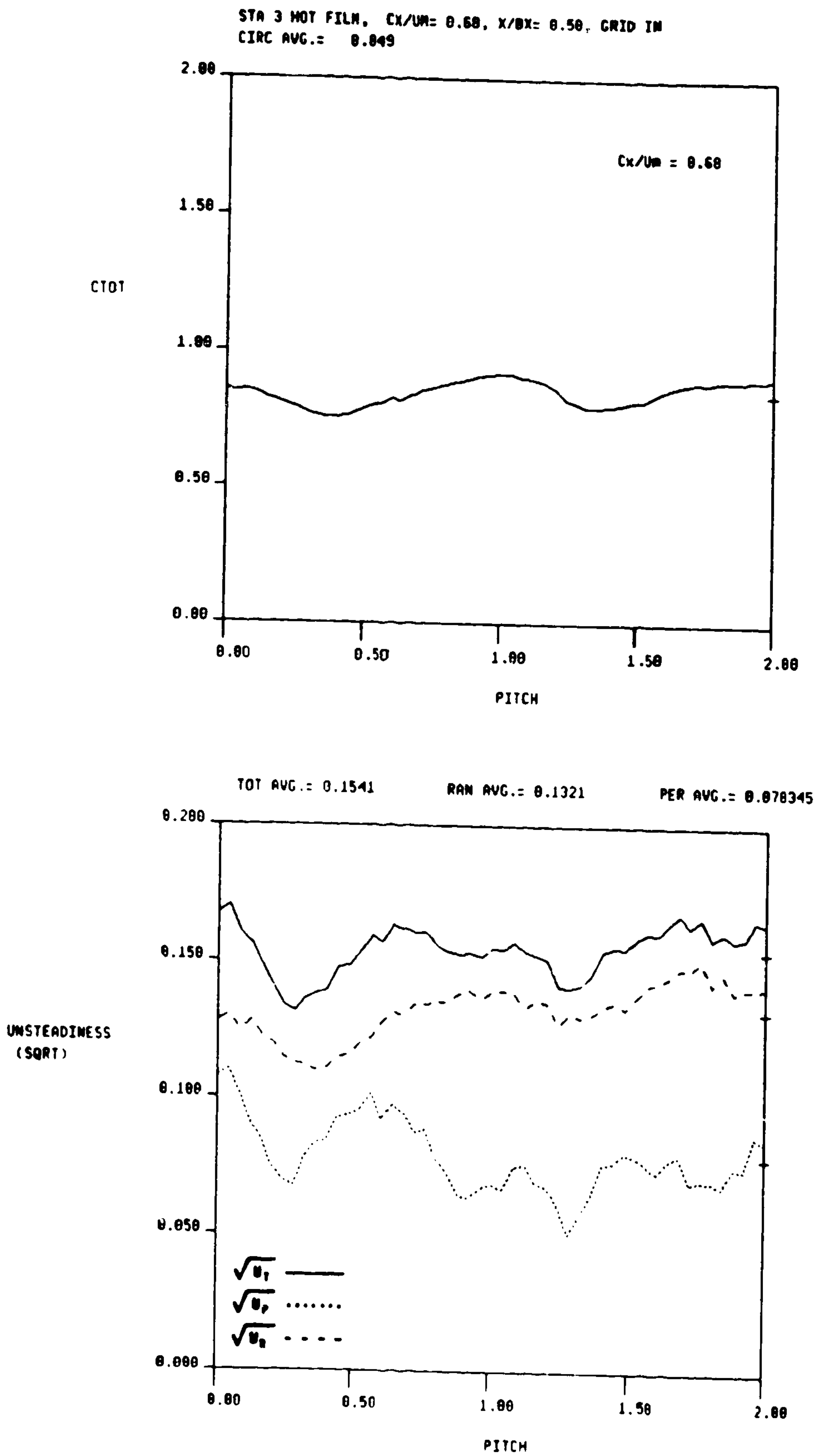

FIG. 34b CIRCUMFERENTIAL DISTRIBUTION OF TIME AVERAGED SPEED AND UNSTEADINESS AT ROTOR EXIT, GRID IN

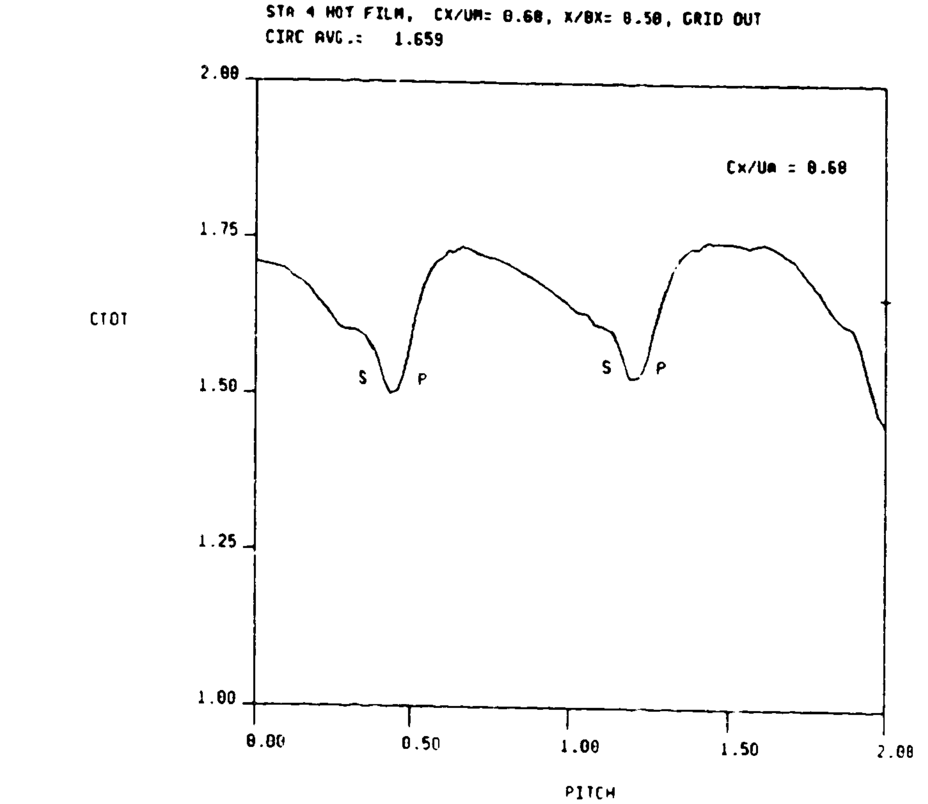

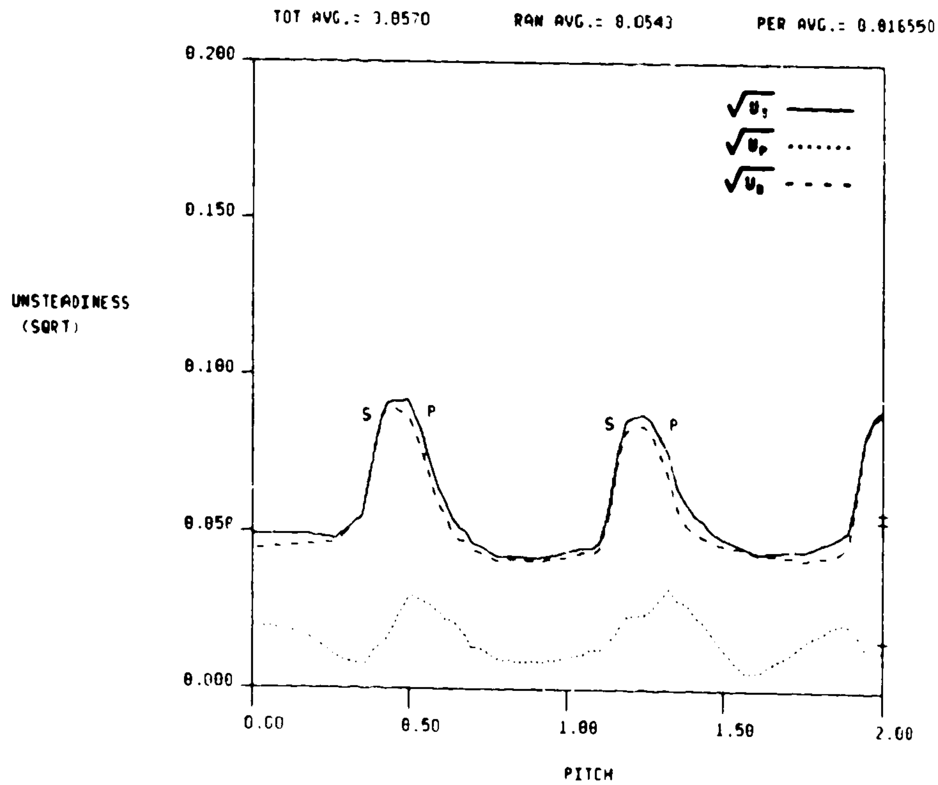

FIG. 35a CIRCUMFERENTIAL DISTRIBUTION OF TIME AVERAGED SPEED AND UNSTEADINESS AT 2ND STATOR EXIT, GRID OUT

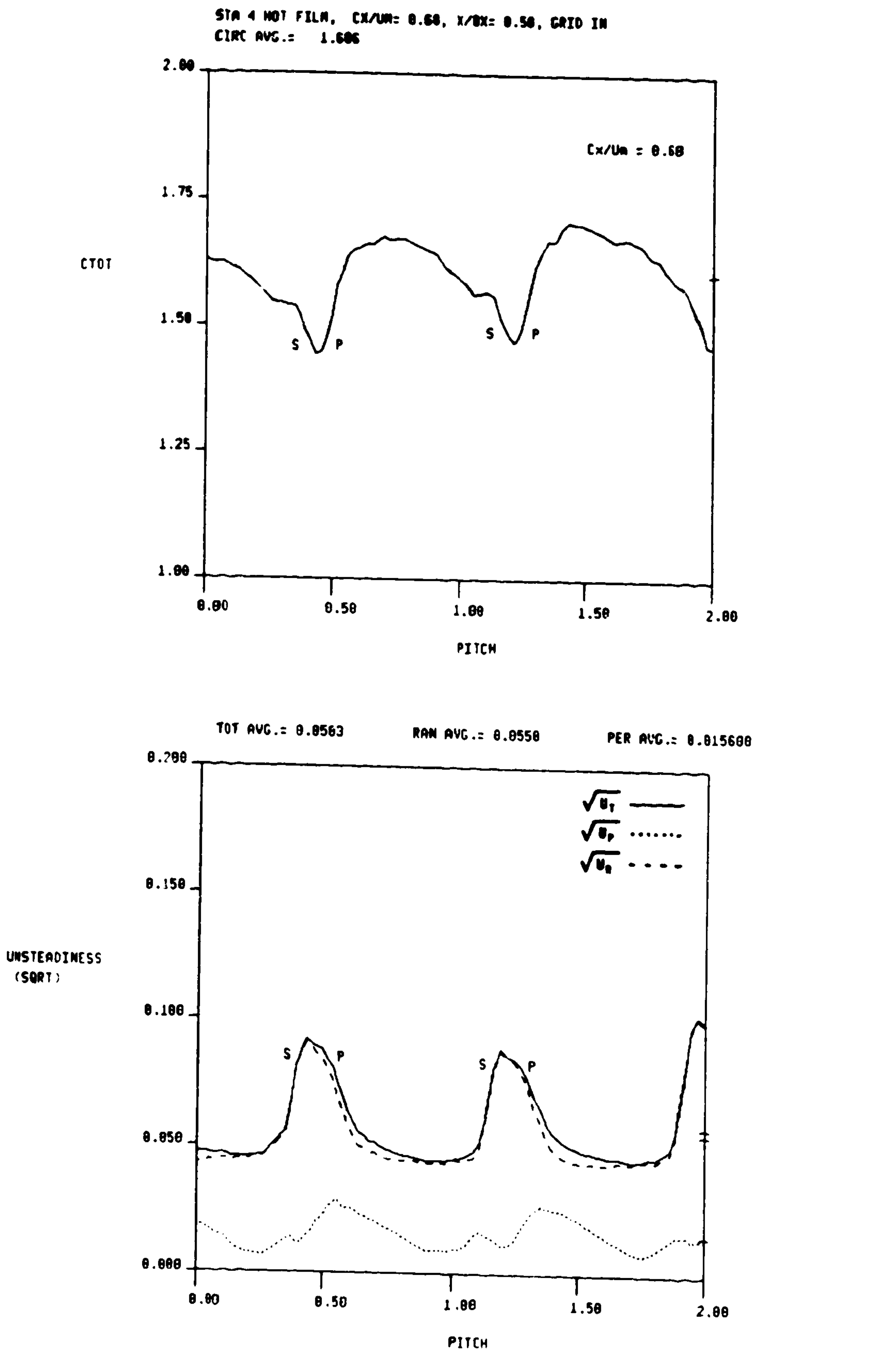

FIG. 35b CIRCUMFERENTIAL DISTRIBUTION OF TIME AVERAGED SPEED AND UNSTEADINESS AT 2ND STATOR EXIT, GRID IN

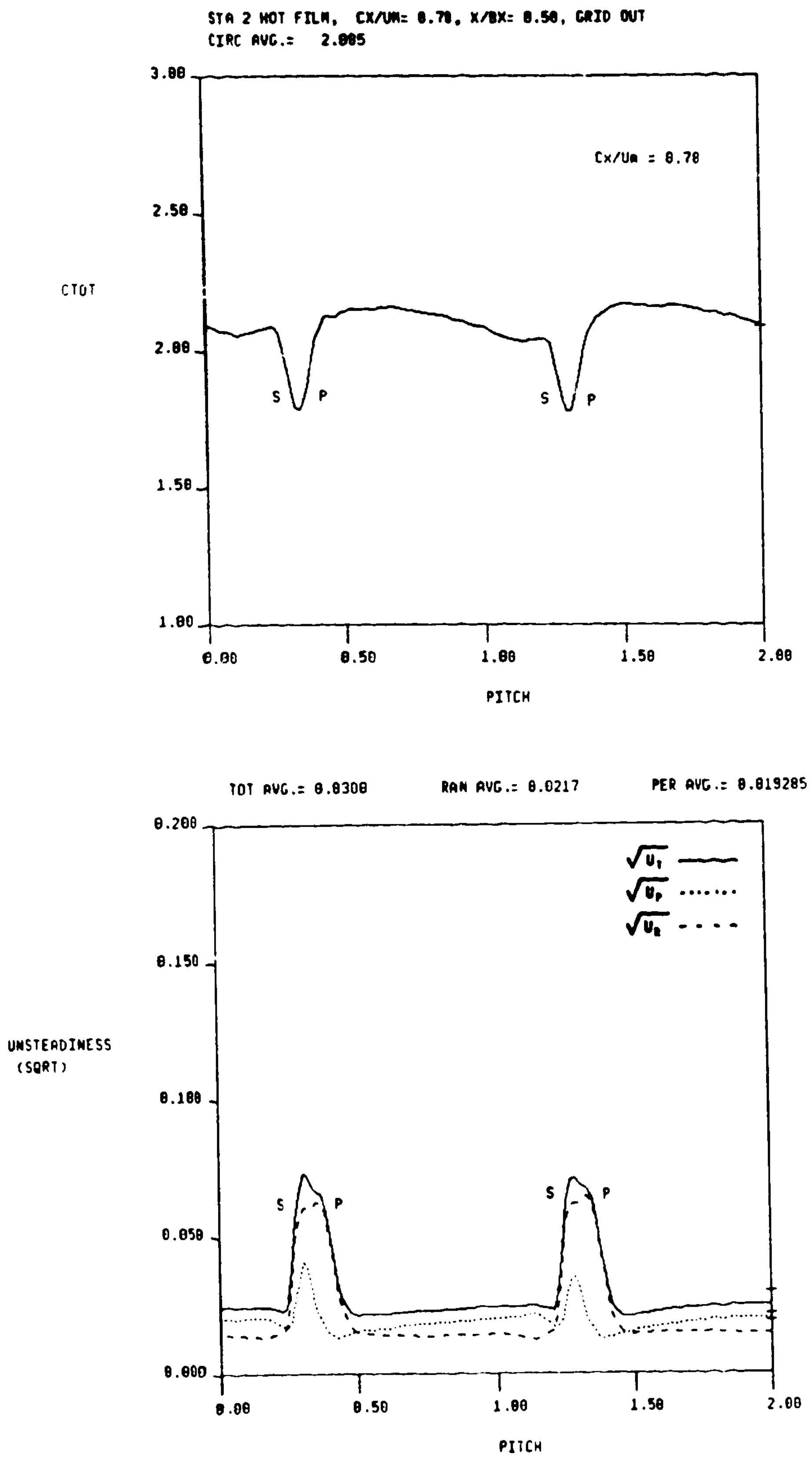

FIG. 36a CIRCUMFERENTIAL DISTRIBUTION OF TIME AVERAGED SPEED AND UNSTEADINESS AT 1ST STATOR EXIT, GRID OUT

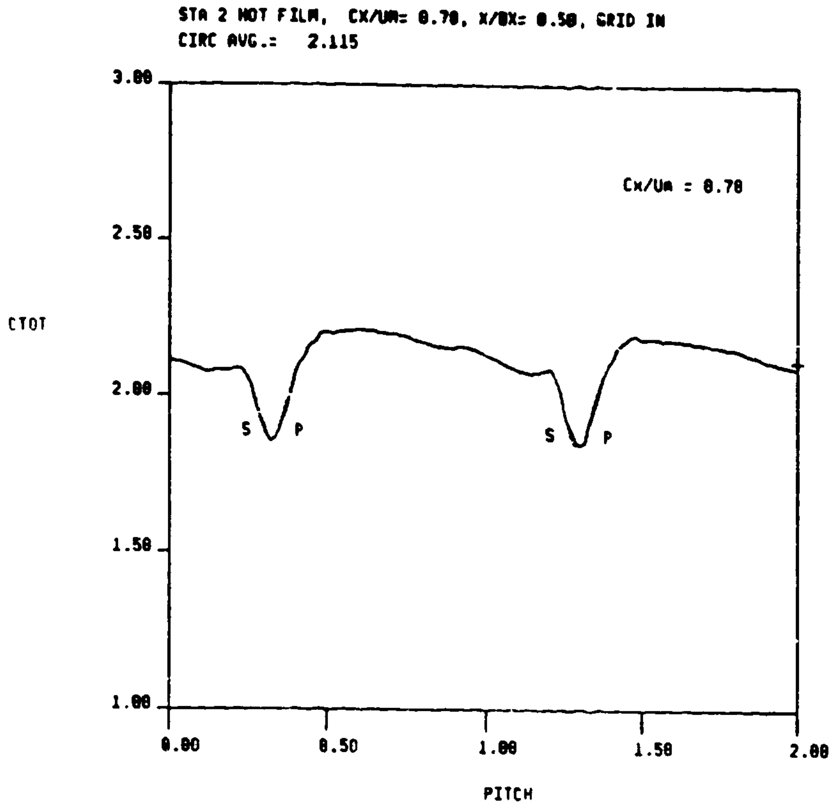

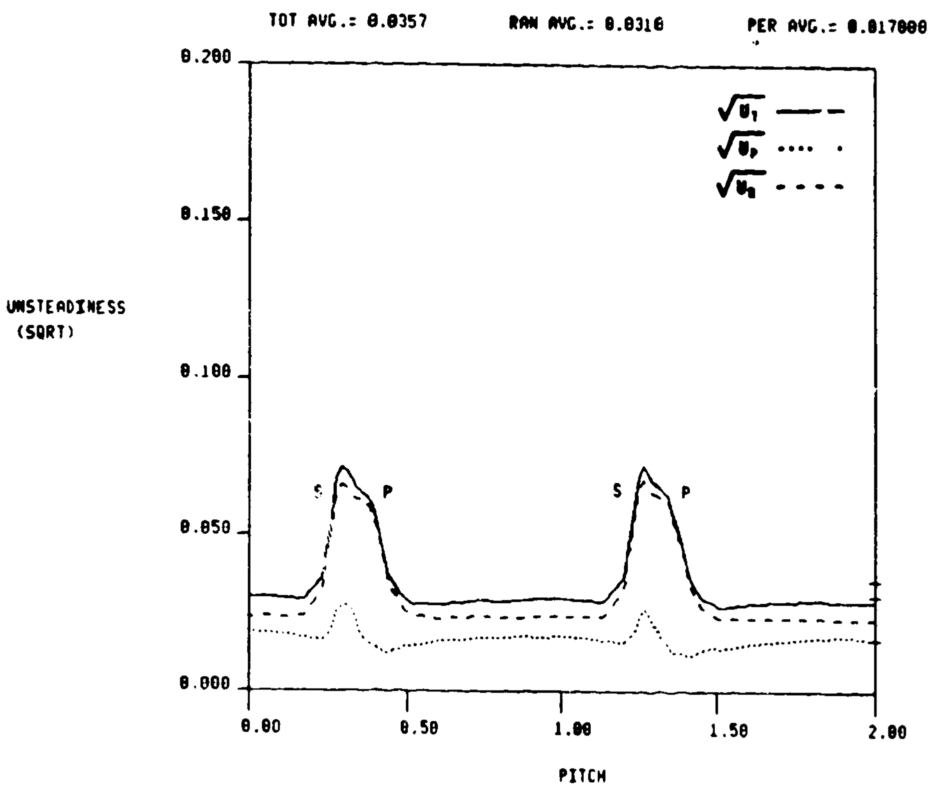

FIG. 36b CIRCUMFERENTIAL DISTRIBUTION OF TIME AVERAGED SPEED AND UNSTEADINESS AT 1ST STATOR EXIT, GRID IN

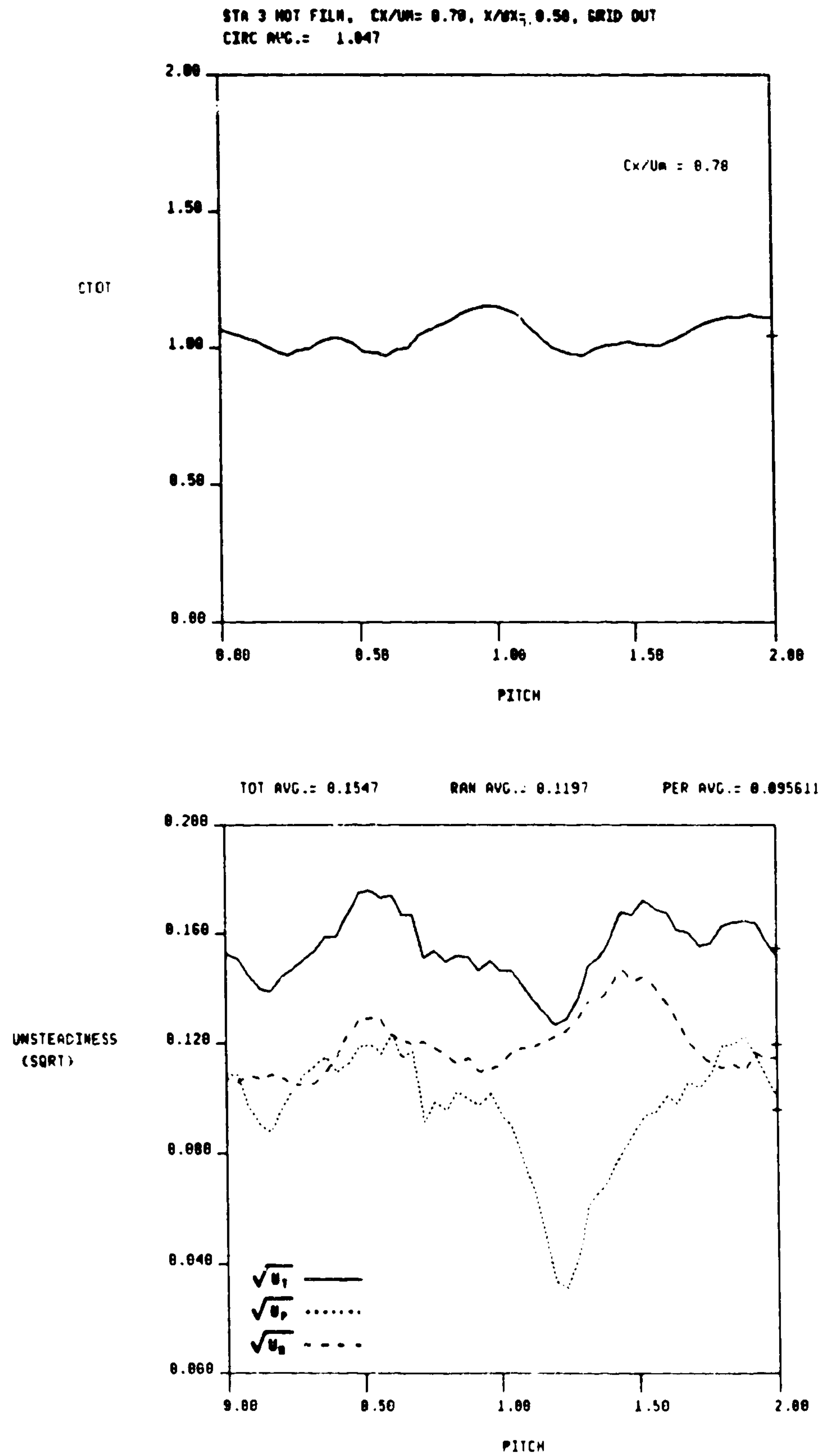

FIG. 37a CIRCUMFERENTIAL DISTRIBUTION OF TIME AVERAGED SPEED AND UNSTEADINESS AT ROTOR EXIT, GRID OUT

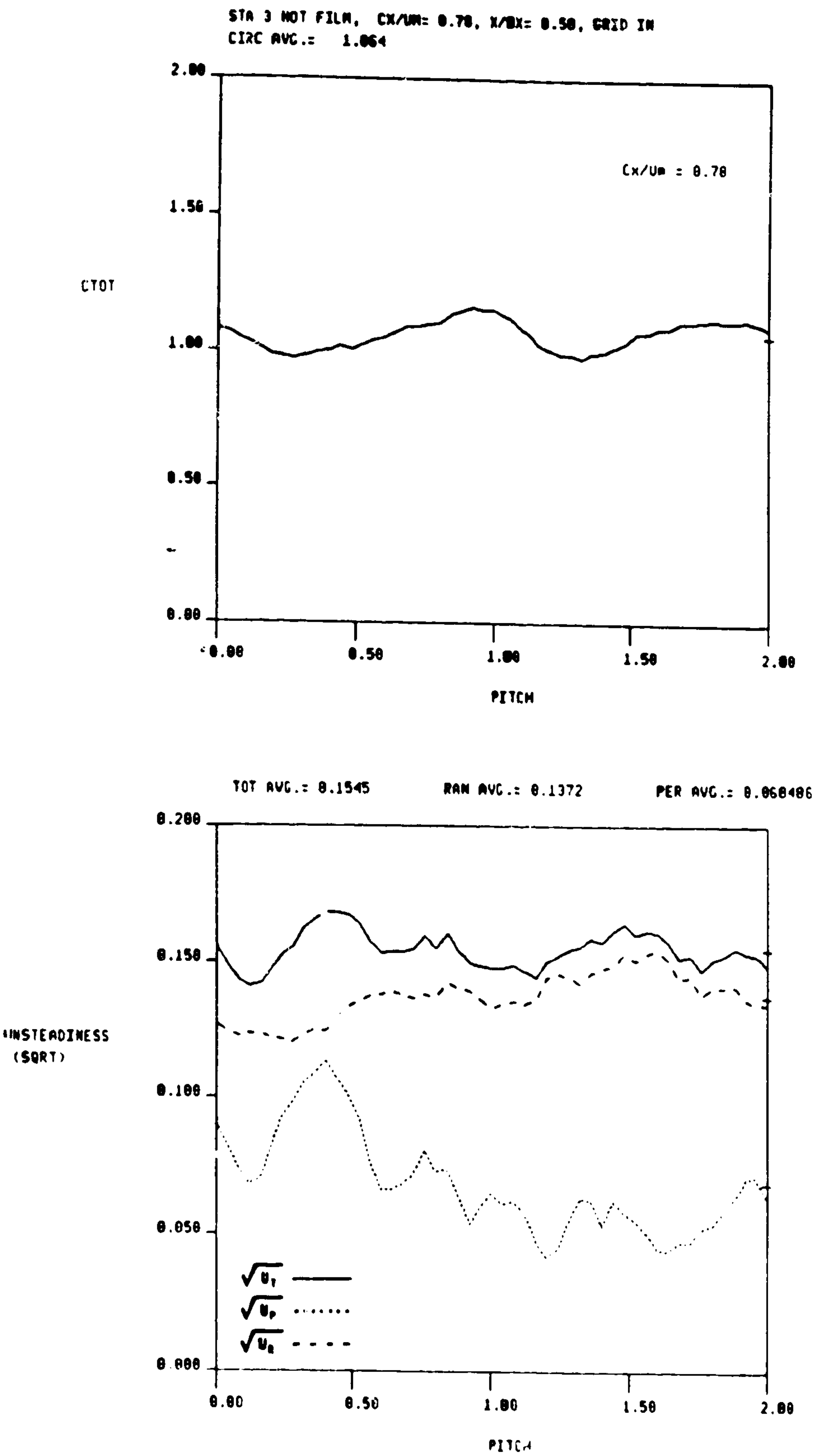

FIG. 37b CIRCUMFERENTIAL DISTRIBUTION OF TIME AVERAGED SPEED AND UNSTEADINESS AT ROTOR EXIT, GRID IN

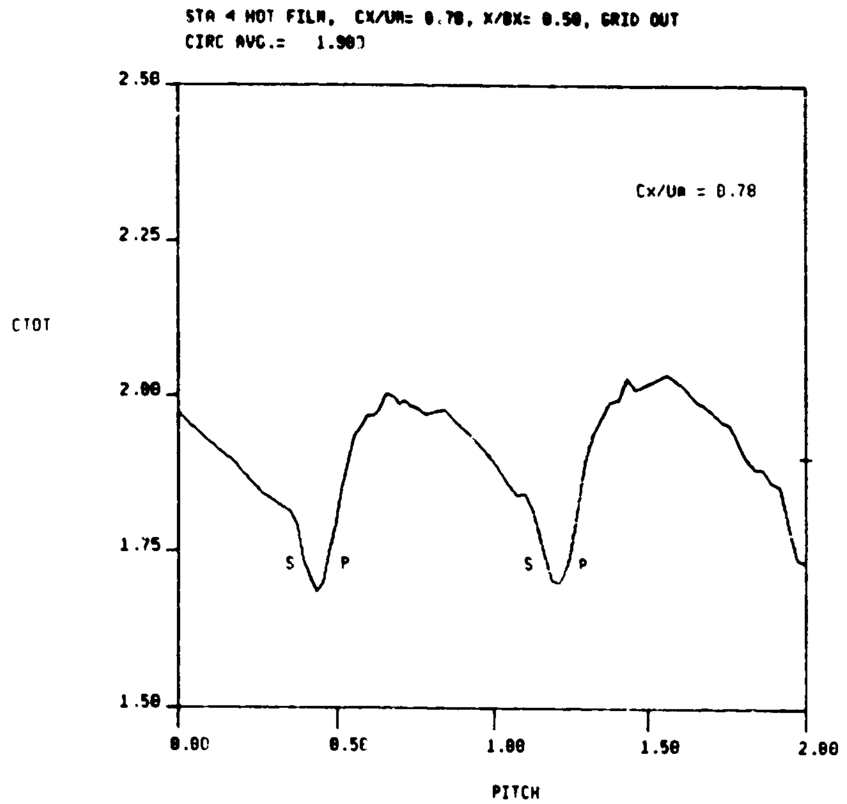

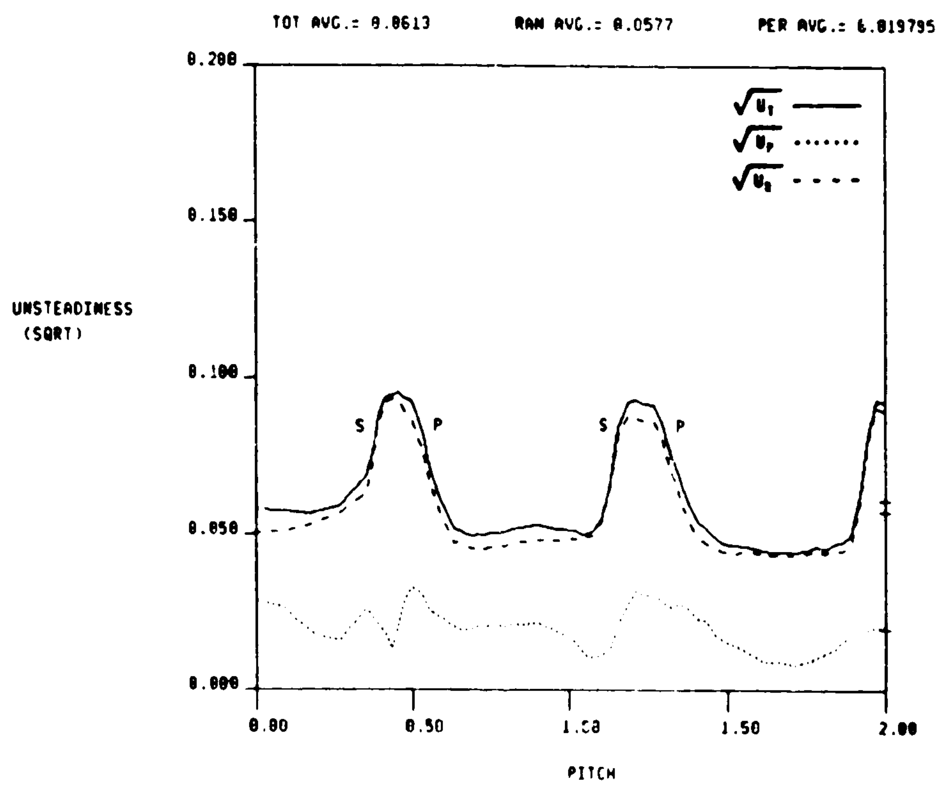

FIG. 38a CIRCUMFERENTIAL DISTRIBUTION OF TIME AVERAGED SPEED AND UNSTEADINESS AT 2ND STATOR EXIT, GRID OUT

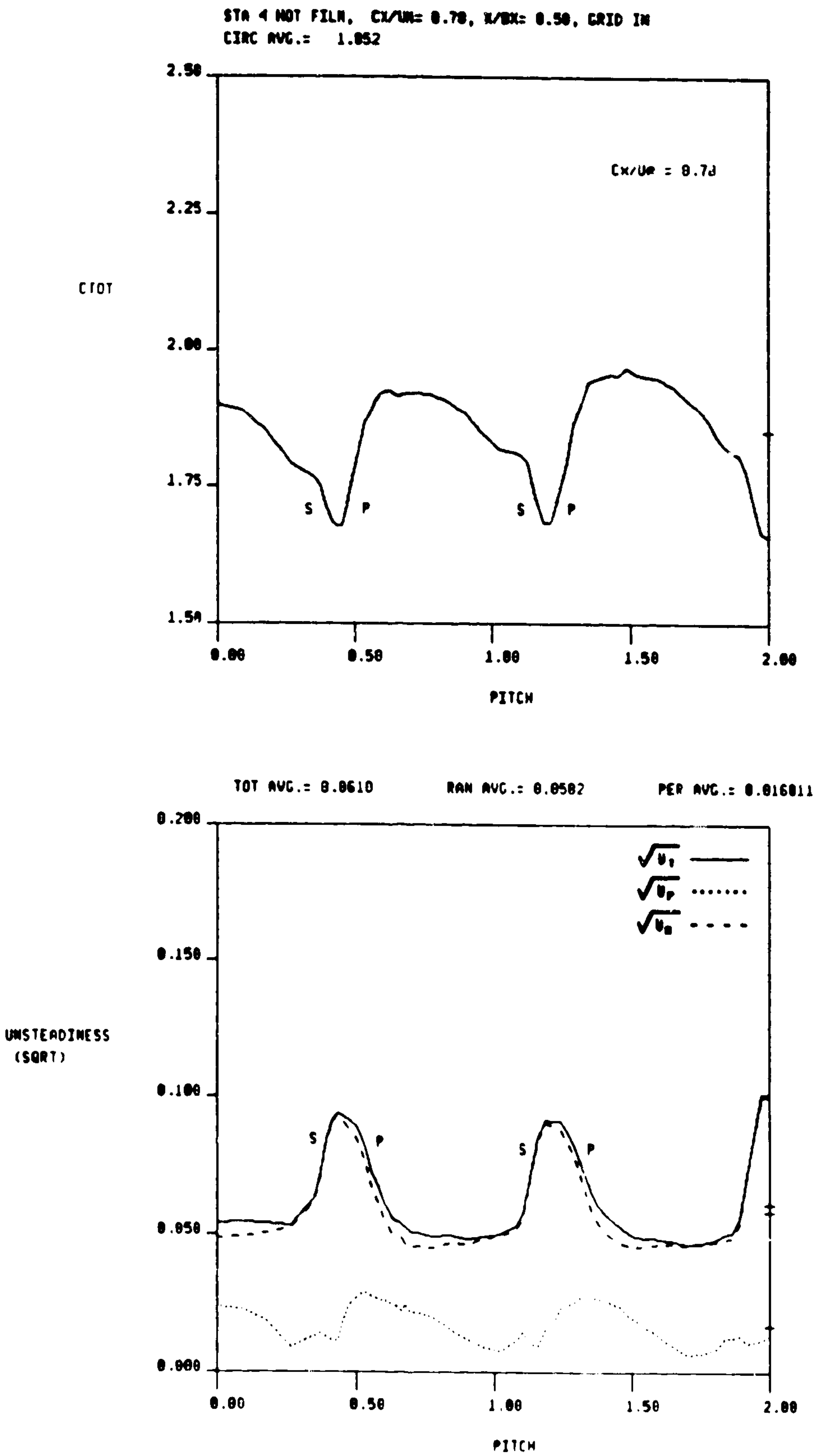

FIG. 38b CIRCUMFERENTIAL DISTRIBUTION OF TIME AVERAGED SPEED AND UNSTEADINESS AT 2ND STATOR EXIT, GRID IN

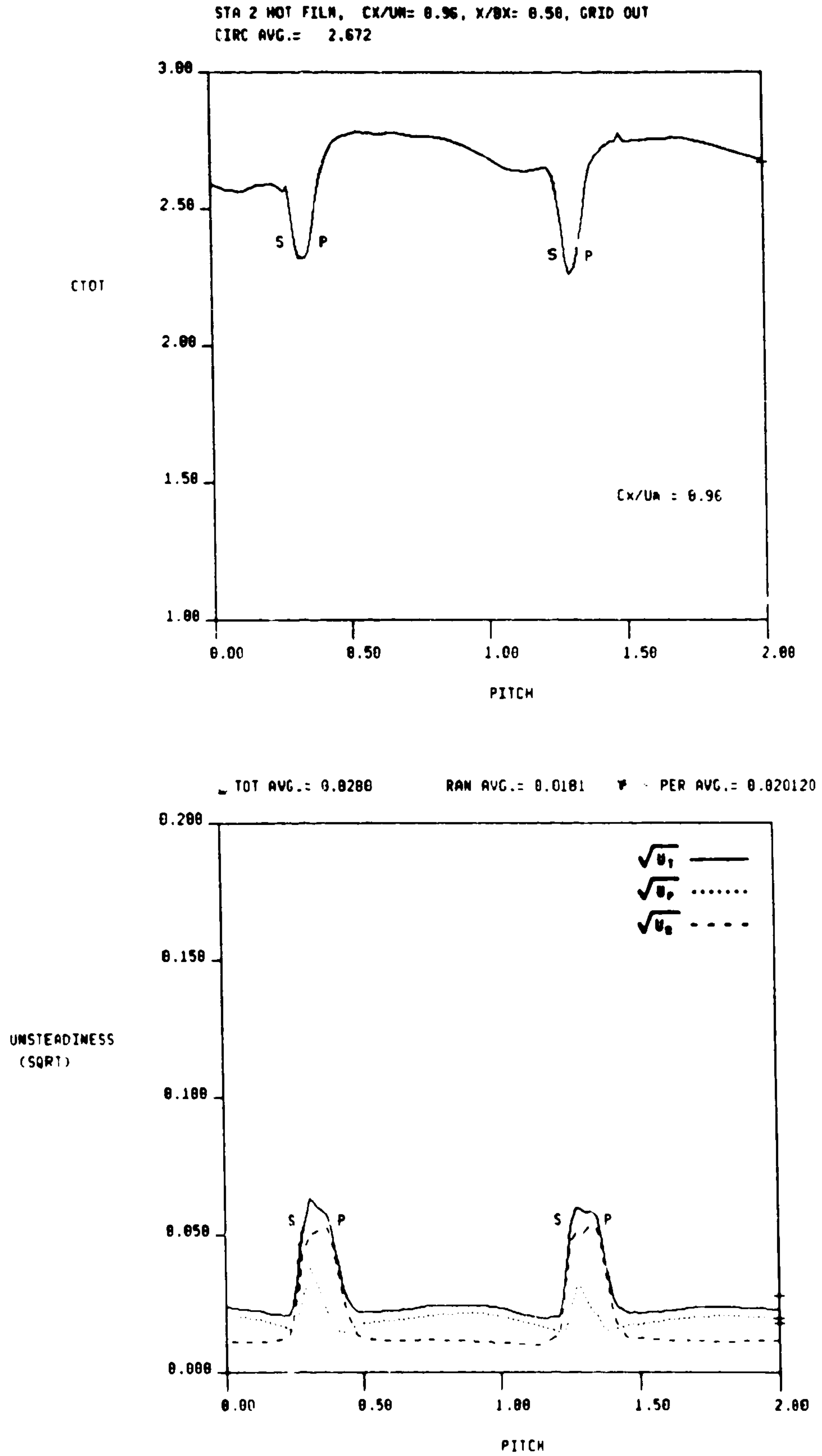

FIG. 39a CIRCUMFERENTIAL DISTRIBUTION OF TIME AVERAGED SPEED AND UNSTEADINESS AT 1ST STATOR EXIT, GRID OUT

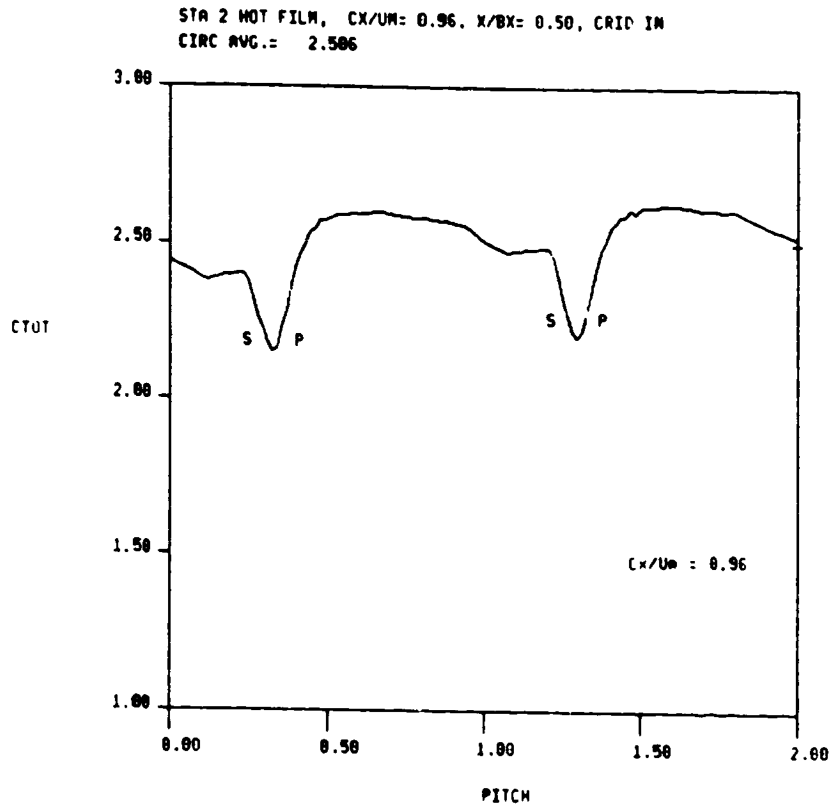

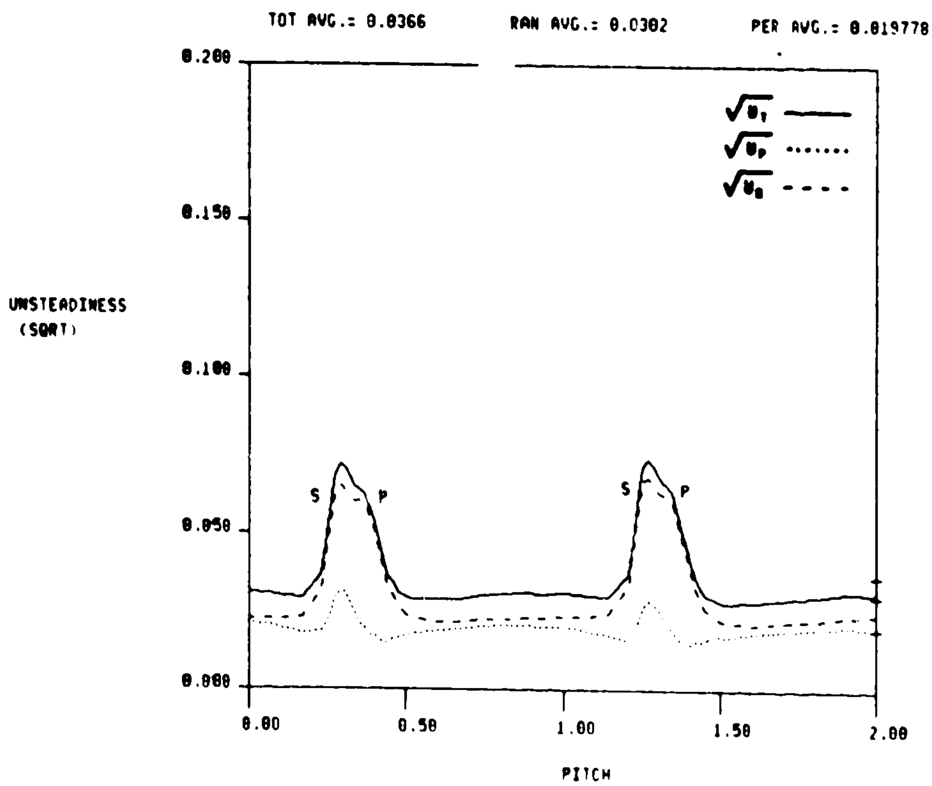

FIG. 39b CIRCUMFERENTIAL DISTRIBUTION OF TIME AVERAGED SPEED AND UNSTEADINESS AT 1ST STATOR EXIT, GRID IN

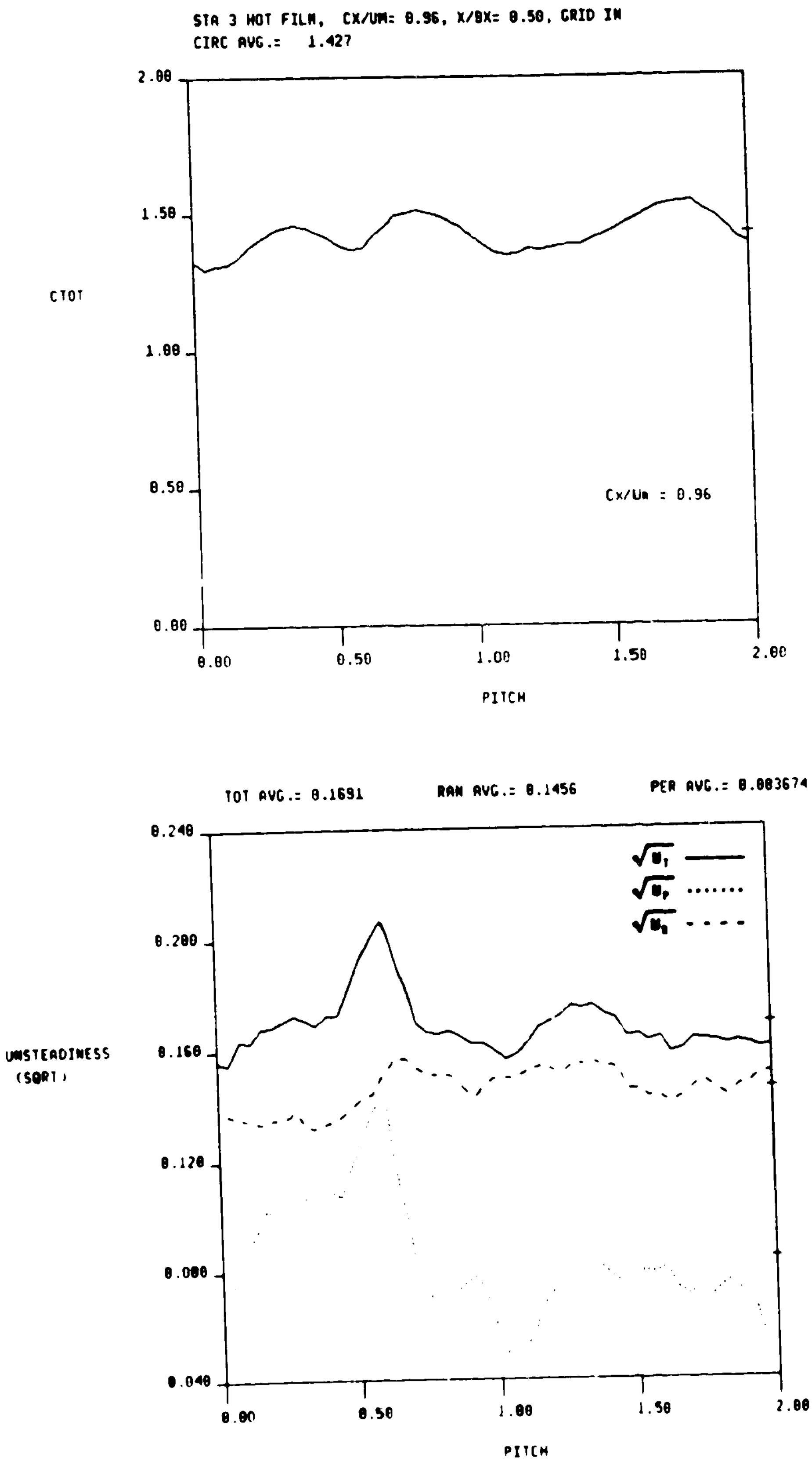

FIG. 40a CIRCUMFERENTIAL DISTRIBUTION OF TIME AVERAGED SPEED AND UNSTEADINESS AT ROTOR EXIT, GRID IN

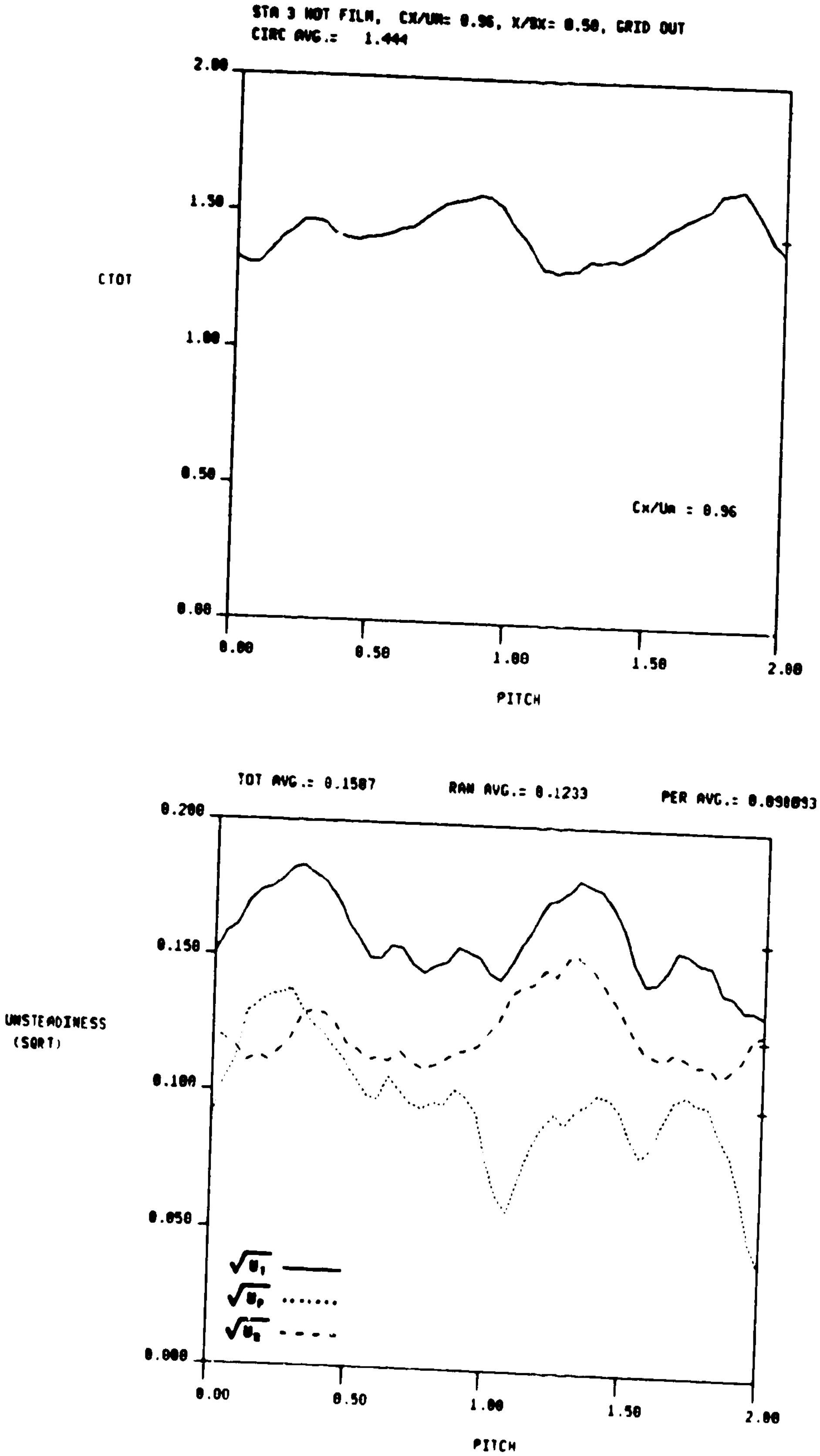

FIG. 40b CIRCUMFERENTIAL DISTRIBUTION OF TIME AVERAGED SPEED AND UNSTEADINESS AT ROTOR EXIT, GRID OUT

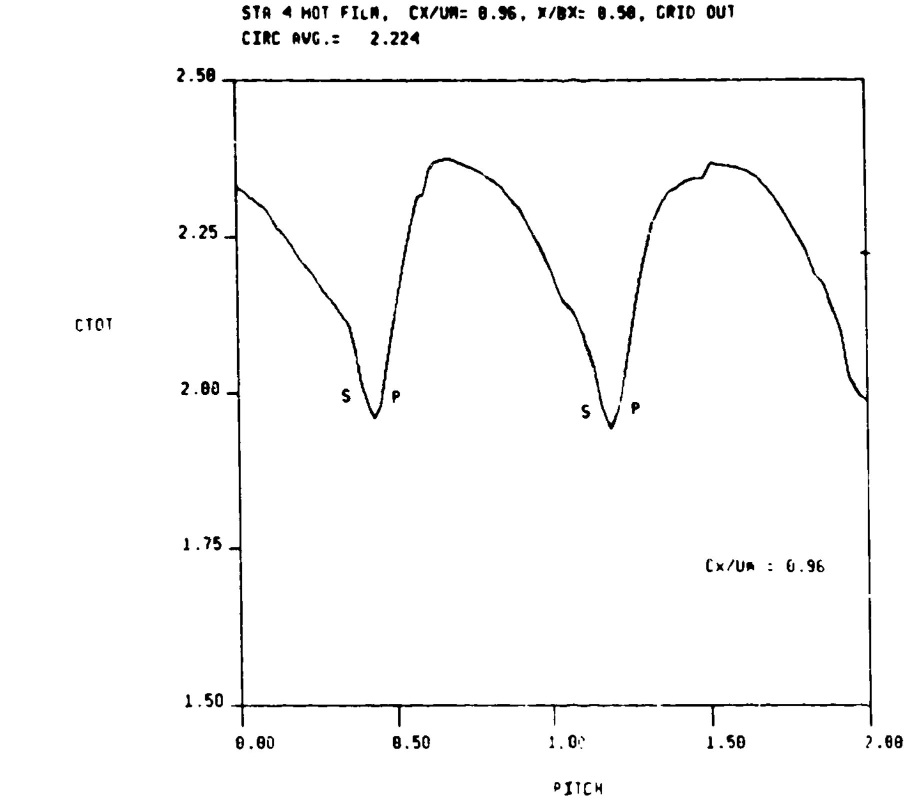

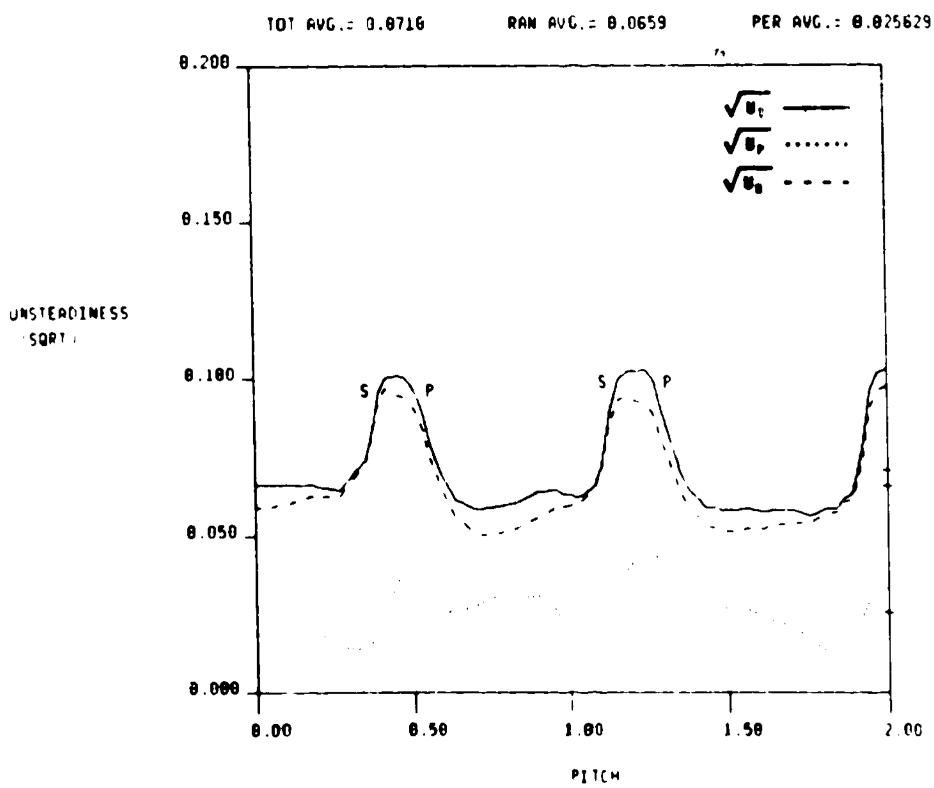

FIG. 41a CIRCUMFERENTIAL DISTRIBUTION OF TIME AVERAGED SPEED AND UNSTEADINESS AT 2ND STATOR EXIT, GRID OUT

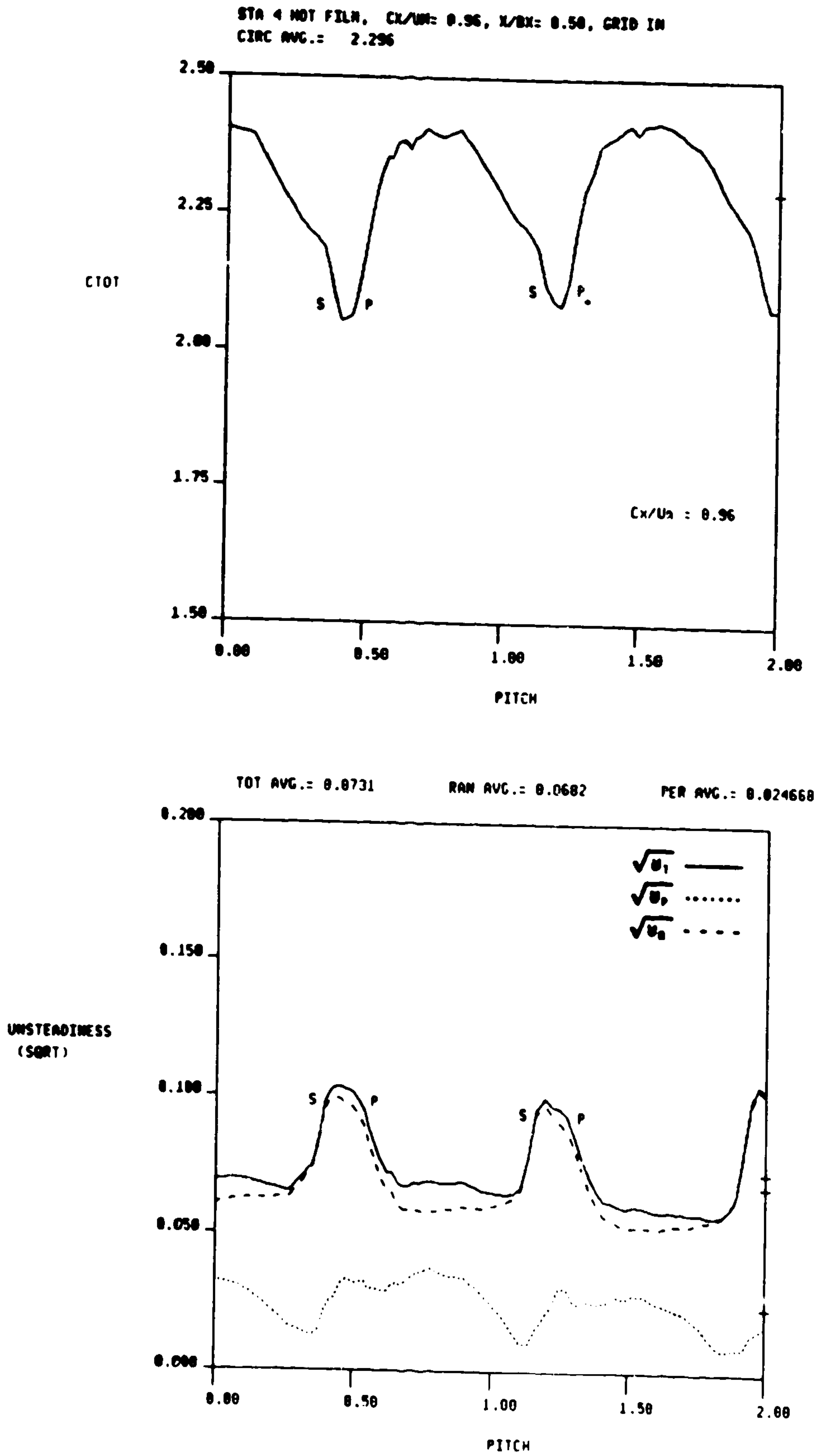

FIG. 41b CIRCUMFERENTIAL DISTRIBUTION OF TIME AVERAGED SPEED AND UNSTEADINESS AT 2ND STATOR EXIT, GRID IN

NASA
National Aeronautics and Space Administration

Report Documentation Page

1. Report No.	2. Government Accession No.	3. Recipient's Catalog No.
NASA CR-179469		

4. Title and Subtitle	5. Report Date
The Effects of Inlet Turbulence and Rotor/Stator Interactions on the Aerodynamics and Heat Transfer of a Large-Scale Rotating Turbine Model IV—Aerodynamic Data Tabulation	November 1987
	6. Performing Organization Code
7. Author(s)	8. Performing Organization Report No.
R.P. Dring, H.D. Joslyn, and M.F. Blair	UTRC-R86-956480-4
	10. Work Unit No. 533-04-11
9. Performing Organization Name and Address United Technologies Research Center Silver Lane East Hartford, Connecticut 06108	11. Contract or Grant No. NAS3-23717
	13. Type of Report and Period Covered Contractor Report Final
12. Sponsoring Agency Name and Address National Aeronautics and Space Administration Lewis Research Center Cleveland, Ohio 44135-3191	14. Sponsoring Agency Code

15. Supplementary Notes

Project Manager, Robert J. Simoneau, Internal Fluid Mechanics Division, NASA Lewis Research Center, Cleveland, Ohio 44135.

16. Abstract

A combined experimental and analytical program was conducted to examine the effects of inlet turbulence on airfoil heat transfer. The experimental portion of the study was conducted in a large-scale (approximately 5× engine), ambient temperature, rotating turbine model configured in both single-stage and stage-and-a-half arrangements. Heat transfer measurements were obtained using low-conductivity airfoils with miniature thermocouples welded to a thin, electrically heated surface skin. Heat transfer data were acquired for various combinations of low or high inlet turbulence intensity, flow coefficient, first-stator/rotor axial spacing, Reynolds number and relative circumferential position of the first and second stators. Aerodynamic measurements obtained as part of the program include distributions of the mean and fluctuating velocities at the turbine inlet and, for each airfoil row, midspan airfoil surface pressures and circumferential distributions of the downstream steady state pressures and fluctuating velocities. Analytical results included airfoil heat transfer predictions produced using existing two-dimensional boundary layer computation schemes and an examination of solutions of the unsteady boundary layer equations. The results of this program are reported in four separate volumes. All four have a common report title and the following volume subtitles:

Report Title: The Effects of Inlet Turbulence and Rotor/Stator Interactions on the Aerodynamics and Heat Transfer of a Large-Scale Rotating Turbine Model.

Volume Titles:			
	Volume I:	UTRC-R86-956480-1 (NASA CR-4079)	Final Report
	Volume II:	UTRC-R86-956480-2 (NASA CR-179467)	Heat Transfer Data Tabulation 15% Axial Spacing
	Volume III:	UTRC-R86-956480-3 (NASA CR-179468)	Heat Transfer Data Tabulation 65% Axial Spacing
	Volume IV:	UTRC-R86-956480-4 (NASA CR-179469)	Aerodynamic Data Tabulation

17. Key Words (Suggested by Author(s))

Heat transfer
Aerodynamics
Turbines
Rotor/stator
Turbulence
Unsteady flow
Airfoils

Date for general release May 1988

STAR Category 34

19. Security Classif. (of this report)	20. Security Classif. (of this page)	21. No of pages	22. Price*
Unclassified	Unclassified	134	A07

NASA FORM 1626 OCT 86